

1989

## Geoelectrical Methods Used to Study Polluted Bedrock Aquifers

Michael Patrick Boland  
*University of Rhode Island*

Follow this and additional works at: <https://digitalcommons.uri.edu/theses>

Terms of Use

All rights reserved under copyright.

---

### Recommended Citation

Boland, Michael Patrick, "Geoelectrical Methods Used to Study Polluted Bedrock Aquifers" (1989). *Open Access Master's Theses*. Paper 2029.  
<https://digitalcommons.uri.edu/theses/2029>

This Thesis is brought to you by the University of Rhode Island. It has been accepted for inclusion in Open Access Master's Theses by an authorized administrator of DigitalCommons@URI. For more information, please contact [digitalcommons-group@uri.edu](mailto:digitalcommons-group@uri.edu). For permission to reuse copyrighted content, contact the author directly.

GEOELECTRICAL METHODS USED TO STUDY  
POLLUTED BEDROCK AQUIFERS  
BY  
MICHAEL PATRICK BOLAND

A THESIS SUBMITTED IN PARTIAL FULFILLMENT OF THE  
REQUIREMENTS FOR THE DEGREE OF  
MASTER OF SCIENCE  
IN  
GEOLOGY

UNIVERSITY OF RHODE ISLAND

1989

## ABSTRACT

Geoelectrical investigations of fractured bedrock aquifers have been performed in three main study areas: (i) Tiverton, R.I. As part of a Rhode Island Department of Environmental Management study evaluating the hydrogeology of an area in which bedrock wells are contaminated with hydrocarbons. (ii) Johnston, R.I. as a part of a study conducted for Solid Waste Management Co., to evaluate the hydrogeology of the fractured bedrock under a landfill. (iii) Presque Isle, Maine as a part of a study by the Geologic Survey of Maine, to place a high yield well in bedrock for the purpose of irrigation. Remote sensing and geophysical methods were used to locate possible fracture zones in the three areas. Vertical electrical soundings, after Schlumberger, have been made over these suspected fractured zones. Other measurements have been made by the profiling and the AB rectangle method.

Theory has been presented that links flow of fluids to flow of direct current through fractured rock. This theory results in an equation for predicting permeability from formation factors,  $k = \alpha F^r$  (Katsube and Hume, 1987). Comparisons to hydraulic parameters have been made using the bulk resistivities of the bedrock, as interpreted in Schlumberger depth soundings, and formation factors, calculated with known ground water resistivities.

The Johnston, RI study area showed a good relationship between permeabilities, predicted by the formation factor, and hydraulic conductivities, averaged from packer tests. This further resulted in the actual estimating equation of  $k = 7.53 \times 10^{-6} F^{1.08}$ .

The Maine study area showed a good linear relationship between bedrock resistivity and well yield on a bilogarithm plot. This relationship keeps the general form of the equation presented. Although actual predictions of yield are not possible, area may be ranked from low to high potential yield.

Correlations were also made to seismic velocities of the bedrock in the Johnston and Tiverton, RI areas. These comparisons yielded interesting results, suggesting that in areas of wide ranging pore water resistivities, the bulk resistivity and not the formation factor may better describe the relative hydraulic characteristics of the bedrock.

Methods have been suggested which would greatly improve and enhance the use of Schlumberger profiling and AB-rectangle techniques. This method involves selecting an optimal current electrode spacing using the depth sounding curve. The expected resistivities are calculated, using a computer program, for the AB-rectangle given the model interpretation from a depth sounding. These values are replotted on the depth sounding curve to view the effect of other layers on the measurement. An ideal size of the rectangle may be found using this technique, giving better control of the inherent change in depth with this method. True anomalies may then be calculated by subtracting the value of the expected resistivity from the measured at the location.

## ACKNOWLEDGEMENTS

I would like to thank my family: my mother for the sacrifices that she has made over the years so that I could obtain an education; my bother Jack for being a safety net when I needed him; my grandmother, "Nanny Pattie", for her wisdom and support; and my aunts Kathy and Dottie for their interest and support.

None of this would have been possible if not for the guidance that I received as a under graduate at the University of Maine at Farmington. I am indebted to: Dr. Eastler, for pulling me into geology in the first place; Dr. Berry for understanding the charades of an over-work undergraduate; "Chuck" for molding and preparing me for graduate work; Dr. Scribner for making math fun; and "Torc" for being their when I needed someone to hit.

I would like to express my deep thanks to the people who helped in so many ways at the University of Rhode Island, to: Dr. Frohlich, without of whom I would not have had the support to finish, he has been my friend as well as my major professor; Sue Ponte, for everything; Larry Hanson, for the endless assistance in my field work and his gumption; Dr. Urish, who taught me what I know about groundwater; The late Dr. Fisher, for his help and many laughs; Dr. Boothroyd, for his respect in me and his assistance in many ways; Dr. Murry, for being "Dan"; Jim Huton, the best office mate anyone could have; Dave Jones, for butting up with stupid computer questions and getting me a job; Tom Dunham, for being a republican to arguing with over a few cold beers ; Dick, Brad and Patty ; for road trips and cookouts that were extremely necessary; Tony, Nancy, Dav-id Law--son, Andrew, Chris, and all the other grad students who were great to be around.

To my friends all of whom helped my in numerous ways that they do and do not know. I would especially like to thank Sue and Elsie, Deano, Mucka, Surfer.

Finally to all those like Jim Owens that I forgot to mention in my haste to finally finish.

## TABLE OF CONTENTS

LIST OF TABLES		vii
LIST OF FIGURES		ix
CHAPTER 1	<b>INTRODUCTION</b>	1
CHAPTER 2	<b>FLOW THROUGH FRACTURED ROCK</b>	4
2.1	GENERAL CHARACTERISTICS	4
2.2	THEORY	5
2.3	RELATION OF FLUID FLOW TO ELECTRICAL FLOW	10
CHAPTER 3	<b>METHODOLOGY</b>	16
3.1	<b>GEOELECTRICAL METHODS</b>	16
3.1.1	Depth Soundings	19
3.1.2	Mapping of Resistivities	19
3.1.3	Instrumentation	23
3.2	<b>INTERPRETATION METHODS</b>	23
3.2.1	Schlumberger Depth Sounding	23
3.2.2	Profiling and AB-Rectangle	24
3.2.3	Electrical Potential/Horizontal Layers	24
3.2.4	The Apparent Resistivity Within the AB-Rectangle	36
3.2.5	Application of the AB-Rectangle Method	46
3.3	<b>LOCATING OF SOUNDINGS</b>	53
CHAPTER 4	<b>DISCUSSION AND RESULTS</b>	54
4.1	<b>AROOSTOOK CO., MAINE</b>	54
4.1.1	Geologic Setting and Lineament Analysis	54
4.1.2	Resistivity Soundings	63
4.1.3	Correlation of Resistivity to Bedrock Parameters	73
4.2	<b>JOHNSTON, RHODE ISLAND</b>	78
4.2.1	Geologic Setting and Lineament Analysis	78
4.2.2	Resistivity Soundings	85
4.2.3	Correlation of Resistivity to Bedrock Parameters	90
4.3	<b>TIVERTON RHODE ISLAND</b>	100
4.3.1	Geologic Setting and Lineament Analysis	100
4.3.2	Resistivity Soundings	105
4.3.3	Correlation of Resistivity to Bedrock Parameters	105
CHAPTER 5	<b>SUMMARY</b>	119
5.1	THEORY	119
5.2	METHODOLOGY	119
5.3	FIELD STUDIES	120
CHAPTER 6	<b>CONCLUSION</b>	123

APPENDIX 1a	Computer Methods	125
APPENDIX 1b	Listing of the depth sounding program	138
APPENDIX 1c	Listing of the AB-rectangle program	164
APPENDIX 2	Plots and Models, Johnston, RI	179
APPENDIX 3	Plots and Models, Tiverton, RI	189
APPENDIX 4	Plots and Models, Aroostook, ME	298
BIBLIOGRAPHY		230



## LIST OF TABLES

Table 4.1	Geoelectrical Parameters, Presque Isle, ME. ....	74
Table 4.2	Geoelectrical Parameters, Johnston, RI. ....	93
Table 4.3	Geoelectrical Parameters II, Johnston, RI.....	97
Table 4.4	Geoelectrical Parameters, Tiverton, RI.....	106

## LIST OF FIGURES

Fig. 2.1	A representative rock sample containing a fracture conduit .....	8
Fig. 3.1a	Schlumberger depth sounding array .....	18
Fig. 3.1b	Generalized four electrode array .....	18
Fig. 3.2a	AB-rectangle electrode configuration.....	22
Fig. 3.2b	Schlumberger profile configuration.....	22
Fig. 3.3	Comparison check of the computer program vs. master curves....	35
Fig. 3.4	Plot of apparent resistivity vs. half electrode spacing .....	38
Fig. 3.5	Contour Plot of the expected resistivities for model in fig. 3.4.....	40
Fig. 3.6	Plot of apparent resistivity vs. half electrode spacing .....	43
Fig. 3.7	Contour Plot of the expected resistivities for model in fig. 3.6.....	45
Fig. 3.8	Sketch showing AB-Rectangle Placement, Plainville, MA .....	48
Fig. 3.9	Sounding Curve w/Layer Model, Plainville, MA.....	50
Fig. 3.10	Contour Map of anomalous bedrock resistivities, Plainville.....	52
Fig. 4.1	Location map showing the two quadrangles of the Maine study ..	56
Fig. 4.2	Location of geoelectrical soundings, Mars Hill.....	58
Fig. 4.3	Location of depth soundings, Fort Fairfield .....	60
Fig. 4.4	Rose diagrams of lineaments, Mars Hill and Fort Fairfield .....	62
Fig. 4.5	Typical sounding curves .....	65
Fig. 4.6	Location of depth soundings in relation to the AB-rectangle.....	67
Fig. 4.7	Layer models for the soundings made in the vicinity of the AB-rectangle.....	69
Fig. 4.8	Contour map of anomalous bedrock resistivity, Presque Isle AB-rectangle.....	72
Fig. 4.9	Plot of bedrock resistivity vs. well yield .....	77
Fig. 4.10	Location map showing study areas in Rhode Island .....	79
Fig. 4.11	Location map of the Central Landfill, Johnston, RI.....	83
Fig. 4.12	Rose diagram showing the trends of the lineaments, Central Landfill .....	84
Fig. 4.13	Location of depth soundings, Johnston .....	87
Fig. 4.14	Plot of depth to bedrock, measured vs. interpreted .....	92
Fig. 4.15	Plot of average hydraulic conductivity vs. estimated permeabil- ity .....	95
Fig. 4.16	Plot of permeability of the bedrock vs. the formation factor.....	99
Fig. 4.17a	Rose diagram showing the trends of the lineaments, Tiverton, RI .....	102
Fig. 4.17b	Histogram showing the trends of the lineaments, Tiverton, RI.....	102
Fig. 4.18	Stereo contour plot of pole to planes of fractures, Tiverton, RI....	104
Fig. 4.19	Location of depth soundings, Tiverton.....	108

Fig. 4.20	Plot of estimated depth to bedrock, seismic vs. geoelectrical depth sounding.....	110
Fig. 4.21	Plot of the apparent formation factor vs. seismic velocity .....	113
Fig. 4.22	Plot of bedrock resistivity vs. seismic velocity .....	116
Fig. 4.23	Geoelectrical profile in relation to the geologic profile.....	118

## 1.0 INTRODUCTION

This investigation will evaluate surface geoelectrical methods for the study of fractured bedrock aquifers. Water bearing fractured rock has a much lower value of electrical resistivity than the nearly infinite value of unfractured rock. It is this contrast which could allow the electrical resistivity method to be used as a geophysical tool for the study of fractured bedrock aquifers. An objective of this study is to investigate the relationship between fluid and electrical flow through fractured rock, both in theory and in field investigations.

Electrical resistivity techniques have been widely used in the study of unconsolidated aquifers. Besides locating aquifers of adequate yield, the method has also been used to detect; (i) zones of ground water recharge (Page, 1968), (ii) contamination from septic tanks (Klefstad, et al., 1974), (iii) acid mine drainage (Merkel, 1972), and (iv) leachate from landfills (Cartwright and McComas, 1968). Several researchers have employed the method to estimate the water transmitting properties of unconsolidated aquifers (Frohlich and Kelly, 1985; Kelly and Reiter, 1984; Kosinski and Kelly, 1981; Urish, 1981). Less experience has been gathered for aquifers in fractured bedrock (Kowalski and Sanders, 1983).

The study of ground water involves the analysis of both unconsolidated and bedrock aquifers. Unconsolidated aquifers are better understood, as they vary in complexity only with their degree of heterogeneity. In exploring for ground water in fractured rock the problem is to find areas of maximum fracture frequency (Summers, 1972). Locating these areas is necessary for evaluating ground water flow within the bedrock. If fractures are sufficiently connected, pollutants may flow at faster rates and at higher concentrations through the fracture network than through the unconsolidated aquifer (Freeze and Cherry, 1979).

Permeability of fractured rocks can vary by several orders of magnitude over short distances. Methods derived for determining the hydraulic characteristics of homogeneous, isotropic systems are unsatisfactory when applied to fractured rock systems. Exploring for groundwater in fractured rock depends on the ability to locate areas of high fracture density for the development of a well. Unless geological and geophysical methods are used, wells will be sited at random (Summers, 1972). The conventional method of installing numerous test wells is costly, time consuming and often produces a low yield well (Stollar and Roux, 1975). Geoelectrical soundings, when used in conjunction with other data, may partially replace this drilling by obtaining ground water information (Frohlich, 1974).

Resistivity measurements have been completed in three main study areas. (i) Tiverton, R.I., as part of a Rhode Island Department of Environmental Management study evaluating the hydrogeology of an area in which bedrock wells are contaminated with hydrocarbons. (ii) Johnston, R.I. as a part of a study conducted for Solid Waste Management Co., to evaluate the hydrogeology of the fractured bedrock under a landfill. (iii) Presque Isle, Maine as a part of a study by the Geologic Survey of Maine, to place a high yield well in bedrock for the purpose of irrigation. Remote sensing and geophysical methods were used to locate possible fracture zones in the three areas. Vertical electrical soundings after Schlumberger have been made over these suspected fractured zones to study the vertical change of resistivity. Other measurements have been made with the profiling and the AB rectangle method (see Zohdy et al., 1974). These last two techniques were used to map lateral changes in resistivities within depth ranges. Measurements with these methods have been considered questionable due to uncertainties with respect to the depth of the investigation.. This study addresses these problems and presents new procedures for the interpretation of data particularly with respect to depth control.

Results of the resistivity interpretations were compared with other available and relevant data in the areas. In Rhode Island seismic refraction soundings have been performed by Larry Hanson (1988). A thesis on bedrock hydrogeology using the magnetic and other methods was completed by Savarese (1987) in Tiverton. The Johnston site is a landfill in which many test wells have been drilled and logged with subsequent packer tests yielding hydraulic conductivity measurements. Some of the soundings were made over these wells. In Maine bedrock resistivities were compared to well yields.

## 2. FLOW THROUGH FRACTURED ROCK

### 2.1 General Characteristics

The main rock types dealt with in this study are limestones, pelites and granites. When characterizing the hydraulic capabilities of a bedrock unit we concern ourselves with the existing conduits through which water flows. These openings originate from two types of permeability. Primary permeability is related to voids which were created during the formation of the rock, and secondary permeability is related to fractures caused by stress. The rock types studied can differ greatly in the amount of primary permeability. However, when fractured the secondary permeability produces units with comparable hydraulic properties.

Unfractured granite is nearly impermeable with permeabilities in the order of  $10^{-4}$  gal/day/ft<sup>2</sup> ( $10^{-11}$  m/s) (Freeze and Cherry, 1979). Thus the most important influence on flow through granite is the degree of fracturing which is often related to regional tectonic stresses. Joints (fractures with no appreciable movement) may also form from contraction during cooling or expansion during the release of overburden stress. Those that form from stress release are known as sheeting joints which are subparallel to the surface topography. The aperture width of fractures may increase in exposed rock due to weathering. However, ground water is usually saturated with silica obtained from the soil above unexposed rock (Freeze and Cherry, 1979). Weathering beneath the water table produces insoluble iron and aluminum oxides that can plug smaller fractures.

The primary permeability of Paleozoic unfractured limestone and dolostone is also low, commonly less than  $10^{-1}$  gal/day/ft<sup>2</sup> ( $\sim 10^{-7}$  m/s) (Freeze and Cherry, 1979). Secondary permeability, which greatly increases the flow network, is caused by fracturing, and by enlargement of fractures or bedding planes by calcite or dolomite dissolution. The

typically horizontal enlargement of bedding planes is more pronounced near vertical fractures in which fresh water can circulate. Particularly in folded limestones, near-vertical fractures form along the crests of anticlines due to tensional stress within the folded layers (Freeze and Cherry, 1979). The zones of highest permeability are located at the intersections of the vertical and horizontal fractures.

Though limestone and pelites do contain a disperse primary permeability, fracture conduits have a greater influence on the permeability of a sample. A fracture network is a much more efficient fluid conductor than a fine-grained intergranular network. Therefore, in both rock types fracture flow is of primary concern.

## 2.2 Theory

The hydraulic conductivity  $K$ , is a property of both the fluid and the porous material through which the fluid flows. In theory these attributes may be separated into fluidity  $f$ , and intrinsic permeability  $k$ .

$$K = kf \tag{2.1}$$

where  $f = \rho g / \mu$

$\rho$  : fluid density  
 $g$  : acceleration of gravity  
 $\mu$  : viscosity

Geologists are concerned with permeability for numerous reasons. The manner in which fluids and gases flow through a rock impacts the rate of magma emplacement and crystallization, the transport of hydrocarbons to an oil or gas well, the migration of leachates from waste disposal sites into an aquifer and, not the least of all, ground water flow to a well. Since permeability is a physical parameter of such importance, many



theoretical and experimental studies have been conducted to estimate it from more readily available rock properties. Approaches of these investigations can be divided into two categories. The first relates  $k$  to microscopic data on pore geometry. The second relates  $k$  to more easily measured properties such as porosity or electrical resistivity (Rothman, 1988)

For fluid flow through rock an empirical law has been developed that relates permeability  $k$ , to porosity  $\phi$ . This equation, known as the Kozeny Equation, is written as

$$k = c \frac{\phi^3}{S_o^2} \quad (2.2)$$

where  $S_o$  is the specific surface area of the rock and  $c$  ( $=0.2$ ) is an empirical constant (Wong, et al., 1984).

The Kozeny-Carman equation relates more specific pore size parameters to permeability. Derivation of this equation is thus critical to our understanding of permeability. Consider a section of rock (fig 2.1), where a fluid flows through a conduit. The flow velocity in the direction of  $l$  is governed by Poiseuille's Law:

$$v_l = - \left( \frac{m^2}{b\mu} \right) \left( \frac{dP}{dl} \right) \quad (2.3)$$

where

- $m$  : hydraulic radius (ratio of the conduit volume to wetted perimeter)
- $b$  : constant dependent on pore shape
- $\mu$  : fluid viscosity
- $dP/dl$  : pressure gradient along the conduit axis

A tortuosity coefficient  $\tau$ , may now be introduced where  $\tau = dl/dx$ . The pressure gradient may now be expressed in the direction of  $x$  as,

$$\frac{dP}{dx} = (\tau) \left( \frac{dP}{dl} \right) \quad (2.4)$$

Figure 2.1: A representative sample of rock with length  $X$ , containing a fracture conduit of length  $l$ . Where  $n$  is a measure of the spacing between conduits,  $d$  is the width of the conduit,  $A_x$  is the cross sectional area of the conduit normal to the sample length  $X$ , and  $A_l$  is the cross sectional area normal to the conduit length  $l$ .

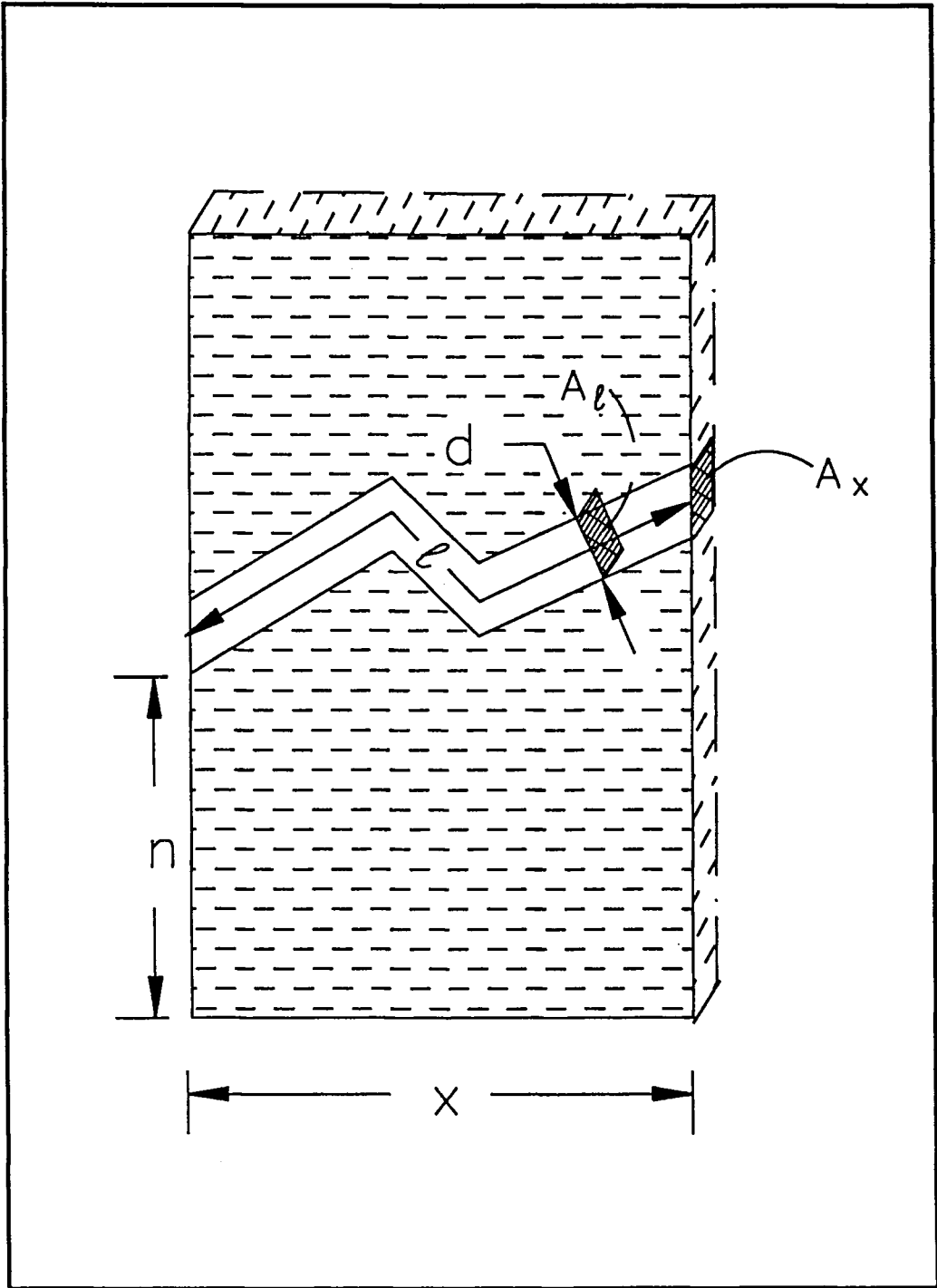


Fig. 2.1

The total flow through the conduit is,

$$q = v_l A_l \quad (2.5)$$

Where  $A_l$  is the cross sectional area of conduit normal to flow direction.

The permeability of the rock section (fig. 2.1) with cross sectional area  $A$  is defined as:

$$k = (q/A) \frac{\mu}{(dP/dx)} \quad (2.6)$$

Combining equations 2.3, 2.4, and 2.5 into equation 2.6 yields

$$k = \left(\frac{m^2}{b}\right) \left(\frac{A_l}{A}\right) \left(\frac{1}{\tau}\right) \quad (2.7)$$

Note that  $A_l = A_x / \tau$ , where  $A_x$  is the conduit area in a plane normal to the sample axis  $x$ .

The porosity  $\phi$  of a sample with isotropically distributed pores is then  $\phi = A_x/A$ .

Thus Equation 2.7 becomes

$$k = \frac{m^2 \phi}{b \tau^2} \quad (2.8)$$

(Walsh and Brace, 1984).

Porosity of more than one conduit can be expressed as  $\phi = \tau n d$ .

Where  $n$  is the conduit density and  $d$  is the aperture width. This expression for porosity may be substituted into equation 2.8. The hydraulic radius  $m$ , as used in equation 2.3, is equivalent to  $d/2$ , for a unit wetted area  $2d^2$ , and volume  $d^3$  (see fig. 2.1). For crack-like pores Walsh and Brace (1984) use a value of  $b = 3$ . Substitution in equation 2.8 yields:

$$k = \frac{n d^3}{12 \tau} \quad (2.9)$$

(Katsube and Hume, 1987).

Expressions like equation (2.9) are often referred to as the "Cubic Law" for flow in a fracture. This equation was originally derived for an open fracture with smooth and parallel planer surfaces, for which  $\tau = 1$ . In equation (2.9)  $\tau$  is a variable of  $x$ . Usually fracture surfaces are rough and have some degree of contact. The validity of the Cubic Law, where fracture surfaces have some degree of contact and fracture widths are decreased under stress, was investigated by Witherspoon, et al. (1980), on rock samples of basalt, granite and marble. For all three rock types the law was found to be valid for rough surfaces with fracture widths that were changed under stress. Permeability was uniquely defined by fracture aperture and found to be independent of the stress history. Deviations from the ideal parallel plate model were accounted for by a roughness coefficient  $f$ , ranging from 1.04 to 1.65, yielding the relation:

$$k = \frac{nd^3}{12f} \quad (2.10)$$

Thus, the aperture width  $d$  influences more effectively  $k$  than the roughness coefficient  $f$ .

Tortuosity of a sample is for all practical purposes impossible to measure. It is therefor desirable to expand the theory to define relationships between  $k$  and the more easily measured electrical resistivity.

### 2.3 Relation of fluid flow to electrical flow

Many attempts to study flow through a fracture network have involved models based on electrical analogs (Greenberg and Brace, 1969; Kiraly, 1971; Shankland and Waff, 1974). The ratio of bulk resistivity of the rock to resistivity of the pore fluid is called the formation factor,  $F$  (Archie, 1942).

The empirical equation which relates  $F$  to porosity in sedimentary rocks, is known as Archie's Law:

$$F = a \cdot \phi^{-m} \quad (2.11)$$

where

$F$  : Formation factor  
 $a, m$  : Material constants

Based on the results of the previous section (eqs. 2.2, 2.8), permeability of fractured rock may be estimated if porosity is known. Since surface resistivity surveys lead to a value of a bulk layer resistivity, a value for the formation factor can be obtained when the pore water resistivity is known (Barker and Griffiths, 1981). The pore water resistivity  $\rho_w$  is the inverse of the specific conductance, and is an easily measured ground water parameter.

Most rock forming minerals are electrical insulators and also impermeable to fluids. Thus the electrical current flows through the same conduits as the fluids, and the bulk resistance is a function of the path length, size and number of the conduits. Hence an expression for the formation factor can be derived using the same model shown in fig (2.1).

When all current is carried by the pore fluid, bulk resistivity is defined as  $\rho_{\text{bulk}} = \rho_w l/A_p$ . For a sample of unit length  $l=1$ , the effective conduit length is  $\tau$ . The total width of the conduits, and thus for a unit depth  $A_p$ , equals  $nd$ . Noting that the resistivity is independent of the current,  $\rho_{\text{bulk}} = \rho_w \tau/nd$ . Therefore,

$$F = \frac{\tau}{nd} \quad (2.12)$$

Referring back to equation (2.9), it can be seen that both formation factor,  $F$ , and permeability,  $k$ , are functions of  $n, d$ , and  $\tau$ , hence  $k \propto F^{-r}$ . Katsube and Hume (1987) suggested the relation:

$$k = \alpha F^{-r} \quad (2.13)$$

Walsh and Brace (1984) have confirmed the validity of this relationship for granitic rocks and report that  $r$  values must be between 1.0 and 3.0. Similar results have been found for samples from Atikokan, Ontario and the Whiteshell Nuclear Research Facility, Pinawa, Manitoba. Katsube and Hume (1987), report two values for  $r$ , 2.22 and 1.96, which fall within this range.

The previous equations containing the formation factor are based on a non-conducting matrix. If the matrix is a conductor with a resistivity,  $\rho_m$ , then it also contributes to the electrical flow. For any number of materials in parallel, the reciprocal of the total resistivity equals the sum of the reciprocal of the individual resistivities. Hence,

$$\frac{1}{\rho_b} = \frac{1}{\rho_{pore}} + \frac{1}{\rho_m} \quad (2.14)$$

thus,

$$\frac{1}{F_a} = \frac{1}{F_i} + \frac{\rho_w}{\rho_m} \quad (2.15)$$

where  $F_a = \rho_b / \rho_w$ , is the apparent formation factor and  $F_i = \rho_{pore} / \rho_w$ , is the intrinsic formation factor. Note:  $\rho_{pore} = \rho_b$  for a non-conducting matrix. Thus the intrinsic formation factor can be calculated by solving equation 2.15 and substituted into equations 2.11 and 2.13.

Still unaccounted for in these models is the "pocket porosity", which is the non-connected "dead end" porosity. However, this pore space is insignificant to the flow of fluids and electrical current (Norton and Knapp, 1977). To accurately relate pore characteristics to resistivity would require a means to distinguish effective porosity from "pocket porosity". Johnson and others (1986) introduced a new geometric parameter which is an intrinsic measure of interconnected pore size and is directly related to transport. This parameter  $\Lambda$ , with the dimensions of length, may provide the long sought link between electrical resistivity and permeability to flow of a viscous fluid.

$$\frac{2}{\Lambda} = \frac{\int |\nabla \psi_0(r)|^2 dS}{\int |\nabla \psi_0(r)|^2 dV_p} \quad (2.16)$$

where

$\psi_0(r)$	:	Microscopic potential for uniform pore fluid conductivity
$S$	:	Surface area of pore space
$V_p$	:	Specific pore volume
$r$	:	$(x^2+y^2+z^2)^{1/2}$
$\nabla$	:	Laplacian $(\partial^2/\partial x^2 + \partial^2/\partial y^2 + \partial^2/\partial z^2)$

If  $\nabla \psi_0(r)$  is constant, independent of  $r$ , then

$$\frac{2}{\Lambda} \propto \frac{\int dS}{\int dV_p} = \frac{\text{surface area of pore space}}{\text{pore volume}}$$

$2/\Lambda$ , is an effective surface to pore volume ratio, analogous to hydraulic radius, where each area-volume is weighted according to  $\nabla \psi_0(r)$ , dependent on location. This weighting may eliminate contributions from those isolated pores.



Using this new pore parameter an expression for the effective conductivity of a porous medium, with a saturating fluid of conductance,  $\sigma_f$ , has been derived.

$$\sigma_{eff} = \frac{1}{F} \{ \sigma_f + 2\Sigma_s/\Lambda \} \quad (2.17)$$

where  $\Sigma_s$  is the interfacial conductivity.

Another problem that needs to be addressed when considering the relationship of dc current and hydraulic permeabilities is that of a matrix containing clay. Increased alteration, such as chloritization, kaolinitization and serpentinization increases the surface conduction. The effect of disseminated clays on rock resistivity becomes increasingly important as the pore water conductance decreases. The contribution of the clay minerals to the surface conductivity is independent of the nature of the ionic solution, except for low ionic concentrations (Ward and Fraser, 1967). To examine how clay affects the conductivity we must consider the double layer theory. Dry clay minerals usually contain charged impurities which are balanced by counter ions bound to the surfaces. However, once the pores are saturated, the hydrated counter ions become mobile within a layer of thickness  $h$ . Depending on the salinity of the pore water, the thickness of this layer is typically less than 40 Å around the clay particle. Since the typical pore sizes are greater than 1000 Å, the conductivity can be written as

$$\sigma_{eff} = \frac{1}{F} \{ \sigma_f + B Q_v \} \quad (2.18)$$

where  $Q_v$  : density of counter ions per unit pore volume  
 $B$  : equivalent conduction per ion

if  $2/\Lambda$  replaces  $S/V_p$  then this equation is identical to equation 2.16, because  $Q_v = n_s(S/V_p)$  where  $n_s$  is the surface charge density of the clay mineral and  $\Sigma_s = n_s B$  (Johnson et al., 1986).

Finally, the problems that develop when pores approach 40 Å must be discussed. It was mentioned above that the effects of clay particles are not explained by the equations for small pores and low fluid conductivities. Some interesting membrane effects can occur in rocks containing a few percent of clays. If the thickness  $h$ , of the hydrated cations in the double layer, is large compared to the pore width, the "cloud" of cations can partially block ionic solution paths (Ward and Fraser, 1967). On application of an electrical potential, positive charge carriers easily pass through the cationic cloud but negative charge carriers, with larger ionic radii, are blocked and accumulate (Bear, 1972). Because of this, a surplus of both cations and anions occurs at one end of the membrane zone, while a deficiency occurs at the other end. This is because the number of positive charges can not deviate significantly from the number of negative charges at any one point in space due to the large electric fields which would then result. These ion concentration gradients oppose the flow of the current, since the mobility of the anions is reduced (Ward and Fraser, 1967).

The preceding theory suggests that a relationship exists for which a range of predicted permeabilities may be estimated from resistivity measurements. However, it will be difficult to verify permeabilities that are estimated from electrical resistivity measurements. Different methods of measuring permeability do not reproduce the same value. Laboratory tests on samples, drawdown curves in test wells and packer tests affect different quantities of the subsurface environment. Neuzil (1986), for instance, states that insitu tests in low-permeable aquifers produce estimates that are restricted to the immediate vicinity of the well.

### 3. METHODOLOGY

#### 3.1 Geoelectrical methods

In making a geoelectrical survey a direct current is introduced into the ground through two electrodes, A and B. The potential difference is measured between a second pair of electrodes, M and N (fig. 3.1b). Values of the apparent resistivity are calculated using the following equation.

$$\rho_a = K \frac{\Delta V}{I} \quad (3.1)$$

where  $\Delta V$  : voltage between the potential electrodes  
 $I$  : current input  
 $K$  : geometric factor

$$K = \frac{2\pi}{\frac{1}{AM} - \frac{1}{BM} - \frac{1}{AN} + \frac{1}{BN}} \quad (3.2)$$

where  $AM, AN, BM, BN$  : Distances between electrodes (see fig. 3.1)

If the measurement is made over a homogeneous isotropic material of infinite depth then  $\rho_a$  is the true resistivity. For an inhomogeneous substratum the value of the apparent resistivity depends on the electrode spacings and the distribution of true resistivities in the subsurface. Standard symmetrical electrode arrays have been developed for which geoelectrical depth soundings depend on only two distance variables. A geoelectrical depth sounding is most useful over a horizontally layer substratum in which the resistivity changes mainly with depth.

Figure 3.1a: Schlumberger depth sounding array. The current electrodes A and B are separated by the distance  $L$ , and the potential electrode M and N are separated by the distance  $b$ .

Figure 3.1b: Generalized four electrode array where the distances  $r$ , are the distances between the electrodes of the subscripts.

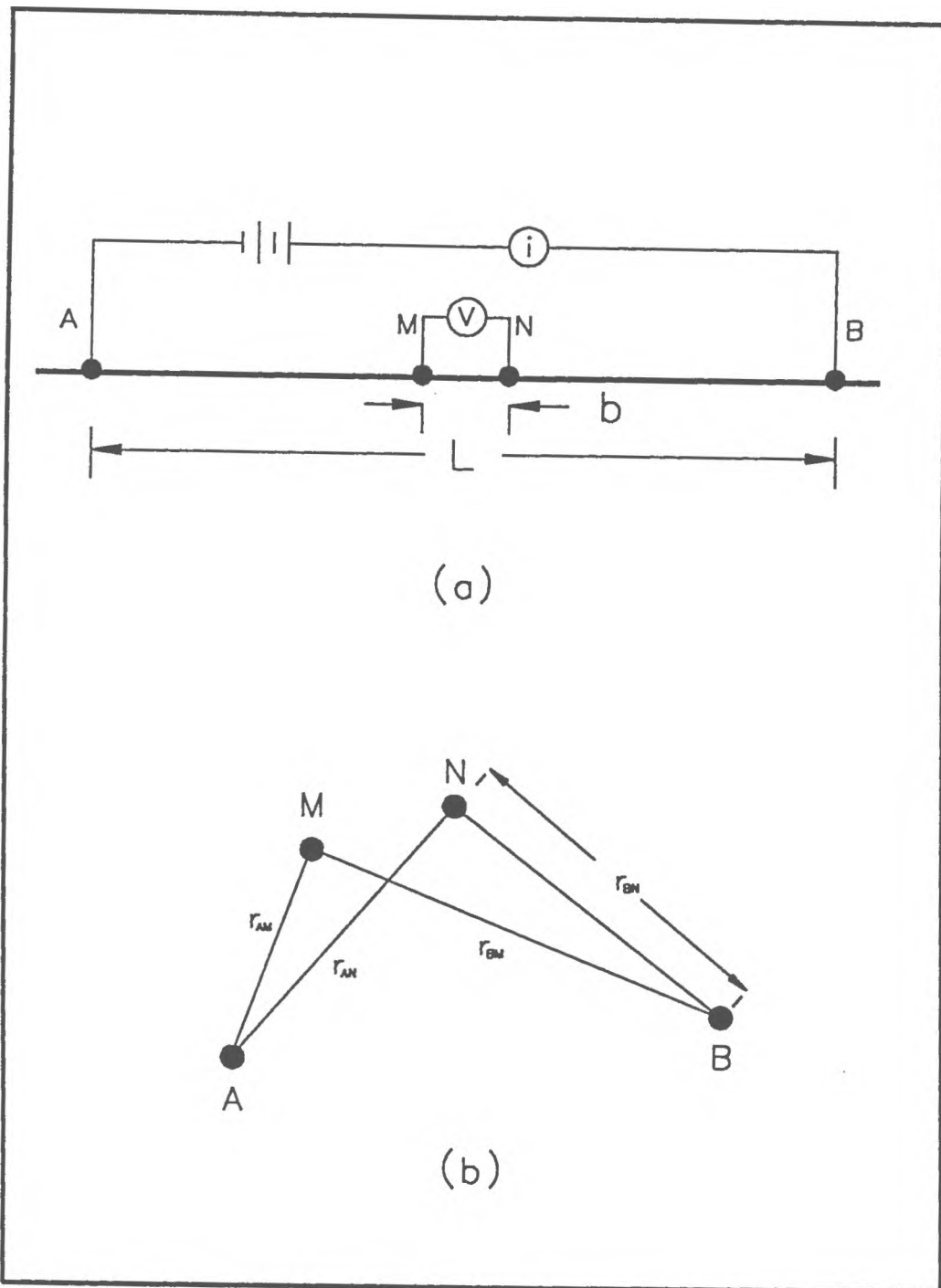


Fig. 3.1

### 3.1.1 Depth Soundings

Geoelectrical depth soundings were performed with the Schlumberger method. This array is characterized by the four electrodes being placed in a straight line with the potential measuring distance  $b$ , kept constant and small relative to the distance,  $L$  of the current electrodes (fig. 3.1a). The sounding proceeds by forcing the current into greater depth with an increase of spacing  $L$ . The spacing in this case,  $b=2$  ft, is kept constant until at large current electrode spacing, the potential becomes too small to measure. Because of the decreasing voltage across  $b=2$  ft, the potential spacing was increased to  $b=8$  ft. Measurements are taken at both forward and reverse current polarity to prevent corrosion of the electrodes. The apparent resistivity is plotted versus  $L/2$  on a bi-logarithmic plot.

### 3.1.2 Mapping of resistivities

The apparent resistivity is influenced by lateral as well as vertical changes of resistivity. Lateral changes of resistivity within a layer may have a variety of causes related to either lithologic or pore water conditions. Changes in the apparent resistivity may indicate porosity or permeability changes, clay (low) or sand (high) lenses, or the spreading of a pollution plume. The advantages gained by being able to map such features with a surface geophysical technique are obvious. Most of the papers found in the literature related to the Wenner electrode array used for profiling, where the entire electrode array was moved along a profile (Klefstad et al, 1975; Fink and Aulenbach, 1974; Merkel, 1972; Seitz et al, 1972; Hackbarth, 1971; Hemud, 1971; Warner, 1971; Cartwright and McComas, 1968). These papers had mixed conclusions on the ability of the method. The most frequently mentioned problems were the lack of geologic control and the inherent problem of nonuniqueness.

The Wenner array with its larger potential measuring distance,  $AM = MN = NB$ , is subject to more noise. Stray currents, either industrial or telluric, affect measurements made with a Wenner array to a greater degree than measurements made with a Schlumberger array. The Wenner array is more subject to near surface inhomogeneities. Moving of the potential electrodes increases the time required to make the measurement. Further it is the belief of the author that the moving of the current electrode presents problems by creating a new current distribution in the subsurface at every measurement. If the current distribution is kept constant then any change in the apparent resistivity will be a result of changes below the potential measuring position and not new lateral effects encountered when the array is shifted.

Geoelectrical profiling was accomplished using the Schlumberger AB profiling method. This technique uses the same equipment and basically the same array as for the depth sounding. While the current electrode spacing is held constant, the potential electrodes are moved off center along the baseline, while the spacing  $b$ , is kept constant (see fig. 3.2b).

The AB rectangle method deviates from the profiling technique only in that the potential electrode "stations" are also moved off the baseline forming an array of measurements (see fig. 3.2a). These two techniques are used to measure lateral changes in the apparent resistivity, as opposed to the vertical layers modeled in the depth sounding method. This allows for the mapping of lateral subsurface influences on the electrical resistivity such as fracture zones and pollution plumes.

Kunetz (1966) pointed out a disadvantage with this method of mapping in that the depth penetration varies if the potential electrodes are moved off center. This problem will be addressed in section 3.2.

Figure 3.2a: AB rectangle electrode configuration showing the typical dimensions of the potential measuring array.

Figure 3.2b: Schlumberger profile configuration showing the similarity to the AB rectangle configuration.



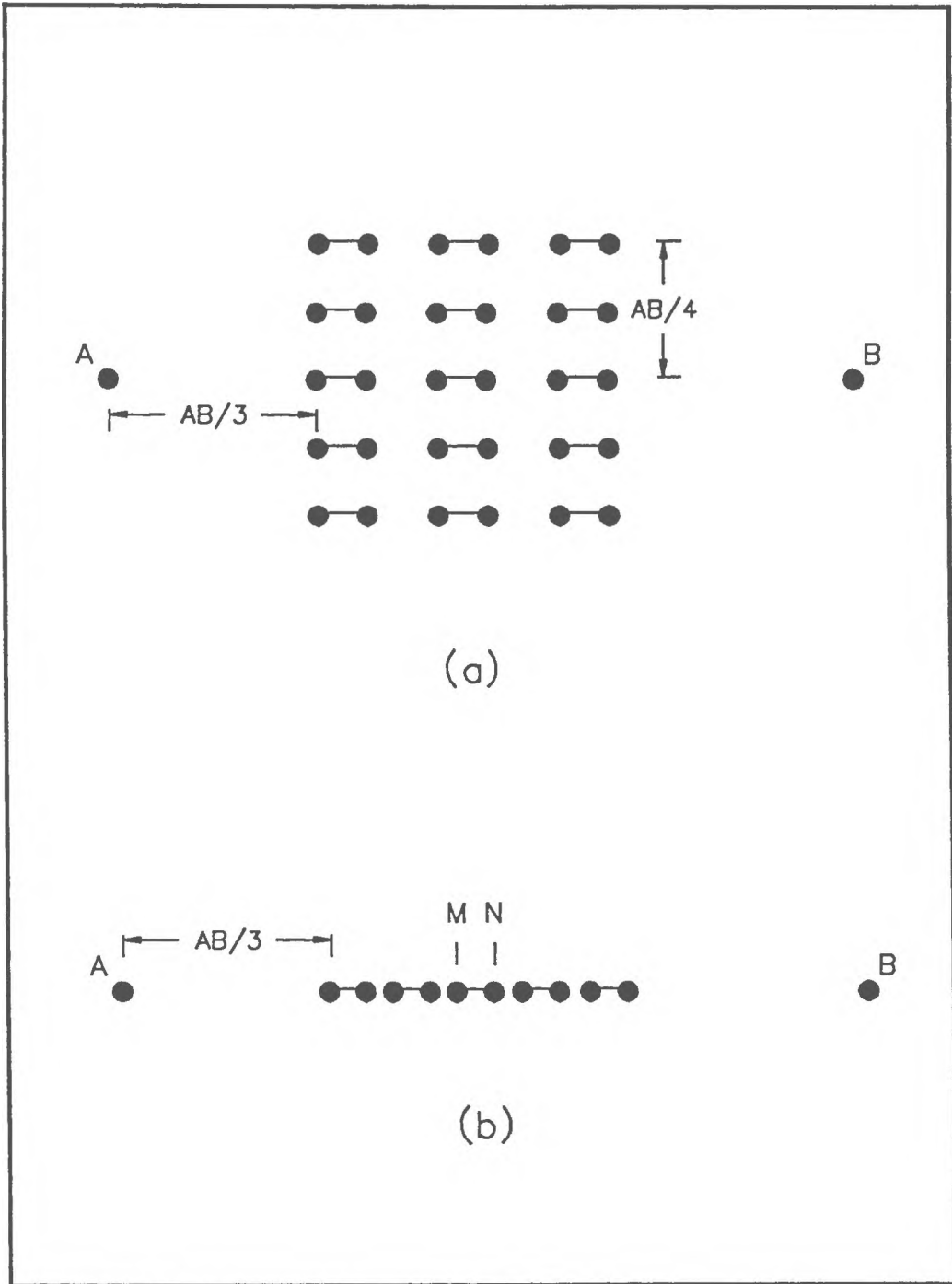


Fig. 3.2

### 3.1.3 Instrumentation

The materials used are two metal current electrodes and two porous-pot non-polarizable potential electrodes. A current is created using two 12 volt batteries wired in series to run a d.c. inverter with an output of 250 volts. This produces a maximum current of about 0.1 amp which is measured using a Sampson model 260 Multitester, and put into the ground through the current electrodes. The potential between the potential electrodes is measured using a Hewlett Packard 3468A Multimeter. In the dry season it is necessary to wet the current electrodes to insure good contact with the ground.

## 3.2 Interpretation Methods

### 3.2.1 Schlumberger depth sounding

The purpose of interpreting the Schlumberger depth sounding curve is to find the resistivity-depth function assuming a horizontally layered substratum. Curves are interpreted in two steps: First the approximate resistivity-depth sequence is found by partial curve matching with two layer master curves and a set of auxiliary curves (Keller and Frischknecht, 1976). Second this starter model is refined by use of an indirect multilayer model program. Refinements are made by comparing the field curve to a multilayer model curve calculated by a computer program (Koefoed, 1979). Model and field curves are compared for optimal fit using standard deviation and goodness of fit statistics. The procedure ends when optimal values for these statistics have been reached. This method of interpretation is known as the indirect interpretation method. Indirect interpretation takes considerably longer than direct methods but offers the advantage of user interaction, which also offers an insight into the layer response.

### 3.2.2 Profiling and AB rectangle

The purpose of interpreting the profiling and AB rectangle data is to map lateral variations in resistivity within a certain depth range. Lateral changes of resistivity are mapped out within a rectangle at constant current electrode separations (see fig. 3.2). However, the depth of investigation changes as the position of the potential electrodes changes relative to the current electrodes. Therefore, a change in the apparent resistivity measured is also a function of the change in the true resistivity with depth. To obtain a value which relates solely to the lateral change requires that the vertical change be estimated separately.

Conventional methods were not found in the literature which show the lateral change of the apparent resistivity over a horizontally layered substratum. However, O'Neill and Merrick (1984), presented the theory for the calculation of apparent resistivities, given a model of horizontal layers, for any four electrode array (fig. 3.1b). It was then possible to write a computer program based on this theory which would calculate expected resistivities for both the profiling and rectangle arrays. The model for a horizontal layer case is derived from a Schlumberger depth sounding.

### 3.2.3 The theory of the electrical potential over a horizontally layered substratum.

The electrical potential,  $V$ , caused by a direct current point source satisfies the differential equation of Laplace:

$$\frac{\partial^2 V}{\partial x^2} + \frac{\partial^2 V}{\partial y^2} + \frac{\partial^2 V}{\partial z^2} = 0 \quad (3.3)$$

The rotational symmetry about the vertical axis through the current source suggests the use of cylindrical coordinates.

The Laplacian differential equation is then written:

$$\frac{\partial^2 V}{\partial r^2} + \frac{1}{r} \frac{\partial V}{\partial r} + \frac{\partial^2 V}{\partial z^2} + \frac{1}{r^2} \frac{\partial^2 V}{\partial \theta^2} = 0 \quad (3.4)$$

Because of axial symmetry the potential is independent of  $\theta$ , hence,

$$\frac{\partial^2 V}{\partial \theta^2} = 0 \quad (3.5)$$

This simplifies eqn. 3.4 to,

$$\frac{\partial^2 V}{\partial r^2} + \frac{1}{r} \frac{\partial V}{\partial r} + \frac{\partial^2 V}{\partial z^2} = 0 \quad (3.6)$$

The partial differential equation 3.6 is solved by finding particular solutions. Solutions of equation 3.6 are obtained by separation of variables  $r$  and  $z$  in the form:

$$V(r, z) = U(r)W(z) \quad (3.7)$$

meaning that solutions are a product of two functions, one dependent on  $r$ , the other on  $z$  only. Thus, the partial differential equation 3.6 can be separated into two ordinary differential equations of the same order.

Substituting eq. 3.7 into eq. 3.6 and dividing all terms by  $U W$  yields,

$$\frac{1}{U} \frac{d^2 U}{dr^2} + \frac{1}{Ur} \frac{dU}{dr} + \frac{1}{W} \frac{d^2 W}{dz^2} = 0 \quad (3.8)$$

This equation is satisfied if,

$$\frac{1}{U} \frac{d^2 U}{dr^2} + \frac{1}{Ur} \frac{dU}{dr} = -\lambda^2 \quad (3.9)$$

and

$$\frac{1}{W} \frac{d^2 W}{dz^2} = \lambda^2 \quad (3.10)$$

where  $\lambda$  is an arbitrary real constant.

The solutions to eq. 3.10 are well known as:

$$W_1(z) = C e^{-\lambda z} \text{ and } W_2(z) = C e^{\lambda z} \quad (3.11)$$

Differential equations of the type of eq. 3.9 have lead to the development of the theory of Bessel functions. In this case, the solution of eq. 3.9 can be written as,

$$U = C J_0(\lambda r) \quad (3.12)$$

where  $J_0$  is the Bessel function of order zero.

Combining eqs. 3.11 and 3.12, we obtain as particular solutions of the differential equation (eq. 3.6)

$$V = C e^{-\lambda z} J_0(\lambda r) \text{ and } V = C e^{\lambda z} J_0(\lambda r) \quad (3.13)$$

where  $C$  and  $\lambda$  are arbitrary constants.

Since any linear combination of solutions leads to a general solution of the differential equation,  $\lambda$  extends from zero to infinity by allowing  $C$  to vary in dependence of  $\lambda$  as:

$$V = \int_0^{\infty} [\Phi(\lambda) e^{-\lambda z} + \Psi(\lambda) e^{+\lambda z}] J_0(\lambda r) d\lambda \quad (3.14)$$

In this equation both  $\Phi(\lambda)$  and  $\Psi(\lambda)$  are different functions of  $\lambda$ .

In order to proceed further it is convenient to write eq. 3.14 in a form which contains a separate term for the potential that is generated by the single point source of intensity  $I$ , located at the surface of the earth. This potential is,

$$V = \frac{\rho_1 I}{2\pi\sqrt{r^2 + z^2}} \quad (3.15)$$

where  $\rho_1$  is the resistivity of the surface layer and  $I$  the current. Eq. 3.14 can then be written in the form of eq. 3.15 using the Lipschitz integral,

$$\frac{1}{\sqrt{r^2 + z^2}} = \int_0^\infty e^{-\lambda z} J_0(\lambda r) d\lambda \quad (3.16)$$

yielding

$$V = \frac{\rho_1 I}{2\pi} \int_0^\infty e^{-\lambda z} J_0(\lambda r) d\lambda \quad (3.17)$$

Thus, the general solution of the differential equation is,

$$V = \frac{\rho_1 I}{2\pi} \int_0^\infty [e^{-\lambda z} + \Theta(\lambda)e^{-\lambda z} + X(\lambda)e^{\lambda z}] J_0(\lambda r) d\lambda \quad (3.18)$$

Where  $\Theta(\lambda)$  and  $X(\lambda)$  are arbitrary functions of  $\lambda$ . Each layer from 1 to  $n$  has a separate solution of the form given in eq. 3.18 which is for the  $i^{\text{th}}$  layer:

$$V_i = \frac{\rho_1 I}{2\pi} \int_0^\infty [e^{-\lambda z} + \Theta_i(\lambda)e^{-\lambda z} + X_i(\lambda)e^{\lambda z}] J_0(\lambda r) d\lambda \quad (3.19)$$

The functions  $\Theta(\lambda)$  and  $X(\lambda)$  are determined by the boundary conditions:

- (1) Continuity of the electrical potential across boundaries.
- (2) Continuity of the vertical component of the current density across boundaries.
- (3) Since the resistivity of the air is infinitely high, at the surface the vertical component of the current density is zero, because of (2).
- (4) The potential must decrease with increasing  $z$  in the  $n^{\text{th}}$  layer.

The first boundary condition applied to layer  $i$  and  $i+1$  implies:

$$\begin{aligned} \int_0^{\infty} [e^{-\lambda h_i} + \Theta_i(\lambda)e^{-\lambda h_i} + X_i(\lambda)e^{+\lambda h_i}]J_0(\lambda r)d\lambda \\ = \int_0^{\infty} [e^{-\lambda h_i} + \Theta_{i+1}(\lambda)e^{-\lambda h_i} + X_{i+1}(\lambda)e^{+\lambda h_i}]J_0(\lambda r)d\lambda \end{aligned}$$

This equation can only be satisfied for all values of  $r$  if the integrands on both sides of the equation are equal, yielding,

$$\Theta_i(\lambda)e^{-\lambda h_i} + X_i(\lambda)e^{+\lambda h_i} = \Theta_{i+1}(\lambda)e^{-\lambda h_i} + X_{i+1}(\lambda)e^{+\lambda h_i} \quad (3.20)$$

Satisfying condition (2) the vertical component of the current density is equal to the derivative of the potential with respect to  $z$  divided by the resistivity of the layer under consideration. From equation (3.19) we obtain,

$$\begin{aligned} \frac{1}{\rho_i} \int_0^{\infty} [\{1 + \Theta_i(\lambda)\}e^{-\lambda h_i} - X_i(\lambda)e^{+\lambda h_i}]J_0(\lambda r)\lambda d\lambda \\ = \frac{1}{\rho_{i+1}} \int_0^{\infty} [\{1 + \Theta_{i+1}(\lambda)\}e^{-\lambda h_i} - X_{i+1}(\lambda)e^{+\lambda h_i}]J_0(\lambda r)\lambda d\lambda \end{aligned}$$

Again, this equation can only be satisfied for all values of  $r$  if the integrands on both sides of the equation are equal, yielding,

$$\frac{1}{\rho_i} [\{1 + \Theta_i(\lambda)\}e^{-\lambda h_i} - X_i(\lambda)e^{+\lambda h_i}] = \frac{1}{\rho_{i+1}} [\{1 + \Theta_{i+1}(\lambda)\}e^{-\lambda h_i} - X_{i+1}(\lambda)e^{+\lambda h_i}] \quad (3.21)$$

To satisfy condition (3) we differentiate the expression for the potential in the first layer (eq. 3.19) with respect to  $z$  and then set  $z = 0$  to obtain the following equation,

$$\int_0^{\infty} [-1 - \Theta_1(\lambda) + X_1(\lambda)]J_0(\lambda r)\lambda d\lambda = 0 \quad (3.22)$$

The first term in the integrand defines the field in a homogeneous earth. This primary field automatically satisfies the boundary condition. However, the last two terms of the integrand together define the effect of the boundaries. The vertical component of the perturbing fields must be zero at all values of  $r$ , including the point at which the current source is located. This can only occur if,

$$\Theta(\lambda) = X(\lambda) \quad (3.23)$$

Condition (4) requires that in the deepest layer,  $n$ , the function  $\chi$  must be zero, otherwise the factor  $e^{+\lambda z}$  would increase the potential at increasing  $z$ . Thus,

$$X_n(\lambda) = 0 \quad (3.24)$$

This set of equations are simultaneously solved to obtain  $\Theta_1(\lambda)$ .

It is desirable to look at another function  $K_1(\lambda)$ ;

$$K_1(\lambda) = 1 + 2\Theta_1(\lambda) \quad (3.25)$$

so that the expression for the potential becomes,

$$V_1 = \frac{\rho_1 I}{2\pi} \int_0^\infty K_1(\lambda) J_0(\lambda r) d\lambda \quad (3.26)$$

where  $K_1(\lambda)$  is known as the kernel function. Koefoed (1979) introduced another function, the resistivity transform,  $T_1(\lambda)$ , where,

$$T_1 = \rho_1 K_1$$

thus yielding,

$$V_1(r) = \frac{I}{2\pi} \int_0^\infty T_1(\lambda) J_0(\lambda r) d\lambda \quad (3.27)$$



This resistivity transform is a function of the layer parameters only. Ghosh (1971a) showed that the relationship between the apparent resistivity function  $\rho_a(x)$  and the resistivity transform  $T(y)$  is linear in nature. Thus it is possible to derive a set of filter coefficients needed to calculate  $\rho_a$  from  $T$  (Ghosh 1971b).

Kunetz (1966) first noticed the possibility of applying the method of digital linear filtering for the resistivity sounding interpretation. However, it was Ghosh (1970, 1971a, 1971b) who worked out and improved the method. The method is applicable because of the fact that the resistivity transform and the apparent resistivity functions are linearly related, thus the principle of digital filter theory can be applied to derive the apparent resistivity from the resistivity transform.

The procedure is then to find values of the function  $T$  at a constant interval along the abscissa. The value of the function  $\rho_a$  is then obtained as a linear expression of the function  $T$ . The coefficients of this linear expression are called the filter coefficients. The filter coefficients are values, sampled at a constant interval, of a sinc function ( $\sin x/x$ ), with the origins at each sample point. The amplitude and period of these functions is determined by the sampling interval. Thus, the basic problem is to determine this sampling interval and the coefficients (Ghosh, 1971b). Fortunately filters have been published for the arrays used in this study.

Two Pascal programs have been written using the linear filter method. The first program after Koefoed (1979) for Schlumberger depth soundings and the second program for Schlumberger profiling and A-B rectangle methods.

For the Schlumberger depth sounding the potential difference for a homogeneous earth using a symmetrical linear electrode configuration is,

$$\Delta V = 2 \left( \frac{\rho I}{2\pi} \right) \left[ \frac{1}{s-b} - \frac{1}{s+b} \right] \quad (3.28)$$

where  $s$  is half the current electrode separation,  $b$  is half the potential electrode separation and  $\rho$  is the resistivity of the homogeneous earth. Thus the expression for the apparent resistivity is found by solving for  $\rho$  and using values of  $\Delta V$  and  $I$ , measured in a realistic non-homogeneous case.

$$\rho_a = \left( \frac{\Delta V}{I} \right) 2\pi s \frac{(s^2 - b^2)}{(4bs)} \quad (3.29)$$

For small values of  $b$  the expression  $(s^2 - b^2)/(4bs)$  reduces to  $(s/4b)$ . One finally can show that eq. (3.28) can be written in differential form as:

$$\rho_a = \frac{-2\pi s^2 \partial V}{I \partial s} \quad (3.30)$$

where for  $s = r$ , the expression (3.26) must be substituted for  $V$  yielding,

$$\rho_a(s) = s^2 \int_0^\infty T(\lambda) J_1(\lambda s) \lambda d\lambda \quad (3.31)$$

Equation (3.26) and equation (3.31) are the basic equations solved in the two program.

Both equations may be written as a convolution integral, by making the following substitutions,

$$x = \ln(s)$$

$$x = \ln(r)$$

$$y = -\ln(\lambda)$$

$$y = -\ln(\lambda)$$

Yielding for the Schlumberger:

$$\rho_{aSchl}(x) = \int_{-\infty}^{\infty} T(y)f(x)dy \quad (3.32)$$

and for the potential:

$$V(r) = \frac{I}{2\pi r} \int_{-\infty}^{\infty} T(y)f(x-y)dy \quad (3.33)$$

These are solved by the convolution of the transform function with a filter function of form,

$f(x) = J_1 [exp(x)] exp(2x)$ , For the Schlumberger and,

$f(x-y) = exp(x-y) J_0 [exp(x-y)]$ , For the potential.

This convolution may be expressed in discrete form as (Rijo, et. al., 1977)

$$\rho(y)_{aSchl} \approx \sum_{j=-n_1}^{n_2} T(y - \eta_j) \cdot C(\eta_j) \quad (3.34)$$

for the Schlumberger and,

$$V(r) = \frac{I}{2\pi r} \sum_{j=-n_1}^{n_2} T(\ln r - \eta_j) \cdot C(\eta_j) \quad (3.35)$$

for the potential, where

- $\eta_j$  : filter coefficient abscissae
- $C(\eta_j)$  : digital filter coefficients
- $n_1$  : number of coefficients to the left of filter origin
- $n_2$  : number of coefficients to the right of the filter origin

For the general case for any four-electrode array (see fig. 3.1b)

$$\Delta V = V(r_{1,1}) - V(r_{1,2}) - V(r_{2,1}) + V(r_{2,2}) \quad (3.36)$$

For any measuring point  $i$ ,

$$\Delta V^i = \frac{I}{2\pi} \sum_{j=-n_1}^{n_2} T_{i,j} C_j \quad (3.37)$$

where

$$T_{i,j} = \frac{T(\ln r_{1,1}^i - \eta_j)}{r_{1,1}^i} - \frac{T(\ln r_{1,2}^i - \eta_j)}{r_{1,2}^i} - \frac{T(\ln r_{2,1}^i - \eta_j)}{r_{2,1}^i} + \frac{T(\ln r_{2,2}^i - \eta_j)}{r_{2,2}^i}$$

and

$$C_j = C(\eta_j)$$

For any array the apparent resistivity is given by equation 3.1

$$\rho_a = K \frac{\Delta V}{I}$$

By Combining (3.36) and (3.1), the expression for the apparent resistivity as measured by a generalized four electrode array becomes

$$\rho_a^i = \left[ \frac{1}{r_{1,1}} - \frac{1}{r_{1,2}} - \frac{1}{r_{2,1}} + \frac{1}{r_{2,2}} \right]^{-1} \sum_{j=-n_1}^{n_2} T_{i,j} C_j \quad (3.38)$$

The filter used in the computer program for the Schlumberger array was from Ghosh (1971), published in Koefoed (1979). The filter for the generalized array, (O'Neill and Merrick, 1984) was designed for the sampling rate of six points per decade. This filter was initially tested for the generalized array adopting the standard configuration of the Schlumberger, Wenner, and various bipole-bipole arrays. It was confirmed that this filter was applicable to any four electrode array. The programs written in this study were tested in comparison to master curve tables by Orellana and Mooney (1966) as shown in fig. 3.3. The "rectangle" program was tested using it to simulate a Schlumberger sounding.

Figure 3.3: Comparison check of the computer program vs. master curves of a plot of apparent resistivity vs. half electrode spacing for a typical Schlumberger depth sounding.

### Master Curve Vs. Computer Program

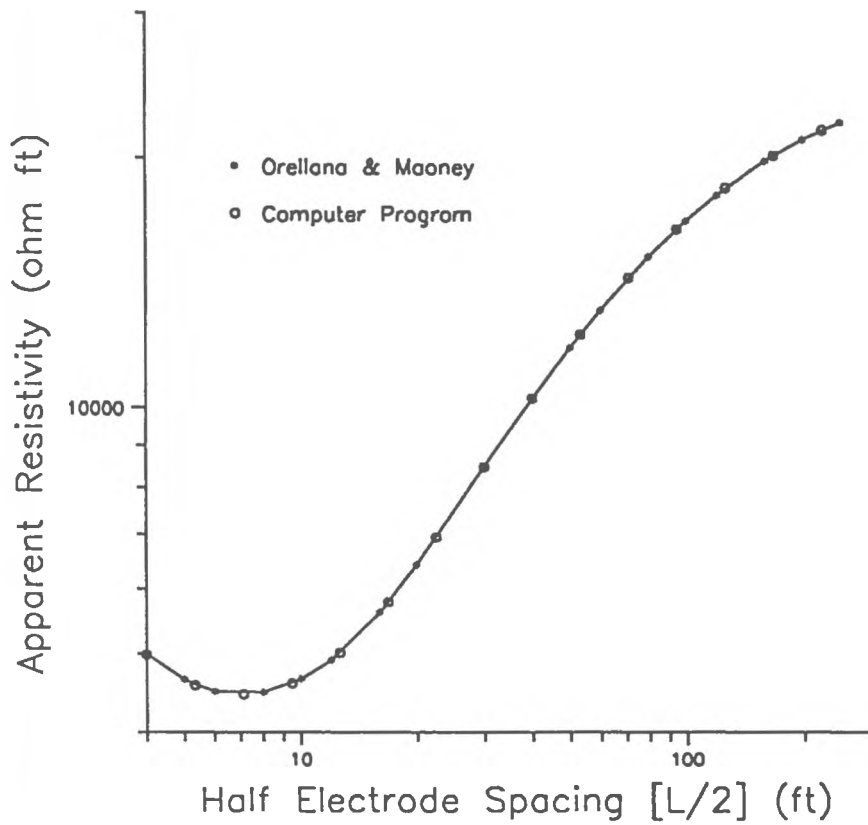


Fig. 3.3

### 3.2.4 Calculation of the apparent resistivity within the AB-rectangle for the horizontally layered case.

For a constant separation of the current electrodes  $L$ , the depth penetration of a resistivity measurement varies, depending on the location of the potential electrodes  $MN$  relative to  $A$  and  $B$  (see fig. 3.2). Moving the potential electrodes  $MN$  towards  $A$  or  $B$  from a center position (as it is used in the Schlumberger sounding), decreases the depth penetration and thus increases the effect of shallower layers on the apparent resistivity. Moving  $MN$  perpendicular to  $AB$  away from the center, increases the depth penetration and thus increases the effect of deeper layers on the apparent resistivity. For any horizontal layer model the change in the apparent resistivity within the rectangle as a function of the location of  $MN$  can be calculated. The horizontal layer model will be established from the interpretation of a Schlumberger depth sounding.

This principle is demonstrated in an example. Fig. 3.4 shows a 3-layer curve with  $\rho_1$ : unsaturated zone (10,000  $\Omega$  ft),  $\rho_2$ : saturated zone (3,200  $\Omega$  ft) and  $\rho_3$ : aquiclude (25,000  $\Omega$  ft). Say, the aquifer ( $\rho_2$ ) is the layer of interest, which causes a relative minimum in the K-type curve ( $\rho_1 > \rho_2 < \rho_3$ ). At an optimal electrode separation of  $L/2 = 20$  ft layer 2 has a maximum influence on the apparent resistivity. If we are interested in the changes of  $\rho_2$  due to pollution of the aquifer (spreading of a plume from a point source), this would be observed with an AB-rectangle at an optimal AB separation of 40 ft ( $L/2 = 20$  ft). Lateral variations due to horizontal layering at varying depth penetrations are shown in fig. 3.5. The contours of constant resistivity are symmetric with respect to the center point of the rectangle. Approaching  $A$  or  $B$  (to the right or left) in fig. 3.5 increases  $\rho_a$  due to the higher resistivity of the upper layer ( $\rho_1$ ). (compare with fig. 3.4) Moving perpendicular away from  $A$  or  $B$  (to the top or bottom of fig. 3.5) will also increase the apparent resistivity due to the higher resistivity of the third layer ( $\rho_3$ ).

Figure 3.4: Plot of apparent resistivity vs. half electrode spacing for the layer model shown. Note the ranges of the apparent resistivities within the AB-rectangles of dimensions 4x10 ft, and 6x15 ft, and how these ranges relate to an apparent shift in the  $L/2$  and therefore the depth penetration.



Ranges of Apparent Resistivities and Equivalent Electrode Spacing for AB Rectangle of given dimension

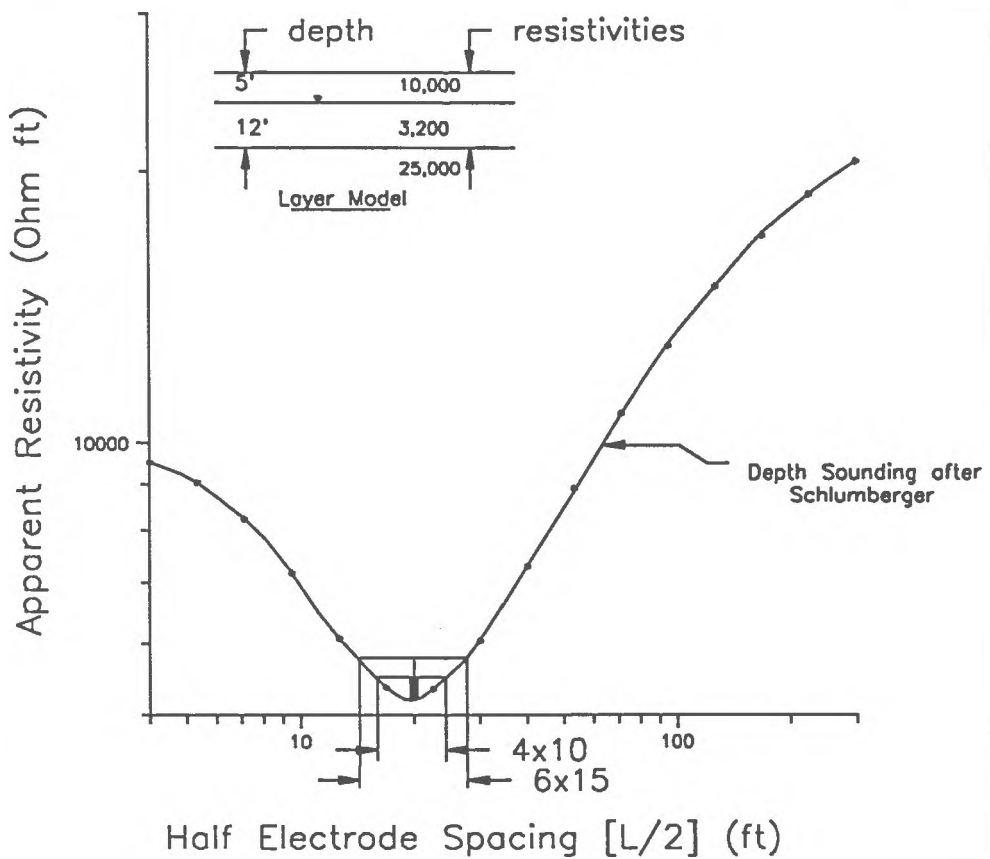


Fig. 3.4

Figure 3.5: Contour plot of the expected resistivities within the 6x15 ft rectangle for the model presented in fig. 3.4. Note the bowl shape caused by the greater effect of the bordering layers of higher resistivity on the edges of the plot.

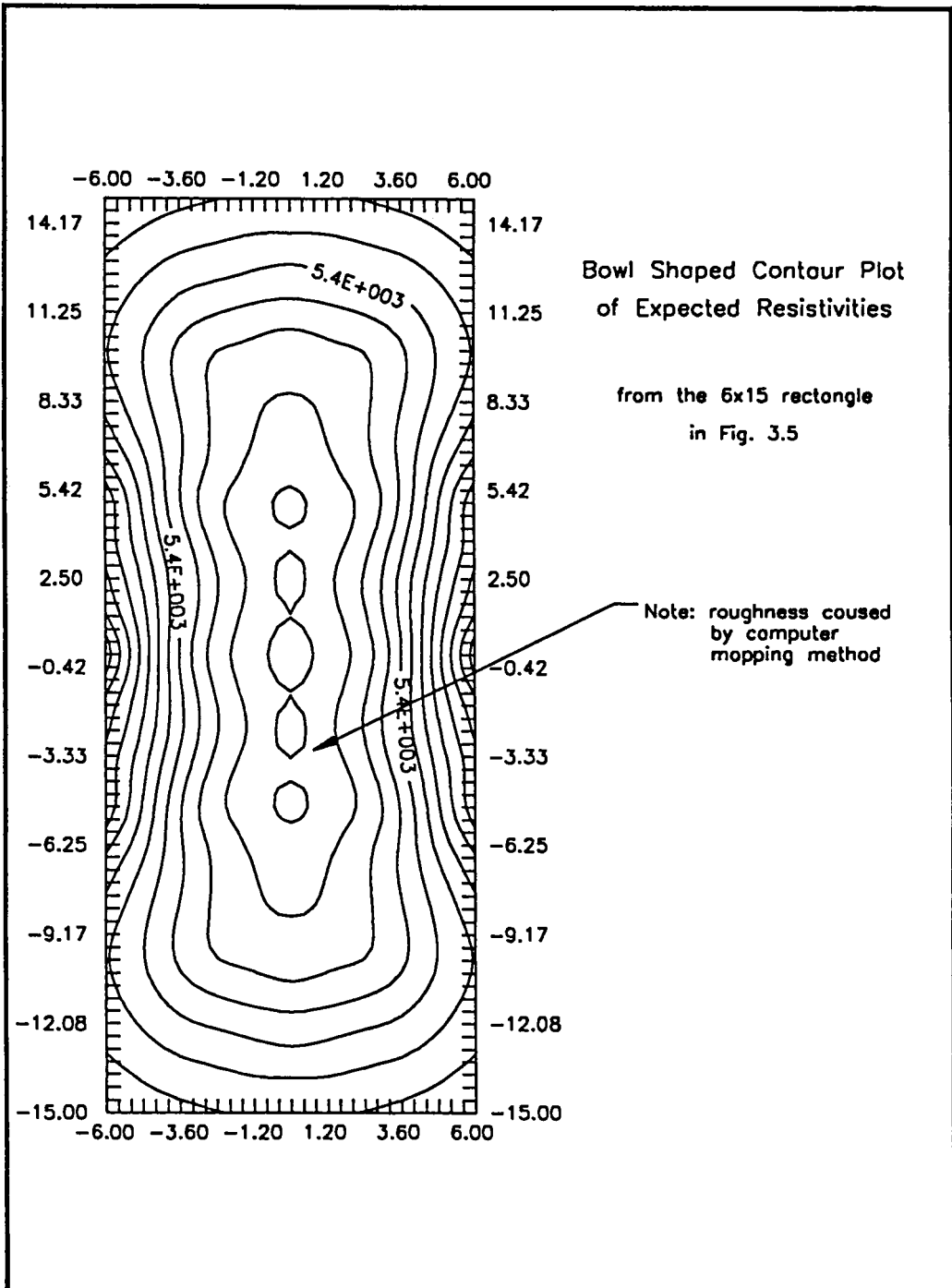


Fig. 3.5

The smaller the rectangle at constant AB, the lesser the effect of  $\rho_1$  and  $\rho_3$  on the apparent resistivity. If the rectangles are too small, however, the method becomes less practical. Selection of the size of the AB-rectangle is a compromise between the number of observations possible for one AB-setup and the admissible influence of the layers above or below the target layer, which in this case is the aquifer. Also, the effect of varying depth penetration is large if the depth sounding curve shows large changes of  $\rho_a$  with respect to  $L/2$ . This is mostly the case with the steeply ascending branch due to highly resistive unfractured bedrock.

The curve in fig. 3.6 is similar to the curve in fig. 3.4. In this case, however, we are interested in lateral resistivity changes in the bedrock. For the AB-rectangle method, therefore, an  $L/2$  of 300 ft was selected. Plotting the expected resistivity values for a rectangle of size 120x200ft on the sounding curve shows the small influence of other layers. A contour map of the expected resistivities for this case was also plotted (fig. 3.7). This map shows a saddle indicating the effect of the slightly higher and lower resistivities about that point on the ascending branch of the sounding curve. In the case approaching A or B (to the right or left) in fig. 3.7  $\rho_a$  decreases due to the lower resistivity of the upper layer ( $\rho_2$ ). (compare with fig. 3.6) Moving perpendicular away from A or B (to the top or bottom of fig. 3.7) will increase the apparent resistivity due to the higher resistivity of the bedrock at depth.

The measurement and the interpretation is conducted in 5 steps:

1. A geoelectrical depth sounding is conducted and interpreted for the derivation of the horizontal layer model.
2. The choices of the optimal distance AB (or L) and the rectangle length and width are made.
3. Calculation of the expected resistivity inside the rectangle due to the horizontal layer case from step 1. or from additional depth soundings.
4. Measurement of the apparent resistivity inside the rectangle.
5. Subtraction of 3. from 4. yielding the residual resistivity due to lateral resistivity changes.

Figure 3.6: Plot of apparent resistivity vs. half electrode spacing for the layer model shown. Note the ranges of the apparent resistivities within the AB-rectangle of dimension 120x200 ft, and how these ranges relate to an apparent shift in the  $L/2$  and therefore the depth penetration.

### Ranges of Apparent Resistivities and Equivalent Electrode Spacing for AB Rectangle in Bedrock Layer

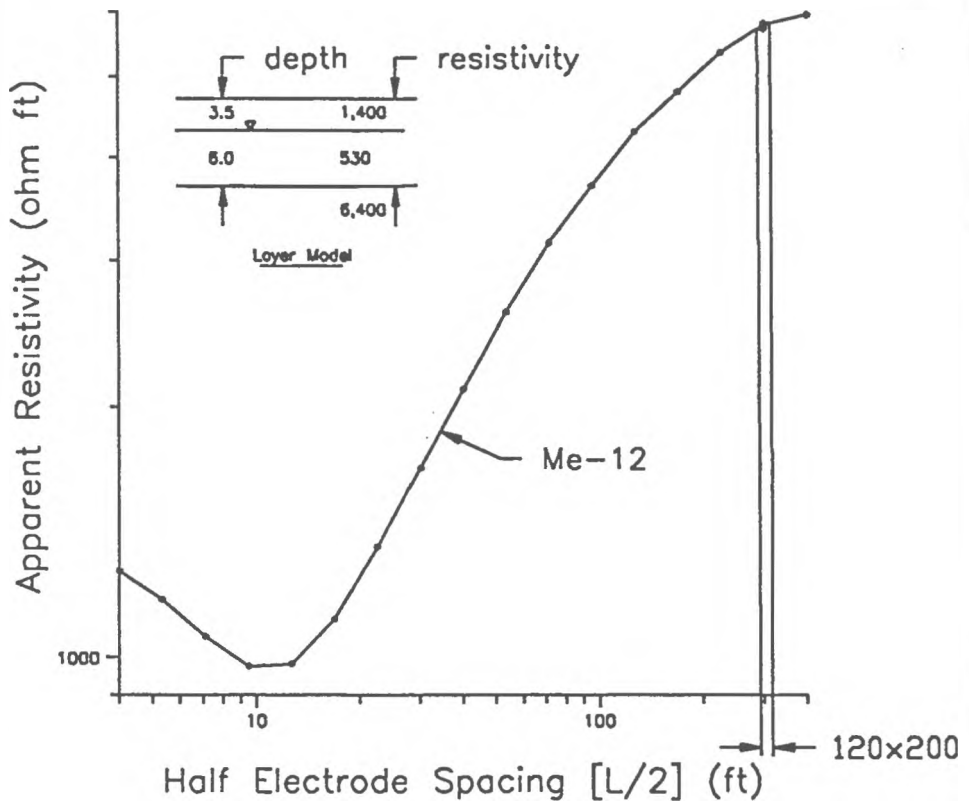
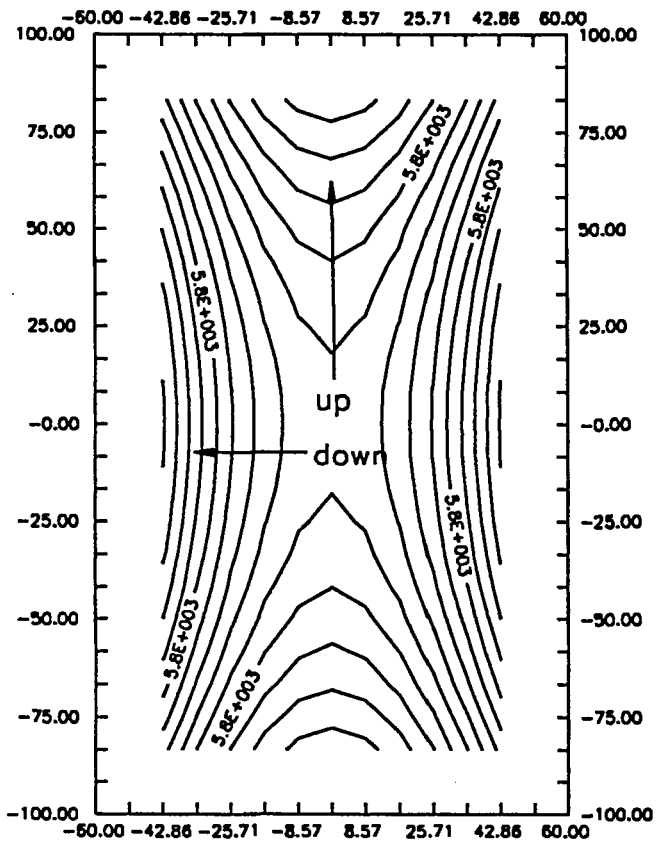


Fig. 3.6

Figure 3.7: Contour plot of the expected resistivities within the 120x200 ft rectangle for the model presented in fig. 3.6. Note the saddle shape caused by the greater effect of the bordering layers of higher and lower resistivities on the edges of the plot.



Saddle Shaped Contour Plot  
of Expected Resistivities

from the rectangle  
in Fig. 3.6

Fig. 3.7



### 3.2.5 Application of the AB rectangle method near a sanitary landfill.

As part of a separate study an AB rectangle measurement was completed on the site of a landfill in Plainville, MA. A location plan of the area shows the measuring site relative to the landfill and other features (see fig 3.8). First a depth sounding was conducted and interpreted for a horizontal layer model (see fig. 3.9). In this area bedrock fractures and high permeability zones were expected, based on fracture trace analysis, which may facilitate the flow of leachates from the landfill. The current electrode spacing  $L$  of 400 ft. was sufficiently large for a satisfactory depth penetration into the bedrock (see fig. 3.9). Measurements were taken within an AB-rectangle with dimensions 80x200 ft. The expected apparent resistivity (due to horizontal layering) at each position was then calculated and subtracted from the actual measured value.

Contours of the residual resistivities, as a result of this AB rectangle measurement are shown in figure 3.10. The most noticeable trend is the decrease in residual resistivity from south to north. The northern part of the rectangle has been affected by the downgradient southward advance of the leachates from the landfill (see fig. 3.8). Further trends in this figure appear to be north-south linear crests and valleys. These features trend in the same general direction as lineaments and measured fractures which correspond to the local geology in the area. The highs might correspond to competent rock and the lows to fracture zones of higher porosity. Note that the main trend, believed to be from the leachate, seems to flow into the suspected fracture zones from the landfill.

Figure 3.8: Sketch showing the placement of the AB-rectangle relative to the landfill, and hydraulic gradient, Plainville, MA.

Sketch Showing Placement  
of the AB Rectangle,  
Plainville, MA.

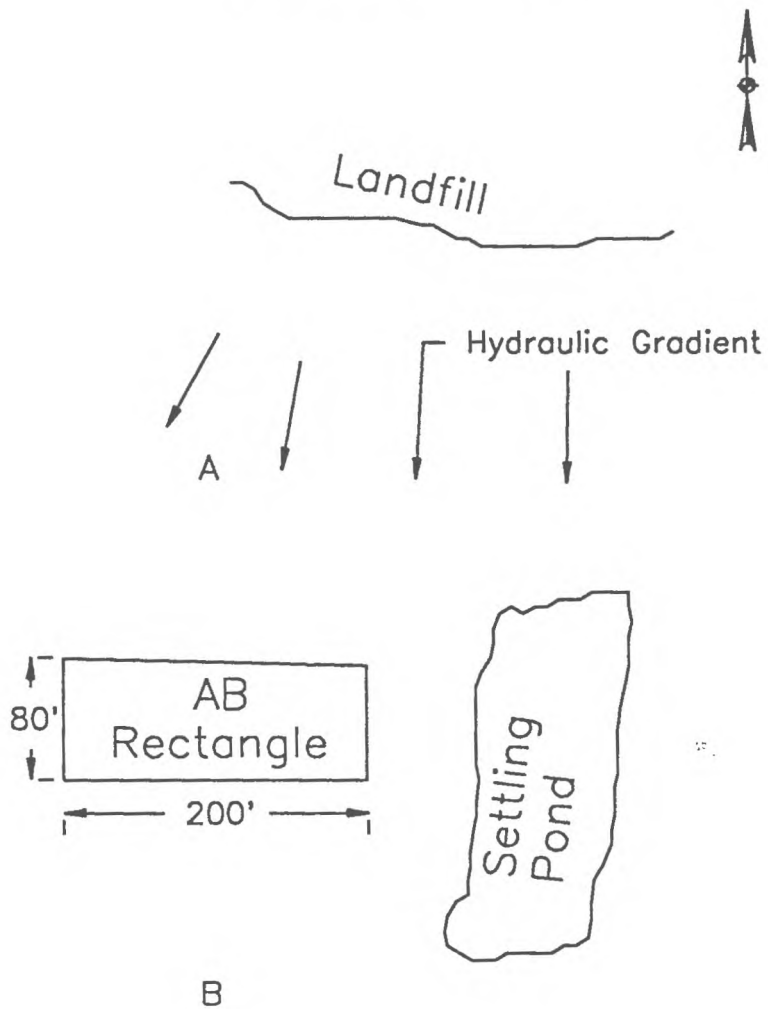


Fig 3.8

Figure 3.9: Sounding curve with layer model interpretation used to calculate the expected resistivities within the AB-rectangle of dimensions 80x200 ft.

Sounding Curve with Layer Model  
and Current Electrode Spacing  
for the AB Rectangle,  
Plainville, MA.

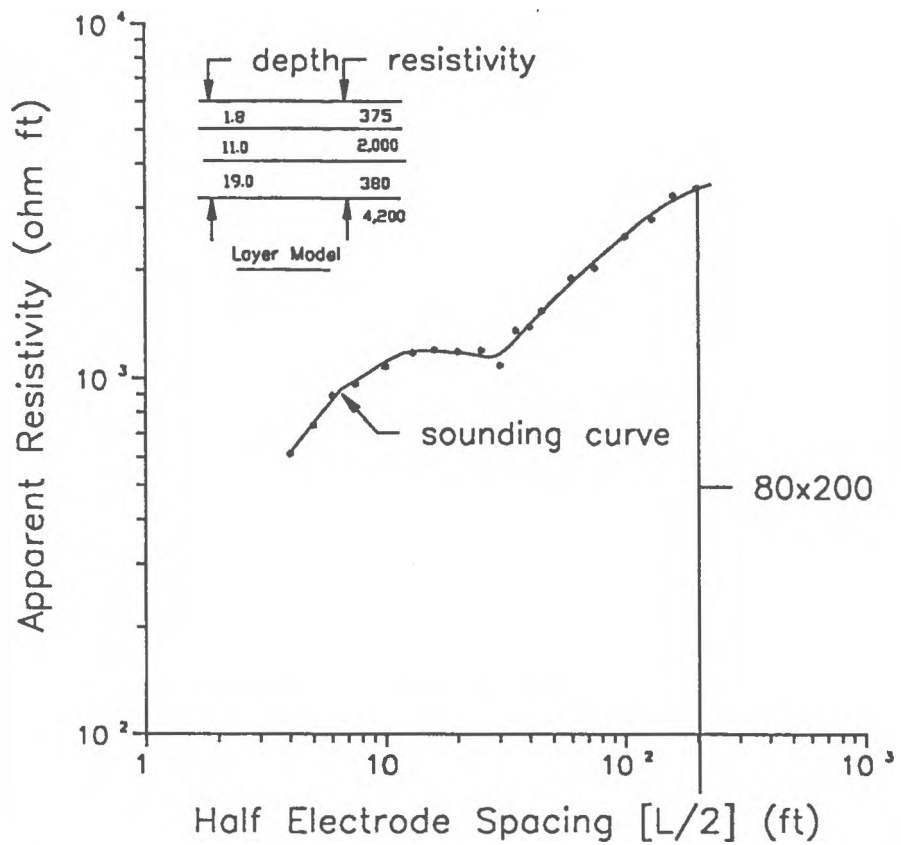


Fig. 3.9

Figure 3.10: Contour map of anomalous bedrock resistivities within the AB-rectangle, Plainville, MA. Note the trend from low to high bedrock resistivity away from the landfill to the north.

### Contours of Anomalous Bedrock Resistivity AB-Rectangle Methode Plainville, MA.

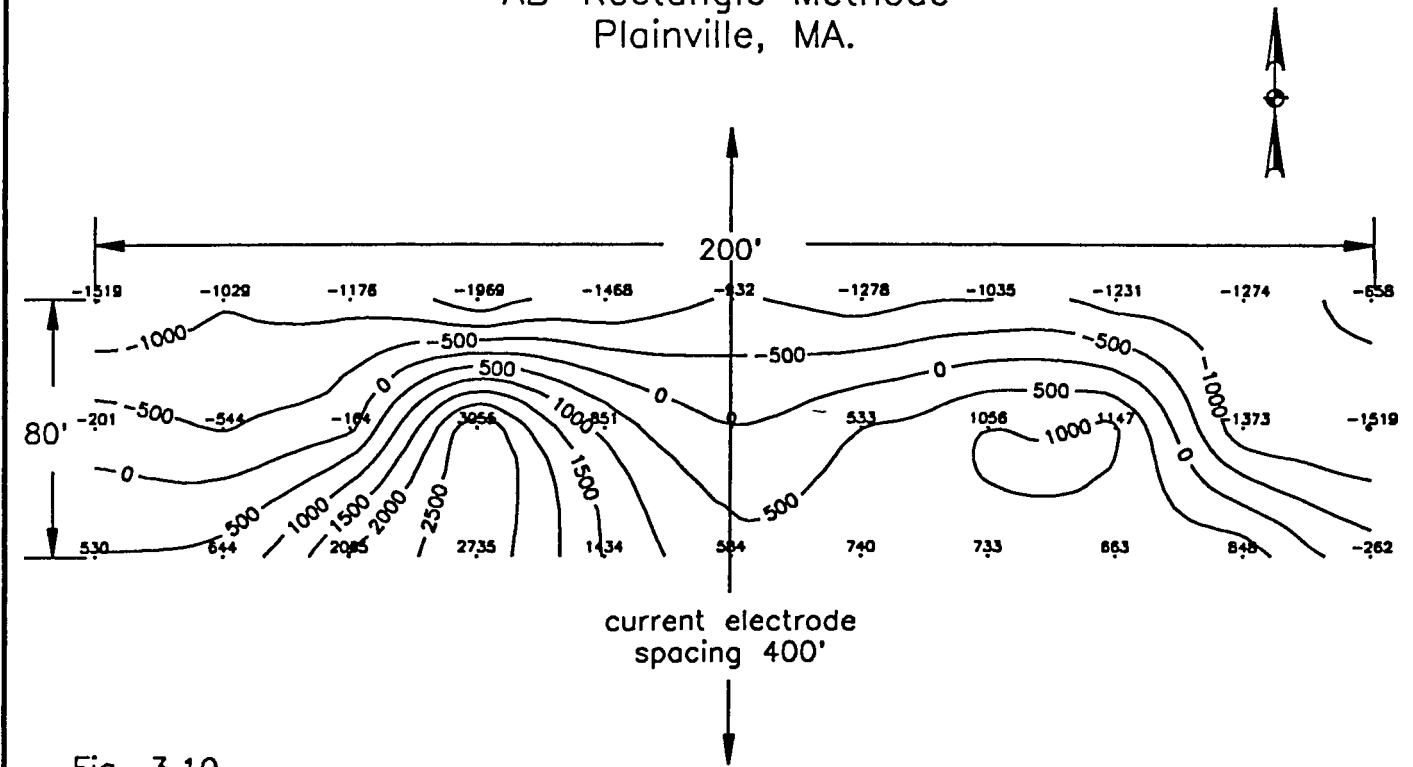


Fig. 3.10

### 3.3 Locating of soundings

Additional supporting evidence for near vertical fractures is fracture trace analysis. This method is concerned with the mapping of lineaments. Lineaments are linear features noticeable on aerial photos, satellite imagery, and other remote sensing maps. The features are from depressions in the topography, stream valleys, swamps, chains of lakes, or even tonal differences indicating different types of vegetation. Some formed from the ease with which the fractured rock is weathered in these zones, others are an indication of the moisture which can be associated with these zones.

Fracture trace analysis does not provide information on the extent of subhorizontal fractures. Since these fractures are just as important to the flow network other techniques are needed to characterize and rank the potential within these zones. Drilling test wells over lineaments will provide much more of the needed information. However, drilling can be expensive and many wells may be required to locate the zones of highest potential. Geoelectrical depth soundings can provide information useful in substantially narrowing the number of wells drilled.

Lineaments in this study had been previously mapped by others. Statistics were calculated and rose diagrams were plotted using software titled Fracture Analysis Software by Rockware Inc. The program to digitize the lineaments from a base map for use with this software was modified by this author. This was written in IBM basic for use with a Huston Instruments HIPad tablet connected via the COM1: port.



## 4.0 RESULTS AND DISCUSSION

### 4.1 Aroostook Co., Maine

The Maine Geologic Survey, under the state Department of Conservation, has been conducting a state-wide survey of both sand and gravel, and bedrock aquifers. A bedrock well was drilled for the hydraulic characterization of the bedrock in an effort to produce a high yield well for crop irrigation. Geophysics, conducted by Dr. R. K. Frohlich, D. Owen, M. Boland and T. Smith, was used to locate an optimal area for test wells.

#### 4.1.1 Geologic Setting and Lineament Analysis

The study area extends over two fifteen minute quadrangles, the Mars Hill and Fort Fairfield, of the extreme northeastern corner of Maine (figure 4.1). Most of the bedrock in the area is a weakly metamorphosed calcareous sediment of middle Ordovician to early Silurian age. It is known as the Cary's Mill formation, which is overlain by younger pelites of the Spragueville formation, localized to the northeast of this area. The structure of the region consists of northeast to north trending folds. There is also a major steeply dipping fault bordering the Spragueville formation trending north (Pavrides, 1978).

The geophysical study began with a map of lineaments for the area. Lineaments aided in the sighting of measurement locations. Lineaments in this area had been previously mapped by the Maine Geologic Survey (figures 4.2 and 4.3.). These lineaments were later digitized and statistically interpreted (figures 4.4a and 4.4b). The statistics for both quadrangles show similarities for the total number and length of lineaments and their averages. The Mars Hill Quadrangle shows three predominant lineament trends: N 40-50 W; N 0-10 W; and N 40-50 E.

Figure 4.1: Location map showing the two quadrangles, Mars Hill and Fort Fairfield, within the state of Maine.

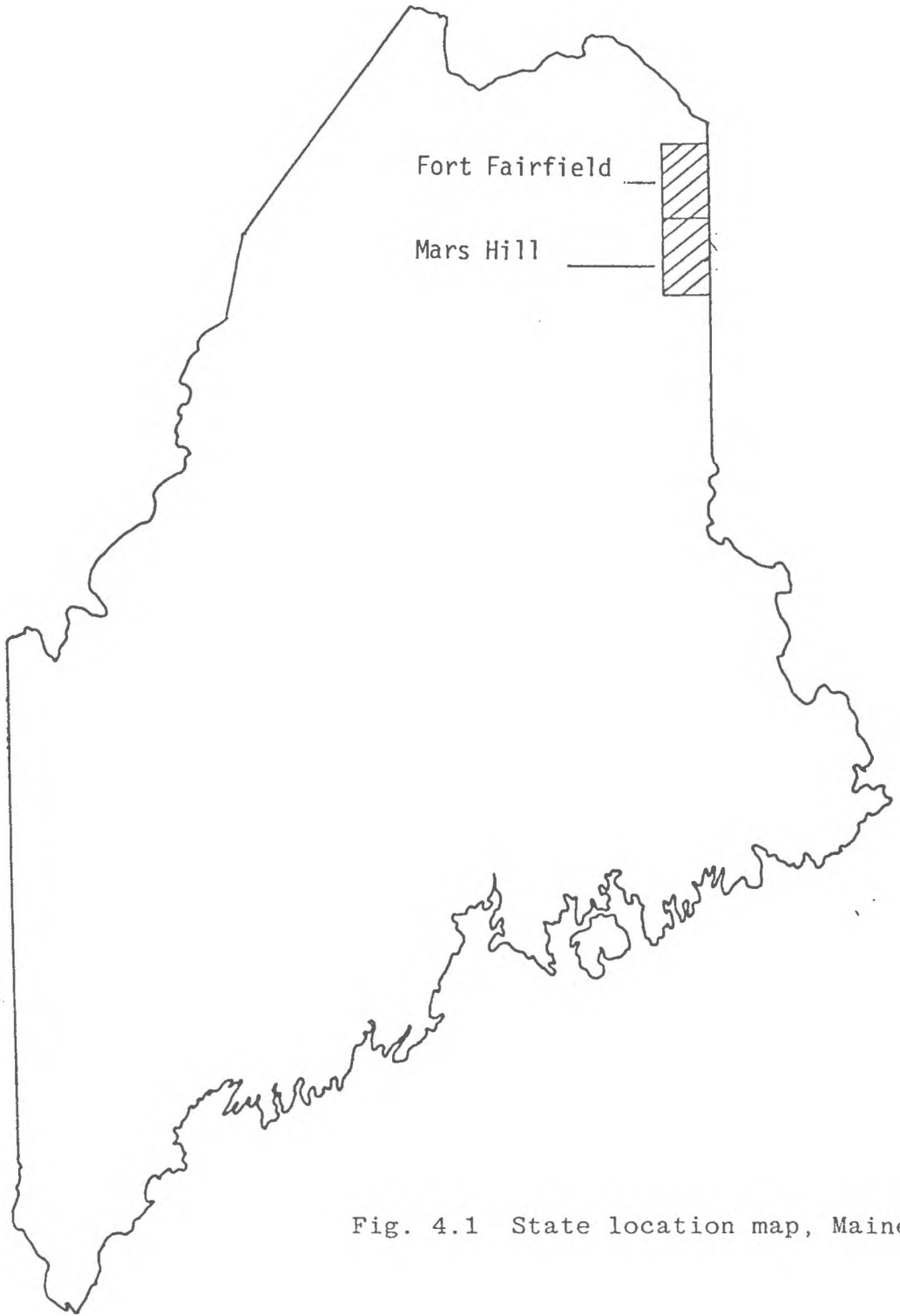


Fig. 4.1 State location map, Maine

Figure 4.2: Location of the geoelectrical soundings in relation to the lineaments in the Mars Hill quadrangle. Lineaments were taken off a map provided by the Maine Geological Survey.

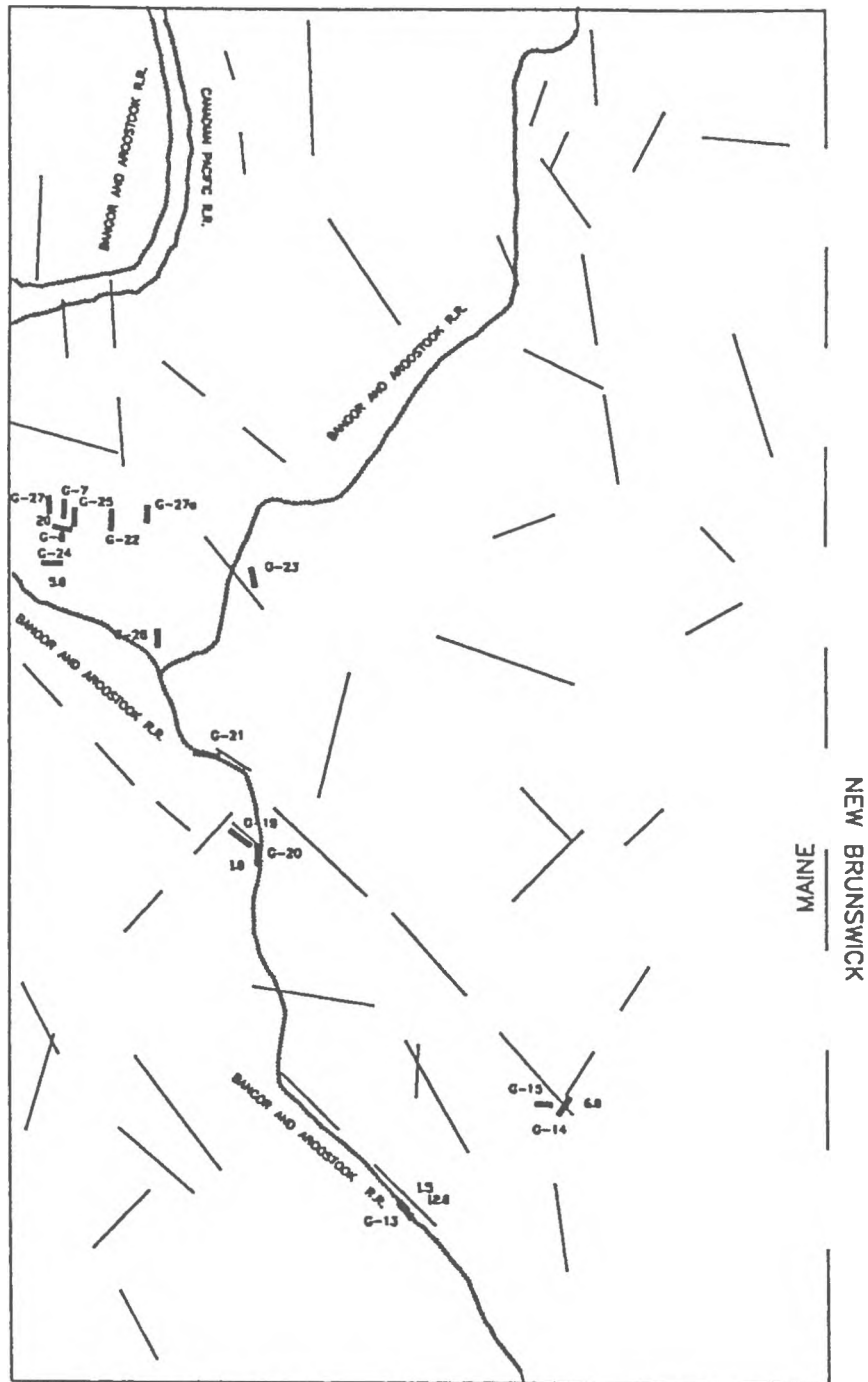


Fig. 4.2 Mars Hill Quadrangle

- G-21** GeoSounding
- Well and Yield
- Lineament

Figure 4.3: Location of the geoelectrical soundings in relation to the lineaments in the Fort Fairfield quadrangle. Lineaments were taken off a map provided by the Maine Geological Survey.

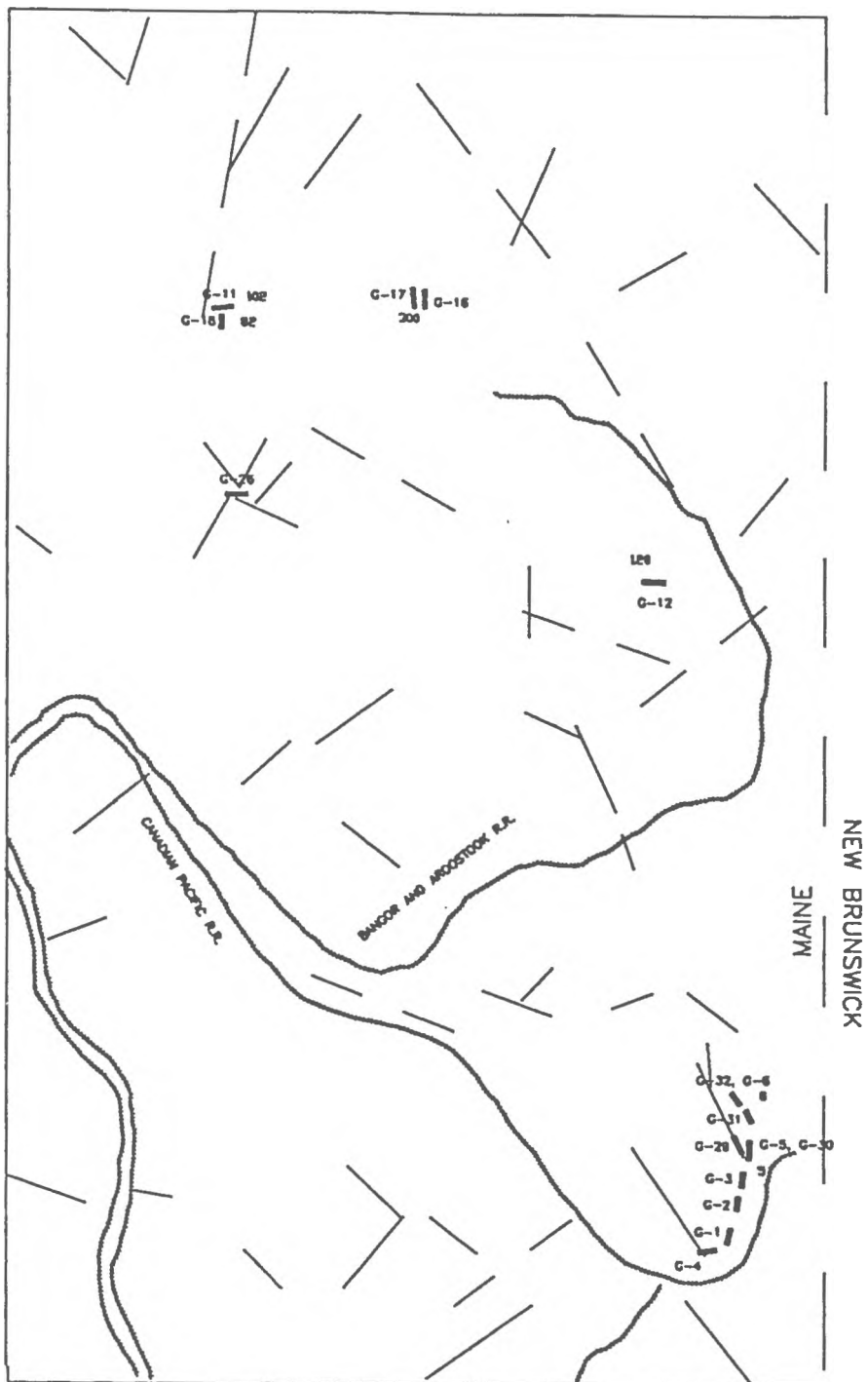


Fig. 4.3 Fort Fairfield Quadrangle

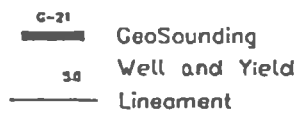


Figure 4.4a: Rose diagram showing the trends of the lineaments within the Mars Hill Quadrangle based on percent length of lineaments.

Figure 4.4b: Rose diagram showing the trends of the lineaments within the Fort Fairfield Quadrangle based on percent length of lineaments.



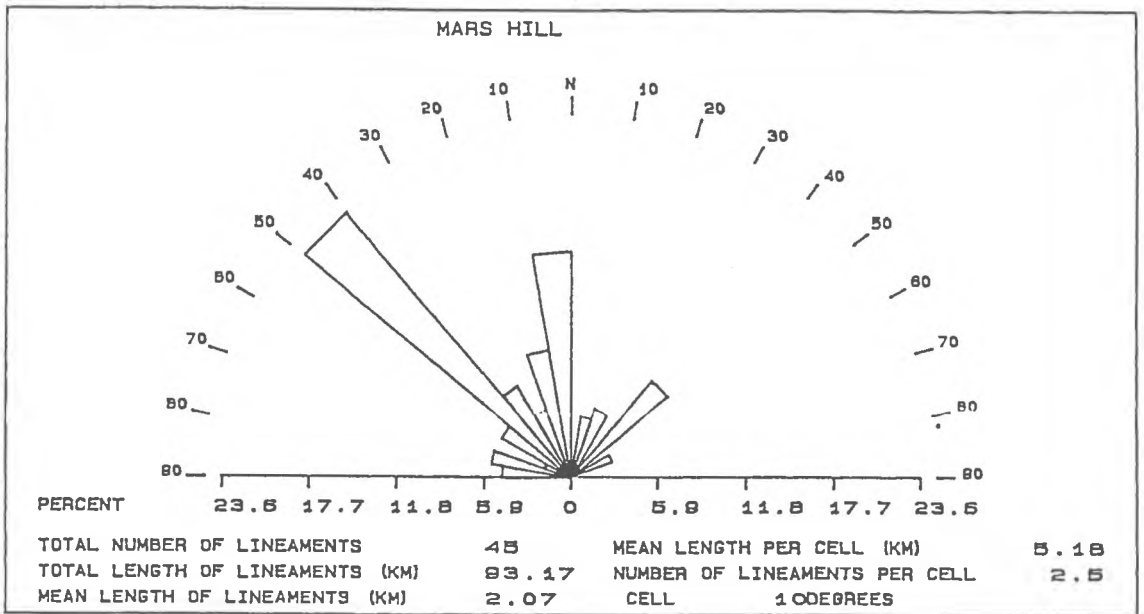


Fig. 4.4a

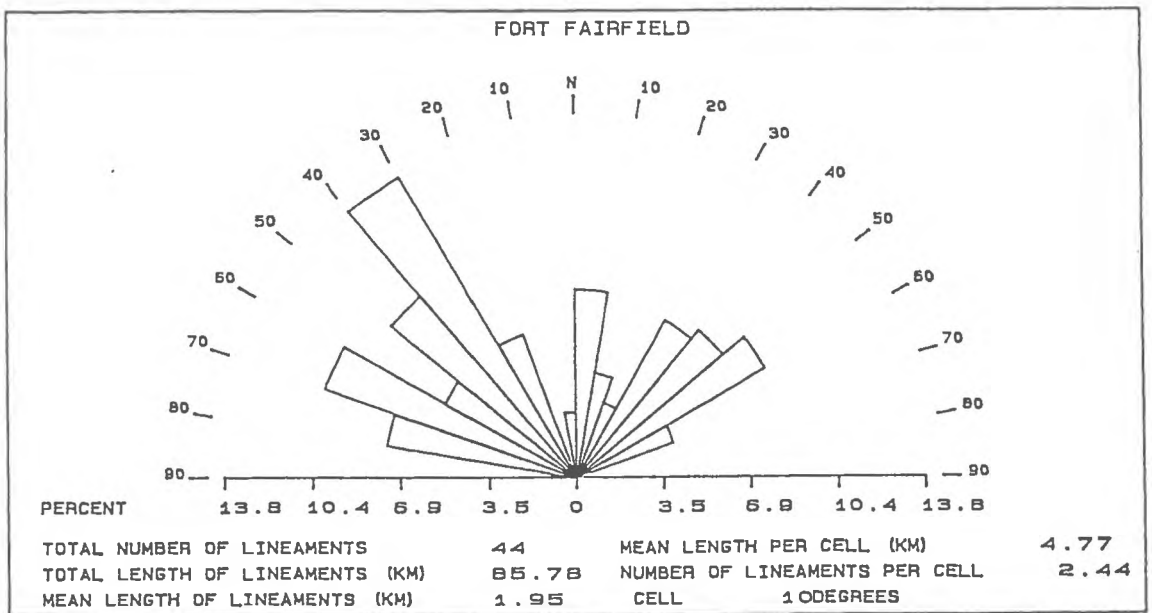


Fig. 4.4b

With a shift of 10 degrees the three trends are preserved on the Fort Fairfield Quadrangle. Lineaments on this quadrangle, however, are scattered over a wider azimuthal range. The lineaments N 0-10 W are parallel to the strike of the regional anticlines.

#### 4.1.2 Resistivity Soundings

The geophysical survey consisted of 32 geoelectrical depth soundings and was conducted over two summers 1986-87. Almost all soundings have been interpreted using a four layer model of AA-type or HA-type. These type curves correspond to layered sequences of relative resistivity changes (see appendix 4). Examples of these types are shown in figure 4.5. Sounding Me-22 represents an AA-type curve with a layer resistivity sequence of  $\rho_1 < \rho_2 < \rho_3 < \rho_4$ , whereas Me-29 is an HA-type curve with a sequence  $\rho_1 > \rho_2 < \rho_3 < \rho_4$ . The initially high resistivity of the HA-type is due to the unsaturated zone above the water table. The AA-type curves can have two hydrogeologic interpretations. The first interpretation is that the saturated zone is at the surface, possibly due to a recent rain. The second interpretation is that the water table is in the bedrock, where the saturated bedrock has a higher resistivity than the overlaying unsaturated sediments.

Again the goal of this study was to locate possible sites for the drilling of high yield test wells in bedrock for the purpose of crop irrigation. This made it advantageous for the farmers to have our work performed on their land. One such site was suggested by professor Forbes of the University of Maine at Presque Isle. This site was also attractive to us because of nearby swamps and springs and the mild suggestion of a N-S lineament (Forbes, pers. communication).

A total of six geoelectrical depth soundings were completed in this area (see fig. 4.6 and appendix 4). Layer model resistivities are shown in Figure 4.7.

Figure 4.5: Typical sounding curves within the study area. Me-22 is an AA type and Me-29 is an HA type.

# GeoElectrical Depth Sounding After Schlumberger

Location : Fort Fairfield

Date : AUG 1987

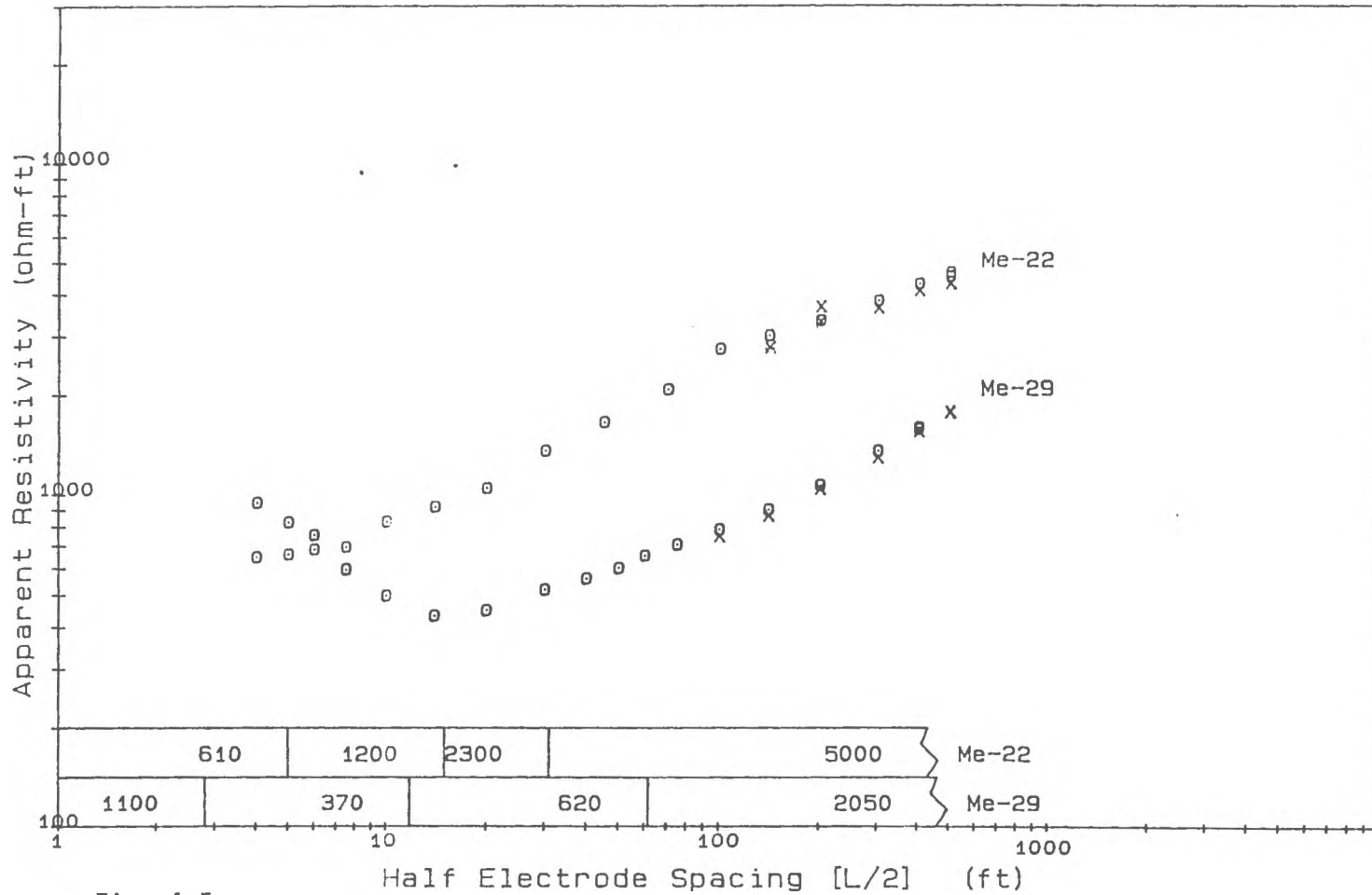


Figure 4.6: Location of depth soundings in relation to the AB-rectangle, Presque Isle, Maine.

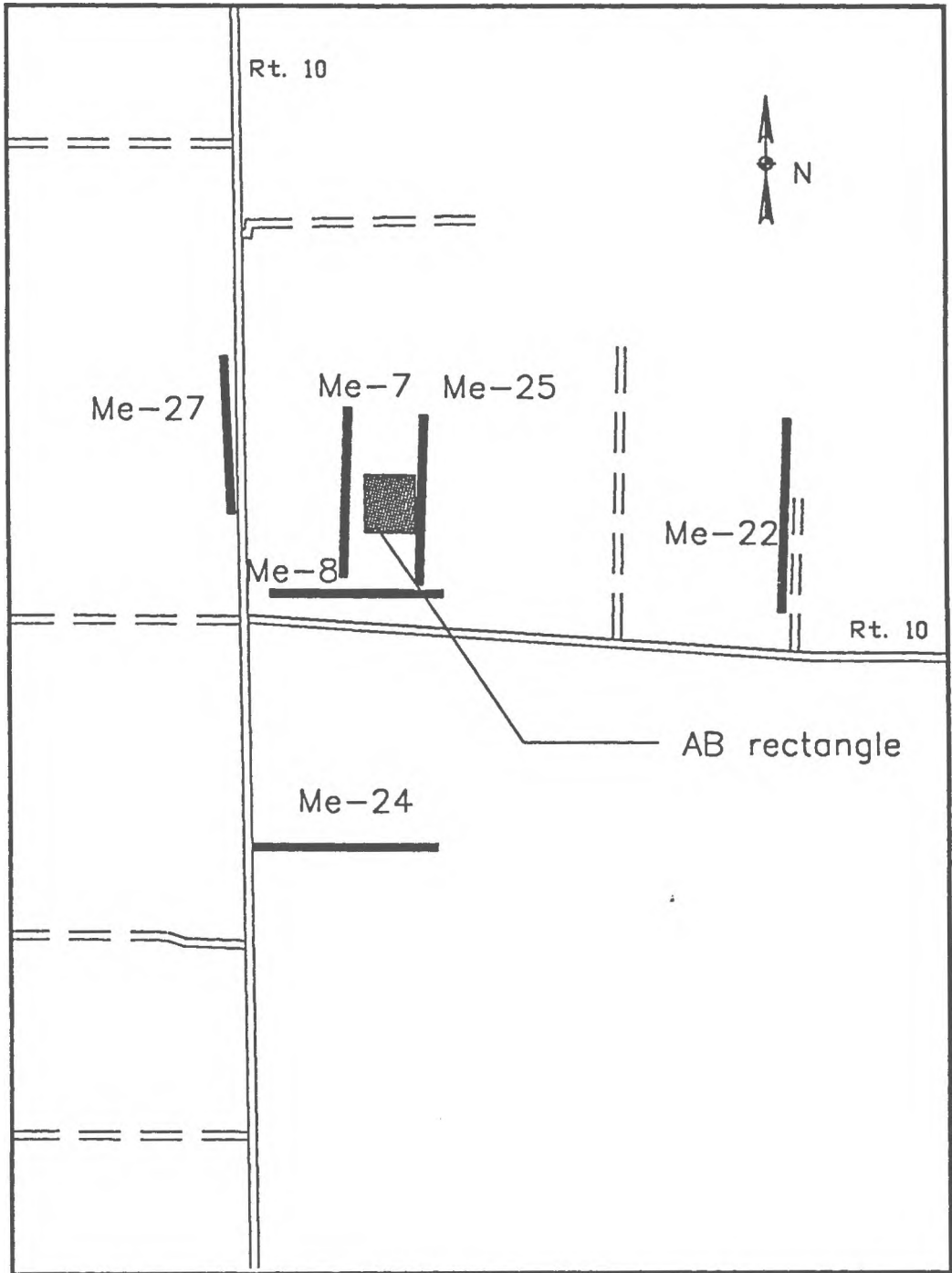


Fig. 4.6

Figure 4.7: Layer models for the soundings made in the vicinity of the AB-rectangle, maintaining the relative positions with respect to the rectangle. Note the position of the soundings with the low bedrock resistivities.

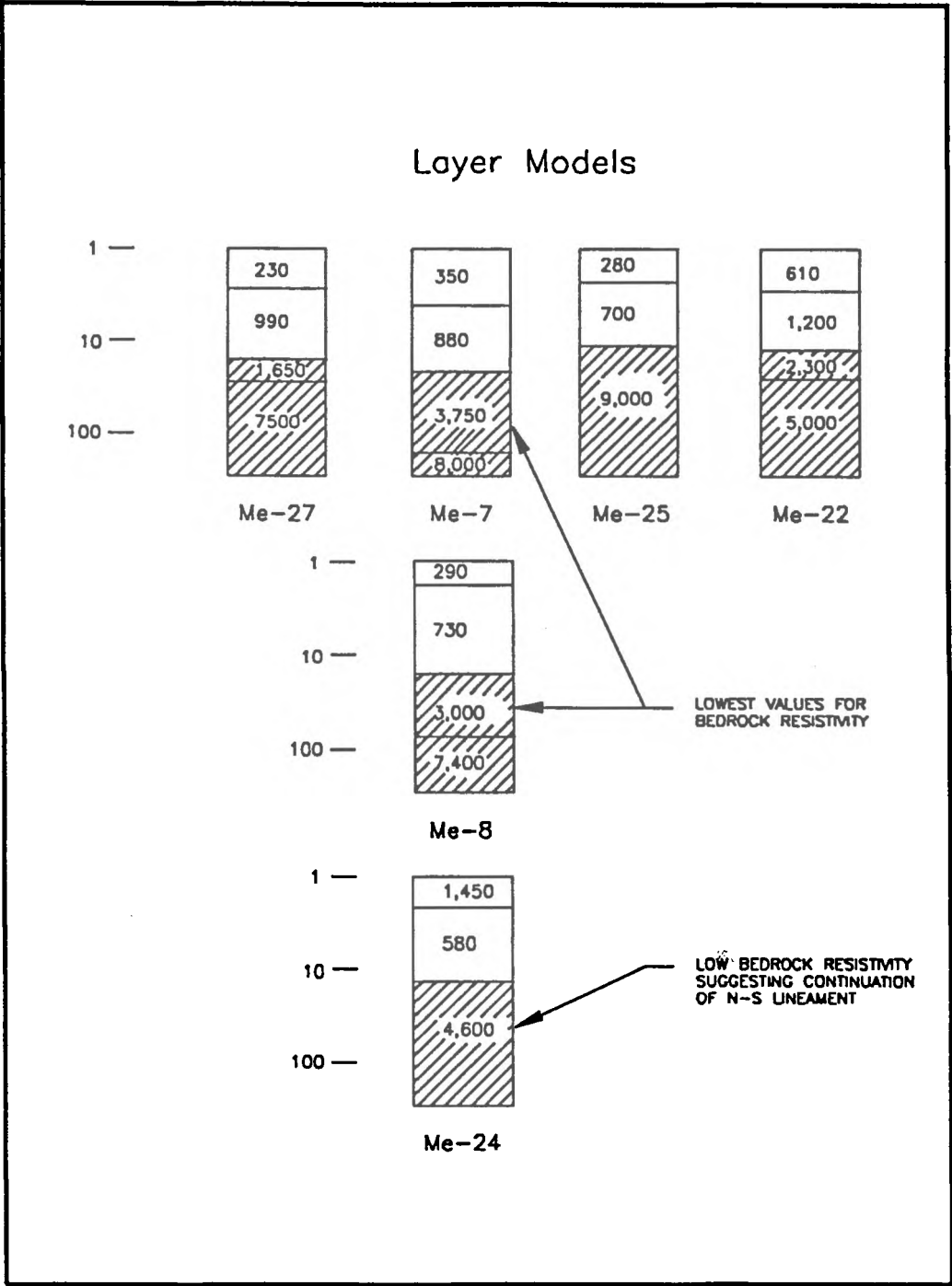


Fig. 4.7



These models have been positioned relative to their actual field locations (fig. 4.6). As is easily seen the lowest bedrock resistivities occur in soundings Me-7 and Me-8. To further investigate this area of lower bedrock resistivity an AB rectangle measurement was performed. The current electrode spacing of  $L/2=500$  ft., was chosen to focus the measurements within the bedrock layer. Figure 4.6 shows the location of the rectangle in relation to other depth soundings made in the area. Since the measurements were made to the west of the sounding line Me-25, the array actually covered half of a typical rectangle. The contours of anomalous bedrock resistivity show a relative low in the southwestern corner (fig 4.8). This is a significant resistivity low relative to the area to the north and east. This low is supported by two depth soundings made within approximately 200ft of the southwestern corner of the rectangle. Figure 4.7 shows the layer models of Me-7&8 which have low resistivity layers at the same depth that a high resistivity bedrock layer is shown for the model of Me-25.

The bedrock resistivity low could be due to a greater depth of the bedrock, contamination of the groundwater, or a more fractured bedrock to the southwest. The depth to bedrock modeled for this area was confirmed by the digging of a trench (Owen, 1987). The low being caused by a more fractured zone of the bedrock is supported by the N-S lineament crossing the area. Although, this site was not the first choice for the placement of a well, based on this information I feel confident that drilling in the southwest corner of this AB-rectangle will produce a well with a higher yield relative to the surrounding area.

Figure 4.8: Contour map of anomalous bedrock resistivity for the Presque Isle AB-rectangle. Note the low situated in the southwest corner corresponding to the low bedrock resistivities as seen in the geoelectrical depth soundings is figure 4.7.

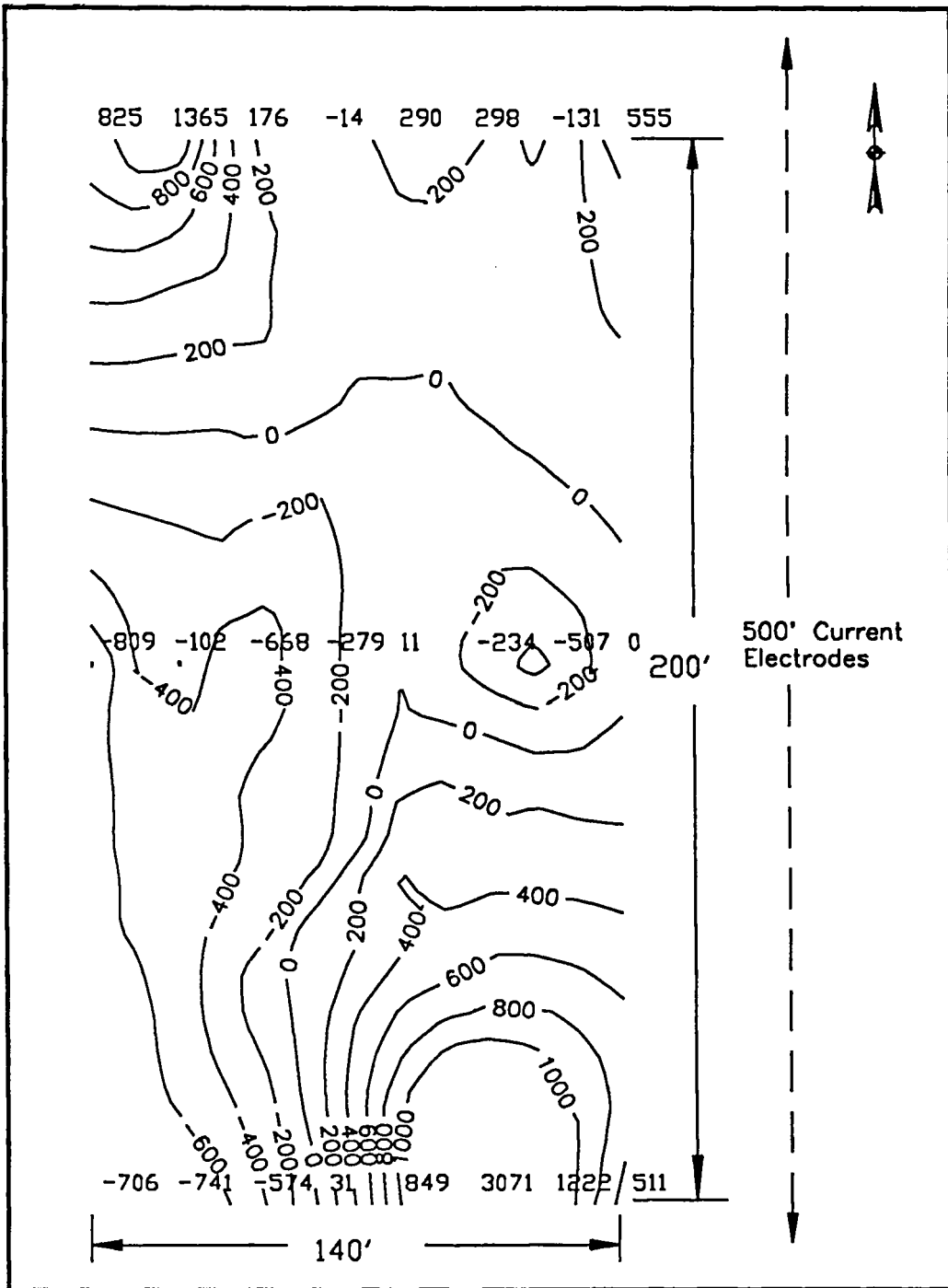


Fig. 4.8

### 4.1.3 Correlation of Resistivity to Bedrock Parameters

As previously presented theory has shown, bedrock resistivities may be used to estimate porosities and permeabilities. Many water conductivity measurements were made and it was determined that a uniform value of  $500 \mu \text{ S/cm}$  was characteristic of the uniform pore water in the bedrock. This provided a value for pore water resistivity of  $65.6 \Omega \text{ ft}$  ( $20 \Omega \text{ m}$ ), from which apparent formation factors were calculated. Intrinsic formation factors were calculated using equation 2.14, with a value of  $25,000 \Omega \text{ ft}$  ( $7,620 \Omega \text{ m}$ ) for the matrix resistivity. This value represents the the resistivity of the unsaturated zone interpreted from sounding Me-27a. The sounding is located on a hill over outcropping bedrock. This value was assumed to be characteristic for the matrix resistivity of the bedrock in this area. The resistivity of this unsaturated zone is the highest found in the study area.

Porosity values were estimated from the intrinsic formation factors with Archie's Law (eq. 2.11). Values for constants  $a, m$  were obtained from laboratory work on similar rock types found in the literature (Keller and Frischknecht, 1976).

- |     |             |            |                     |
|-----|-------------|------------|---------------------|
| 1.) | $a = 0.55;$ | $m = 1.85$ | dolomite-limestone  |
| 2.) | $a = 1.20;$ | $m = 1.88$ | siliceous limestone |

These values were used to estimate a range of possible porosities between  $\phi_1$  and  $\phi_2$  in table 4.1.

Permeability estimates were made in the same manner using equation 2.13. Constants used here are from Katsube and Hume (1987) determined experimentally for two fractured granites of the Canadian Shield.

- |     |                              |            |                          |
|-----|------------------------------|------------|--------------------------|
| 1.) | $\alpha = 2.51 \times 10^7;$ | $r = 2.22$ | Lac du Bonnet (Manitoba) |
| 2.) | $\alpha = 3.31 \times 10^6;$ | $r = 1.96$ | Atikokan (Ontario)       |

Table: 4.1 Geoelectrical Parameters, Presque Isle, ME.

Column 1: Depth sounding number  
 Column 2: Bedrock resistivity  
 Column 3: Well yield (gallons per minute)  
 Column 4: Apparent formation factor  
 Column 5: Intrinsic formation factor  
 Column 6/7: Permeability estimate after Katsube & Hume (1987)  
 Column 8/9: Porosity estimates after Archie (1942)

VES #	$\rho_s$ ( $\Omega$ ft)	GPM	Fa	Fi	k1	k2	$\phi$ 1	$\phi$ 2
1	2,000		30.49	32.67	10921.70	3565.49	0.11	0.17
2	1,700		25.91	27.47	16042.50	5006.63	0.12	0.19
3	7,000	5.0	106.71	139.25	436.98	207.97	0.05	0.08
4	2,100		32.01	34.43	9722.88	3217.64	0.11	0.17
5	1,500		22.86	24.07	21515.26	6487.70	0.13	0.20
6	2,400		36.58	39.77	7056.87	2424.69	0.09	0.16
7	8,000		121.95	166.38	294.29	146.69	0.04	0.07
8	7,400		112.80	149.81	371.48	180.19	0.05	0.08
11	3,200	102.0	48.78	54.61	3490.13	1302.26	0.09	0.14
12	6,400	120.0	97.56	124.07	564.60	260.76	0.05	0.08
13	20,000	6.8	304.88	917.43	6.65	5.17	0.02	0.03
14	10,000	6.0	152.44	228.83	145.06	78.55	0.04	0.06
15	9,000		137.20	196.12	204.30	106.29	0.04	0.07
16	2,500	300.0	38.11	41.58	6393.66	2222.36	0.09	0.14
18	5,000	82.0	76.22	91.49	1110.22	473.72	0.06	0.10
19	11,000		167.68	265.00	104.73	58.92	0.04	0.06
20	25,000	1.0	381.10	2304.15	0.86	0.85	0.01	0.02
21	25,000		381.10	2304.15	0.86	0.85	0.01	0.02
22	5,000		76.22	91.49	1110.22	473.72	0.06	0.10
23	23,000		350.61	1510.18	2.20	1.95	0.01	0.02
24	4,600		70.12	82.84	1383.99	575.49	0.07	0.11
25	9,000	20.00	137.20	196.12	204.30	106.29	0.04	0.07
26	8,000		121.95	166.39	294.29	146.70	0.05	0.07
27	7,500	20.00	114.33	152.52	357.03	173.99	0.05	0.08
27a	25,000		381.10	2304.15	0.86	0.85	0.01	0.02
28	20,000		304.88	917.43	6.65	5.17	0.02	0.03
29	2,100		32.01	34.43	9722.88	3217.65	0.11	0.17
30	2,000		30.49	32.67	10921.70	3565.50	0.11	0.17
31	2,500		38.11	41.58	6393.66	2222.36	0.09	0.14
32	2,500		38.11	41.58	6393.66	2222.36	0.10	0.15

These are the only values for these constants which could be found in the literature.

Again a range was calculated between  $k_1$  and  $k_2$  (table 4.1).

These values of porosity and permeability, in table 4.1, are tentative at best. This is due to the lack of specific knowledge about the rocks and therefore their constants critical for the estimating equations 2.11 and 2.13. In order to prove that these values are even partially related to the actual parameters it must be shown that the basic relationships in the predicting equations are true. Both equation 2.11 and 2.13 are of the same form. These equations may be simplified to the form of a line by taking the logarithm of both sides. A bi-logarithm plot should then show a linear trend. Therefore, if the theory is correct, a plot of the logarithm of the intrinsic formation factor versus the logarithm of the porosity or the permeability will produce a straight line.

Before this comparison can be made it is necessary to have the values of porosity or permeability with which to compare to the bedrock resistivity. Porosity and permeability are parameters seldom measured in domestic wells. However, the yield of the well is almost always determined. Minimizing somewhat the changing depth factor from well to well by pointing out that yield decrease at depth, then yield should be a function of both the permeability and the porosity of the formation. As part of the Maine Survey's study, data on yield in the area had been mapped. Some depth soundings were made in close proximity to these wells so that a comparison could be made (table 4.1).

A graph was then prepared of bedrock resistivity and yield in 10 wells located very near soundings (fig. 4.9). This graph does show a good relationship between the logarithm of these two parameters as suggested by the theory. The trend shown on the graph has a correlation coefficient of -0.73, as calculated by standard linear regression techniques.

Figure 4.9: Plot of bedrock resistivity versus well yield, Aroostook Co., Maine. The correlation coefficient is -0.73.

Bedrock Resistivity vs. Well Yield  
Aroostook Co., Maine

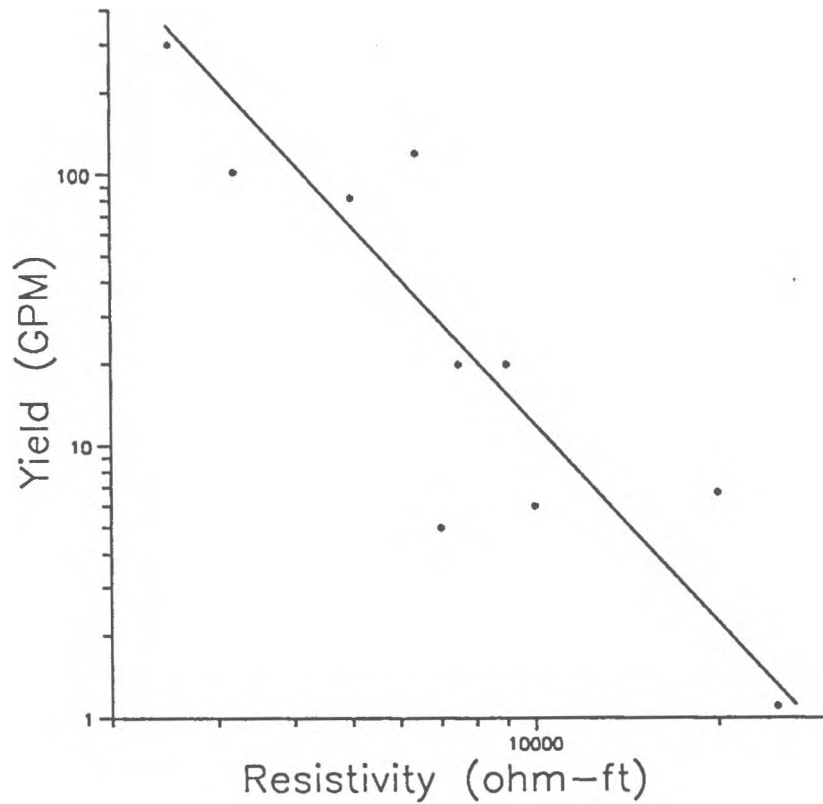


Fig. 4.9



Results of this study lead Frohlich et al. (1988), to suggest a site for the drilling of a high yield bedrock well based on the lowest bedrock resistivities. The test well terminated at 200 ft (70m) and produced a yield of 100 GPM ( $6.3 \times 10^{-3} \text{ m}^3/\text{s}$ ).

#### 4.2 Johnston, Rhode Island

The Solid Waste Management Corporation has been conducting a survey to evaluate the hydrogeology of fractured bedrock under the Central Landfill in Johnston, RI (fig. 4.10). This study has been headed by the engineering firm of Goldberg Zoino and Associates, who contracted Dr. R. K. Frohlich, Dr. D. W. Urish and the late Dr. J. J. Fisher, to perform geophysics and lineament analysis to locate fracture zones in the bedrock. The study was assisted by Joe Savarese, lineaments; Larry Hanson, seismic; and Mike Boland, geoelectrics. The purpose was to suggest three sites in which to drill deep bedrock wells to monitor any contaminant transport within the suggested fracture zones.

##### 4.2.1 Geologic Setting and Lineament Analysis

The study was located about the Landfill (fig 4.11) on the North Scituate Quadrangle. The bedrock in the area is a hypersolvus granite known as the Devonian Scituate Pluton, with a radiometric age measured at 370 my (Hermes and Zartman, 1985). The Scituate Granite is bordered to the east and northeast by the Proterozoic metadiorite associated with the Esmond Plutonic Suite and the Late Proterozoic Blackstone Series (Quinn, 1971). The northwestern edge is bordered by Esmond Granite, the Carboniferous Bellingham Conglomerate, the Precambrian Absalona Gneiss, and the Woonasquatucket Shists.

Figure 4.10: Location map showing the study areas in Rhode Island.

1. Johnston - centered at the Central Landfill
2. Tiverton - centered at Florence ave.

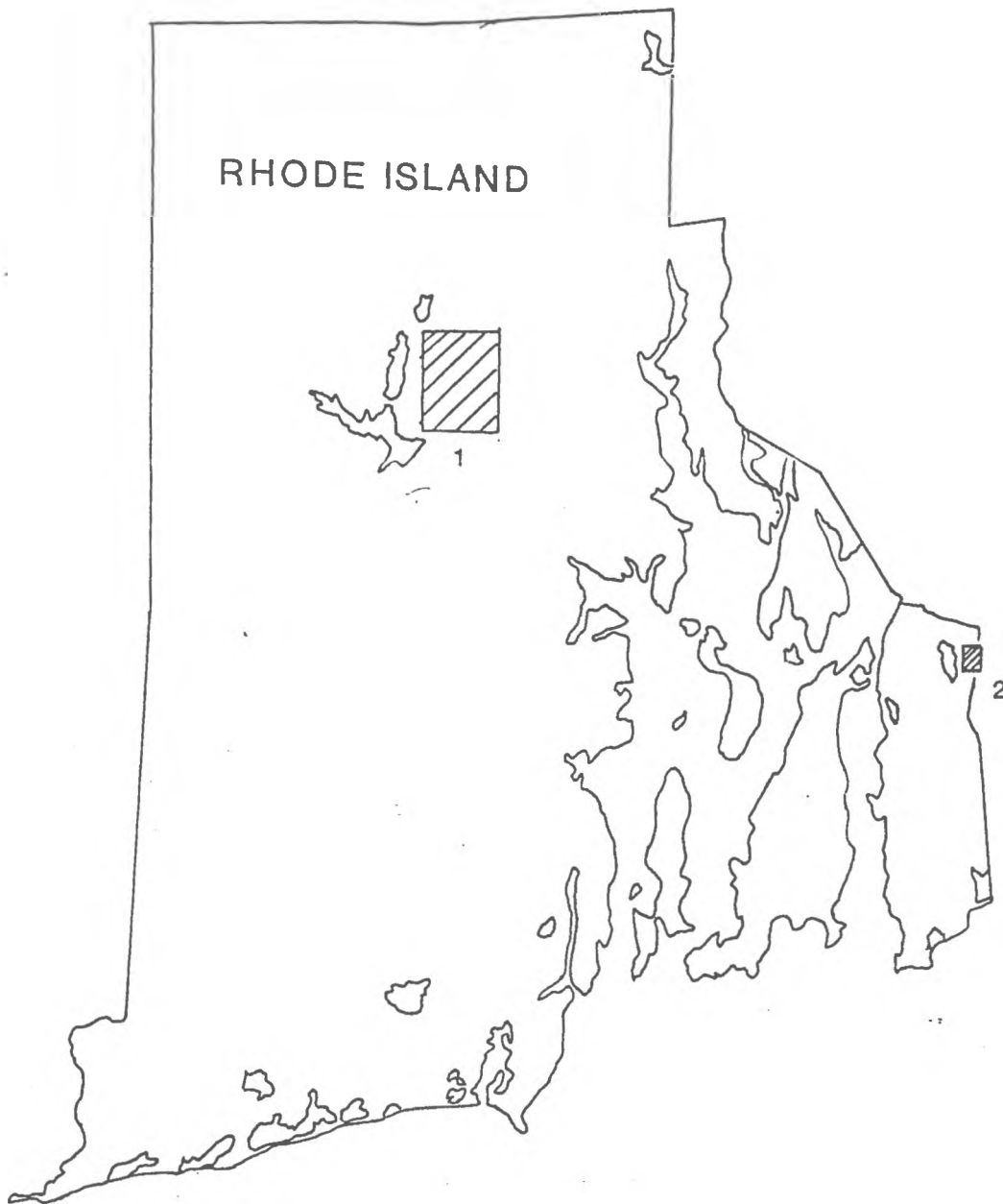


Fig. 4.10 Location map of study areas

1. Johnston - Central Landfill
2. Tiverton

Figure 4.11: Location map of the Central Landfill, Johnston RI. with lineaments mapped by Joesph Savarese.

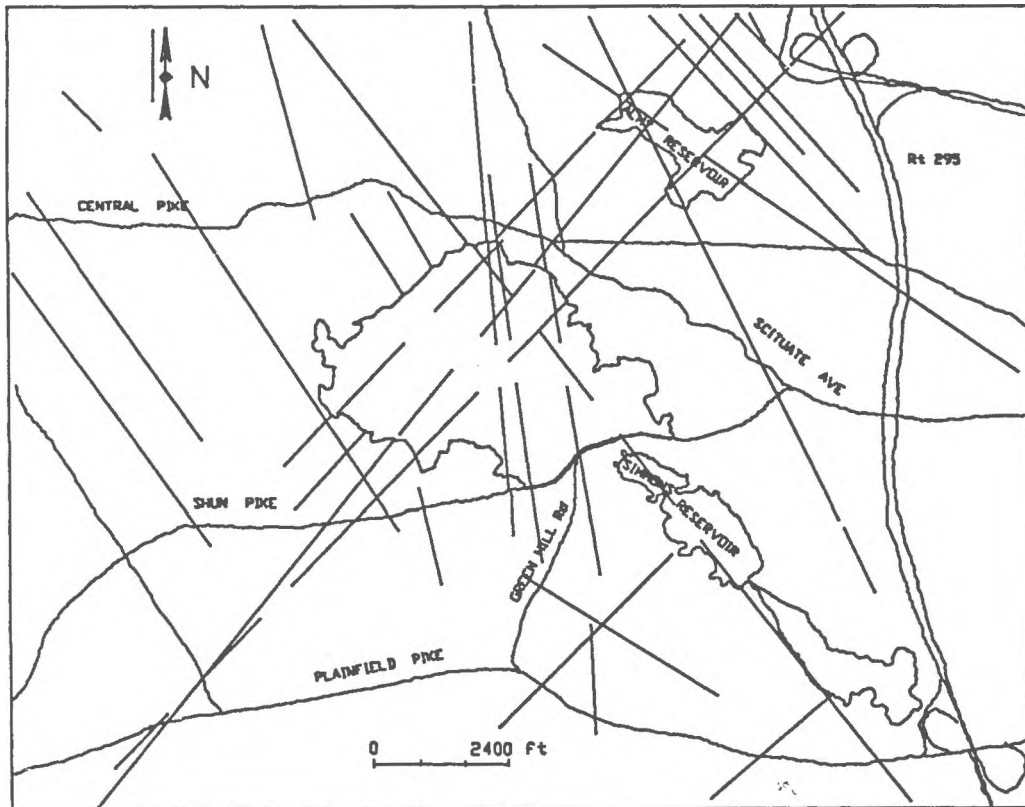


Fig. 4.11

Figure 4.12: Rose diagram showing the trends of the lineaments within the area of the Central Landfill based on percent length of lineaments.

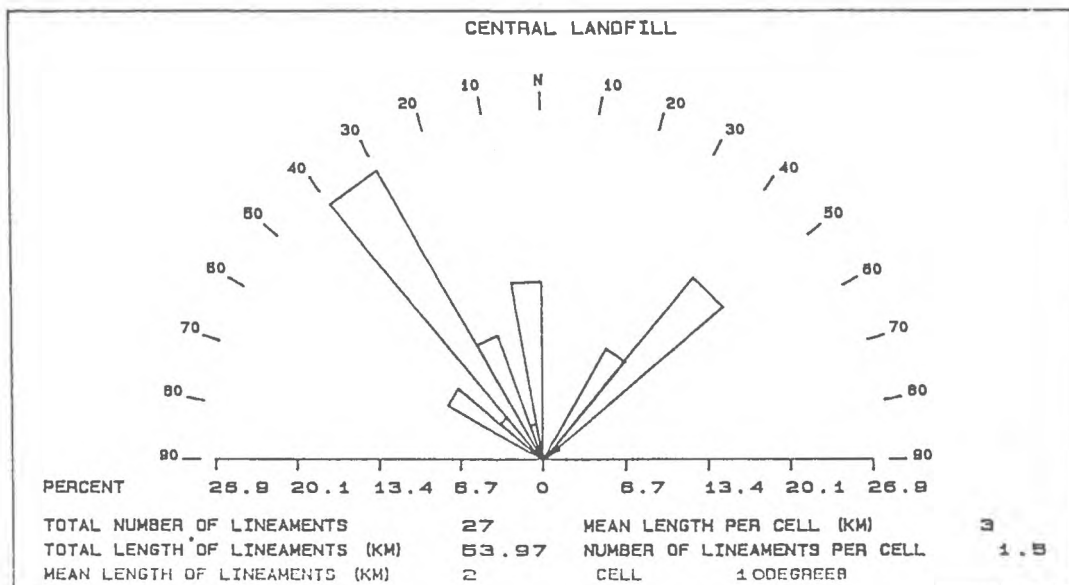


Fig. 4.12

The Esmond Granite and Bellingham Conglomerate are interpreted to be in fault contact with the Scituate Granite (Hamidzada, 1988 and Quinn, 1951). The Scituate Granite constitutes an 'A' type granite, typical of an anorogenic, extensional tectonic regime (Danforth, 1986).

There is one major lineament in the area visible on landsat imagery. This lineament is of most concern because it passes through the Scituate reservoir and the Central Landfill. It strikes N 40-50 E which is one of three major trends (fig. 4.12). The northwest trend may be associated with ductile shear zones which strike N 30-40 W, and dip northeast and are exposed to the northeast of the landfill (Hamidzada and Hermes, 1984). They describe another set of shear zones which could fit the north trend. These shear zones are near the southeast end of the Scituate Reservoir, striking N 0-5 W. There are also dolomite dikes striking N 0. These dikes are characteristic of those produced by magmas in intraplate zones of tensional igneous activity which could have occurred during Mesozoic rifting along eastern North America during the opening of the Atlantic (Hermes et al, 1984). The northeast trend could relate to a fault described by Hamidzada (1988), near the Rt. I 295 - I 195 interchange. This near vertical fault has a 4 ft. wide zone of gouge and was measured by Hanson (1988) at N 30 E, 74 W.

The surficial geology, though of minor importance to this study, is complex in the area. Most of the visible surface that has not been removed is a deposit of ground moraine (till). A glacial fluvial deposits (outwash) is present and a glacial channel is mapped to the west of the landfill in the Cedar Brook valley (Robinson, 1961).

#### 4.2.2 Resistivity Soundings

A total of ten geoelectrical depth soundings were conducted for this study (see appendix 2). The locations of these soundings are shown in figure 4.13.



Figure 4.13: Location of depth soundings Clf, and seismic soundings S (Hanson, 1988), Johnston, RI.

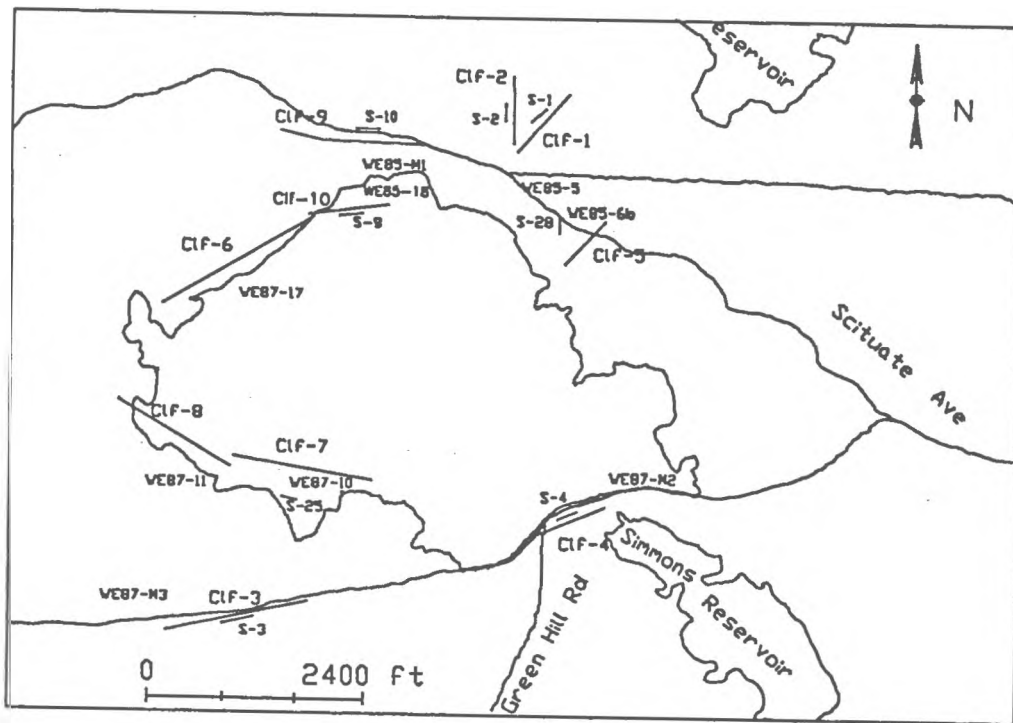


Fig. 4.13

The sounding curves with layer model interpretations along with the sounding data are located in appendix 3a and 3b. Sites for these soundings were selected on the basis of the fracture trace analysis, a gravity survey and a map showing contour lines of hydraulic head from a report by Goldberg & Zoino (Frohlich et al, 1987). Most of the interpreted models have a thin top layer with resistivities that indicate the top soil moisture conditions. High resistivity indicates dry soil and low resistivities prevail during the moist season. Unique for this study is that the area has had many test wells drilled, providing much data for comparison and evaluation of the geoelectrical method. The next few paragraphs discuss the interpreted layer models and how those models relate to features uncovered by other geologic or geophysical methods

Soundings Clf-1 and 2, were conducted away from any wells and near one of the major mapped lineaments. Depths to bedrock coincide well with those from seismic refraction interpretations (Hanson, 1988). The low bedrock resistivities between 6000 and 8000  $\Omega$ ft to a depth below 200 ft (Clf-1) and 80 ft (Clf-2) suggest fractured bedrock. The decrease in bedrock resistivity from 8000  $\Omega$  ft to 6000  $\Omega$  ft further supports the effect of a fracture zone which is closer to Clf-2.

Sounding Clf-3 was located near a well that was recommended on the basis of this study: WE87-M3. The depth to bedrock is 53 ft as measured in the well. A low resistivity of 3900  $\Omega$  ft extends from 59 to 250 ft. This zone coincides with four permeable zones interpreted on the basis on tube waves delineated by surface to hole seismic techniques. This seismic work was performed by Weston Geophysics for Goldberg Zoino and Associates. Below 250 ft the resistivity increases to 5400  $\Omega$  ft which is evidence of further fracturing though less than the section above. The high resistivity layer of 8500  $\Omega$  ft above the fractured zone is probably a compact till that may form a confining layer.

The most noticeable feature of sounding Clf-4 is the very low apparent resistivity of 680  $\Omega$  ft between 10 and 140ft. This is due mainly to the low pore water resistivity of 30  $\Omega$  ft as measured in well WE87-M2. It was also noted in this sounding that it was impossible to distinguish between a layer that was logged as boulder till and the top of the fractured bedrock. This is due to the fact that the bedrock is probably highly fractured and that the low resistivity of the pore water is such a good conductor. The resistivity rises strongly below a depth of 140 ft, suggesting a compact and less fractured bedrock. The fractured nature of the bedrock above this is supported by the core logs. However, the well penetrated only to a depth of 151 ft, which leaves no support for a continuation of compact rock beneath.

Sounding Clf-5 shows an unusually low bedrock resistivity. No logs were available for this well for comparison. The packer tests do indicate the highest permeabilities of the area. Shallow and relatively compact bedrock was measured in sounding Clf-6. Packer tests indicate low permeability except for the very first packer interval. This could be due to an inadequate seal of the top packer. Therefore average hydraulic conductivities were also calculated minus the first packer in hope to get as characteristic a value of the hydraulic conductivity of the bedrock as possible.

A sounding that was made close to the landfill, Clf-7, is believed to be located over the major northeast trending lineament. This curve shows a bedrock bulk resistivity of 1200  $\Omega$  ft with a high pore water conductance in well WE87-10. This corresponds to a high bedrock permeability. Clf-8 is located adjacent to this sounding and shows a high resistivity off the lineament indicating a decreasing fracture frequency and a more competent bedrock .

Sounding Clf-9 and Clf-10 suggests a sequence of high and low resistivities to a depth below 300 ft. The strong variations of the apparent resistivity versus  $L/2$  make these sounding curves look different from the others. It is very likely that lateral inhomogeneities influence these variations.

To evaluate the accuracy of the electrical resistivity method in this area and to meet concerns of equivalence, common in most geoelectrical studies, a plot of depth to bedrock from sounding models to well logs was made. This was to confirm that the models can accurately predict the depth to bedrock. Figure 4.14, shows an excellent, one to one relationship between these two measurements. The graph has a correlation coefficient of 0.99 and standard deviation of 0.42.

#### 4.2.3 Correlation of Resistivity to Bedrock Parameters

Porosities and permeabilities were estimated in the same manner as discussed in chapter 4.1.  $35,000 \Omega \text{ ft}$  ( $7,620 \Omega \text{ m}$ ) was used for the matrix resistivity. This value represents the the resistivity of the unsaturated zone interpreted from sounding Clf-6. As before this sounding was located over outcropping bedrock. This value was assumed to be characteristic for the matrix resistivity of the bedrock in this area. These values along with data from soundings is presented in table 4.2. In this study we were able to compare permeabilities from Katsube and Hume (1987) with hydraulic conductivities obtained from packer tests. A graph of this result is shown in figure 4.15. One point on the graph had the average hydraulic conductivity calculated without the first 5 ft packer interval. This is because this first interval was extremely high and uncharacteristic of the rest of the well. It is believed that the packer may not have had a good seal near the bedrock-overburden interface.

Figure 4.14: Plot of depth to bedrock, measured in a well vs. interpreted from geoelectrical depth sounding. The correlation coefficient is 0.99.

Measured Depth to Bedrock  
Central Landfill, Johnston, RI

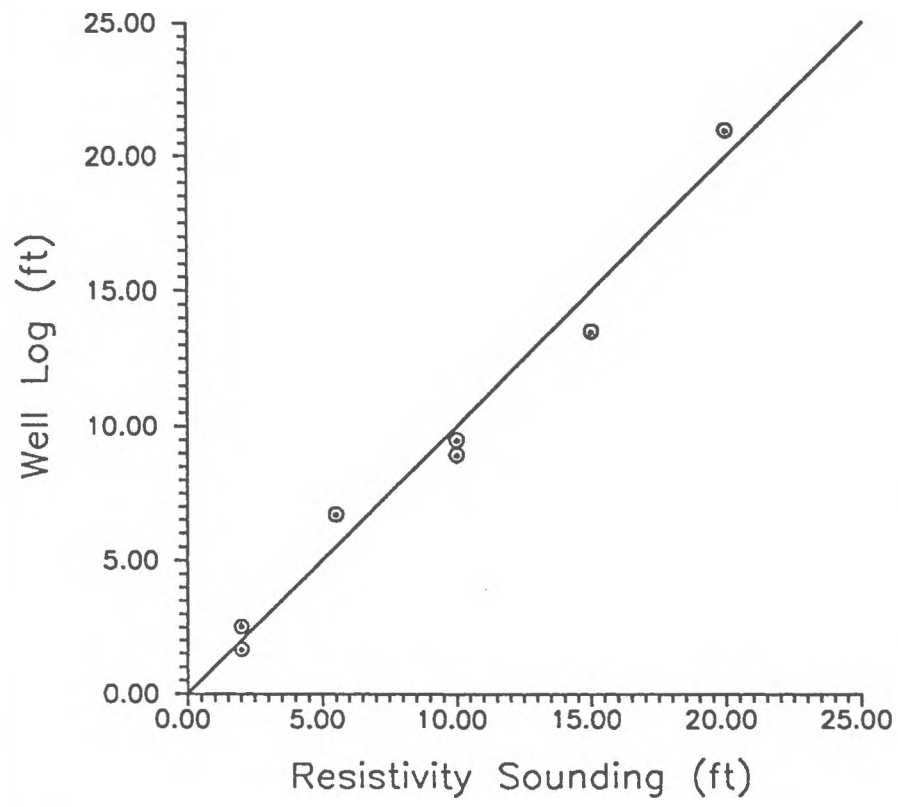


Fig. 4.14

Table: 4.2 Geoelectrical Parameters, Johnston, RI

Column 1: Depth sounding number  
 Column 2: Seismic profile number (Hanson, 1988)  
 Column 3: Monitoring well number  
 Column 4: Depth to bedrock from the Resistivity model  
 Column 5: Depth to bedrock from the seismic model (Hanson, 1988)  
 Column 6: Depth to bedrock from well data  
 Column 7: Bedrock resistivity  
 Column 8: Bedrock seismic velocity (Hanson, 1988)

Column 9: Pore-water resistivity  
 Column 10: Average hydraulic conductivity (minus first packer interval)  
 Column 11: Average hydraulic conductivity (entire bedrock section)  
 Column 12: Apparent formation factor  
 Column 13: Intrinsic formation factor  
 Column 14: Permeability estimates after Katsube & Hume (1987)  
 ( $\alpha = 3.31 \times 10^6$ ,  $r = 1.96$ )  
 Column 15: Porosity estimates after Archie (1942)  
 ( $a = 1.85$ ,  $m = 0.55$ )

Resistivity Sounding	Seismic Profile	Well #	Resistivity Depths (ft)	Seismic Depths (ft)	Well Depths (ft)	Bulk Resistivity ( $\Omega$ -ft)	Seismic Velocity (ft/s)	Pore Water Resistivity ( $\Omega$ -ft)	K AVE (ft/yr)	K AVE (ft/yr)	F <sub>a</sub>	F <sub>i</sub>	k (am <sup>2</sup> )	$\phi$
clf-1	s-1		19.00	20.00		8,000	12,112		3.21	3.59				
clf-2	s-2		19.50	16.00		6,000	12,970		3.21	3.59				
clf-3	s-3	WE87M3	19.00	24.00	53.00	8,500	15,400	219.00	19.35	18.34	38.81	51.26	1474.5	0.10
clf-4	s-4	WE87M2	10.00	24.67	9.5 till, 29	680	9,333	30.00	56.98	51.50	22.67	23.12	7021.2	0.13
clf-5	s-28	WE85-6	20.00	35.00	21.00	2,000	9,173	469.00	75.89	83.39	4.26	4.52	172090.0	0.33
clf-6	s-15	WE87-17	2.00	3.65	1.65	9,500	15,070	410.00	4.45	48.30	23.17	31.80	3759.0	0.13
clf-7	s-25	WE87-10	10.00	6.50	8.95	1,200	8,840	9.00	7.80	55.12	133.33	138.06	211.5	0.04
clf-8	s-35	WE87-11	2.00	5.21	2.53	8,000	11,477	22.00	3.53	4.75	363.64	471.39	19.1	0.01
clf-9	s-10	WE85M1	15.00	25.00	13.50	9,000	12,228	137.00	16.49	14.52	65.69	88.43	506.4	0.07
clf-10	s-9	WE85-18	5.50	6.69	6.70	5,200	14,088	800.00	51.47	44.77	6.50	7.63	61670.8	0.26



Figure 4.15: Plot of the average hydraulic conductivity versus the permeability estimated by the geoelectrical depth sounding after Katsube and Hume (1987).

Average Conductivity Vs. Estimated Permeability  
 after Katsube & Hume (1987)  
 Johnston, RI.

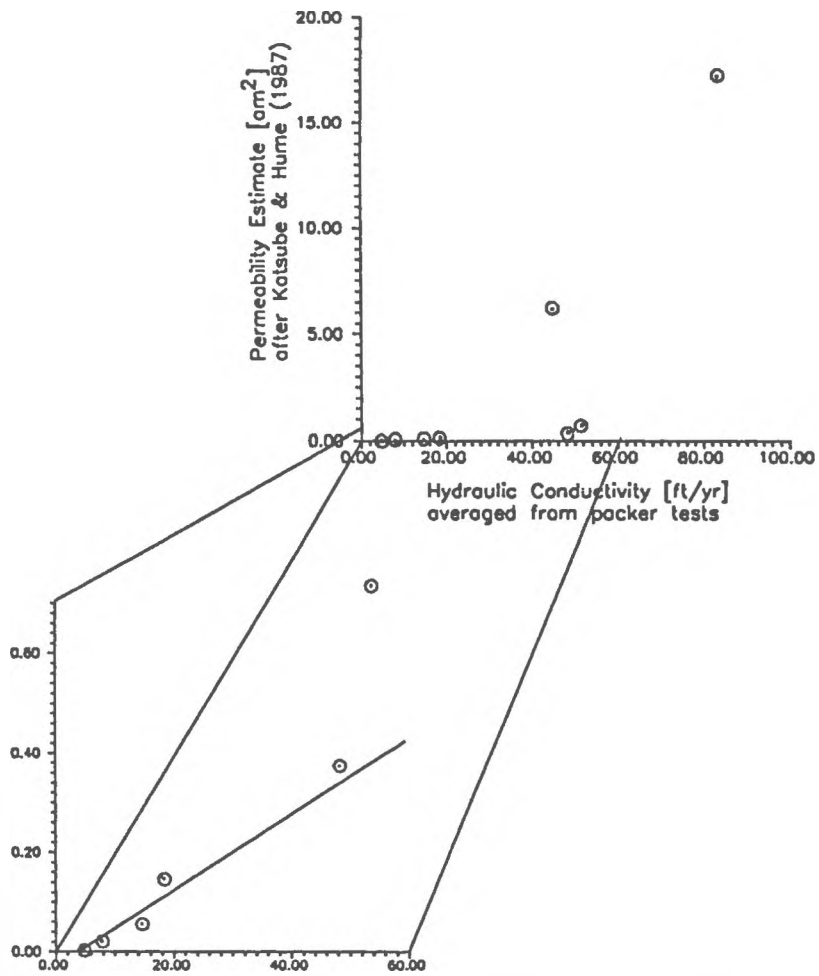


Fig. 4.15

As seen in figure 4.15 two of the points stretch the scale beyond which a relationship may be distinguished. Those two points are data from sounding Clf-10 and Clf-5. These points have the highest values for pore water resistivity which could be the cause for this deviation. When the plot is re-scaled a good linear trend appears. There is one point on this trend which also seems not to fit. This point from Clf-8 has a low pore water resistivity. The effect that the pore water resistivity has on this relationship was addressed in chapter 2.3. These predictive equations are believed not to be valid for extremes in pore water resistivity. Further discussion on this element will be made in the following chapter.

Actual coefficients for the permeability predicting equation 2.13, have never been reported for formation factors measured on the surface. Using equation 2.1, with values  $\rho = 1 \text{ g/cm}^3$ ,  $g = 9.78 \text{ m/s}^2$ ,  $\mu = 1.005 \text{ centipoise at } 20^\circ \text{ C}$ , values for hydraulic conductivity were transformed into values of permeability (see table 4.3). The logarithm of this data was plotted vs. the logarithm of the intrinsic formation factor. Plotted were the five points which fitted the previous linear trend best. (fig. 4.16). This plot shows a good linear relationship with a correlation coefficient of 0.98. The slope of this trend is -1.08 and the y-intercept is -11.80.

The coefficients for the estimating equation 2.13 are now determined to be  $r = 1.08$  and  $\alpha = 7.53 \times 10^{-6}$ . As noted in chapter 2.3, Walsh and Brace (1984) report that  $r$  must be within the range 1 to 3. Also the value for  $\alpha$  falls between the two values used by Katsube and Hume (1987).

$$k = 7.53 \times 10^{-6} F^{-1.08} \quad [am^2] \quad (4.1)$$

note:  $am^2 = \text{atto}(\text{meter})^2 = 10^{-18} \text{ m}^2$

Table: 4.3 Geoelectrical Parameters, Johnston, RI

Column 1: Depth sounding number  
 Column 2: Monitoring well number  
 Column 3: Actual hydraulic conductivity (ft/yr)  
 Column 4: Actual hydraulic conductivity (m/s)  
 Column 5: Actual permeability (m<sup>2</sup>)  
 Column 6: Logarithm of the Actual permeability  
 Column 7: Logarithm of the Intrinsic formation factor  
 Column 8: Permeability estimates after Katsube & Hume (1987)  
 ( $\alpha = 3.31 \times 10^6$ ,  $r = 1.96$ )

Resistivity Sounding	Well #	$K_a$ (ft/yr)	$K_a$ (m/s) [ $\times 10^{-3}$ ]	$k_a$ (m <sup>2</sup> ) [ $\times 10^{-14}$ ]	Log $k_a$ (m <sup>2</sup> )	Log $F_i$	$k_p$ (m <sup>2</sup> ) [ $\times 10^{-14}$ ]
clf-3	WE87M3	18.34	1.77	1.82	-13.74	1.71	0.147
clf-4	WE87M2	51.50	4.98	5.12	-13.29	1.36	0.702
clf-5	WE85-6	83.39	8.06	8.28	-13.08	0.65	17.209
clf-6	WE87-17	48.30	4.67	4.80	-13.32	1.50	0.375
clf-7	WE87-10	7.80	0.75	0.77	-14.11	2.14	0.021
clf-8	WE87-11	4.75	0.43	0.47	-14.33	2.67	0.002
clf-9	WE85M1	14.52	1.40	1.44	-13.84	1.95	0.051
clf-10	WE85-18	44.77	4.33	4.45	-13.35	0.88	6.167

Figure 4.16: Plot of the permeability of the bedrock versus the formation factor, Johnston RI. The correlation coefficient is 0.98.

# Permeability Vs. Formation Factor

Johnston, RI

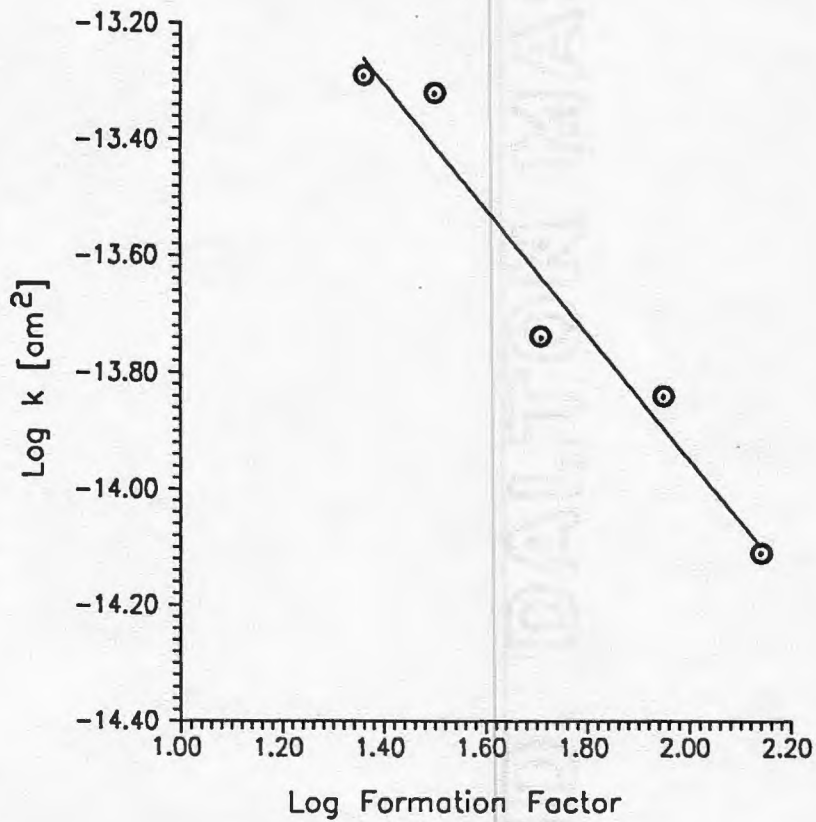


Fig. 4.16

### 4.3 Tiverton, Rhode Island

Several bedrock wells in Northeastern Tiverton, Rhode Island (fig.4.9), have been contaminated with petroleum hydrocarbons since November 1984. The impacted wells are located in the southwest portion of the Fall River Quadrangle. The study, performed for the Water Resources Division of the RI Department of Environmental Management, determined that ground water in the bedrock aquifer was polluted with #2 fuel oil with dissolved concentrations of up to 3600 mg/L. The URI Department of Geology was contracted to study the hydrogeology of the area using their remote sensing and geophysical techniques (Frohlich and Fisher, 1988). Assisting in this study were: J. Savarese (1987, hydrogeology), L. Hanson (1988, seismic refraction) and this author, geoelectrics.

#### 4.3.1 Geologic Setting and Lineament Analysis

The area is underlain by coarse-grained, pink to gray Bulgarmarsh Granite, (Quinn,1971). This granite, a member of the Fall River Pluton, intruded and crystallized during the Precambrian (Zen, 1983). Above the granite, is a cover of poorly sorted till with an average thickness of 20 ft (Allen and Ryan, 1960). This till contains boulders of granite derived locally from the Bulgarmarsh granite. The clay component of the till may originate from the shales of the Narragansett Basin to the north.

Lineaments mapped by Savarese (1987), and lineament orientations, expressed in percent of total length were determined and plotted on a rose diagram (fig 4.17a). This diagram shows a strong, major trend of N15°-30°W. Because of its dominance other trends are suppressed. A histogram of the data (fig. 4.17b), however, shows the minor trends of N65°E, N20°E, N05°E and N45°W. These trends were field checked by measuring the orientations of approximately 300 fractures in the area. A contoured stereo net (fig. 4.18), was then constructed. The strike directions of the measured fractures coincide with the lineaments shown in fig. 4.17.

Figure 4.17a: Rose diagram showing the trends of the lineaments within the Tiverton, RI. area based on percent length of lineaments. Lineaments mapped by Joseph Savarese, (1987).

Figure 4.17b: Histogram showing the trends of the lineaments within the Tiverton, RI. area based on percent length of lineaments. Lineaments mapped by Joseph Savarese, (1987).



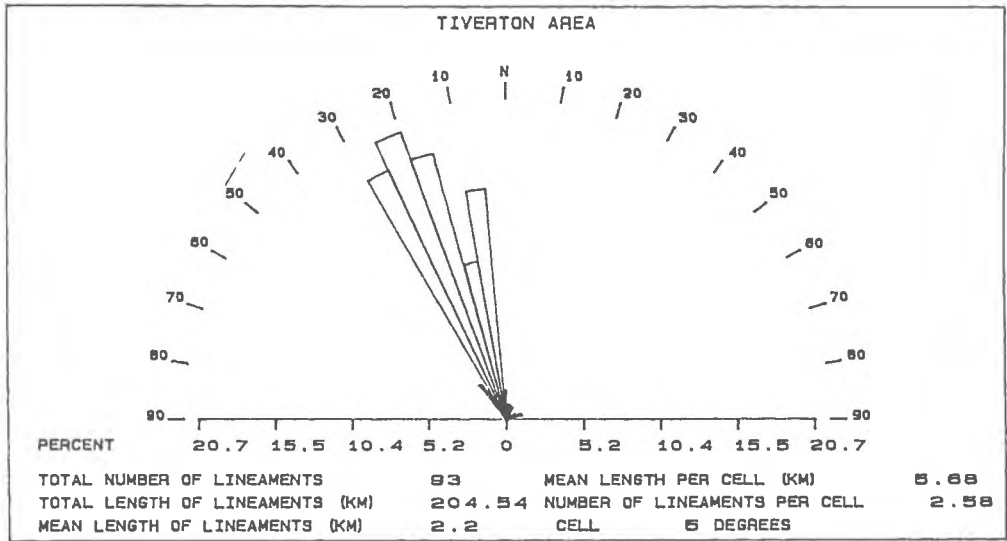


Fig. 4.17a

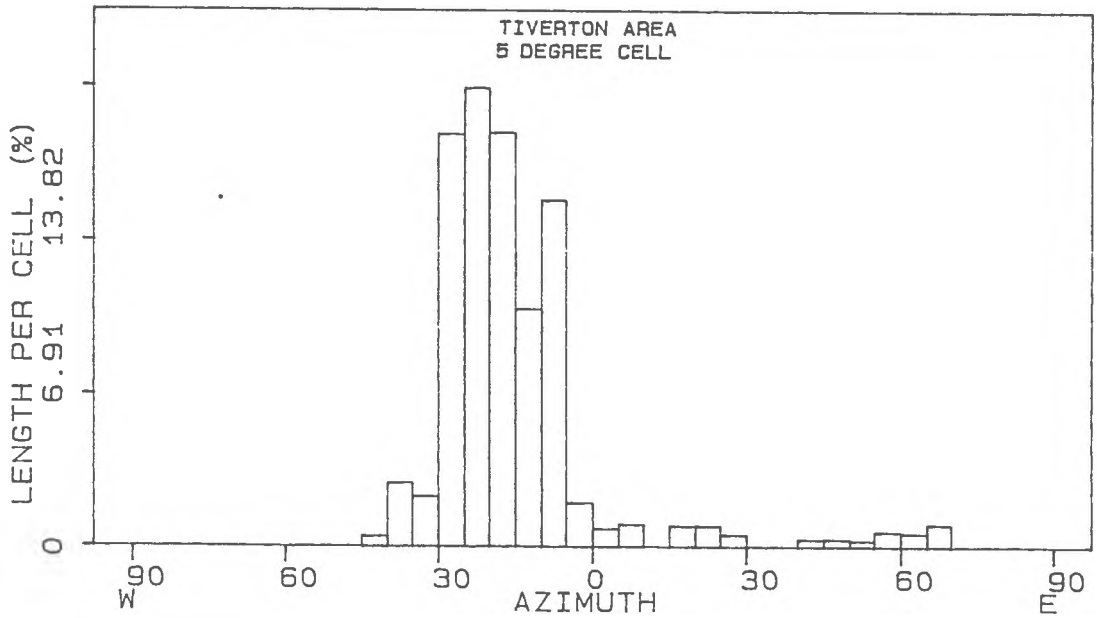


Fig 4.17b

Figure 4.18: Stereo contour plot of poles to fracture planes, Tiverton, RI. Based on 300 measurements.



Stereo Contour Plot  
Poles to Fracture Planes  
Tiverton, RI

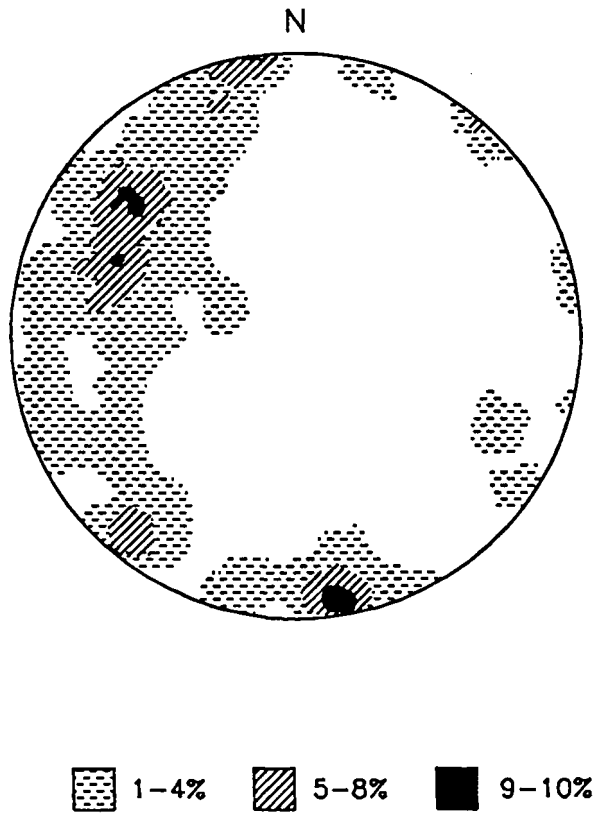


Fig. 4.18

### 4.3.2 Resistivity Soundings

Eight geoelectrical depth soundings after Schlumberger were completed in this study area (fig. 4.19 and appendix 3). All but three of the soundings were interpreted using a two layer model. The three remaining soundings show a dry layer of soil above the water table. Apparent resistivities for the bedrock range from 4,000 to 50,000  $\Omega$  ft (Table 4.4). All soundings showing bedrock resistivities below 10,000  $\Omega$  ft are located along a lineament that is expressed on the ground surface as an elongate swamp (Saverese, 1987). Frohlich et al. (1988), conclude from the interpretation of ground magnetic data that this is a 30 to 40 m wide fracture zone dipping 70°-80° to the east. The suggestion that this lineament is the surface expression of a fracture zone is further supported by low seismic bedrock velocities (table 4.4), which decrease along this zone by approximately 20 % of the compact velocity of 16,000 ft/s (Hanson, 1988).

### 4.3.3 Correlation of Resistivity to Bedrock Parameters

Sjogren et al. (1979) found a correlation between seismic velocity and RQD-factors for crystalline rocks in Sweden. They also suggested a correlation between permeability and RQD-factor. Hanson (1988) showed on the Central landfill also a correlation between seismic velocity and RQD-factor. Because of a relation between permeability and formation factor, a correlation is expected between seismic velocity and formation factor.

Before relationships between resistivity and seismic velocity can be tested, we can compare how these two methods independently measure depth to bedrock (DTB) (fig. 4.20). This plot shows an identity line with only three points differing by more than a few feet in DTB. A linear regression computed on DTB seismic vs. resistivity shows a correlation coefficient of 0.78.

Table: 4.4 Geoelectrical Parameters, Tiverton, RI

Column 1:	Depth sounding number	Column 7:	Pore-water resistivity
Column 2:	Seismic profile number (Hanson, 1988)	Column 8:	Apparent formation factor
Column 3:	Depth to bedrock from the Resistivity model	Column 9:	Intrinsic formation factor
Column 4:	Depth to bedrock from the seismic model (Hanson, 1988)	Column 10:	Permeability estimates after Katsube & Hume (1987) ( $\alpha = 3.31 \times 10^6$ , $r = 1.96$ )
Column 5:	Bedrock resistivity	Column 11:	Porosity estimates after Archie (1942) ( $a = 1.85$ , $m = 0.55$ )
Column 6:	Bedrock seismic velocity (Hanson, 1988)		

Resistivity Sounding	Seismic Profile	Resistivity Depths (ft)	Seismic Depths (ft)	Bulk Resistivity ( $\Omega$ -ft)	Seismic Velocity (ft/s)	Pore Water Resistivity ( $\Omega$ -ft)	$F_a$	$F_i$	k	$\phi$
fl-1	s-2	6.50	6.50	8,000	13,350	54.67	146.25	215.34	88.49	0.04
fl-2	s-2	5.00	6.50	12,000	13,350	65.60	182.92	305.19	44.68	0.03
fl-3	s-2	9.50	6.50	6,000	13,350	59.64	100.67	129.14	241.06	0.05
fl-4	---	25.00	---	50,000	---	79.00	640.20	---	---	---
fl-5	s-1	13.15	11.00	20,000	16,250	79.00	256.08	583.09	12.56	0.02
fl-6	s-4	6.50	8.80	4,000	11,000	72.89	54.90	62.36	1004.25	0.08
fl-7	s-3	9.52	6.50	19,000	15,900	82.00	228.92	459.05	20.07	0.03
fl-8	---	8.60	---	8,500	---	72.89	116.60	156.58	165.25	0.05

Figure 4.19: Location of Tiverton study area. Geoelectrical soundings are labeled Fl, and seismic soundings S.

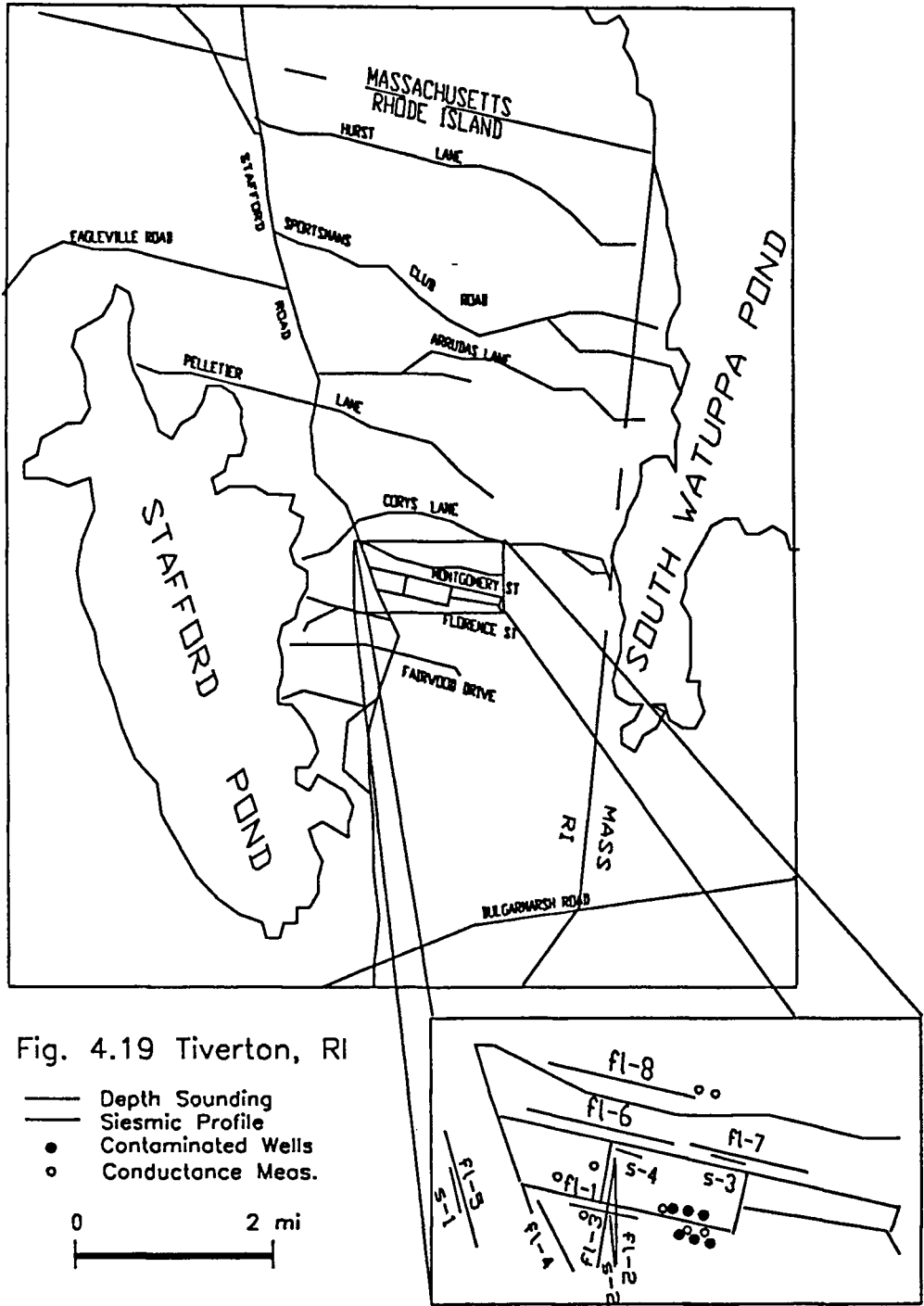


Figure 4.20: Plot of estimated depth to bedrock, seismic versus geoelectrical sounding. The line drawn represents an identity line since the two should be equal.



Estimated Depth to Bedrock  
Johnston and Tiverton, RI

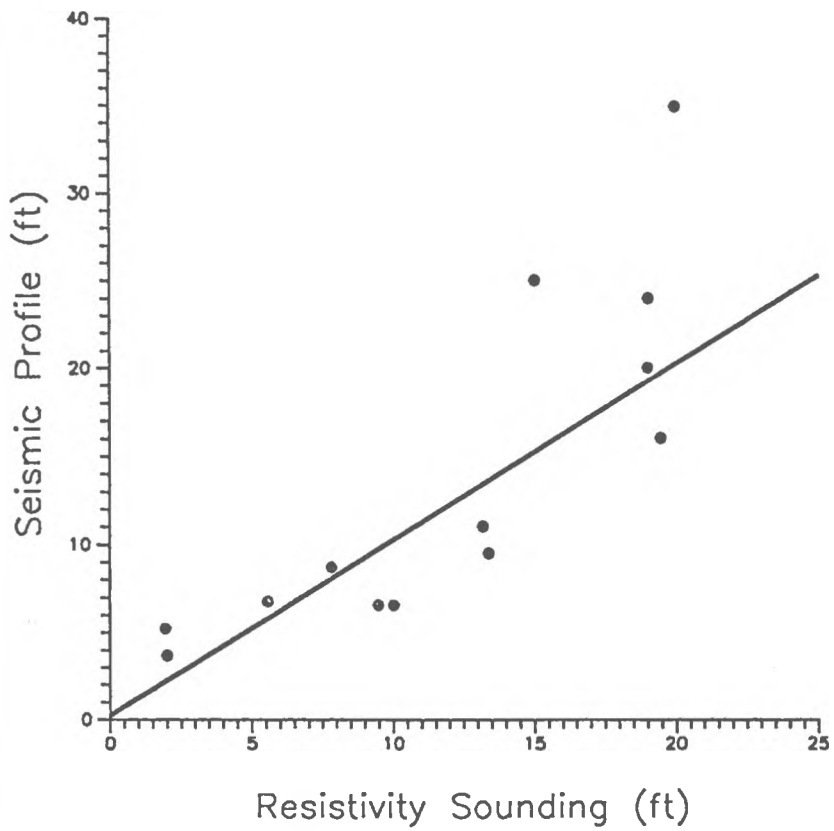


Fig. 4.20

The standard deviation of the difference between DTB interpreted from these two methods amounts to 5.0 ft. This is an expected deviation, given the accuracy of both methods (note the scatter in fig. 4.14, in which resistivity was compared to the actual depth). Seismic refraction and electrical depth sounding interpretation produce similar depths to bedrock which agree with borehole data.

As mentioned in chapter 2.3 the logarithmic function of the formation factor should be linearly related to the logarithm of porosity and permeability, and thus to the logarithm of bedrock velocity. Figure 4.21 shows seismic velocities versus apparent formation factors on a bilogarithmic scale. While the data are widely scattered, one set (black points) shows a linear trend indicated by the least squares' regression line. Points that do not follow this trend are characterized by extreme pore water resistivities. The group to the top left (clf-3,5,6,10) has pore water resistivities of 219  $\Omega$ ft and greater. Points to the bottom right (clf-7 and 8) have pore water resistivities of 22  $\Omega$ ft or less. All data about this trend have pore water resistivities that lie between these extreme values.

The theory discussed in chapter 2.2 suggests clay effects, though constant within a range of conductivities, may alter the values of formation factor, when dealing with high and low pore water resistivity. It is well known that the relationship between ionic concentration and conductance is linear up to the point when the solution becomes so concentrated that ionic mobility is restricted. Charged clay particles within a fracture have the effect of increasing this concentration and further restricting ionic mobility by the creation of the double layer. Thus, for high specific conductances (low resistivities) the measured pore water resistance does not account for the total resistance of the pore, which is higher under these conditions. This leads to a higher value for the formation factor than would be consistent with equations for hydrogeologic parameters. This could explain the shift to the right of points Clf-7 and Clf-8 in fig. 4.21.

Figure 4.21: Plot of apparent formation factor versus seismic velocity, Johnston and Tiverton, RI. Soundings marked by x had high pore water resistivities, those marked by o had low pore water resistivities relative to the points about the line.

# Formation Factor Vs. Velocity

Johnston and Tiverton, RI

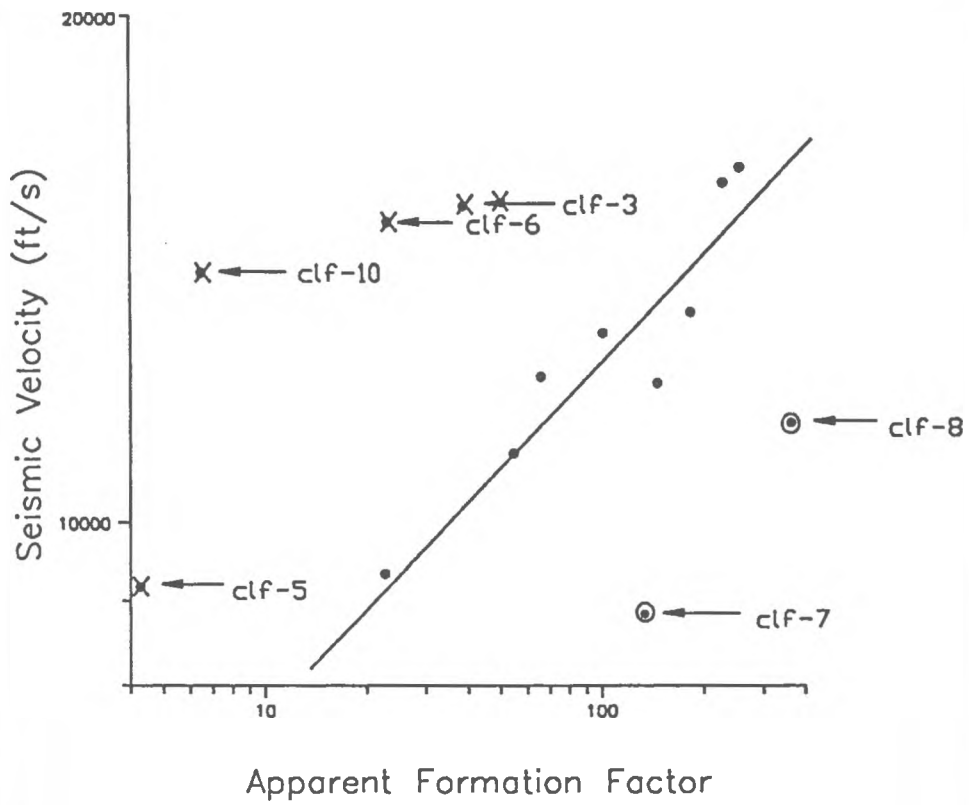


Fig. 4.21

Also noted in section 2.2 is that equation 2.17, is invalid for high pore water resistivities. The theory for the effect of low pore water conductivity is complex, particularly if clay effects are considered.

The added conduction of the clay particles themselves is also not accounted for in the apparent formation factor. Thus, the bulk resistivity must be divided by what would amount to a lower resistivity for the pore system. This would have the effect of increasing the formation factor, thus, shifting those points to the right. If this bit of digression means anything, then using formation factors with extremely high or low pore water resistivities can decrease the inherent correlation between these two parameters considerably. A plot of seismic velocity versus bulk resistivity was made to see if the relationship became better defined (fig. 4.22). Replacing apparent formation factors with bulk resistivities produces a better correlation with seismic velocities, which includes points of extreme pore water resistivities.

From these observations, it would appear that in dealing with an area with an extreme variability in pore water resistivity, the bulk resistivity, and not the formation factor, better describes the relative hydraulic characteristics of the bedrock.

A geoelectrical profile after Schlumberger was also completed in the Tiverton area. This profile supports the interpretation of a fracture zone located roughly perpendicular to Florence Ave. Profile FI-1p shows the relationship of resistivity to the actual bedrock profile as shown in Savarese (1987), (fig. 4.23). It should be pointed out that profiling and AB-rectangle measurements show larger and sometimes discontinuous lateral variations than depth sounding data taken with increased electrode separations.

Figure 4.22: Plot of bedrock resistivity versus seismic velocity, Johnston and Tiverton, RI.

# Bedrock Resistivity Vs. Seismic Velocity

Johnston and Tiverton, RI

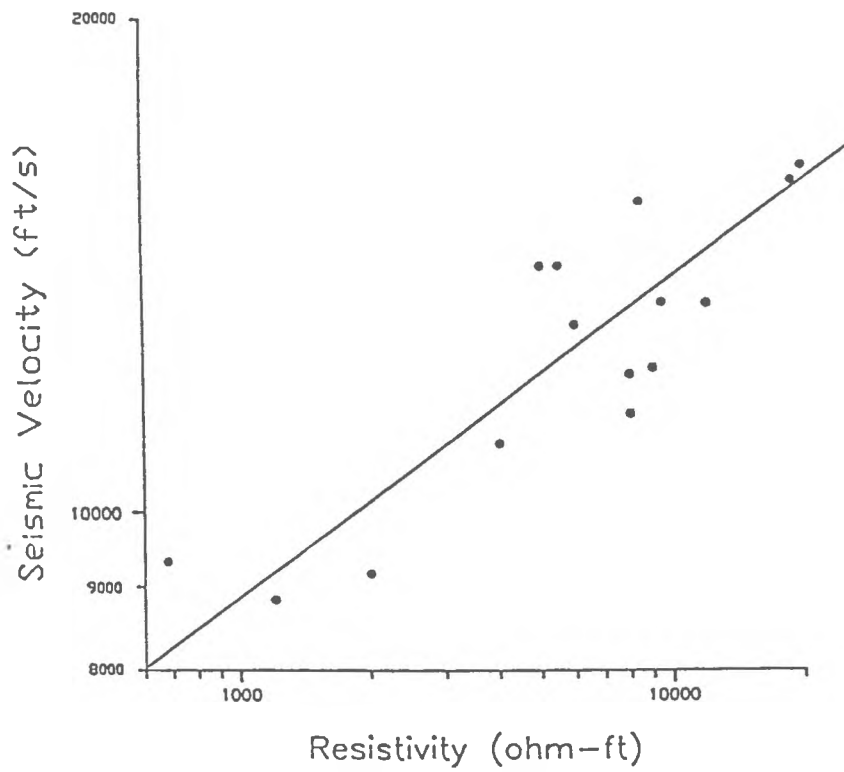


Fig. 4.22

Figure 4.23: Geoelectrical profile FI-1p shown in relation to the geologic profile by Savarese (1987).



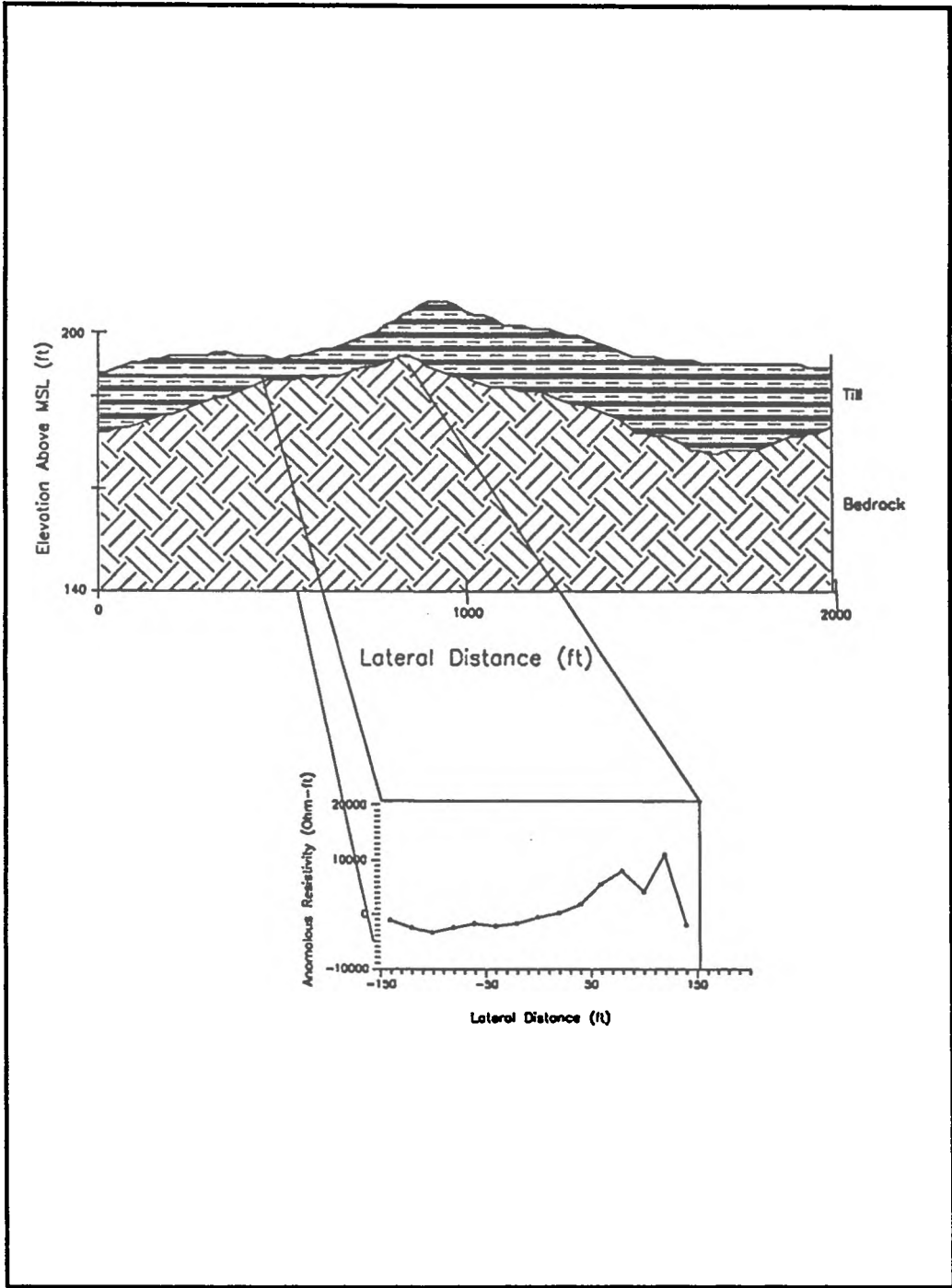


Fig. 4.23

## 5. SUMMARY

This study has presented the theory, the methodology and practical examples for using direct current resistivity to estimate the water transmitting properties of fractured bedrock.

### 5.1 Theory

The theory presented is an up to date summary relating electrical resistivity to hydraulic parameters. It was the authors intent to have this theory in this paper to help those who are not already familiar with it. This background information is crucial in the understanding that the relationships found are based on actual physical properties. It has been shown that the logarithm of permeability in fractured rock is inversely related to the log function of the formation factor. The effects of fracture frequency, fracture tortuosity, roughness and degree of weathering on the formation factor have been discussed.

### 5.2 Methodology

The methods used in this study have also been presented. The main tool used in the field studies has been the geoelectrical depth sounding after Schlumberger. This is a common technique and has been presented only to clarify the specific procedures and interpretation techniques used by the author.

A second method, the AB-rectangle technique, has also been presented. This technique has been presented because it allows for many more measurements to be made spatially over an area in substantially less time than multiple depth soundings. However, in the past this method was not able to give "true" apparent resistivity changes within a layer. This was due to the relative change in the depth penetration of the measurement as the potential electrodes were moved. Though this method was not used extensively in this study, procedures have been developed and presented to aid future studies for which

the AB-rectangle would be useful. Simply put the procedure includes a method to focus the measurements within a layer and "filter" out the effect of the change in measurement depth. The measurement and the interpretation is conducted in 5 steps:

1. A geoelectrical depth sounding is conducted and interpreted for the derivation of the horizontal layer model.
2. The choices of the optimal distance AB (or L) and the rectangle length and width are made.
3. Calculation of the expected resistivity inside the rectangle due to the horizontal layer case from step 1. or from additional depth soundings.
4. Measurement of the apparent resistivity inside the rectangle.
5. Subtraction of 3. from 4. yielding the residual resistivity due to lateral resistivity changes.

### 5.3 Field Studies

Fifty depth soundings were completed to analyze the theory relating electrical resistivity to fluid flow through fractured bedrock. Comparisons have been made with available information believed to characterize flow in two separate study areas (Johnston, RI and northeastern Maine). Relationships have been demonstrated which are specific to each study area, but which can be applied in a broad sense elsewhere. These relationships have been predicted by theory of both flow of fluid and electrical current through fractured rock.

In the Maine study area bedrock resistivity was compared to yields in domestic wells. This relationship proved not to be significant enough to predict well yields. However, apparent resistivity of the bedrock was used to locate areas of potentially higher well yield. Although actual predictions of that yield are not possible, a relative ranking from high to low in an area is possible (fig. 4.9).

In the Johnston study area a relationship between hydraulic conductivity and predicted permeability, after Katsube and Hume (1987), was suggested (fig. 4.16). Although this relationship lacks sufficient data to be statistically valid, it again shows that a general

ranking from low to high values in an area is possible. Coefficients calculated for this relationship correspond to the lower limit of the range,  $1 < r < 3$ , in equation 2.13, presented by Walsh and Brace (1986). It should be further noted that permeability estimates were compared to hydraulic conductivity found by averaging packer intervals in a well. It is not known whether this is an accurate characterization of the bedrock aquifer. It would have been preferred if more conventional, yet more inconvenient, pumping tests were run on these wells.

Eight soundings were completed near wells. Another eight were completed next to complementary seismic refraction profiles. This allowed for the evaluation of the resistivity depth sounding method to accurately characterize the bedrock layer given the inherent problem with equivalence. Depth sounding interpretations were all made without the above mentioned prior information. Comparisons between the depth to bedrock as interpreted by the depth sounding to the actual depth to bedrock and that measured by seismic refraction were good (fig. 4.14, and fig. 4.20). This is due to accurate interpretations of, in most cases the final asymptotic branches, which characterize the bedrock.

Comparison to another method of characterizing aquifers, that of seismic velocity, shows some very interesting results. Suggested in figure 4.20 is the possible dependence of this relationship on a range of pore water resistivities. This range of pore water resistivities was  $22 < \rho_w < 220 \Omega \text{ ft}$ , or  $150 < \sigma_w < 1,500 \mu \text{ S/cm}$ . It appears, comparing fig. 4.21 to fig. 4.23, that in an area of inhomogeneous pore water resistivities, the apparent resistivity is a better parameter to rank sites than would be the formation factor of the bedrock.

Two computer programs totaling 2,580 lines of code were written. These programs provide for storage, interpretation, and presentation of all geoelectrical methods in use by the Department of Geology (URI). The interpretation procedures in the first program

were rewritten from Koefoed (1979). These procedures in the second program were developed using general theory, and linear filters found in Merrick and O'Neill (1984). The programs were written in Turbo Pascal for IBM PC's with parallel printers accommodated by PC DOS, and HP plotters using the COM1: port. The implementation of these programs has been checked by comparisons to master curve sets by Orellana and Mooney (1966) and by, comparison to an older version of the depth sounding interpretation program, and by evaluation of a depth sounding using both the first and second programs to obtain equal results. These programs speed interpretation and presentation of geoelectrical data and also provide the option of storage that will facilitate use of new and old data in the future.

## 6. CONCLUSION

The geoelectrical depth sounding has proved a useful tool in evaluating the hydrogeology of three areas. Attempts were made producing good results with the direct comparison of bedrock resistivity to hydrogeologic parameters. It was not the intent of this study to suggest that the geoelectrical depth sounding method could replace exploratory drilling and in-hole hydraulic testing. However, drilling into bedrock is costly and the results of this study show that good estimates of the hydraulic conductivity may be made between wells for which the hydraulic conductivity has been calculated.

The limitations of AB Rectangle and Schlumberger profiling techniques have been minimized. It must be pointed out that, in fractured bedrock, resistivity highs and lows may be due to other than changes in the porosity and permeability. Since all interpretations are made based on the layer model from a depth sounding, deviations from this model will cause anomalous resistivity values. For instance, if the depth to bedrock increases, this will produce an resistivity low. Changes in the pore water resistivity will also change values without indicating changes in the hydraulic characteristics of the bedrock aquifer. However, both of these observations may be useful in placing a monitoring well. Hanson (1988) has indicated a relationship between depth of bedrock and degree of fracturing in a glaciated area. High pore water resistivities may indicate contamination of aquifers from salt water intrusion or non-organic pollutants. Therefore, resistivity lows located with the profiling or AB rectangle techniques are worth investigating even if not directly related to changes in porosity and permeability.

In final conclusion it has been found that:

1. Electrical resistivity measurements can aid in the siting of bedrock production or monitoring wells.
2. Electrical resistivity measurements can provide good estimates of the hydraulic conductivity between existing bedrock wells with known hydraulic conductivities. This is extremely valuable for subsequent placing of monitoring wells and groundwater modeling of an area.
3. These methods can also aid in verifying buried fracture zones as seen on areal photos or satellite imagery which may be geologically significant to the regional structure.

## **APPENDIX 1a.**

### Computer Methods



## COMPUTER METHODS

Programs written, in Pascal, for these interpretation are; "Sounding", and "Rectangle". The first program is a data collection, storage, and interpretation routine for the Schlumberger resistivity depth sounding. The interpretation procedures were actually rewritten from the language of Fortran in Koefoed (1979). This is an interactive program that has prompts that allow anyone to enter error free data when using the program for the first time. The program allows for data to be entered to either include or not, forward and reverse measurements. Final draft data sheets are produced in either mode. These sheets are best when the program is used with the letter quality printers.

The second half of the first program is a graphing routine to produce final draft plots on a HP 7475 plotter. The only important information that is needed to run this program, which is automatically started by the first program, is the "Dip Switch" settings on the plotter itself. Just follow the settings for the HP Basic, which are explained in the manual for the plotter. The program draws single or multiple plots. It can also use two scales for the resistivity (ordinate axis), 100 - 30,000 or 1,000 - 300,000, for those rare curves with resistivities over 30,000. You will be asked to input the model at the end of the plot. Confusing here might be the thickness on the last layer. This is the depth to which you "feel" the sounding has reached. These plots are to the scale of the master curves for easy reinterpretation using the auxiliary point method.

The second program "Rectangle", was written to analyze AB Rectangles or Schlumberger profiles. The program produces data sheets for final copies (tab. 3.3) and can export data files specifically designed for easy import into other plotting software. The program calculates resistivities from a horizontal layer case. These values differ spa-

tially, forming a surface resembling a saddle function, as seen in a typical model case. A contour map can then be prepared plotting the difference between the measured apparent resistivity and the resistivity calculated by the program at that point.

Almost all of the figures created for this study were done so on the computer drafting package AutoCAD. The contour maps mentioned about were created using Surfer, a contouring package. These maps may be written to a .dxf file easily readable by AutoCAD. Note that AutoCAD may only read one .dxf file into a drawing. If you must import more than one create a new drawing import the .dxf file into it then insert that new drawing into your destination drawing by using the insert (Block) command.

The stereo plot for Tiverton was created using STEREO by Rockware, Inc. This plot was imported into AutoCAD by reformatting the drawing in GRIDZO by Rockware, as a script file and calling it up in AutoCAD as the same. The lineaments were digitized into FAS, software also by Rockware, using a digitizing routine I modified for the Huston instruments HiPAD. The program is stored on the departments main student computers hard drive. The Title is Digitize and its written in IBM basica.

**APPENDIX 1b.**

Listing of the Depth Sounding Program

## DEPTH SOUNDING PROGRAM

```
program sounding (input,output,diskfile);
(*$I GRAPH.P*)
{$U+}
const pi = 3.1415927;

type
  taray      = array[1..5,1..100] of real;
  wastary    = array[1..100] of real;
  sterioray  = array[1..200] of integer;
  symblaray  = array[1..200] of string[3];
  dataray    = array[1..5,1..100,1..4] of real;
  char12arr  = array[1..12] of char;
  strary     = array[1..5] of string[20];
  string20   = string[20];
  regrec =
    record
      ax,bx,cx,dx,bp,si,di,ds,es,flags : integer;
    end;

var
  project      : string[20];
  locat       : string[30];
  oper        : strary;
  prof        : string[8];
  date        : string[10];
  ra,l,yhat,dev : taray;
  b           : wastary;
  potelc,a    : integer;
  potnum      : sterioray;
  modl        : char;
  outfile,diskfile : text;
  cnprog,sies : file;
  volt,amp    : dataray;
  n,meas,m1,count : integer;
  filename    : string[10];
  save,graph,inptype : char;
  pos,kr      : taray;
  reverse,view,zofa : char;
  mn,s,th     : wastary;
  f,x1,x2,y,bo : real;
  t,resist,thick : wastary;
  num,nu,m    : integer;

  plott : char;
  Port,Baud,StopBits,DataBits,Par: Integer;
  Message: String[80];
  xz,yz,xz1,yz1,i,j,pen,q,r,u,layers,curve,curv : integer;
```

```

xx,yy,mult,xp,yp,depth : real;
scale,model : char;
yayer,layers,layer,labl : wastary;
return : text;

```

```

type
  String19=String[19];

```

```

Type
  __RegisterSet=Record case Integer of
    1: (AX,BX,CX,DX,BP,DI,SE,DS,ES,Flags: Integer);
    2: (AL,AH,BL,BH,CL,CH,DL,DH: Byte);
  end;
  __ParityType=(None,Even,Odd);

```

```

var
  __Regs: __RegisterSet;
  InError,OutError: Array [1..2] of Byte;

```

```

procedure __Int14(PortNumber,Command,Parameter: Integer);
{ do a BIOS COM driver interrupt }

```

```

begin
  with __Regs do
    begin
      DX:=PortNumber-1;
      AH:=Command;
      AL:=Parameter;
      Flags:=0;
      Intr($14,__Regs);
    end;
end;

```

```

procedure SetSerial(PortNumber,BaudRate,StopBits,DataBits: Integer;
  Parity: __ParityType);
{ Set serial parameters on a COM port }

```

```

var
  Parameter: Integer;
begin
  case BaudRate of
    110: BaudRate:=0;
    150: BaudRate:=1;
    300: BaudRate:=2;
    600: BaudRate:=3;
    1200: BaudRate:=4;
    2400: BaudRate:=5;
    4800: BaudRate:=6;
    else BaudRate:=7; { Default to 9600 baud }
  end;
  if StopBits=2 then StopBits:=1
  else StopBits:=0; { Default to 1 stop bit }

```

```

if DataBits=7 then DataBits:=2
else DataBits:=3; { Default to 8 data bits }
Parameter:=(BaudRate Shl 5)+(StopBits Shl 2)+DataBits;
case Parity of
  Odd: Parameter:=Parameter+8;
  Even: Parameter:=Parameter+24;
  else; { Default to no parity }
end;
__Int14(PortNumber,0,Parameter);
end;

```

```

Function SerialStatus(PortNumber: Integer): Integer;
{ Return the status of a COM port }
begin
  __Int14(PortNumber,3,0);
  SerialStatus:=__Regs.AX;
end;

```

```

procedure __OutPort1(C: Byte);
{ Called by Write to Aux or Usr when assigned to COM1 }
begin
  while (SerialStatus(1) and $30)=0 do ;
    __Int14(1,1,C);
    OutError[1]:=OutError[1] Or (__Regs.AH and $8E);
end;

```

```

procedure __OutPort2(C: Byte);
{ Called by Write to Aux or Usr when assigned to COM2 }
begin
  while (SerialStatus(2) and $30)=0 do ;
    __Int14(2,1,C);
    OutError[2]:=OutError[2] Or (__Regs.AH and $8E);
end;

```

```

Function __InPort1: Char;
{ Called by Read from Aux or Usr when assigned to COM1 }
begin
  __Int14(1,2,0);
  __InPort1:=Chr(__Regs.AL);
  InError[1]:=InError[1] Or (__Regs.AH and $8E);
end;

```

```

Function __InPort2: Char;
{ Called by Read from Aux or Usr when assigned to COM2 }

```

```

begin
  __Int14(2,2,0);
  __InPort2:=Chr(__Regs.AL);
  InError[2]:=InError[2] Or (__Regs.AH and $8E);
end;

```

```

procedure __AssignPort(PortNumber: Integer; var InPtr,OutPtr: Integer);
{ Assign either Aux or Usr to either COM1 or COM2 }

```

```

begin
  if PortNumber=2 then
    begin
      OutPtr:=Ofs(__OutPort2);
      InPtr:=Ofs(__InPort2);
    end
  else { Default to port 1 }
    begin
      OutPtr:=Ofs(__OutPort1);
      InPtr:=Ofs(__InPort1);
    end;
  InError[PortNumber]:=0;
  OutError[PortNumber]:=0;
end;

```

```

procedure AssignAux(PortNumber: Integer);
{ Assign Aux to either COM1 or COM2 }

```

```

begin
  __AssignPort(PortNumber,AuxInPtr,AuxOutPtr);
end;

```

```

procedure AssignUsr(PortNumber: Integer);
{ Assign Usr to either COM1 or COM2 }

```

```

begin
  __AssignPort(PortNumber,UsrInPtr,UsrOutPtr);
end;

```

```

Function Binary(V: Integer): String19;

```

```

var
  I: Integer;
  B: Array [0..3] of String[4];
begin
  For I:=0 To 15 do
    if (V and (1 Shl (15-I)))<>0 then B[I Div 4][(I Mod 4)+1]:='1'
    else B[I Div 4][(I Mod 4)+1]:='0';
  For I:=0 To 3 do B[I][0]:=Chr(4);
  Binary:=B[0]+' '+B[1]+' '+B[2]+' '+B[3];
end;

```

```

procedure resmodel;
begin
  writeln(' Do You wish to include a model ');
  repeat
    read(model);
  until model in ['y','n'];
  if model = 'y' then
    begin
      clrscr;
      writeln(' Input the Number of Layers');
      readln(layers);
      depth := 0;
      for r := 1 to layers do
        begin
          writeln(' Input the thickness of Layer ',r);
          readln(layer[r]);
          writeln('Input the Resistivity of Layer ',r);
          readln(layres[r]);
        end;
      writeln(usr,'sm;');
      if scale = '1' then
        begin
          writeln(usr,'sp3;pa1000,1250;pd;');
          for u := 1 to layers do
            begin
              depth := depth + layer[u];
              ylayer[u] := ((ln(depth)/ln(10))+1)*1000;
              if u = layers then
                begin
                  writeln(usr,'pa',ylayer[u]:7:2,',1250;');
                  writeln(usr,'pa',(ylayer[u]-30):7:2,',1175;');
                  writeln(usr,'pa',(ylayer[u]+50):7:2,',1050;');
                  writeln(usr,'pa',ylayer[u]:7:2,',1000;');
                end;
              if u < layers then
                begin
                  writeln(usr,'pa',ylayer[u]:7:2,',1250;');
                  writeln(usr,'pa',ylayer[u]:7:2,',1000;');
                end;
              writeln(usr,'pu;di0,1;cp-1,1;lb',layres[u]:6:0,'^O;');
              writeln(usr,'pu1000,1250;pd');
            end;
        end;
      if scale = '2' then
        begin
          writeln(usr,'sp3;pa1000,2250;pd;');
          for u := 1 to layers do
            begin
              depth := depth + layer[u];
              ylayer[u] := ((ln(depth)/ln(10))+1)*1000;
              if u = layers then
            
```



```

begin
  writeln(usr,'pa',ylayer[u]:7:2,',2250;');
  writeln(usr,'pa',(ylayer[u]-30):7:2,',2175;');
  writeln(usr,'pa',(ylayer[u]+50):7:2,',2050;');
  writeln(usr,'pa',ylayer[u]:7:2,',2000;');
end;
if u < layers then
begin
  writeln(usr,'pa',ylayer[u]:7:2,',2250;');
  writeln(usr,'pa',ylayer[u]:7:2,',2000;');
end;
writeln(usr,'pu;di0,1;cp-1,1;lb',layres[u]:6:0,'^O;');
writeln(usr,'pu1000,2250;pd');
end;
end;
end;
end;
procedure graf;
var   ab,b,bb : integer;
begin
  a := 0;
  b := 0;
  bb := 0;
  writeln(' Input y the scale you want');
  writeln(' 1 for 100-30,000');
  writeln(' 2 for 1,000-300,000');
  repeat
    readln(scale);
  until scale in ['1','2'];
  writeln(usr,chr(27),'.@');
  writeln(usr,'ip 355,710,10365,6920');
  if scale = '1' then
  begin
    WriteLn(Usr,'pa;dt^O;sc 1000,5000,1000,3477');
    if modl = 'y' then resmodel;
    writeln(usr,'sp1;pa1000,1000;pd1000,3477,5000,3477,5000,1000,1000,1000;pu;');
    mult := 1;
    for xz1 := 1 to 4 do
    begin
      mult := mult * 10;
      for xz := 1 to 10 do
      begin
        xx := (ln(mult*xz)/ln(10))*1000;
        writeln(usr,'pa',xx:7:2,',',1000,',');
        writeln(usr,'xt;');
      end;
    end;
    mult := 1;
    for yz1 := 1 to 3 do
    begin

```

```

mult := mult * 10;
for yz := 1 to 10 do
begin
  yy := (ln(mult*yz)/ln(10))*1000;
  if yy < 3478 then
  begin
    writeln(usr,'pa',1000,',',yy:7:2,',');
    writeln(usr,'yt');
  end;
end;
end;
writeln(usr,'dt^O;pa 980,940;lb1^O;');
writeln(usr,'pa 1954,940;lb10^O;');
writeln(usr,'pa 2940,940;lb100^O;');
writeln(usr,'pa 3905,920;lb1000^O;');
writeln(usr,'pa 940,1000;lb100^O;');
writeln(usr,'pa 940,2000;lb1000^O;');
writeln(usr,'pa 940,3000;lb10000^O;');
writeln(usr,'sp1;si0.24,0.32;pa 2000,820;');
writeln(usr,'lbHalf Electrode Spacing [L/2] (ft)^O;');
writeln(usr,'pa 910,1400;di0,1;lbApparent Resistivity (ohm-ft)^O;');
writeln(usr,'di;sp2;pa 1260,3800;si.3,.41');
writeln(usr,'lbGeoElectrical Depth^O;');
writeln(usr,'lb Sounding After Schlumberger^O;');
writeln('Please Hit a Key When Plotting Stops');
  repeat
    until keypressed;
  writeln(usr,'sp3;si;pa1500,3700;');
  writeln(usr,'lbProject : ',project,'^O');
  writeln(usr,'pa1500,3620;');
  writeln(usr,'lbLocation : ',locat,'^O');
  writeln(usr,'pa1500,3540;');
  writeln(usr,'lbOperators:^O');
  for ab := 1 to (a-1) do
  begin
    write(usr,'lb ',oper[ab],', ^O');
  end;
  writeln(usr,'lb ',oper[a],'^O');
  writeln(usr,'pa3500,3620;');
  writeln(usr,'lbProfile : ',prof,'^O');
  writeln(usr,'pa3500,3540;');
  writeln(usr,'lbDate : ',date,'^O');
  writeln(potelc,' ',potnum[1]);
  clrscr;
  writeln(' Hit any Key to Plot Data');
  repeat
  until keypressed;
  pen := 3;
  for i := 1 to potelc do
  begin
    pen := pen + 1;
    writeln(usr,'sp4;smo');
  end;
end;

```

```

if i = 2 then writeln(usr,'smx');
if i = 3 then writeln(usr,'sm*');
for j := 1 to potnum[i] do
begin
  xp := ((ln(l[i,j])/ln(10))+1)*1000;
  yp := ((ln(ra[i,j])/ln(10))-1)*1000;
  writeln(usr,'pa',xp:7:2,',',yp:7:2,',');
  writeln(usr,'pd;pu');
  writeln(l[i,j],ra[i,j]);
end;
end;
end;
if scale = '2' then
begin
  WriteLn(Usr,'pa;sc 1000,5000,2000,4477');
  if modl = 'y' then resmodel;
  writeln(usr,'sp1;pa1000,2000;pd1000,4477,5000,4477,5000,2000,1000,2000;pu');
  mult := 1;
  for xz1 := 1 to 4 do
  begin
    mult := mult * 10;
    for xz := 1 to 10 do
    begin
      xx := (ln(mult*xz)/ln(10))*1000;
      writeln(usr,'pa',xx:7:2,',',2000,',');
      writeln(usr,'xt;');
    end;
  end;
  mult := 10;
  for yz1 := 1 to 3 do
  begin
    mult := mult * 10;
    for yz := 1 to 10 do
    begin
      yy := (ln(mult*yz)/ln(10))*1000;
      if yy < 4478 then
      begin
        writeln(usr,'pa',1000,',',yy:7:2,',');
        writeln(usr,'yt');
      end;
    end;
  end;
  writeln(usr,'dt^O;pa 980,1940;lb1^O;');
  writeln(usr,'pa 1954,1940;lb10^O;');
  writeln(usr,'pa 2940,1940;lb100^O;');
  writeln(usr,'pa 3905,1920;lb1000^O;');
  writeln(usr,'pa 940,2000;lb10000^O;');
  writeln(usr,'pa 940,3000;lb100000^O;');
  writeln(usr,'pa 940,4000;lb1000000^O;');
  writeln(usr,'sp1;si0.24,0.32;pa 2000,1820;');
  writeln(usr,'lbHalf Electrode Spacing [L/2] (ft)^O;');
  writeln(usr,'pa 910,2400;di0,1;lbApparent Resistivity (ohm-ft)^O;');

```

```

writeln(usr,'di;sp2;pa 1260,4800;si.3,.41');
writeln(usr,'lbGeoElectrical Depth^O;');
writeln(usr,'lb Sounding After Schlumberger^O;');
writeln(usr,'sp3;si;pa1500,4700;');
writeln('Please Hit a Key When Plotting Stops');
  repeat
  until keypressed;
writeln(usr,'lbProject : ',project,'^O');
writeln(usr,'pa1500,4620;');
writeln(usr,'lbLocation : ',locat,'^O');
writeln(usr,'pa1500,4540;');
writeln(usr,'lbOperators:^O');
for ab := 1 to (2) do
begin
write(usr,'lb ',oper[ab],', ^O');
end;
writeln(usr,'lb ',oper[3],'^O');
writeln(usr,'pa3500,3620;');
writeln(usr,'lbProfile : ',prof,'^O');
writeln(usr,'pa3500,4540;');
writeln(usr,'lbDate : ',date,'^O');
writeln(potelc,' ',potnum[1]);
clrscr;
writeln(' Hit any Key to Plot Data');
repeat
until keypressed;
pen := 3;
for i := 1 to potelc do
begin
writeln(potelc);
pen := pen + 1;
writeln(usr,'sp4;smo');
if i = 2 then writeln(usr,'smx');
if i = 3 then writeln(usr,'sm*');
writeln(usr,'sp4;sm*');
for j := 1 to potnum[i] do
begin
xp := ((ln(l[i,j])/ln(10))+1)*1000;
yp := ((ln(ra[i,j])/ln(10))-1)*1000;
writeln(usr,'pa',xp:7:2,',',yp:7:2,',');
writeln(usr,'pd;pu');
writeln(l[i,j],ra[i,j]);
end;
end;
end;
end;
end;

```

```

procedure resmodel2;

```

```

begin
  writeln(' Do You wish to include a model ');
  repeat
  read(model);
  until model in ['y','n'];
  if model = 'y' then
  begin
    clrscr;
    writeln(' Input the Number of Layers');
    readln(layers);
    depth := 0;
    for r := 1 to layers do
    begin
      writeln(' Input the thickness of Layer ',r);
      readln(layer[r]);
      writeln('Input the Resistivity of Layer ',r);
      readln(layres[r]);
    end;
    writeln(usr,'sm;');
    if scale = '1' then
    begin
      writeln(usr,'sp3;pa1000,',(1150+150*curve),',');
      for u := 1 to layers do
      begin
        depth := depth + layer[u];
        ylayer[u] := ((ln(depth)/ln(10))+1)*1000;
        if u = layers then
        begin
          writeln(usr,'pd;pa',ylayer[u]:7:2,',',(1150+150*curve),',');
          writeln(usr,'pa',(ylayer[u]-20):7:2,',',(1100+150*curve),',');
          writeln(usr,'pa',(ylayer[u]+30):7:2,',',(1050+150*curve),',');
          writeln(usr,'pa',ylayer[u]:7:2,',',(1000+150*curve),',pu;pa',(ylayer[u]+100):7:2,',',(1050+150*curve),',lb',prof,'^O;');
          writeln(usr,'pu;pa',(ylayer[u]-400):7:2,',',(1050+150*curve),',lb',layres[u]:6:0,'^O;');
        end;
        if u < layers then
        begin
          writeln(usr,'pd;pa',ylayer[u]:7:2,',',(1150+150*curve),',');
          writeln(usr,'pa',ylayer[u]:7:2,',',(1000+150*curve),',');
          writeln(usr,'pu;pa',(ylayer[u]-400):7:2,',',(1050+150*curve),',lb',layres[u]:6:0,'^O;');
        end;
        writeln(usr,'pu1000,',(1150+150*curve),',');
      end;
    end;
    if scale = '2' then
    begin
      writeln(usr,'sp3;pa1000,',(2150+150*curve),',');
      for u := 1 to layers do
      begin
        depth := depth + layer[u];

```

```

yayer[u] := ((ln(depth)/ln(10))+1)*1000;
if u = layers then
begin
  writeln(usr, 'pd;pa', yayer[u]:7:2, ',', (2150+150*curve), ',');
  writeln(usr, 'pa', (yayer[u]-20):7:2, ',', (2100+150*curve), ',');
  writeln(usr, 'pa', (yayer[u]+30):7:2, ',', (2050+150*curve), ',');
  writeln(usr, 'pa', yayer[u]:7:2, ',', (2000+150*curve), ';pu;pa', (yayer[u]+100):7:2, ',', (2
050+150*curve), ';lb', prof, '^O');
  writeln(usr, 'pu;pa', (yayer[u]-
400):7:2, ',', (2050+150*curve), ';lb', layres[u]:6:0, '^O');
  end;
  if u < layers then
  begin
    writeln(usr, 'pd;pa', yayer[u]:7:2, ',', (2150+150*curve), ',');
    writeln(usr, 'pa', yayer[u]:7:2, ',', (2000+150*curve), ',');
    writeln(usr, 'pu;pa', (yayer[u]-
400):7:2, ',', (2050+150*curve), ';lb', layres[u]:6:0, '^O');
    end;
    writeln(usr, 'pu1000', (2150+150*curve), ',');
  end;
end;
end;
end;
end;
procedure graf2;
var a, ab, b, bb : integer;
begin
  a := 0;
  ab := 0;
  b := 0;
  bb := 0;
  clrscr;
  writeln('Input the # of the curve on this plot ? (1) first, (2) second, ect. ');
  readln(curv);
  curve := curv-1;
  clrscr;
  writeln(' Input y the scale you want');
  writeln(' 1 for 100-30,000');
  writeln(' 2 for 1,000-300,000');
  repeat
    readln(scale);
  until scale in ['1', '2'];
  writeln(usr, chr(27), '@');
  writeln(usr, 'ip 355,710,10365,6920');
  if scale = '1' then
  begin
    writeln(usr, 'pa;dt^O;sc 1000,5000,1000,3477');
    writeln(usr, 'sp1;pa1000,1000;pd1000,3477,5000,3477,5000,1000,1000,1000;pu;');
    if modl = 'y' then resmodel;
    writeln(usr, 'sp1;');
  end;
  if curv = 1 then

```

```

begin
  mult := 1;
  for xz1 := 1 to 4 do
  begin
    mult := mult * 10;
    for xz := 1 to 10 do
    begin
      xx := (ln(mult*xz)/ln(10))*1000;
      writeln(usr,'pa',xx:7:2,',',1000,');
      writeln(usr,'xt,');
    end;
  end;
  mult := 1;
  for yz1 := 1 to 3 do
  begin
    mult := mult * 10;
    for yz := 1 to 10 do
    begin
      yy := (ln(mult*yz)/ln(10))*1000;
      if yy < 3478 then
      begin
        writeln(usr,'pa',1000,',',yy:7:2,');
        writeln(usr,'yt');
      end;
    end;
  end;
  writeln(usr,'dt^O;pa 980,940;lb1^O;');
  writeln(usr,'pa 1954,940;lb10^O;');
  writeln(usr,'pa 2940,940;lb100^O;');
  writeln(usr,'pa 3905,920;lb1000^O;');
  writeln(usr,'pa 940,1000;lb100^O;');
  writeln(usr,'pa 940,2000;lb1000^O;');
  writeln(usr,'pa 940,3000;lb10000^O;');
  writeln(usr,'sp1;si0.24,0.32;pa 2000,820;');
  writeln(usr,'lbHalf Electrode Spacing [L/2] (ft)^O;');
  writeln(usr,'pa 910,1400;di0,1;lbApparent Resistivity (ohm-ft)^O;');
  writeln(usr,'di;sp2;pa 1260,3800;si.3,.41');
  writeln(usr,'lbGeoElectrical Depth^O;');
  writeln(usr,'lb Sounding After Schlumberger^O;');
  writeln('Please Hit a Key When Plotting Stops');
  repeat
  until keypressed;
  writeln(usr,'sp3;si;');
  writeln(usr,'pa1500,3620;');
  writeln(usr,'lbLocation : ',locat,'^O');
  writeln(usr,'pa3500,3620;');
  writeln(usr,'lbDate : ',date,'^O');
  writeln(potelc,' ',potnum[1]);
  clrscr;
  writeln(' Hit any Key to Plot Data');
  repeat
  until keypressed;

```

```

end;
pen := 3+(curv-1);
for i := 1 to potelc do
begin
writeln(usr,'sp',pen,';smo');
if i = 2 then writeln(usr,'smx');
if i = 3 then writeln(usr,'sm*');
for j := 1 to potnum[i] do
begin
xp := ((ln(lf[i,j])/ln(10))+1)*1000;
yp := ((ln(ra[i,j])/ln(10))-1)*1000;
writeln(usr,'pa',xp:7:2,',',yp:7:2,',');
writeln(usr,'pd;pu');
writeln(lf[i,j],ra[i,j]);
end;
end;
writeln(usr,'sm ;pa',(xp+100):7:2,',',(yp+50):7:2,';lb',prof,'^O');
end;
if scale = '2' then
begin
WriteLn(Usr,'pa;sc 1000,5000,2000,4477');
writeln(usr,'sp1;pa1000,2000;pd1000,4477,5000,4477,5000,2000,1000,2000;pu');
if modl = 'y' then resmodel;
writeln(usr,'sp1;pa1000,2000;pd1000,4477,5000,4477,5000,2000,1000,2000;pu');
if curve = 1 then
begin
mult := 1;
for xz1 := 1 to 4 do
begin
mult := mult * 10;
for xz := 1 to 10 do
begin
xx := (ln(mult*xz)/ln(10))*1000;
writeln(usr,'pa',xx:7:2,',',2000,',');
writeln(usr,'xt;');
end;
end;
mult := 10;
for yz1 := 1 to 3 do
begin
mult := mult * 10;
for yz := 1 to 10 do
begin
yy := (ln(mult*yz)/ln(10))*1000;
if yy < 4478 then
begin
writeln(usr,'pa',1000,',',yy:7:2,',');
writeln(usr,'yt;');
end;
end;
end;
end;
writeln(usr,'dt^O;pa 980,1940;lb1^O;');

```



```

writeln(usr,'pa 1954,1940;lb10^O;');
writeln(usr,'pa 2940,1940;lb100^O;');
writeln(usr,'pa 3905,1920;lb1000^O;');
writeln(usr,'pa 940,2000;lb1000^O;');
writeln(usr,'pa 940,3000;lb10000^O;');
writeln(usr,'pa 940,4000;lb100000^O;');
writeln(usr,'sp1;si0.24,0.32;pa 2000,1820;');
writeln(usr,'lbHalf Electrode Spacing [L/2] (ft)^O;');
writeln(usr,'pa 910,2400;di0,1;lbApparent Resistivity (ohm-ft)^O;');
writeln(usr,'di;sp2;pa 1260,4800;si.3,.41');
writeln(usr,'lbGeoElectrical Depth^O;');
writeln(usr,'lb Sounding After Schlumberger^O;');
writeln(usr,'sp3;si;pa1500,4700;');
writeln('Please Hit a Key When Plotting Stops');
  repeat
  until keypressed;
writeln(usr,'pa1500,4620;');
writeln(usr,'lbLocation : ',locat,'^O');
writeln(usr,'pa3500,4620;');
writeln(usr,'lbDate : ',date,'^O');
writeln(potelc,' ',potnum[1]);
clrscr;
writeln(' Hit any Key to Plot Data');
repeat
until keypressed;
end;
pen := 3+(curv-1);
for i := 1 to potelc do
begin
  writeln(potelc);
  writeln(usr,'sp',pen,';smo');
  if i = 2 then writeln(usr,'smx');
  if i = 3 then writeln(usr,'sm*');
  writeln(usr,'sp4;sm*');
  for j := 1 to potnum[i] do
  begin
    xp := ((ln(l[i,j])/ln(10))+1)*1000;
    yp := ((ln(ra[i,j])/ln(10))-1)*1000;
    writeln(usr,'pa',xp:7:2,',',yp:7:2,',');
    writeln(usr,'pd;pu');
    writeln(l[i,j],ra[i,j]);
  end;
end;
writeln(usr,'sm ;pa',(xp+100):7:2,',',(yp+50):7:2;',lb',prof,'^O');
end;
end;
procedure chan;
begin
  clrscr;
  writeln('You must know turn on the HP 7475a plotter, with the proper');
  writeln('dip switch settings. Follow the setting for the HP Basic. ');

```

```

writeln('The program will then ask whether or not this is to be a ');
writeln('multiple plot. The lay out is slightly different for the ');
writeln('two kinds or plots, so it may be desirable to plot a single');
writeln('using the multiple option. If this is a multiple plot then');
writeln('when the plotting is through simply leave the plotter be ');
writeln('and run the program again. ');
writeln;
writeln;
writeln('          Hit any key to continue          ');
repeat
until keypressed;
{ Write('Enter port number:          ');
  ReadLn(Port);}
port := 1;
AssignUsr(Port);
{ Write('Enter baud rate:          ');
  ReadLn(Baud);}
baud := 9600;
{ Write('Enter stop bits:          ');
  ReadLn(StopBits);}
stopbits := 2;
{ Write('Enter data bits:          ');
  ReadLn(DataBits);}
databits := 8;
{ Write('Enter parity (0=none, 1=even, 2=odd): ');
  ReadLn(Par);}
par := 0;
SetSerial(1,Baud,StopBits,DataBits,__ParityType(Par));
clrscr;
writeln(' Will this be a multiple plot?');
repeat
readln(plott);
until plott in ['y','n'];
if plott = 'y' then
begin
  graf2;
  resmodel2;
end;
if plott = 'n' then
begin
  graf;
  resmodel;
end;
end;
end;

```

procedure direct;

```

var
  regs      : regrec;
  dta      : array [1..43] of byte;
  mask     : char12arr;
  namr     : string20;
  error,I,count : integer;

begin
  textcolor(5);
  count := 0;
  fillchar(dta,sizeof(dta),0);
  fillchar(mask,sizeof(mask),0);
  fillchar(namr,sizeof(namr),0);
  writeln('Directory for Data Disk');
  writeln;
  regs.ax := $1a00;
  regs.ds := seg(dta);
  regs.dx := ofs(dta);
  MSDos(regs);
  mask := '?????????.???';
  regs.ax := $4e00;
  regs.ds := seg(mask);
  regs.dx := Ofs(mask);
  regs.cx := 22;
  MSDos(regs);
  error := regs.ax and $ff;
  I := 1;
  if (error = 0) then
    repeat
      namr[i] := chr(mem[seg(dta):Ofs(dta)+29+i]);
      I := I + 1;
    until not (namr[I-1] in [' '..'~']) or (I>20);
  namr[0] := chr(I-1);
  while (error = 0) do
    begin
      error := 0;
      regs.ax := $4f00;
      regs.cx := 22;
      MSDos(regs);
      error := regs.ax and $ff;
      I := 1;
      repeat
        namr[i] := chr(mem[seg(dta):Ofs(dta)+29+I]);
        I := I + 1;
      until not (namr[I-1] in [' '..'~']) or (i>20);
      namr[0] := chr(I-1);
      if (error = 0)
        then write(namr,' ');
      count := count + 1;
      if count = 5 then
        begin

```

```

    count := 0;
    writeln;
    writeln;
end;
end;
textcolor(14);
end;

```

```

procedure datafile;

```

```

var    i,j,k,h,t : integer;

```

```

begin
  clrscr;
  h := 0;
  writeln('Input the name of the data file. *****.*');
  readln(filename);
  assign (diskfile, filename);
  rewrite (diskfile);
  writeln(diskfile,a);
  writeln(diskfile,reverse);
  writeln(diskfile,potelc);
  for t:= 1 to potelc do
  begin
    writeln(diskfile,potnum[t]);
  end;
  writeln(diskfile,project);
  writeln(diskfile,locat);
  for i := 1 to a do
  begin
    writeln(diskfile,oper[i]);
  end;
  writeln(diskfile,prof);
  writeln(diskfile,date);
  for i := 1 to potelc do
  begin
    for j := 1 to potnum[i] do
    begin
      h := h +1;
      if reverse = 'y' then
      begin
        write(diskfile,h:5,b[i]:10:3,l[i,j]:10:3,volt[i,j,1]:10:3,amp[i,j,1]:10:3,volt[i,j,2]:10:3,amp[
i,j,2]:10:3);
        writeln(diskfile);
      end;
      if reverse = 'n' then
      begin
        write(diskfile,h:5,b[i]:10:3,l[i,j]:10:3,volt[i,j,1]:10:3,amp[i,j,1]:10:3);
        writeln(diskfile);
      end;
    end;
  end;
end;

```

```

    end;
    end;
    end;
    close (diskfile);
end;

```

```

procedure titles;

```

```

    var i : integer;
begin
    writeln(' Input the Name of the Project (max 20 char.)');
    readln(project);
    writeln(' Input the Location of the Project (max 30 char.)');
    readln(locat);
    writeln(' Input the Profile Designation (max 8 char)');
    readln(prof);
    writeln(' Input tht Date of the Sounding (30 MAR 87)');
    readln(date);
    repeat
        i := i + 1;
        writeln(' Input the Name of the Operator ',i:1);
        readln(oper[i]);
        until oper[i] = '';
        a := i-1;
    end;

```

```

procedure initialize;

```

```

    var i,j,k : integer;

```

```

begin
    meas := 0;
    clrscr;
    if zof0 = 'u' then
        begin
            writeln('You will be asked for the # of potential electrode seperations. ');
            writeln('This the total number of different b/2 s used in the sounding. ');
            writeln('It does not matter whether or not measurements were made at all');
            writeln('the b/2 locations. (example measurements were made at both ');
            writeln('b/2 = 1 and 4, the last measurements were not made at b/2 = 1, ');
            writeln('enter the value 2');
            writeln;
            writeln('The program will then ask if you want to enter forward or reverse');
            writeln('data. The program accounts for both, it just simply averages the');
            writeln('values if this is choosen. If there are sharp contrasts between ');
            writeln('forward and reverse measurements you may want to create two files');
            writeln('of just forward and then one of just reverse measurements. ');
            writeln;
            writeln;
        end;

```

```

end;
writeln('How Many Potential Electrode Separations Were There ?');
readln(potelc);
writeln('Do you Wish to include Forward and Reverse Data ? (y,n)');
repeat
  readln(reverse);
until reverse in ['y','n'];
clrscr;
if zofo = 'u' then
begin
writeln('If a mistake is made in the data input simply correct yourself');
writeln('at the next data point. Most mistakes are fixable latter in ');
writeln('the program. If this is not the case then saving the file and');
writeln('then using a simple text editor (ex. Norton Commander or the ');
writeln('Turbo Pascal editor) may save retying of large files. ');
writeln;
writeln('Enter all measurements made at b/2[1], then type 0 s when ');
writeln('measurements run out. This will bring you back to enter a new');
writeln('b/2[i] seperation if required ');
writeln;
writeln;
end;
for i := 1 to potelc do
begin
  writeln;
  writeln;
  writeln('input the B/2');
  readln(b[i]);
  writeln;
  j := 0;
  repeat
    j := j + 1;
    meas := meas + 1;
    clrscr;
    writeln('Measurement Number ',meas);
    writeln;
    writeln;
    writeln('input the L/2');
    readln(l[i,j]);
    writeln;
    write('Input the Forwad Voltage',j:2,' ');
    readln(volt[i,j,1]);
    writeln;
    if reverse = 'y' then
      begin
        write('Input Reerves Voltage',j:2,' ');
        readln(volt[i,j,2]);
        writeln;
      end;
    write('Input the Forward Current',j:2,' ');
    readln(amp[i,j,1]);
    writeln;
  end;
end;

```

```

    if reverse = 'y' then
    begin
        write('Input Reverse Current',j:2,' ');
        readln(amp[i,j,2]);
        end;
    until l[i,j] = 0;
    j := j -1;
    meas := meas -1;
    potnum[i] := j;
    clrscr;
    write(chr(7));
    writeln(' Starting A New Potential Separation');
    writeln;
end;
end;

```

```

procedure help (var
b:wastaray;l:taray;volt,amp:dataray;potelc:integer;potnum:sterioray;reverse:char);

```

```

var i,j,check,z,meas : integer;
    view,hard : char;

```

```

begin
z := 0;
meas := 0;
clrscr;
if zofo = 'u' then
begin
writeln('This routine allows you to correct mistakes in the data. ');
writeln('It will list the data entered. You Then change the data ');
writeln('according to the measurement numbers ');
writeln;
writeln;
end;
writeln(' View These Values On The Screen (s) or Printer (p) ?');
repeat
    readln(view);
until view in ['s','p'];
if view = 'p' then
    assign (outfile,'lst:');
if view = 's' then
    assign(outfile,'con:');
if reverse = 'n' then
begin
    writeln(outfile,' Meas # B/2 L/2 U I ');
    writeln(outfile,' -----');
end;
end;

```

```

if reverse = 'y' then
begin
  writeln(outfile,'Meas # B/2 L/2 U for I for U rev I rev');
  writeln(outfile,'-----');
end;
for i := 1 to potelc do
begin
  for j := 1 to potnum[i] do
  begin
    meas := meas + 1;
    if reverse = 'n' then
      writeln(outfile,meas:5,b[i]:10:1,l[i,j]:11:3,volt[i,j,1]:11:3,amp[i,j,1]:11:3);
    if reverse = 'y' then
      writeln(outfile,meas:4,b[i]:10:3,l[i,j]:10:3,volt[i,j,1]:10:3,amp[i,j,1]:10:3,volt[i,j,2]:1
0:3,amp[i,j,2]:10:3);
    if view = 's' then
    begin
      check := meas div 20;
      if check > z then
      begin
        writeln('note any mistakes and hit any key to continue');
        repeat
          until keypressed;
          z := z + 1;
          clrscr;
          if reverse = 'n' then
          begin
            writeln(outfile,' Meas # B/2 L/2 U I ');
            writeln(outfile,'-----');
          end;
          if reverse = 'y' then
          begin
            writeln(outfile,'Meas # B/2 L/2 U for I for U rev I rev');
            writeln(outfile,'-----');
          end;
        end;
      end;
    end;
  end;
end;
end;
end;
end;
end;
end;

```

```

procedure calculate (var b:wastary;l:taray;volt,amp:dataray);

```

```

var i,j,k,x,ab,ac,check,c : integer;
    voltav,ampav : real;

```



```

begin
k := 0;
x := 0;
ab := 0;
ac := 0;
clrscr;
if zofo = 'u' then
begin
writeln('The program will now show you the final data and measured ');
writeln('resistivities. To have a quality copy use a letter quality ');
writeln('printer or select NLQ using the pannel mode of your printer. ');
writeln;
writeln('If you select Graph the data sheet will also print and when ');
writeln('all else is finished a plot of the data will be drafted on ');
writeln('the HP 7475a plotter. ');
writeln;
writeln;
end;
writeln(' View The Results On The Screen (s) or Printer (p) or Graph on Plotter (g)?');
repeat
readln(view);
until view in ['s','p','g'];
if inptype = 's' then titles;
if view in ['p','g'] then
begin
assign(outfile,'lst:');
writeln(outfile,'GEOELECTRICAL DEPTH SOUNDING AFTER SCHLUM-
BERGER');
writeln(outfile,'PROJECT : ',project);
writeln(outfile,'LOCATION : ',locat);
write(outfile,'OPERATORS: ');
for c := 1 to a-1 do
begin
write(outfile,oper[c],', ');
end;
write(outfile,oper[a]);
writeln(outfile);
writeln(outfile,'PROFILE : ',prof);
writeln(outfile,'DATE : ',date);
end;
if view = 's' then
assign(outfile,'con:');
if reverse = 'n' then
begin
writeln(outfile);
writeln(outfile);
writeln(outfile);
writeln(outfile);
write(outfile,' Meas # B/2 L/2 ');
write(outfile,' U I RHO');
writeln(outfile);
write(outfile,' -----');

```

```

    write(outfile,'-----');
    writeln(outfile);
end;
if reverse = 'y' then
begin
    writeln(outfile);
    writeln(outfile);
    writeln(outfile);
    writeln(outfile);
    writeln(outfile,'Meas #   B/2   L/2   U for   I for   U rev   I rev   RHO');
    writeln(outfile,'-----');
end;
for i := 1 to potelc do
begin
    for j := 1 to potnum[i] do
    begin
        x := x + 1;
        if reverse = 'n' then
        begin
            ra[i,j] := pi/(2*b[i])*(sqr(l[i,j])-sqr(b[i]))*(volt[i,j,1]/amp[i,j,1]);
            writeln(outfile,x:8,b[i]:15:1,l[i,j]:13:1,volt[i,j,1]:12:1,amp[i,j,1]:12:1,ra[i,j]:12:1);
        end;
        if reverse = 'y' then
        begin
            voltav := (volt[i,j,1] + volt[i,j,2])/2;
            ampav := (amp[i,j,1] + amp[i,j,2])/2;
            ra[i,j] := pi/(2*b[i])*(sqr(l[i,j])-sqr(b[i]))*(voltav/ampav);
            writeln(outfile,x:3,b[i]:11:1,l[i,j]:10:1,volt[i,j,1]:11:3,amp[i,j,1]:11:3,volt[i,j,2]:11:3,am
p[i,j,2]:11:3,ra[i,j]:11:2);
        end;
        k := K + 1;
        if view = 's' then
        begin
            check := k div 20;
            if check = 1 then
            begin
                writeln('      hit any key to continue');
                repeat
                until keypressed;
                clrscr;
            end;
        end;
    end;
end;
begin
    writeln(outfile);
    writeln(outfile);
    writeln(outfile);
    writeln(outfile);
    write(outfile,'   Meas #   B/2   L/2   ');
    write(outfile,' U   I   RHO');
    writeln(outfile);
    write(outfile,' -----');
    write(outfile,'-----');
end;

```

```

    writeln(outfile);
end;
if reverse = 'y' then
begin
    writeln(outfile);
    writeln(outfile);
    writeln(outfile);
    writeln(outfile);
    writeln(outfile,'Meas #   B/2   L/2   U for   I for   U rev   I rev   RHO');
    writeln(outfile,'-----');
end;
    writeln(outfile);
    k := 0;
end;
end;
end;
end;
writeln('Do You Want To Save This Data ? (y,n)');
repeat
    readln(save);
until save in ['y','n'];
if save = 'y' then
begin
    datafile;
end;
end;
end;

```

```

procedure change (var
b:wastaray;l:taray;volt,amp:dataray;potelc:integer;potnum:sterioray;reverse:char);

```

```

var   save,dumb       : char ;
      i,j,k,n,meas   : integer;

```

```

begin
repeat
meas := 0;
dumb := '-';
writeln('Do you wish to change a value ? (y,n)');
readln(dumb);
if dumb = 'y' then
begin
write('enter the number of the measurement to change ');
readln(n);
for i := 1 to potelc do
begin
for j := 1 to potnum[i] do

```

```

begin
  meas := meas + 1;
  if meas = n then
  begin
    writeln;
    writeln('Changing Measurement ',meas:2);
    writeln;
    write('enter the new L/2  ');
    read(l[i,j]);
    writeln;
    write('enter the new Forward Voltage ',n:2,' ');
    readln(volt[i,j,3]);
    volt[i,j,1] := volt[i,j,3];
    writeln;
    if reverse = 'y' then
    begin
      write('enter the new Reverses Voltage ',n:2,' ');
      read(volt[i,j,2]);
      writeln;
    end;
    write('enter the new Forward Current',n:2,' ');
    read(amp[i,j,1]);
    if reverse = 'y' then
    begin
      writeln('enter the new Reverse Current ',n:2,' ');
      read(amp[i,j,2]);
    end;
  end;
end;
end;
end;
end;
until dumb in ['n'];
calculate(b,l,volt,amp);
end;

```

```

procedure inpdata;

```

```

var  i,j,k,h,r,c  : integer;
     dr           : char;

```

```

begin
  j := 0;
  k := 0;
  a := 0;
  clrscr;
  writeln(' Do You Wish A Directory ? (y,n)');

```

```

repeat
  readln(dr);
until dr in ['y', 'n'];
if dr = 'y' then direct;
  writeln;
  writeln ('input the file name. *****.***');
  read(filename);
  assign (diskfile, filename);
  reset (diskfile);
  clrscr;
  readln(diskfile,a);
  readln(diskfile,reverse);
  readln(diskfile,potelc);
  for h := 1 to potelc do
  begin
    readln(diskfile, potnum[h]);
  end;
  readln(diskfile,project);
  readln(diskfile,locat);
  for c := 1 to a do
  begin
    readln(diskfile,oper[c]);
  end;
  readln(diskfile,prof);
  readln(diskfile,date);
  for i := 1 to potelc do
  begin
    for j := 1 to potnum[i] do
    begin
      if reverse = 'y' then
      begin
        read(diskfile,h,b[i],l[i,j],volt[i,j,1],amp[i,j,1],volt[i,j,2],amp[i,j,2]);
        readln(diskfile);
      end;
      if reverse = 'n' then
      begin
        read(diskfile,h,b[i],l[i,j],volt[i,j,1],amp[i,j,1]);
        readln(diskfile);
      end;
    end;
  end;
  end;
  close(diskfile);
end;

```

```

procedure statistics(var l,ra:taray;th,s:wastary;potnum:sterioray;potelc,count:integer);

```

```

var  i,j,k,d,n,az,c : integer;
     slope,sumy,sumys,sumyh,sumyhs,ssdev : real;
     sumdev,sumdevs,corr,sst,ssr,stddev : real;
     reply : char;

```

```

begin
sumdev := 0;
sumdev := 0;
sumys := 0;
sumy := 0;
sumyh := 0;
sumyhs := 0;
for i := 1 to potelc do
begin
for j := 1 to potnum[i] do
begin
k := 0;
d := 0;
repeat
k := k + 1;
if l[i,j] < th[k] then
begin
n := n + 1;
slope := (s[k]-s[k-1])/(th[k]-th[k-1]);
yhat[i,j] := (l[i,j]-th[k-1])*slope+s[k-1];
dev[i,j] := (ra[i,j] - yhat[i,j]);
sumdev := sumdev + dev[i,j];
sumdevs := sumdevs + (dev[i,j]*dev[i,j]);
sumyh := sumyh + yhat[i,j];
sumyhs := sumyhs + (yhat[i,j]*yhat[i,j]);
sumy := sumy + ra[i,j];
sumys := sumys + (ra[i,j] * ra[i,j]);
d := 1;
end;
if k = m then d := 1
until d >=1;
end;
end;
ssdev := sumdevs - ((sumdev * sumdev)/n);
sst := sumys - ((sumy * sumy)/n);
ssr := sumyhs - ((sumyh * sumyh)/n);
corr := sqrt(ssr/sst);
assign(outfile,'con:');
writeln(outfile,'          Model # ',count:2);
writeln(outfile);
writeln(outfile,' Layer Resistivity Thickness');
writeln(outfile);
for az := 1 to num do
begin
writeln(outfile,az:8,resist[az]:15:2,thick[az]:14:2);
end;
writeln(outfile);
writeln(outfile,'goodness of fit = ',corr:8:5);
stddev := sqrt(abs(ssdev/(n-1)));
writeln(outfile,'standard deviation = ',stddev:8:5);
writeln;
writeln(' Do You Wish To Have This Printed ? (y,n)');

```

```

readln(reply);
if reply = 'y' then
begin
  assign(outfile,'lst:');
  writeln(outfile,'          Model # ',count:2);
  writeln(outfile);
  writeln(outfile,'  Layer  Resistivity  Thickness');
  writeln(outfile);
  for az := 1 to num do
  begin
    writeln(outfile,az:8,resist[az]:15:2,thick[az]:14:2);
  end;
  writeln(outfile);
  writeln(outfile,'goodness of fit = ',corr:8:5);
  stddev := sqrt(abs(ssdev/(n-1)));
  writeln(outfile,'standard deviation = ',stddev:8:5);
  writeln(outfile);
  writeln('Would you like the model curve printed out ? (y/n)');
repeat
  readln(modl);
until modl in ['y','n'];
if modl = 'y' then
begin
  assign(outfile,'lst:');
  writeln(outfile);
  writeln(outfile);
  writeln(outfile,'          Model # ',count:2);
  writeln(outfile);
  writeln(outfile,'  L/2  resistivity');
  writeln(outfile,'  -----');
  writeln(outfile);
  for c := 1 to m1 do
  begin
    writeln(outfile,th[c]:10:2,s[c]:10:2);
  end;
end;
end;
  writeln;
  writeln(' Hit any key to see plot and any key to return from the plot');
end;

procedure plotmodel(s,th:wastary;m1:integer);
var x5,x6,y5,y6,y7,y8,i,n : integer;
begin
  for i:= 1 to m1 do
  begin
    x5 := round(ln(th[i])/ln(10)*100);
    y5 := round((ln(s[i])/ln(10)-2)*78.26087);
    y7 := abs(y5-180);

```

```

x6 := round(ln(th[i+1])/ln(10)*100);
y6 := round((ln(s[i+1])/ln(10)-2)*78.26087);
y8 := abs(y6-180);
for n := 1 to 10 do
draw(x5,y7,x6,y8,3);
end;
repeat
until keypressed;
end;

```

```

procedure plotdata(l,ra:taray;potnum:sterioray;potelc:integer);

```

```

var i,j,x9,y9,y10 : integer;

```

```

begin
for i := 1 to potelc do
begin
for j := 1 to potnum[i] do
begin
x9 := round(ln(l[i,j])/ln(10)*100);
y9 := round((ln(ra[i,j])/ln(10)-2)*78.26087);
y10 := abs(y9-180);
draw(x9-2,y10-2,x9-2,y10+2,2);
draw(x9-2,y10+2,x9+2,y10+2,2);
draw(x9+2,y10+2,x9+2,y10-2,2);
draw(x9+2,y10-2,x9-2,y10-2,2);
plot(x9,y10,2);
end;
end;
end;
end;

```

```

procedure startplot;

```

```

var x,x3,x4,mult,y1,y2,y3,y4 : integer;

```

```

begin
graphcolormode;
palette(2);
textcolor(1);
draw(0,0,300,0,1);
draw(0,0,0,180,1);
draw(300,0,300,180,1);
draw(0,180,300,180,1);
mult := 1;
for x3 := 1 to 3 do
begin
for x4 := 2 to 10 do
begin

```



```

    x := round(ln(mult*x4)/ln(10)*100);
    draw(x,177,x,180,1);
end;
mult := mult * 10;
end;
mult := 1;
for y3 := 1 to 2 do
begin
    for y4 := 2 to 10 do
    begin
        y2 := round(ln(mult*y4)/ln(10)*78.26087);
        if y2 < 200 then
        begin
            y1 := abs(y2-180);
            draw(0,y1,3,y1,1);
        end;
    end;
    mult := mult * 10;
end;
end;
end;

```

```

procedure transform(y,x1,x2:real;resist,thick:wastary);

```

```

var k,i : integer;
    u,a1,a2 : real;
begin
    bo := resist[num];
    for k := 1 to num-1 do
    begin
        i := num-k;
        u := thick[i]/y;
        if (5-u) > 0 then
        begin
            a1 := exp(u);
            a2 := (a1-1/a1)/(a1+1/a1);
            bo := (bo+a2*resist[i])/(1+a2*bo/resist[i]);
        end;
        if (5-u) < 0 then bo := resist[i];
    end;
end;

```

```

procedure instruct;

```

```

begin
writeln('This is the interpretation part of the program. You will first ');
writeln('be asked how many layers in you model. Do not worry for you ');
writeln('can change this for the next model. If you do change the number');
writeln('of layers the print might look funny until you fix the thickness');
writeln('of the layers. The program calculates the standard deviation ');
writeln('and a goodness of fit. The smaller the std. dev. the better, ');
writeln('however it is relative to the measured range of resistivities. ');
writeln('The goodness of fit is best at 1.00. These statistics are ');
writeln('calculated for every point of data within the specified range. ');
writeln('This range must not exceed the range of measured l/2 points. ');
writeln('To clear the graph and continue hit any key ');
writeln;
writeln(' Hit any Key to continue ');
repeat
until keypressed;
end;

```

```

procedure ghosh;

```

```

var   j,m,d,e,c,ca   : integer;
      q               : real;
      cont,param     : char;

```

```

begin
if zofo = 'u' then instruct;
count := 0;
repeat
count := count +1;
clearscreen;
m := 0;
f :=1.3335214;
writeln('input the number of layers');
readln(num);
if count > 1 then
begin
repeat
writeln(' Layer Resistivity Thickness');
writeln;
for c := 1 to num do
begin
writeln(c:8,resist[c]:15:2,thick[c]:14:2);
end;
writeln;
writeln;
writeln('Would you like to change a layer parameter ? (y/n)');
repeat
readln(parm);
until parm in ['y','n'];
if parm = 'y' then
begin

```

```

writeln;
writeln('enter the layer # to change ');
readln(ca);
writeln('input the resistivity of layer ',ca:1);
readln(resist[ca]);
if ca < num then
begin
  writeln('input the thickness of layer ',ca:1);
  readln(thick[ca]);
end;
if ca = num then
begin
  thick[ca] := 0;
end;
end;
until parm = 'n';
end;
if count < 2 then
begin
  for j := 1 to num do
  begin
    writeln('input the resistivity of layer ',j:1);
    readln(resist[j]);
    if j < num then
    begin
      writeln('input the thickness of layer ',j:1);
      readln(thick[j]);
    end;
    if j = num then
    begin
      thick[j] := 0;
    end;
  end;
end;
writeln('input the range you wish calculated eg. (4 500) ');
writeln;
writeln(' Do Not exceed range of measured values ');
readln(x1,x2);
y := x1/822.8;
for j := 1 to 34 do
begin
  transform(y,x1,x2,resist,thick);
  t[j] := bo;
  y := y * f;
end;
nu := round(x2);
repeat
  m := m + 1;
  transform(y,x1,x2,resist,thick);
  t[35] := bo;
  y := y*f;
  s[m] :=42*t[1]-103*t[3]+144*t[5]-211*t[7]+330*t[9]-574*t[11];

```

```

s[m] :=s[m]+1184*t[13]-3162*t[15]+10219*t[17]-24514*t[19];
s[m] :=s[m]+18192*t[21]+6486*t[23]+1739*t[25]+79*t[27]+200*t[29];
s[m] :=(s[m]-106*t[31]+93*t[33]-38*t[35])/10000;
for d := 1 to 34 do
begin
  t[d] := t[d+1];
end;
th[m] := x1;
x1 := th[m]*1.3335214;
until th[m] > x2;
m1 := m-1;
statistics(l,ra,th,s,potnum,potelc,count);
startplot;
plotdata(l,ra,potnum,potelc);
plotmodel(s,th,m1);
textmode;
writeln('Do you wish a new model ? (y/n)');
repeat
readln(cont);
until cont in ['y','n'];
until cont = 'n';
end;

```

```

procedure start_res;

```

```

begin
  assign (outfile,'lst:');
  clrscr;
  if zofo = 'u' then
  begin
    writeln('Input may be entered interactively from the screen or');
    writeln('from any file created by this program. The file must');
    writeln('be in the current directory (or on the same disk) as ');
    writeln('the program. You will be able to get a listing of ');
    writeln('files in that directory before the program asks for ');
    writeln('the name of the input file. ');
    writeln;
    writeln;
  end;
  writeln(' Input on Screen (s) of File (f)');
  repeat
    readln(inptype);
  until inptype in ['s','f'];
  if inptype = 's' then
  initialize

```

```

else
inpdata;
help(b,l,volt,amp,potelc,potnum,reverse);
change(b,l,volt,amp,potelc,potnum,reverse);
writeln;
writeln('Do You want to see the plot ? (y,n)');
repeat
  readln(graph);
until graph in ['y','n'];
if graph = 'y' then
begin
  startplot;
  plotdata(l,ra,potnum,potelc);
  textmode;
  ghosh;
  if view = 'g' then
  begin
    assign(cnprog,'geophys.chn');
    chain(cnprog);
  end;
end;
if view = 'g' then chan;
end;

```

procedure menu;

```

begin
  writeln('          Welcome to GeoPhysics III. ');
  writeln(' This Program was designed by M. Boland for Data Calculation');
  writeln(' and Storage for Input to Subsiquent Plotting Software');
  writeln;
  writeln;
  writeln;
  writeln(' You Have The Following Choices So Far');
  writeln;
  writeln('    Resistivity Depth Sounding    ');
  writeln('    Data Storage          (d)');
  writeln('    Use w/ instruction      (u)');
  writeln('    Plot Model on Res. Plot    (m)');
  writeln('    ');
  repeat
    read(zof);
until zof in ['d','u','m'];
if zof in ['d','u'] then start_res;
if zof = 'm' then
begin

```

```
    modl := 'y';  
    chan;  
end;  
end;
```

```
begin  
clrscr;  
menu;  
end.
```

**APPENDIX 1c.**

Listing of the AB-rectangle Program

## AB-RECTANGLE PROGRAM

```
program rectangle (input,output,diskfile);
```

```
{ Calculates actual resistivities given a homogeneous layered  
model. It Uses a filter by O'Neill and Merrick (1984) to  
map the composite resistivity transform to apparent  
resistivities for any four electrode array.
```

```
However, this algorithm is for uniform arrays of rectangular  
potential measurements. Including linear Profiles. }
```

```
type thrdim = array [1..18,1..10,1..4] of real;  
mesdim = array [1..18,1..10,1..2] of real;  
twodim = array [1..40,1..40] of real;  
onedim = array [-25..50] of real;  
chadim = array [1..5] of string[20];
```

```
var xmax,ymax,xshift,yshift : integer;  
xint,yint,l2,i,j,num,a : integer;  
r,volt,amp : thrdim;  
k,tr,mucka,ra,res : twodim;  
thick,resist,t,s,n : onedim;  
locx,locy,bo,y,shift,b2 : real;  
mcfly,reverse,view,inp,plot : char;  
outfile,diskfile : text;  
project : string[20];  
locat : string[30];  
oper : chadim;  
prof,filename : string[9];  
date : string[10];
```

```
procedure input;
```

```
{ To manually input values from keyboard }
```

```
begin
```

```
writeln('input b/2');
```

```
readln(b2);
```

```
writeln;
```

```
writeln('input l/2');
```

```
readln(l2);
```

```
writeln;
```

```
writeln('input the maximum measurement distance along the x-axis');
```

```
readln(xmax);
```

```
writeln;
```

```
writeln('input the maximum measurement distance away from the x-axis');
```

```
writeln;
```

```
readln(ymax);
```

```
writeln;
```

```
writeln('input the interval between measurements on the x-axis');
```



```

readln(xshift);
writeln;
writeln('input the interval between measurement away from the x-axis');
writeln(' NOTE: MUST BE ATLEAST A VALUE OF 1');
readln(yshift);
xint := round(xmax/xshift) +1;
yint := round(ymax/yshift) +1;
end;

```

```

procedure inpdata;
  { To input previously saved data }
var  i,j,k,h,r,a : integer;
     dr          : char;
begin
  j := 0;
  k := 0;
  a := 0;
  clrscr;
  writeln;
  writeln ('input the file name. *****.***');
  read(filename);
  assign (diskfile, filename);
  reset (diskfile);
  clrscr;
  readln(diskfile,reverse);
  readln(diskfile,xmax);
  readln(diskfile,ymax);
  readln(diskfile,xshift);
  readln(diskfile,yshift);
  readln(diskfile,b2);
  readln(diskfile,l2);
  readln(diskfile,project);
  readln(diskfile,locat);
  repeat
    a := a + 1;
    read(diskfile,oper[a]);
  until oper[a] = '';
  readln(diskfile);
  readln(diskfile,prof);
  readln(diskfile,date);
  xint := round(xmax/xshift) +1;
  yint := round(ymax/yshift) +1;
  for i := 1 to (2*xint-1) do
  begin
    for j := 1 to (2*yint-1) do
    begin
      if reverse = 'y' then
      begin
        readln(diskfile,i,j,volt[i,j,1],amp[i,j,1],volt[i,j,2],amp[i,j,2],ra[i,j],res[i,j]);

```

```

end;
if reverse = 'n' then
begin
  read(diskfile,i,j,volt[i,j,1],amp[i,j,1]);
  readln(diskfile);
end;
end;
end;
close(diskfile);
end;

```

```

procedure kvalues;

```

```

  { To compute primary K values }

```

```

var   x,y   : real;
      i,j   : integer;

```

```

begin
  for i := 1 to xint do
  begin
    x := xmax - (xshift*(i-1));
    for j := 1 to yint do
    begin
      y := ymax - (yshift*(j-1));
      r[i,j,1] := sqrt(sqr(y)+sqr(12-x-b2));
      r[i,j,4] := sqrt(sqr(y)+sqr(12+x-b2));
      r[i,j,2] := sqrt(sqr(y)+sqr(12-x+b2));
      r[i,j,3] := sqrt(sqr(y)+sqr(12+x+b2));
      k[i,j] := 2*3.14159/((1/r[i,j,1])-(1/r[i,j,2])-(1/r[i,j,3])+(1/r[i,j,4]));
    end;
  end;
end;

```

```

  { The Quad procedures calculate the other k values
    Using the simitry of the array }

```

```

procedure quad2(var mcfly : char);

```

```

var   n,i,j : integer;

```

```

begin
  n:= 0;
  for i := (xint +1) to (2*xint-1) do
  begin
    n := n+2;
    for j := 1 to yint do
    begin
      if mcfly = 'k' then k[i,j] := k[i-n,j];
      if mcfly = 'r' then mucka[i,j] := mucka[i-n,j];
    end;
  end;
end;

```

```

procedure quad3(var mcfly : char);
var  n,i,j : integer;

begin
  for i := 1 to xint do
    begin
      n := 0;
      for j := (yint +1) to (2*yint-1) do
        begin
          n := n+2;
          if mcfly = 'k' then k[i,j] := k[i,j-n];
          if mcfly = 'r' then mucka[i,j] := mucka[i,j-n];
        end;
      end;
    end;
end;

```

```

procedure quad4(var mcfly : char);
var  nx,ny,i,j : integer;

begin
  nx := 0;
  for i := (xint +1) to (2*xint-1) do
    begin
      ny := 0;
      nx := nx + 2;
      for j := (yint + 1) to (2*yint-1) do
        begin
          ny := ny +2;
          if mcfly = 'k' then k[i,j] := k[i-nx,j-ny];
          if mcfly = 'r' then mucka[i,j] := mucka[i-nx,j-ny];
        end;
      end;
    end;
end;

```

```

procedure transform(a:integer;y:real;resist,thick:onedim);
  { To calculate the resitivity Transform }
var  k,i : integer;
     u,a1,a2,kab,kbc,tprime,tbc : real;
     kcd,tcd,tbcd : real;

begin
  u := exp(y);
  kab := (resist[2]-resist[1])/(resist[2]+resist[1]);
  tprime := resist[1]*((1-exp(-2*thick[1]/u))/(1+exp(-2*thick[1]/u)));
  if num = 2 then
    bo := resist[1]*(1+kab*exp(-2*thick[1]/u))/(1-kab*exp(-2*thick[1]/u));
  if num = 3 then

```

```

begin
  kbc := (resist[3]-resist[2])/(resist[3]+resist[2]);
  tbc := resist[2]*(1+kbc*exp(-2*thick[2]/u))/(1-kbc*exp(-2*thick[2]/u));
  bo := (tprime + tbc)/(1 + (tprime*tbc/(resist[1]*resist[1])));
end;
if num = 4 then
begin
  kcd := (resist[4]-resist[3])/(resist[4]+resist[3]);
  tcd := resist[3]*(1+kcd*exp(-2*thick[3]/u))/(1-kcd*exp(-2*thick[3]/u));
  tbcd:= (tprime + tcd)/(1 + (tprime*tcd/(resist[2]*resist[2])));
  bo := (tprime + tbcd)/(1 + (tprime*tbcd/(resist[1]*resist[1])));
end;
end;

```

```

procedure ghosh;

```

```

var   m,j,d,e,g,h,v   : integer;
      q,f,x           : real;
      cont            : char;

```

```

begin
  m := 0;
  f := 0.3837642;
  shift := -0.046339794;
  writeln('input the number of layers');
  readln(num);
  for j := 1 to num do
  begin
    writeln('input the resistivity of layer ',j:1);
    readln(resist[j]);
    if j < num then
    begin
      writeln('input the thickness of layer ',j:1);
      readln(thick[j]);
    end;
  end;
  for g := 1 to xint do
  begin
    x := xmax - (xshift*(g-1));
    for h := 1 to yint do
    begin
      for a := 1 to 4 do
      begin
        for j := -25 to 10 do
        begin
          n[j] := shift + j*f;
          y := ln(r[g,h,a])-(n[j]);
          transform(a,y,resist,thick);
          tr[j,a] := bo;
        end;
      end;
    end;
  end;
end;

```

```

    end;
    end;
    for v:= -25 to 10 do
begin
    t[v] := (tr[v,1]/r[g,h,1])-(tr[v,2]/r[g,h,2])-(tr[v,3]/r[g,h,3])+(tr[v,4]/r[g,h,4]);
end;
m := 1;
s[m] :=0.00039053314*t[-25]-0.0010087715*t[-24]+0.0018339484*t[-23]-0.00223724
33*t[-22];
s[m] :=s[m]+0.0026864314*t[-21]-0.0024139139*t[-20]+0.002685288*t[-19]-0.00182
92607*t[-18];
s[m] :=s[m]+0.0024492093*t[-17]-0.00082138589*t[-16]+0.0024664738*t[-15]+0.00
069159672*t[-14];
s[m] :=s[m]+0.0032120792*t[-13]+0.0032357338*t[-12]+0.0055210545*t[-11]+0.008
0328605*t[-10];
s[m]
:=s[m]+0.011157895*t[-9]+0.017713717*t[-8]+0.023921121*t[-7]+0.037878738*t[-6];
s[m]
:=s[m]+0.05186661*t[-5]+0.080094716*t[-4]+0.11087382*t[-3]+0.16458964*t[-2];
s[m] :=s[m]+0.22063809*t[-1]+0.29147621*t[0]+0.29934872*t[1]+0.1586253*t[2];
s[m] :=s[m]-0.32349971*t[3]-0.53249164*t[4]+0.51481121*t[5]-0.19282817*t[6];
s[m]
:=(s[m]+0.051125704*t[7]-0.0126355*t[8]+0.0028267073*t[9]-0.00040198125*t[10]);
mucka[g,h] := (s[m]*k[g,h]/(2*3.1415));
end;
end;
end;

```

procedure initialize;

var i,j,k : integer;

```

begin
    clrscr;
    writeln('Do you Wish to include Forward and Reverse Data ? (y,n)');
    repeat
        readln(reverse);
    until reverse in ['y','n'];
    clrscr;
    for i := 1 to (2*xint-1) do
    begin
        for j := 1 to (2*yint-1) do
        begin
            clrscr;
            writeln('Measurement Number ',i:2,', ',j:2);
            write('Input the Forwad Voltage',j:2,' ');
            readln(volt[i,j,1]);
            writeln;
            if reverse = 'y' then
            begin

```

```

    write('Input Reverses Voltage',j:2,' ');
    readln(volt[i,j,2]);
    writeln;
end;
write('Input the Forward Current',j:2,' ');
readln(amp[i,j,1]);
writeln;
if reverse = 'y' then
begin
    write('Input Reverse Current',j:2,' ');
    readln(amp[i,j,2]);
end;
end;
end;
end;

```

```

procedure help (var volt,amp:thrdim;reverse:char);

```

```

var i,j,check,z,meas : integer;
    view ,hard : char;

```

```

begin
z := 0;
meas := 0;
clrscr;
writeln(' View These Values On The Screen (s) or Printer (p) ?');
repeat
    readln(view);
until view in ['s','p'];
if view = 'p' then
    assign (outfile,'lst:');
if view = 's' then
    assign(outfile,'con:');
if reverse = 'n' then
begin
    writeln(outfile,' Location U I ');
    writeln(outfile,' -----');
end;
if reverse = 'y' then
begin
    writeln(outfile,'Location U for I for U rev I rev');
    writeln(outfile,'-----');
end;
for i := 1 to (2*xint-1) do
begin
    for j := 1 to (2*yint-1) do
begin
meas := meas + 1;
if reverse = 'n' then

```

```

    writeln(outfile,i:2,j:2,volt[i,j,1]:8:3,amp[i,j,1]:8:3);
if reverse = 'y' then
    writeln(outfile,i:2,j:2,volt[i,j,1]:10:3,amp[i,j,1]:10:3,volt[i,j,2]:10:3,amp[i,j,2]:10:3);
if view = 's' then
begin
    check := meas div 20;
    if check > z then
    begin
        writeln('note any mistakes and hit any key to continue');
        repeat
            until keypressed;
        z := z + 1;
        clrscr;
        if reverse = 'n' then
        begin
            writeln(outfile,' Location   U   I ');
            writeln(outfile,'-----');
            end;
            if reverse = 'y' then
            begin
                writeln(outfile,'Location   U for I for U rev I rev');
                writeln(outfile,'-----');
            end;
        end;
    end;
end;
end;
end;
end;
end;

```

```

procedure change (var volt,amp:thrdim;reverse:char);

```

```

var   save,dumb      : char ;
      i,j,k,x,y     : integer;

```

```

begin
    repeat
        dumb := '-';
        writeln('Do you wish to change a value ? (y,n)');
        readln(dumb);
        if dumb = 'y' then
        begin
            write('enter the number of the measurement to change (x,y) ');
            readln(x,y);
            writeln('Changing Measurement ',x:2,', ',y:2);
            write('enter the new Forward Voltage ',x:2,', ',y:2,' ');
            read(volt[x,y,1]);
            writeln;
            if reverse = 'y' then
            begin

```

```

        write('enter the new Reerves Voltage ',x:2,',',y:2,' ');
        read(volt[x,y,2]);
        writeln;
    end;
    write('enter the new Forward Current',x:2,',',y:2,' ');
    read(amp[x,y,1]);
    writeln;
    if reverse = 'y' then
    begin
        write('enter the new Reverse Current ',x:2,',',y:2,' ');
        read(amp[x,y,2]);
        writeln;
    end;
end;
until dumb in ['n'];
end;

```

```

procedure datafile (var res,ra:twodim;volt,amp:thrdim;revers:char);

```

```

var    i,j,k,h,t,a : integer;

```

```

begin
    clrscr;
    h := 0;
    a := 0;
    writeln('Input the name of the data file. *****.*');
    readln(filename);
    assign (diskfile, filename);
    rewrite (diskfile);
    writeln(diskfile,reverse);
    writeln(diskfile,xmax:8);
    writeln(diskfile,ymax:8);
    writeln(diskfile,xshift:8);
    writeln(diskfile,yshift:8);
    writeln(diskfile,b2:5:2);
    writeln(diskfile,l2:5);
    writeln(diskfile,project);
    writeln(diskfile,locat);
    repeat
        a := a + 1;
        write(diskfile,oper[a],' ');
        until oper[a] = ' ';
        writeln(diskfile);
        writeln(diskfile,prof);
        writeln(diskfile,date);
    for i := 1 to (2*xint-1) do

```



```

begin
  for j := 1 to (2*yint-1) do
    begin
      if reverse = 'y' then
        begin
          write(diskfile,i:3,j:3,volt[i,j,1]:10:3,amp[i,j,1]:10:3);
          write(diskfile,volt[i,j,2]:10:3,amp[i,j,2]:10:3,ra[i,j]:14:3,res[i,j]:14:3);
          writeln(diskfile);
        end;
      if reverse = 'n' then
        begin
          write(diskfile,i:3,j:3,volt[i,j,1]:14:3,amp[i,j,1]:14:3);
          writeln(diskfile);
        end;
      end;
    end;
  close (diskfile);
end;

```

```

procedure calculate (var volt,amp:thrdim;mucka:twodim);

```

```

var i,j,h,x,a,ab,ac,check : integer;
    voltav,ampav          : real;
    save                  : char;
begin
  h := 0;
  x := 0;
  a := 0;
  ab := 0;
  ac := 0;
  clrscr;
  writeln(' View The Results On The Screen (s) or Printer (p) ?');
  repeat
    readln(view);
  until view in ['s','p','g'];
  if view in ['p','g'] then
    begin
      assign (outfile,'lst:');
      writeln(' Input the Name of the Project (max 20 char.)');
      readln(project);
      writeln(' Input the Location of the Project (max 30 char.)');
    end;

```

```

readln(locat);
writeln(' Input the Profile Designation (max 8 char)');
readln(prof);
writeln(' Input tht Date of the Sounding (30 MAR 87)');
readln(date);
repeat
a := a + 1;
writeln(' Input the Name of the Operator ',a:1);
readln(oper[a]);
until oper[a] = '';
end;
if view in ['p','g'] then
begin
writeln(outfile,'GEOELECTRICAL A-B RECTANGLE METHOD');
writeln(outfile,'PROJECT : ',project);
writeln(outfile,'LOCATION : ',locat);
write(outfile,'OPERATORS: ');
repeat
ab := ab + 1;
write(outfile,oper[ab],', ');
until ab = a-2;
write(outfile,oper[a-1]);
writeln(outfile);
writeln(outfile,'PROFILE : ',prof);
writeln(outfile,'DATE : ',date);
end;
if view = 's' then
assign(outfile,'con:');
if reverse = 'n' then
begin
writeln(outfile);
writeln(outfile);
writeln(outfile);
writeln(outfile);
write(outfile,' Location ');
write(outfile,' U I RHOapp Residual');
writeln(outfile);
write(outfile,' -----');
write(outfile,' -----');
writeln(outfile);
end;
if reverse = 'y' then
begin
writeln(outfile);
writeln(outfile);
writeln(outfile);
writeln(outfile);
writeln(outfile,' Location U for I for U rev I rev RHO (meas)
Residual');
writeln(outfile,' -----');
end;
for i := 1 to 2*xint-1 do

```

```

begin
  for j := 1 to 2*yint-1 do
  begin
    locx := xmax-((i-1)*xshift);
    locy := ymax-((j-1)*yshift);
    x := x + 1;
    if reverse = 'n' then
    begin
      ra[i,j] := k[i,j]*(volt[i,j,1]/amp[i,j,1]);
      res[i,j] := mucka[i,j]-ra[i,j];
      writeln(outfile,locx:6:0,lo-
cy:6:0,volt[i,j,1]:14:1,amp[i,j,1]:14:1,ra[i,j]:14:1,res[i,j]:14:1);
    end;
    if reverse = 'y' then
    begin
      voltav := (volt[i,j,1] + volt[i,j,2])/2;
      ampav := (amp[i,j,1] + amp[i,j,2])/2;
      ra[i,j] := k[i,j]*(voltav/ampav);
      res[i,j] := mucka[i,j]-ra[i,j];
      write(outfile,locx:4:0,locy:5:0,volt[i,j,1]:10:2,amp[i,j,1]:11:2);
      write(outfile,volt[i,j,2]:11:2,amp[i,j,2]:11:2,ra[i,j]:11:2,res[i,j]:14:2);
      writeln(outfile);
      h := h + 1;
    end;
    if view = 's' then
    begin
      check := h div 20;
      if check = 1 then
      begin
        writeln('          hit any key to continue');
        repeat
          until keypressed;
        clrscr;
      end;
    end;
    if reverse = 'n' then
    begin
      writeln(outfile);
      writeln(outfile);
      writeln(outfile);
      writeln(outfile);
      write(outfile,' Location      ');
      write(outfile,' U      I      RHO      Residual');
      writeln(outfile);
      write(outfile,' -----');
      write(outfile,' -----');
      writeln(outfile);
    end;
    if reverse = 'y' then
    begin
      writeln(outfile);
      writeln(outfile);
      writeln(outfile);
      writeln(outfile);
    end;
  end;
end;

```

```

writeln(outfile,'Location      U for   I for   U rev   I rev   RHO   Residual');
writeln(outfile,'-----');
end;
  writeln(outfile);
  h := 0;
  end;
end;
end;
end;
writeln('Do You Want To Save This Data ? (y,n)');
repeat
  readln(save);
until save in ['y','n'];
if save = 'y' then
begin
  datafile(res,ra,volt,amp,reverse);
end;
end;

```

```

procedure lotusfile (var res,ra:twodim;volt,amp:thrdim;revers:char);

```

```

var   i,j,k,h,t,a : integer;

```

```

begin
  clrscr;
  h := 0;
  a := 0;
  writeln('Input the name of the data file. *****.*');
  readln(filename);
  assign (diskfile, filename);
  rewrite (diskfile);
  for i := 1 to (2*xint-1) do
  begin
    for j := 1 to (2*yint-1) do
    begin
      locx := xmax-((i-1)*xshift);
      locy := ymax-((j-1)*yshift);
      write(diskfile,locx:5:2,locy:5:2,mucka[i,j]:14:3);
      writeln(diskfile);
    end;
  end;
  close (diskfile);
end;

```

```

begin
writeln(' Input data from (s)creen or (f)ile ? ');
repeat
readln(inp);
until inp in ['s','f'];
if inp = 'f' then inpdata;
if inp = 's' then
begin
input;
initialize;
end;
help(volt,amp,reverse);
change(volt,amp,reverse);
kvalues;
mcfly := 'k';
quad2(mcfly);
quad3(mcfly);
quad4(mcfly);
for i := 1 to (2*yint-1) do
begin
for j := 1 to (2*xint-1) do
begin
write(k[j,i]:6:0,' ');
end;
writeln;
end;
ghosh;
mcfly := 'r';
quad2(mcfly);
quad3(mcfly);
quad4(mcfly);
for i := 1 to (2*yint-1) do
begin
for j := 1 to (2*xint-1) do
begin
write(mucka[j,i]:8:2,' ');
end;
writeln;
end;
calculate(volt,amp,mucka);
writeln(' Do You Wish To Save This For a Plot Of Residuals ? (y,n) ');
repeat
readln(plot);
until plot in ['y','n'];
if plot = 'y' then lotusfile(res,ra,volt,amp,reverse);
end.

```

## APPENDIX 2

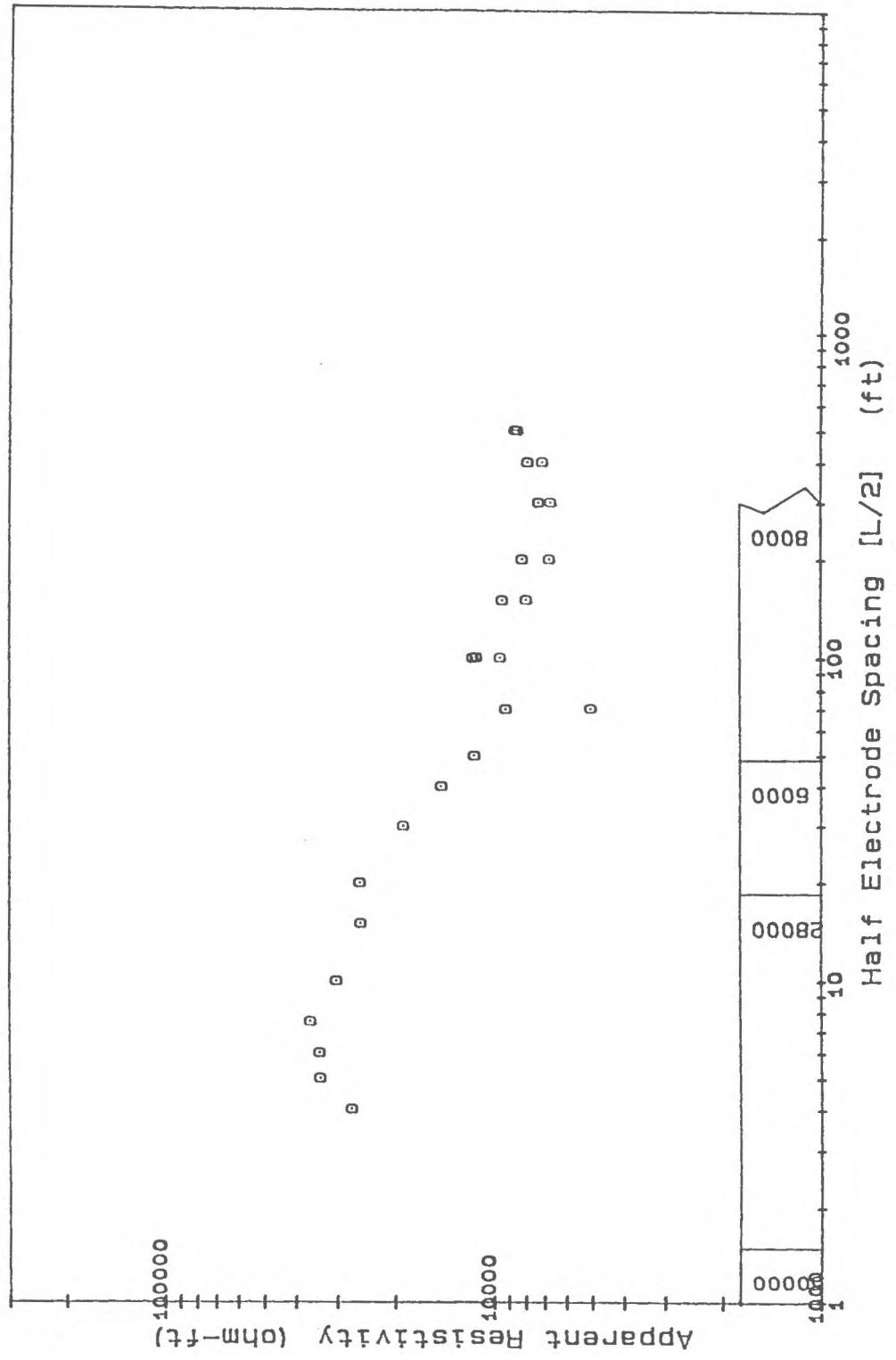
Depth Sounding Curves with layer model interpretations,  
Johnston, Rhode Island

see header for profile number and location

# GeoElectrical Depth Sounding After Schlumberger

Project : Central Landfill  
 Location : Johnston R.I.  
 Operators: Frohlich, Boland

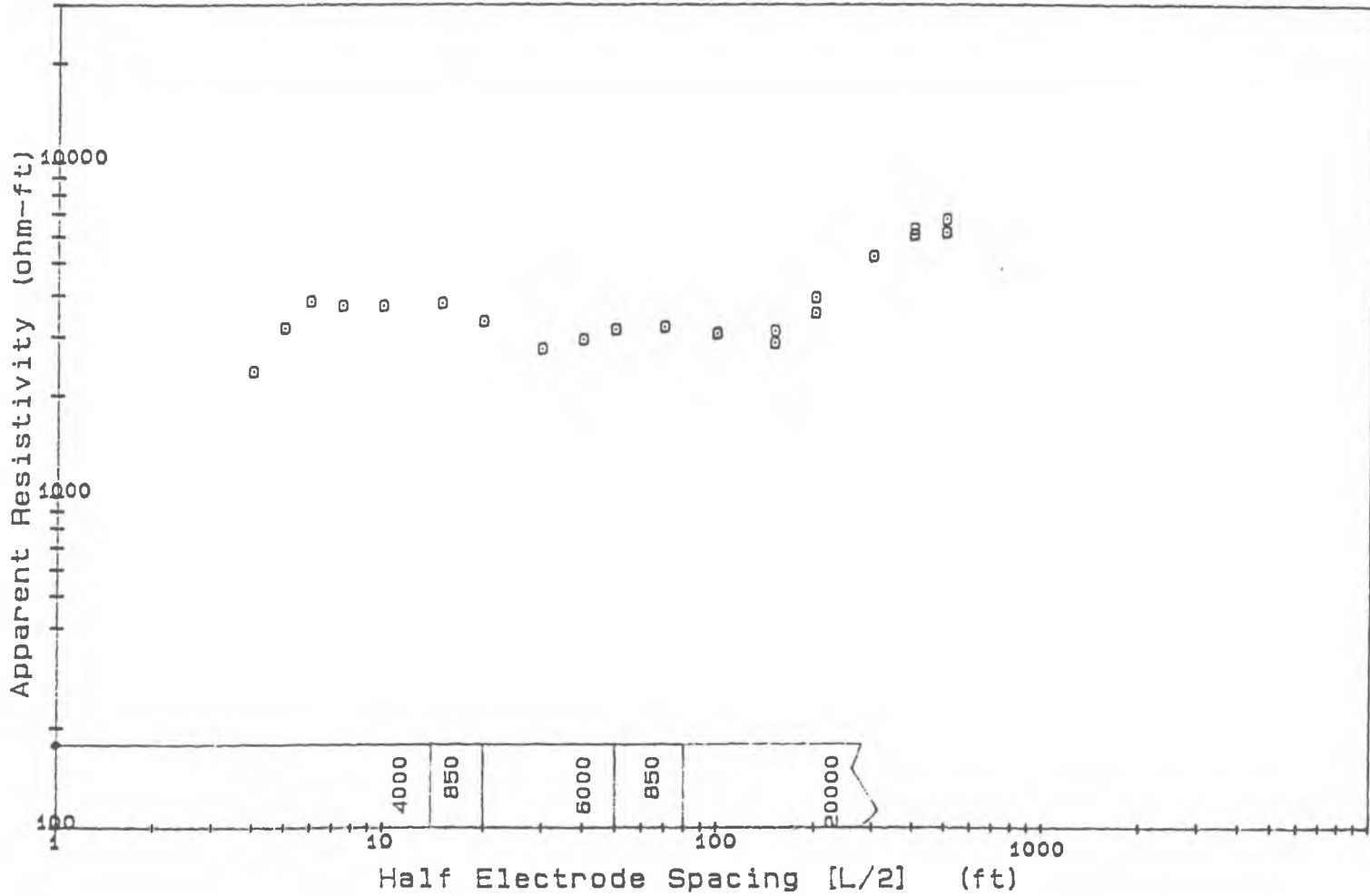
Profile : CLF-1  
 Date : 19 JUN 87



# GeoElectrical Depth Sounding After Schlumberger

Project : Central Landfill  
Location : Johnston R.I.  
Operators Frohlich, Boland

Profile : CLF-2  
Date : 19 JUN 87

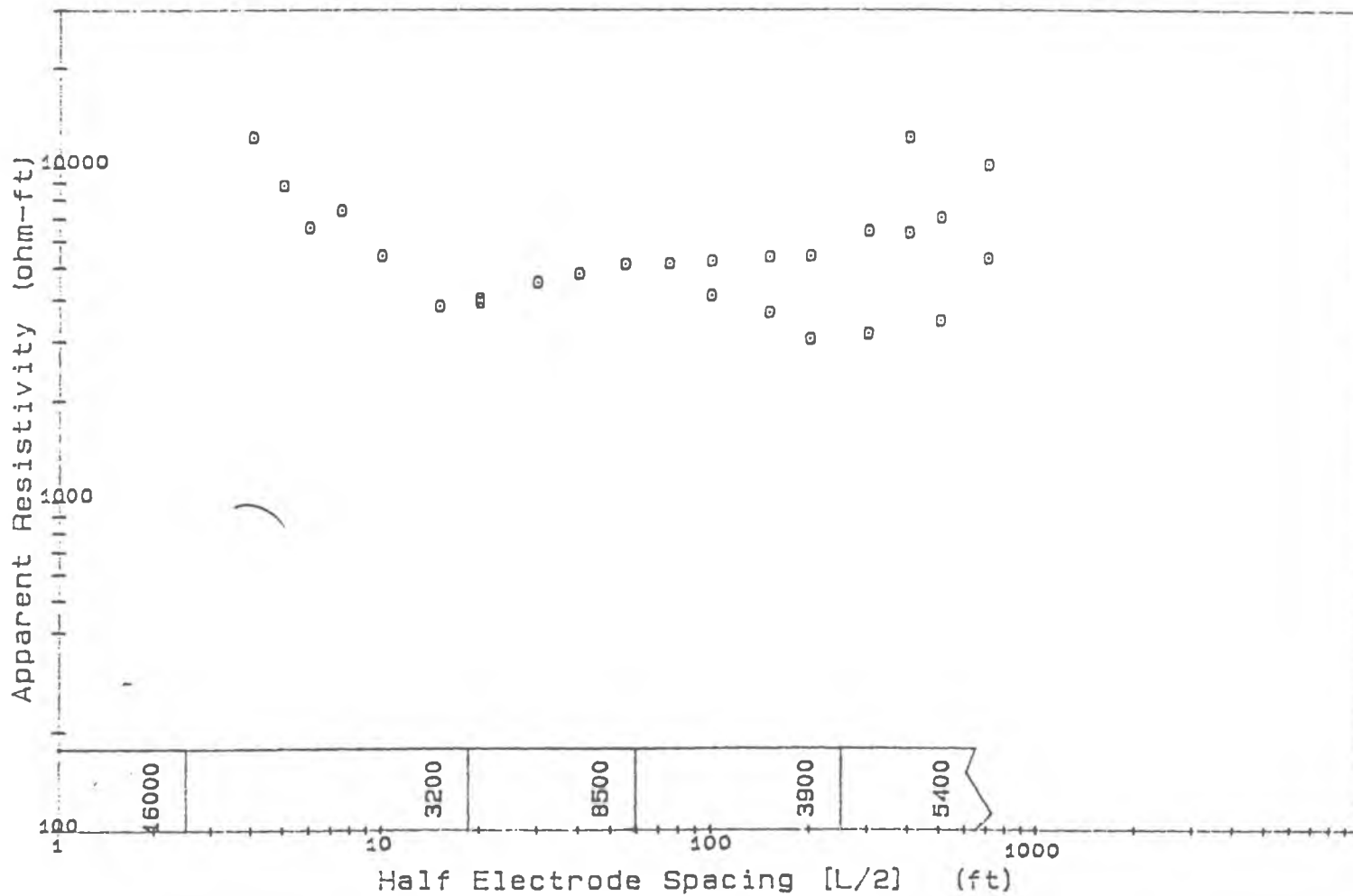




# GeoElectrical Depth Sounding After Schlumberger

Project : Central Landfill  
Location : Johnston R.I.  
Operators Frohlich, Boland

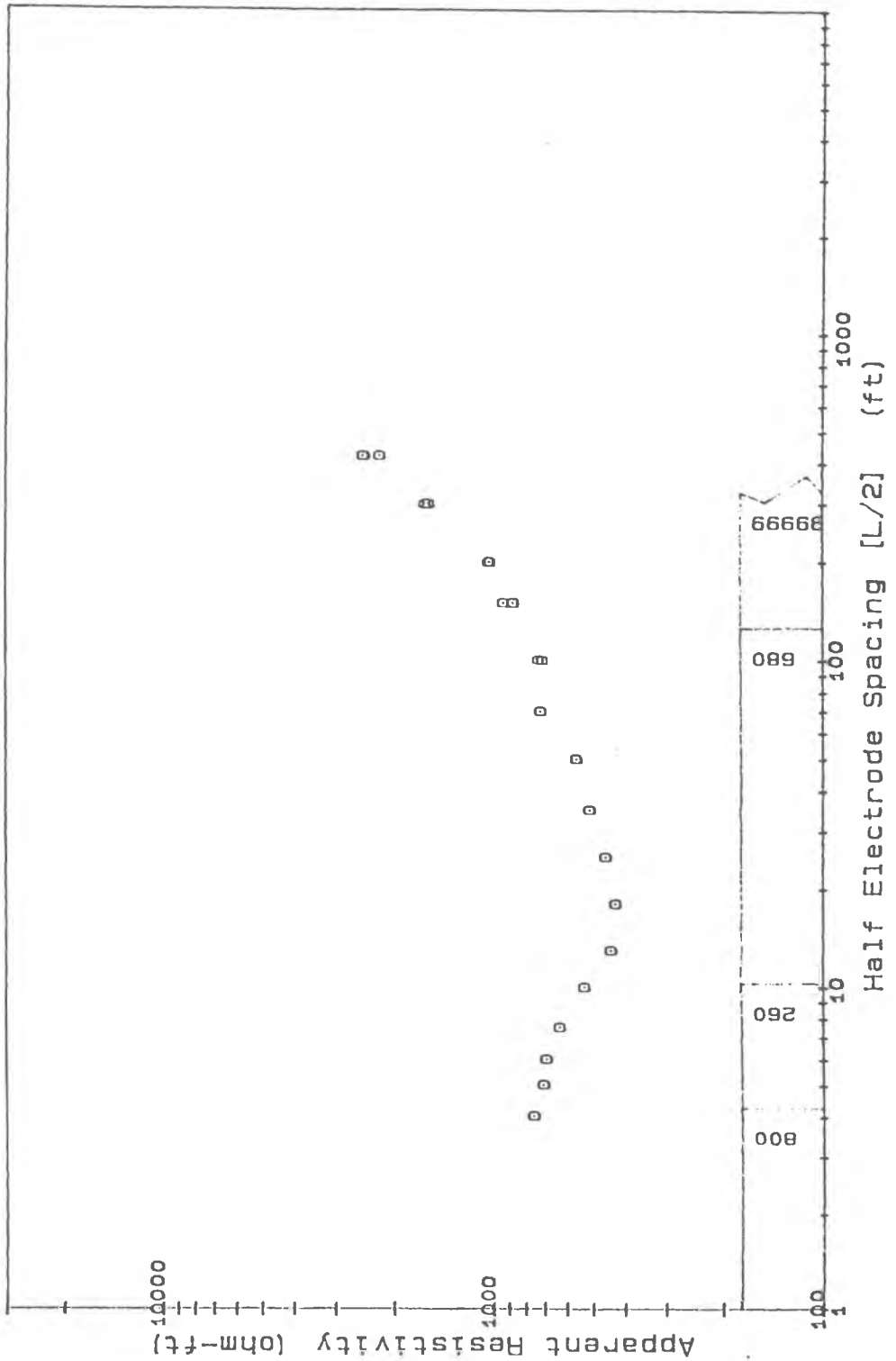
Profile : CLF-3  
Date : 20 JUN 87



# GeoElectrical Depth Sounding After Schlumberger

Project : Central Landfill  
 Location : Johnston R.I.  
 Operators: Frhlich, Boland

Profile : CLF-4  
 Date : 20 JAN 87



# GeoElectrical Depth Sounding After Schlumberger

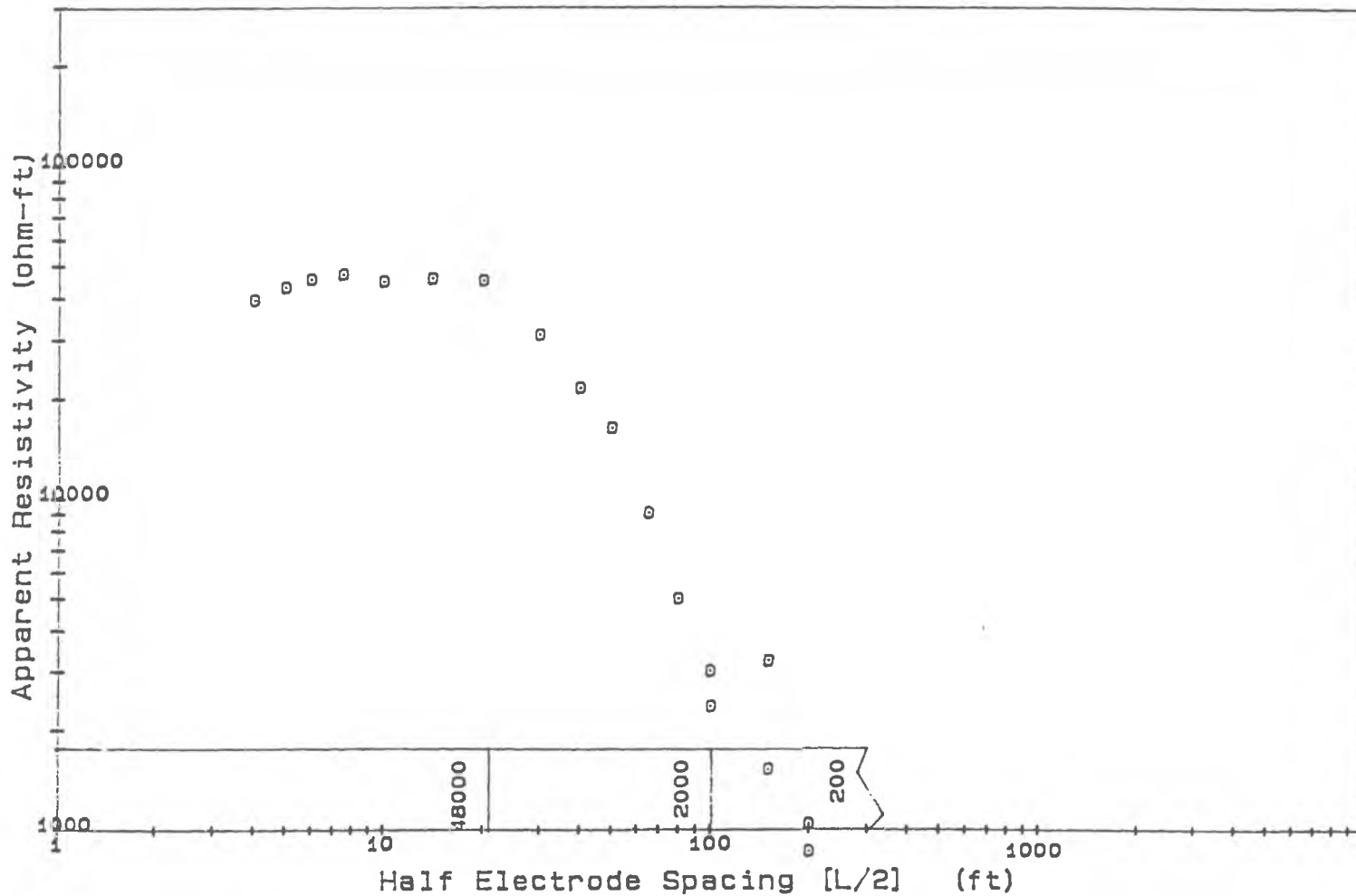
Project : Central Landfill

Location : Johnston R.I.

Operators: Frohlich, Boland, Savarese

Profile : CLF-5

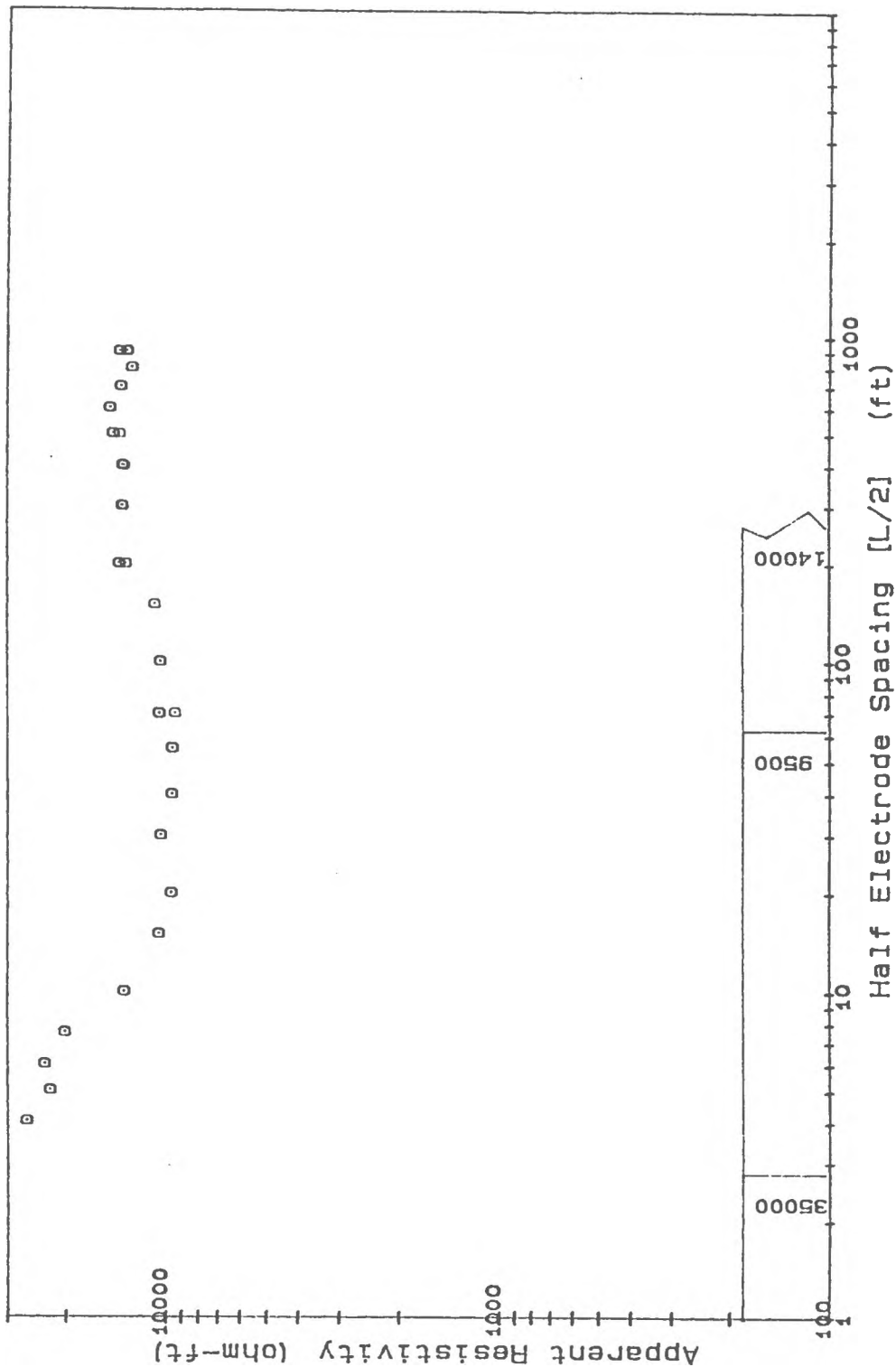
Date : 24 JUN 87



# GeoElectrical Depth Sounding After Schlumberger

Project : Central Landfill  
 Location : Johnston R.I.  
 Operators: Frohlich, Boland, Savarese

Profile : CLF-6  
 Date : 24 JUN 87



# GeoElectrical Depth Sounding After Schlumberger

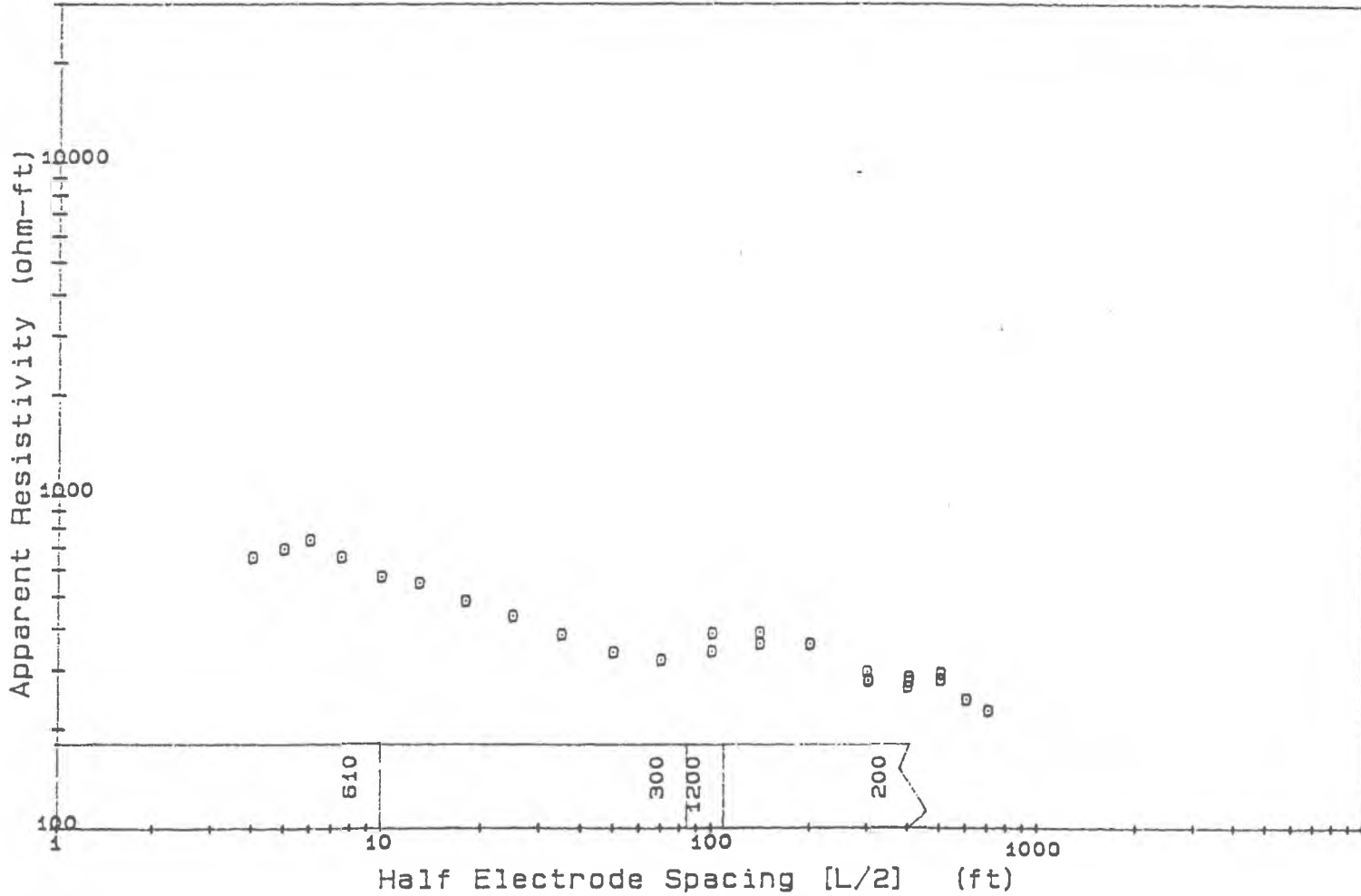
Project : Central Landfill

Location : Johnston R.I.

Operator: Frohlich, Boland, Hanson

Profile : CLF-7

Date : 01 JUL 87



# GeoElectrical Depth Sounding After Schlumberger

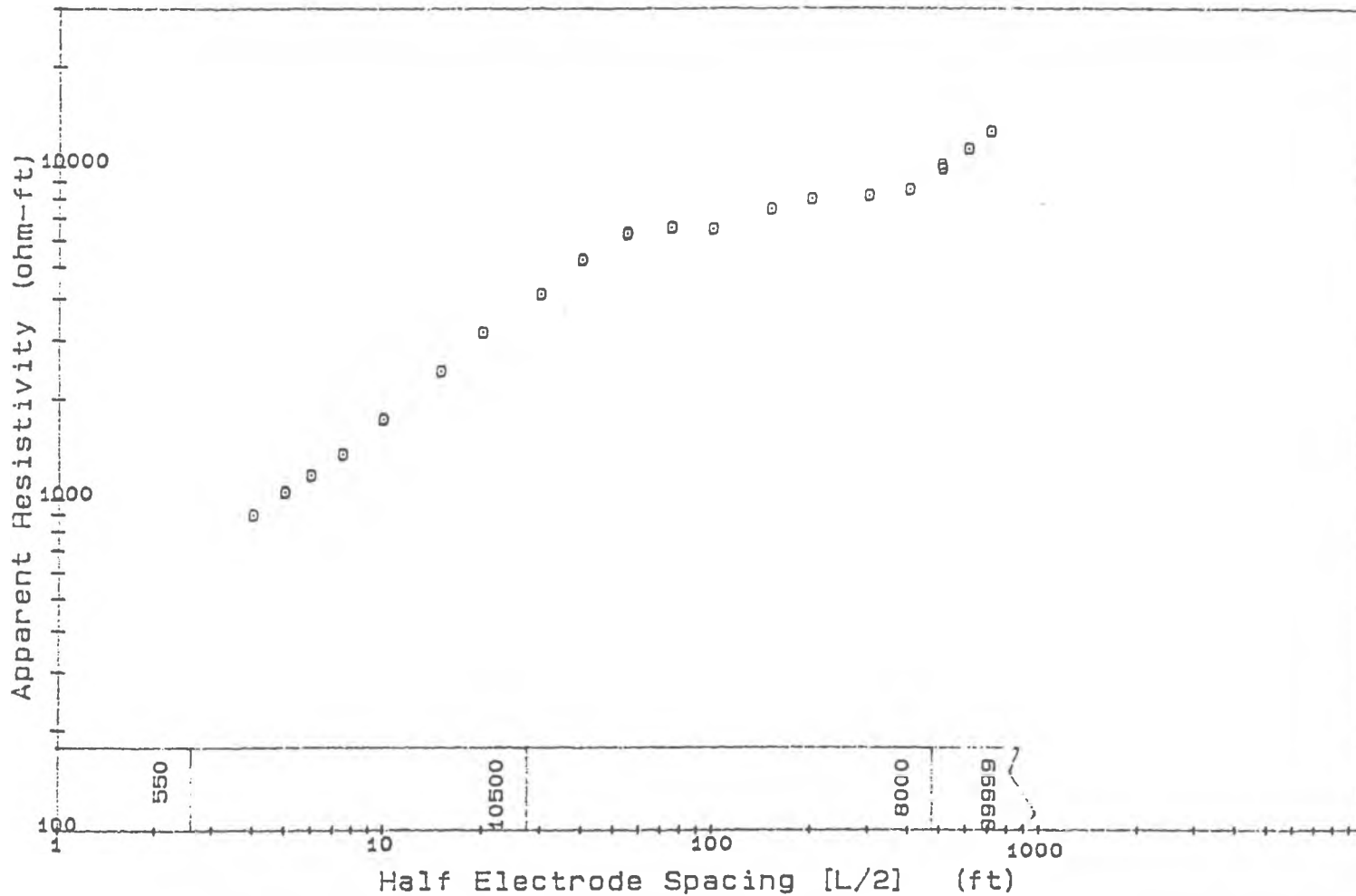
Project : Central Landfill

Location : Johnston R.I.

Operators: Frohlich, Boland, Hanson

Profile : CLF-8

Date : 01 JUL 87



# GeoElectrical Depth Sounding After Schlumberger

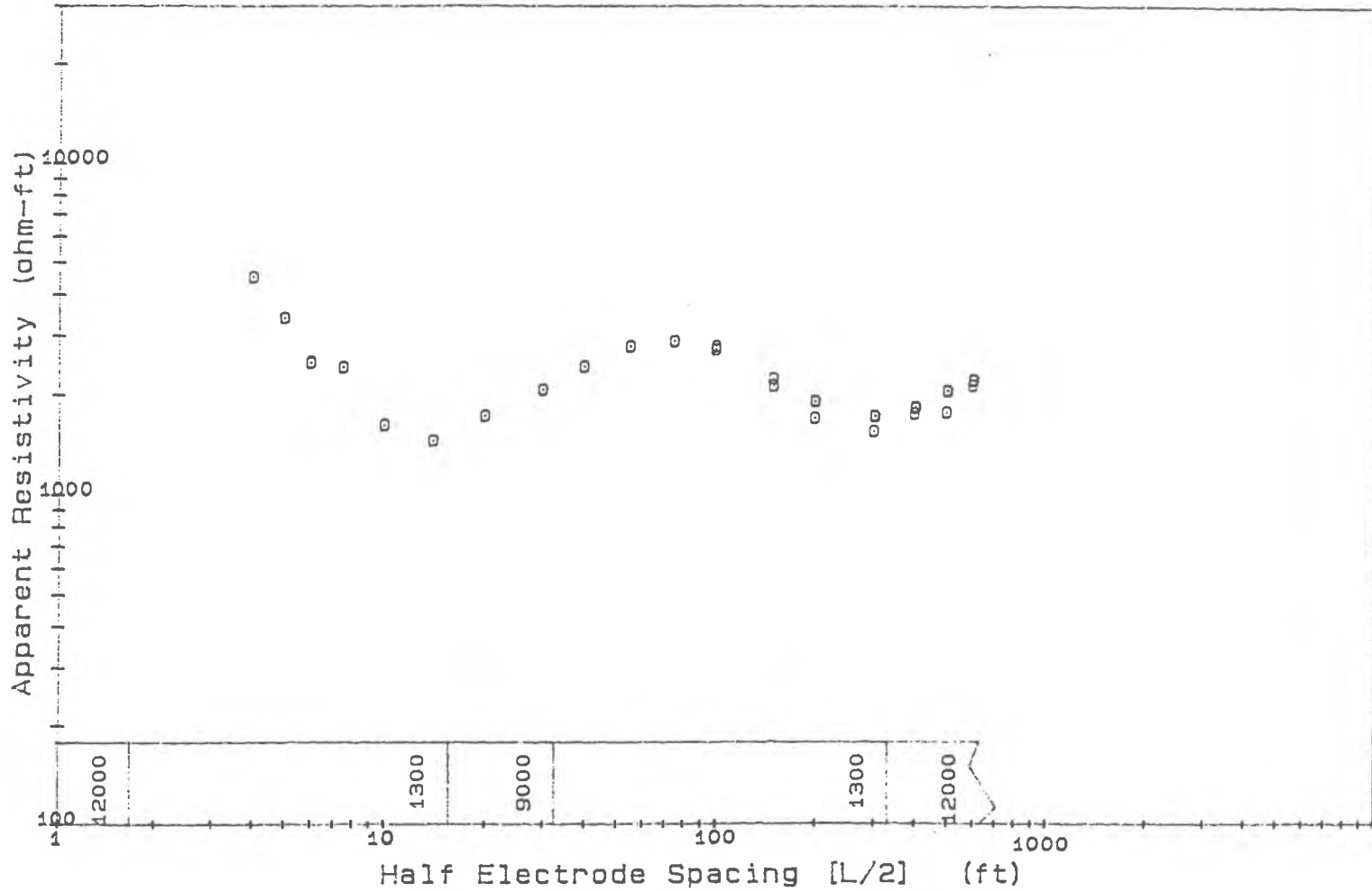
Project : Central Landfill

Location : Johnston R.I.

Operator: Frohlich, Boland, Hanson

Profile : CLF-9

Date : 01 JUL 87



### APPENDIX 3

Depth Sounding Curves with layer model interpretations,  
Tiverton, Rhode Island

see header for profile number and location



# GeoElectrical Depth Sounding After Schlumberger

Project : Tiverton/D.E.M.

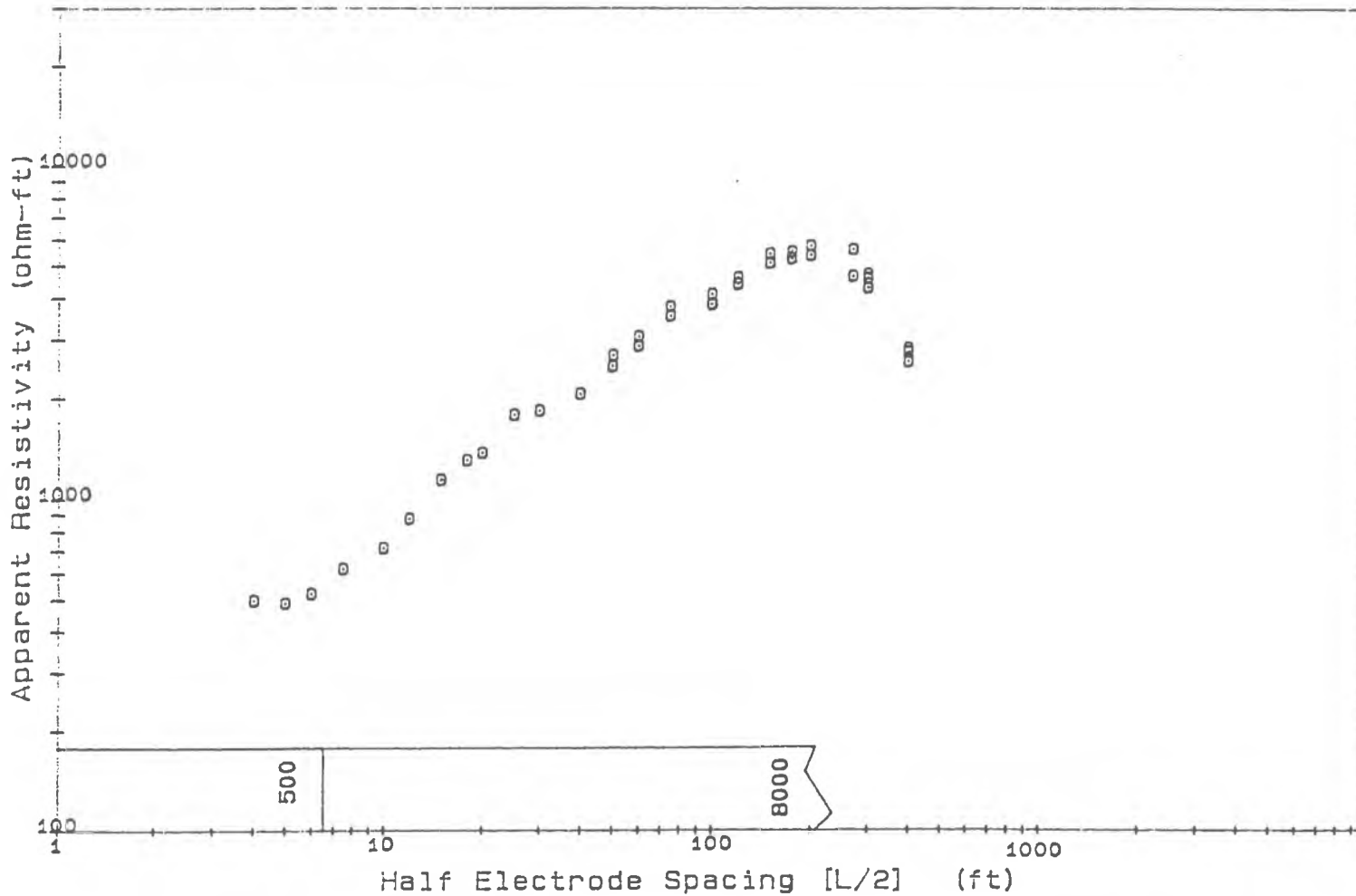
Location : Florence Ave.

Operators Frohlich, Boland, Hanson

Profile : FL-1

Date : 19 MAY 87

190



# GeoElectrical Depth Sounding After Schlumberger

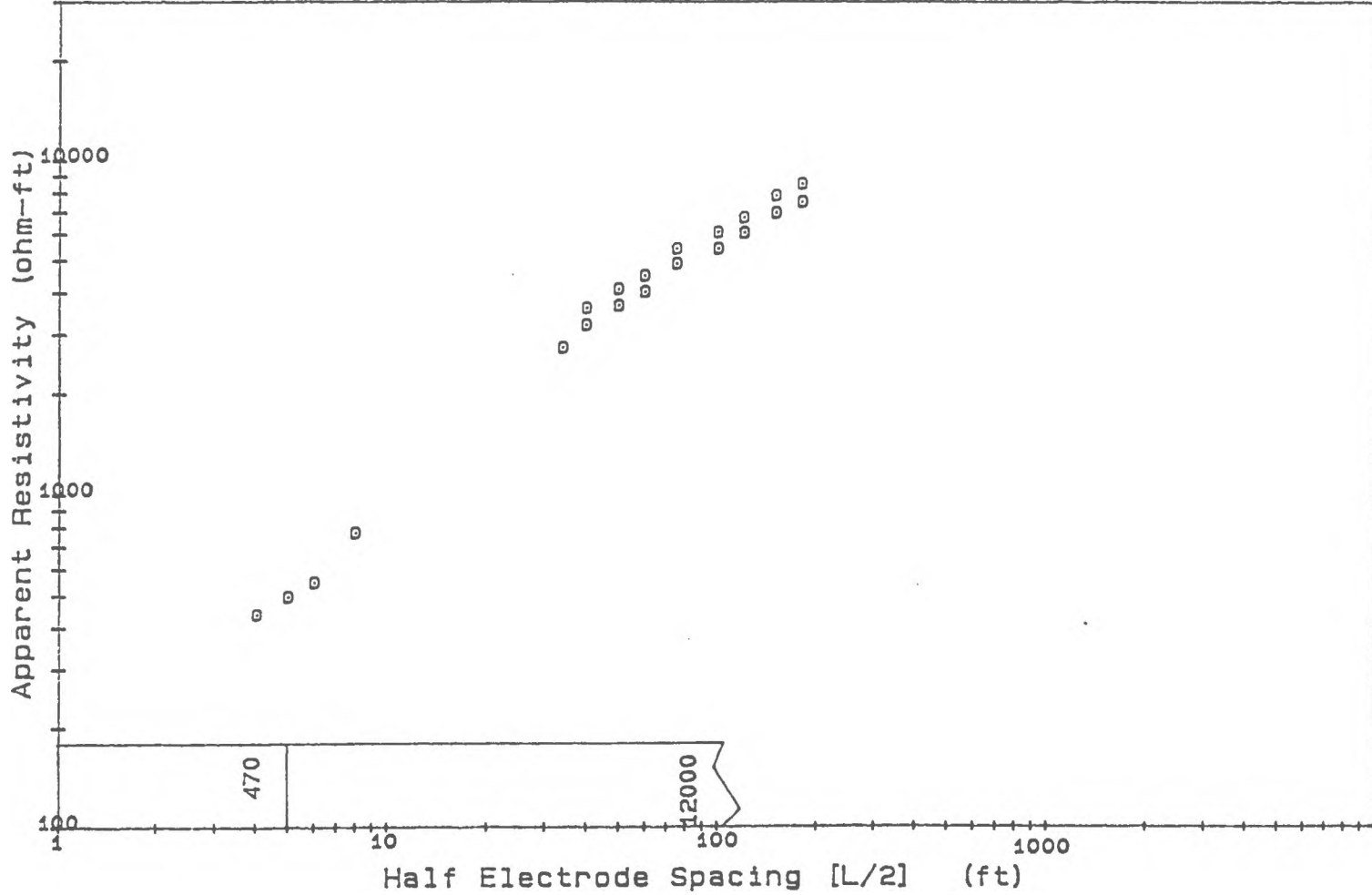
Project : Tiverton/D.E.M.

Location : Florence Ave.

Operators Frohlich, Boland, Hanson

Profile : f1-2

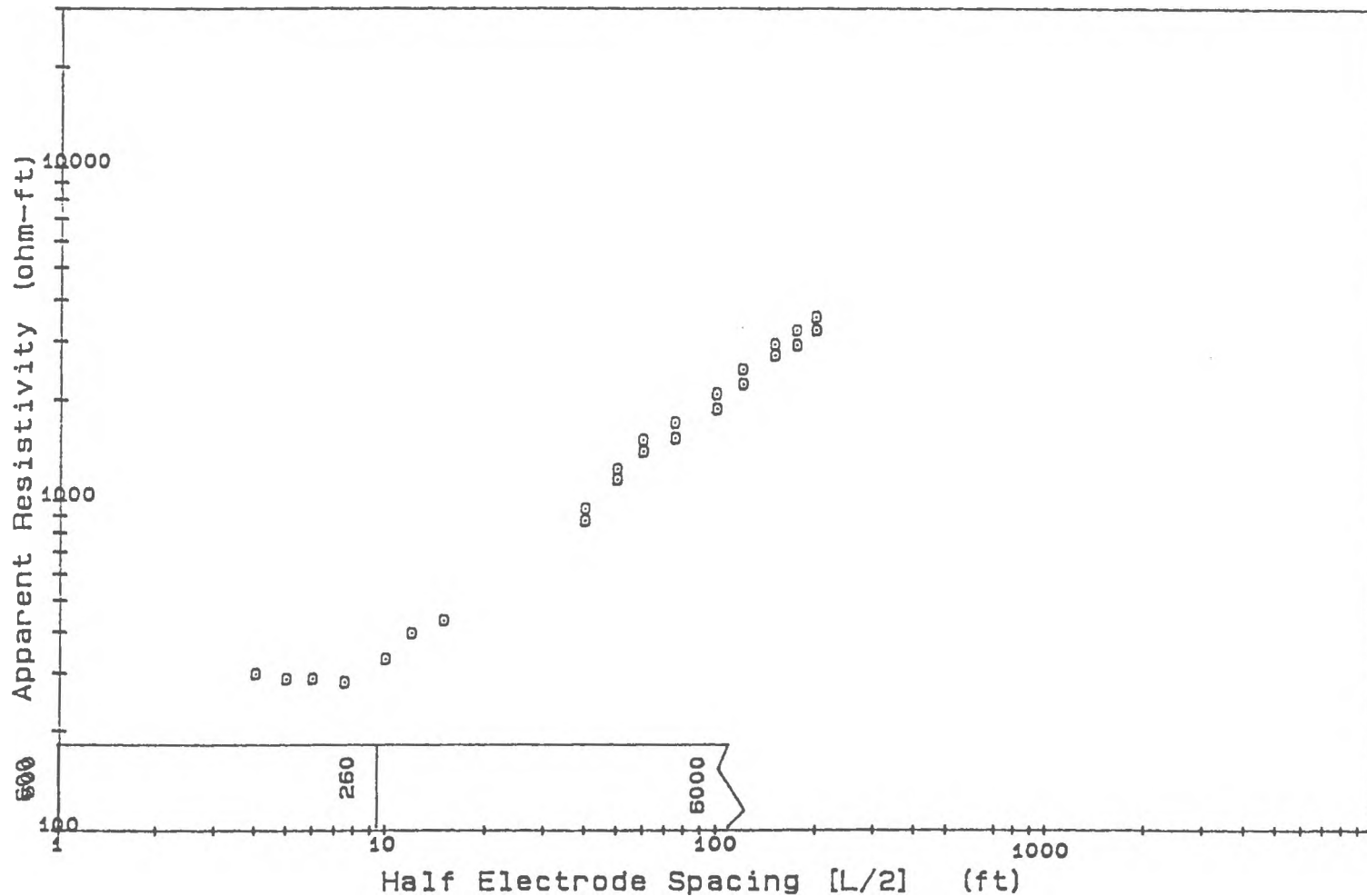
Date : 19 MAY 87



# GeoElectrical Depth Sounding After Schlumberger

Project : Tiverton/D.E.M.  
Location : Florence Ave.  
Operators Frohlich, Boland, Hanson

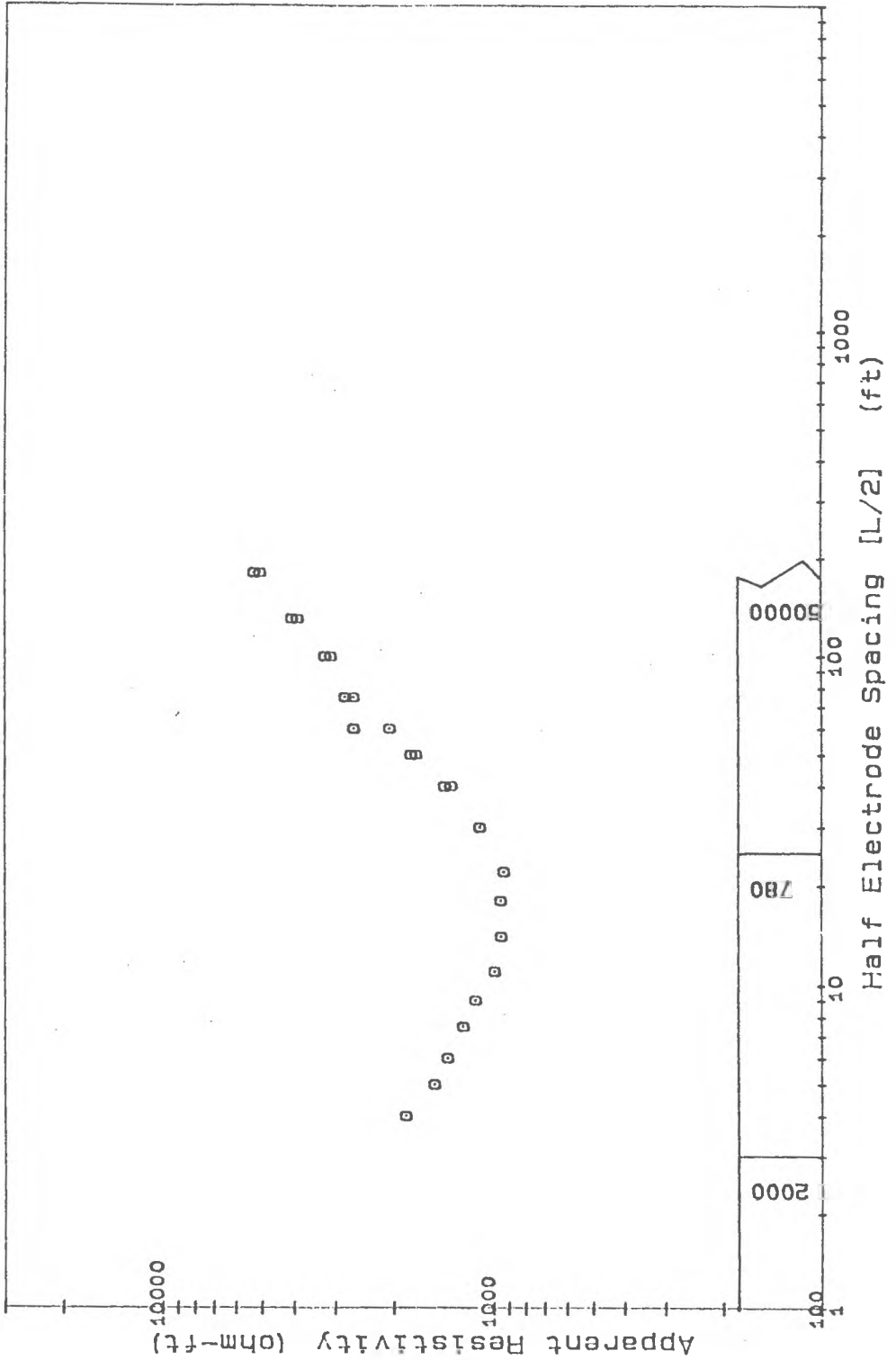
Profile : FL-3  
Date : 19 MAY 87



# GeoElectrical Depth Sounding After Schlumberger

Project : Tiverton/D.E.M.  
 Location : Stafford Rd.  
 Operators: Frohlich, Boland, Hanson

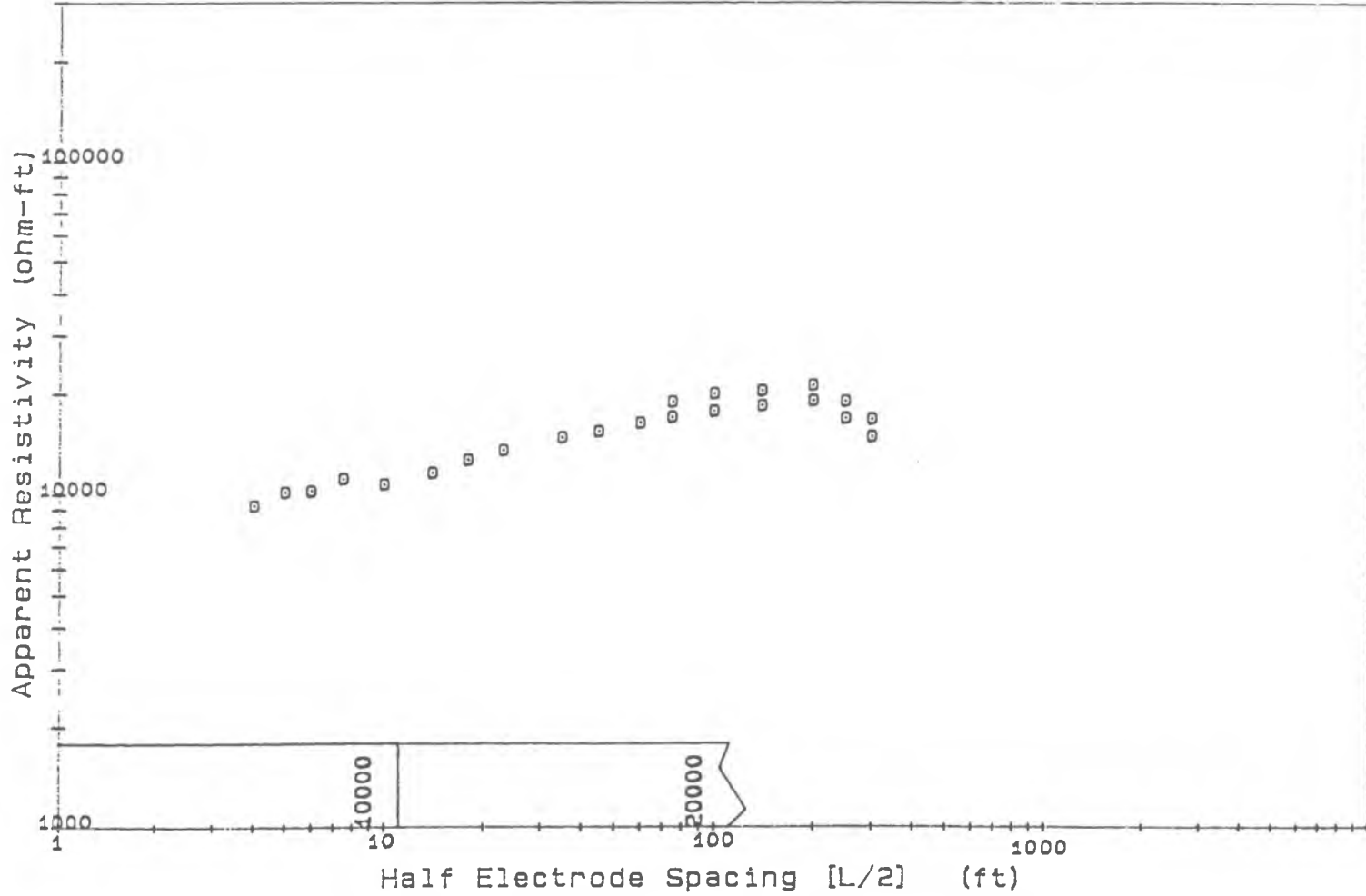
Profile : f1-4  
 Date : 27 MAY 67



# GeoElectrical Depth Sounding After Schlumberger

Project : Tiverton/D.E.M.  
Location : Behind Irene's  
operators: Frohlich, Boland, Hanson

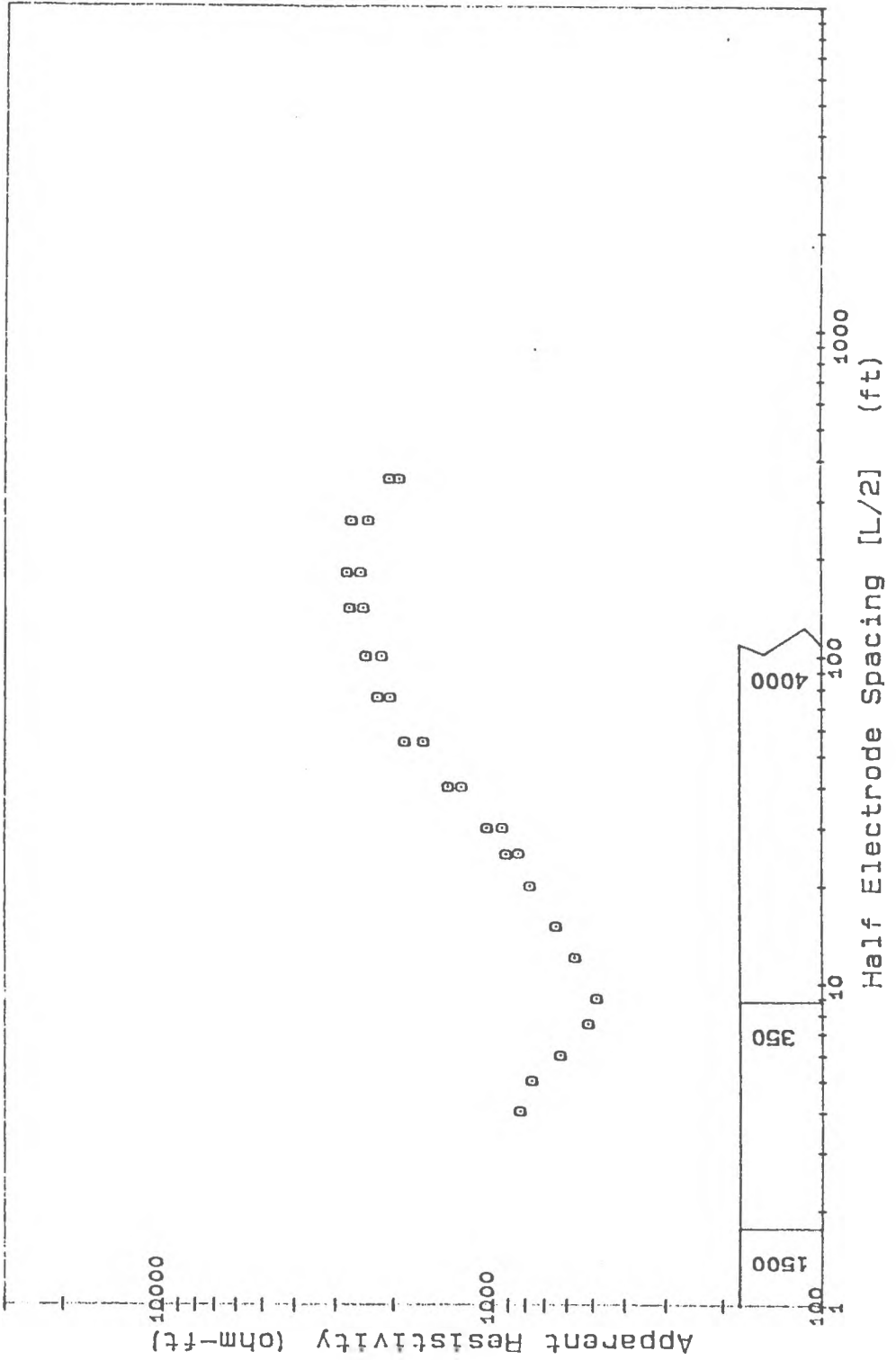
Profile : FL-5  
Date : 27 MAY 87



# GeoElectrical Depth Sounding After Schlumberger

Project : Tiverton/D.E.M.  
 Location : Montgomery Ln.  
 Operator: Frohlich, Boland, Hanson

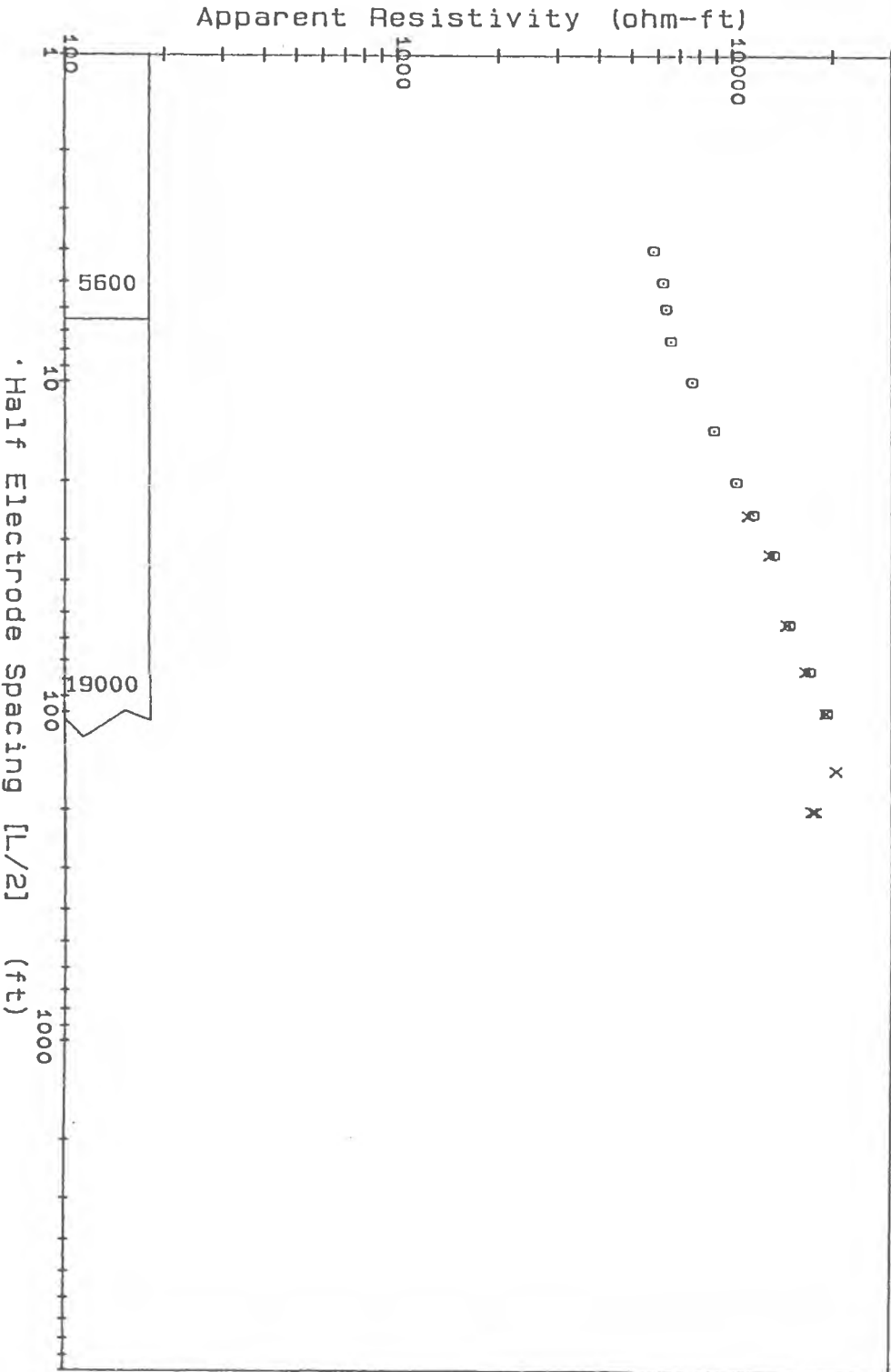
Profile : FL-6  
 Date : 29 MAY 87



# Geoelectrical Depth Sounding After Schlumberger

Project : Tiverton/D.E.M.  
Location : Montgomery Ave.  
Operators : Ave.

Profile : FL-7  
Date : 29 MAY 87



# GeoElectrical Depth Sounding After Schlumberger

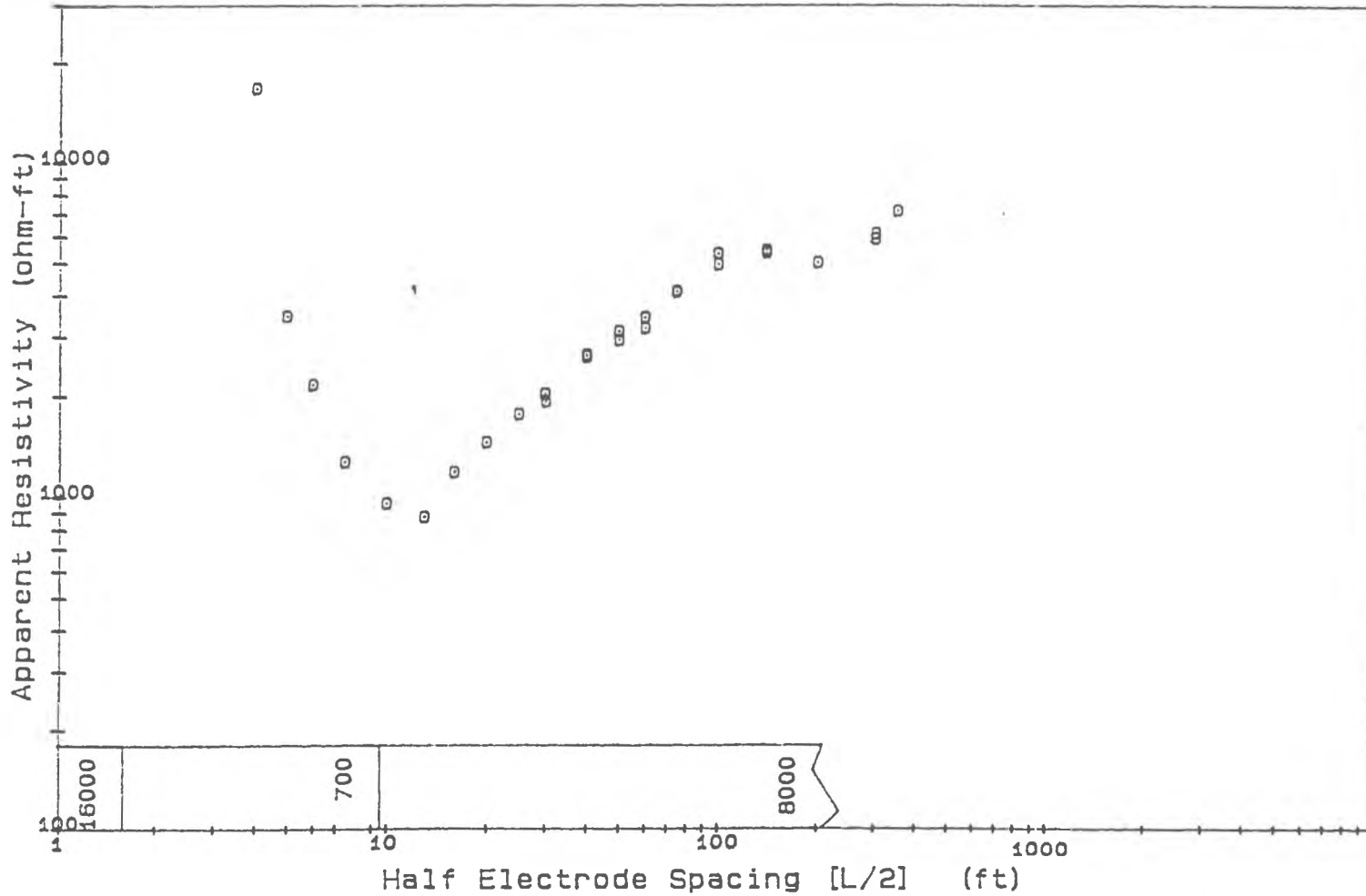
Project : Tiverton/D.E.M.

Location : Bridal Way

Operators: Fohlich, Boland, Hanson

Profile : FL-8

Date : 16 JUN 87





## APPENDIX 4

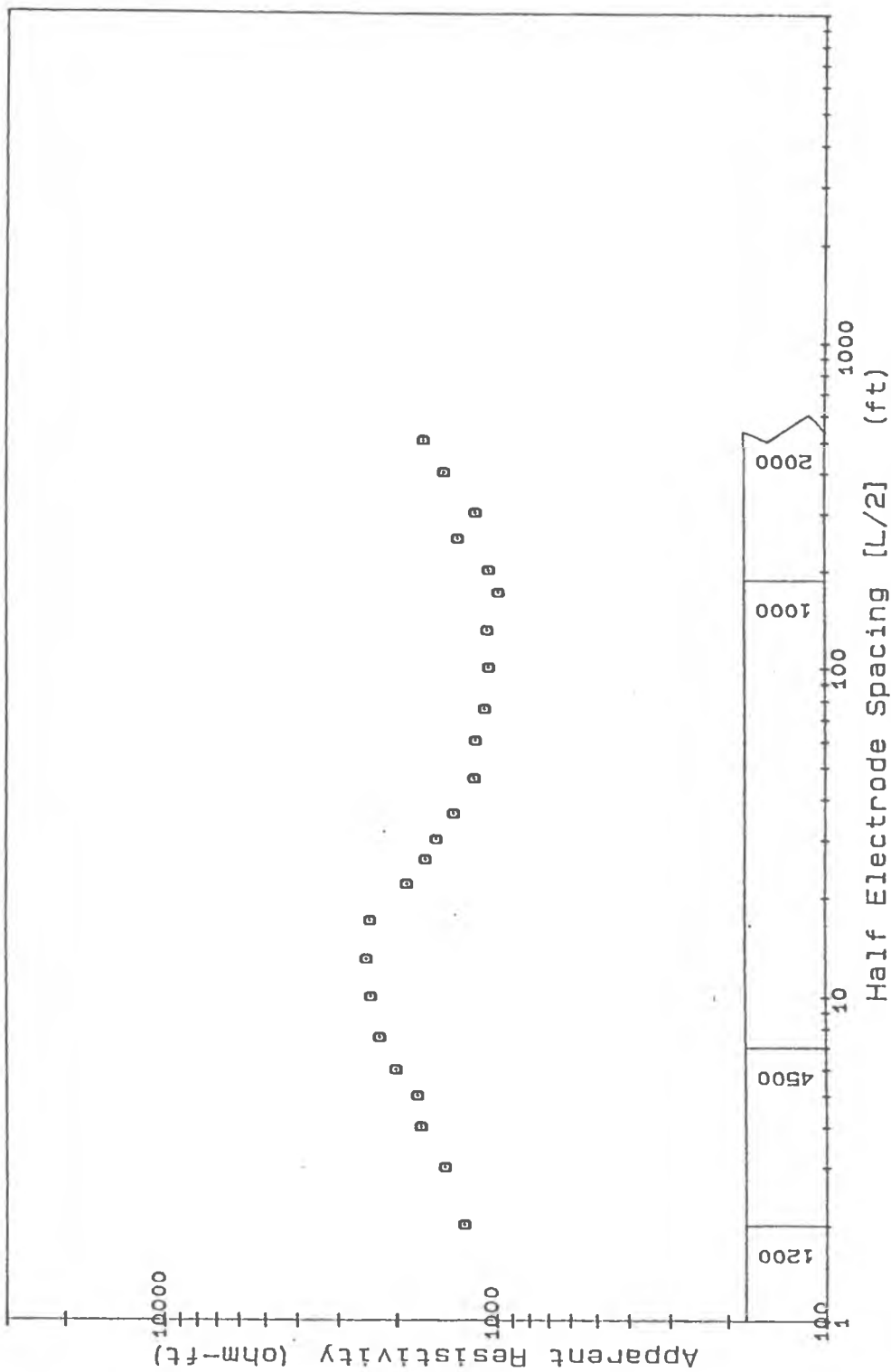
### Depth Sounding Curves with layer model interpretations, Aroostook Co. Maine

see header for profile number and location

# GeoElectrical Depth Sounding After Schlumberger

Project : Maine Survey  
 Location :  
 Operators: Frohlich, Owen

Profile : Me-1  
 Date : AUG 86



# GeoElectrical Depth Sounding After Schlumberger

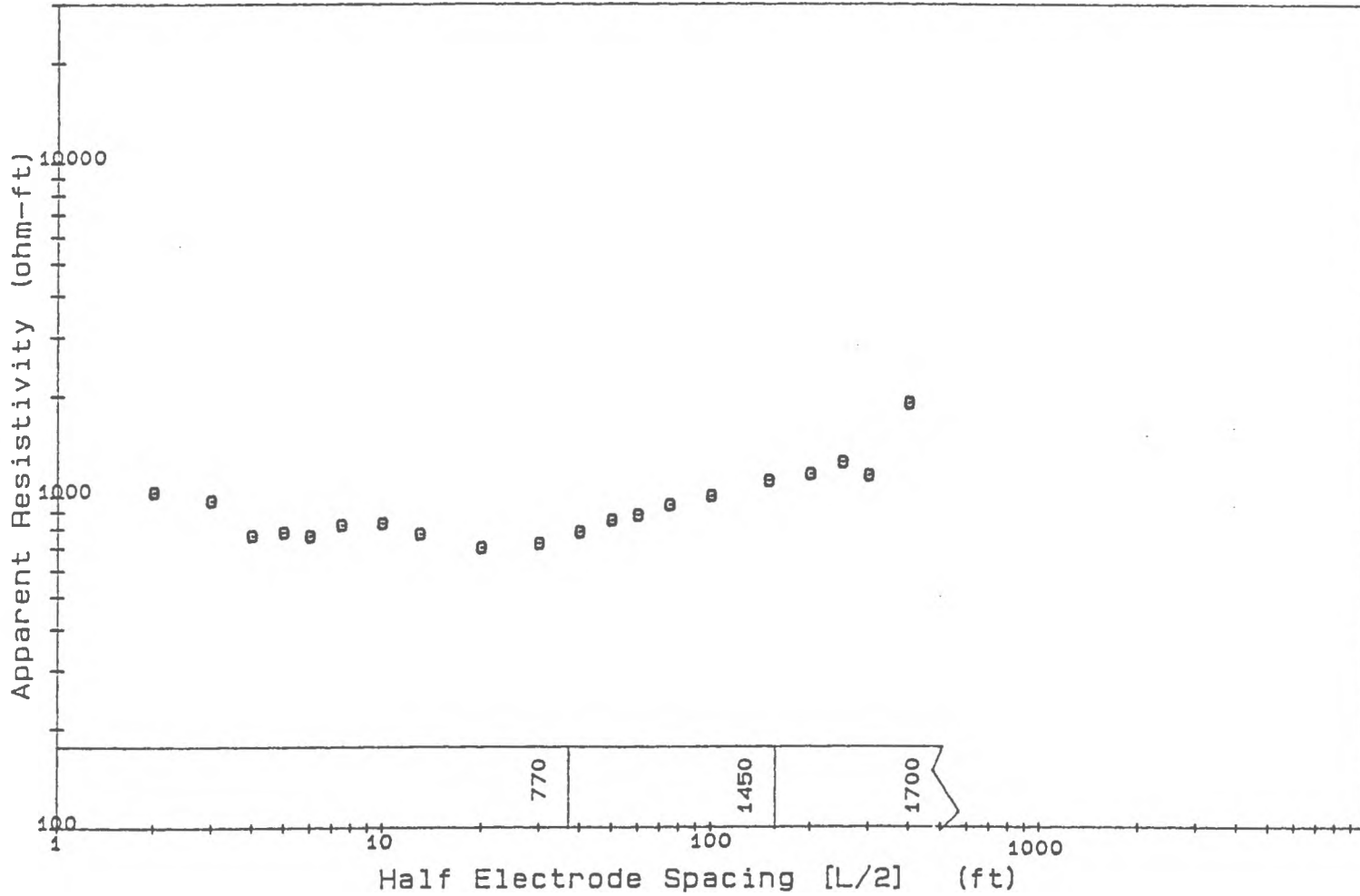
Project : Maine Survey

Location :

Operators: Frohlich, Owen

Profile : Me-2

Date : AUG 86

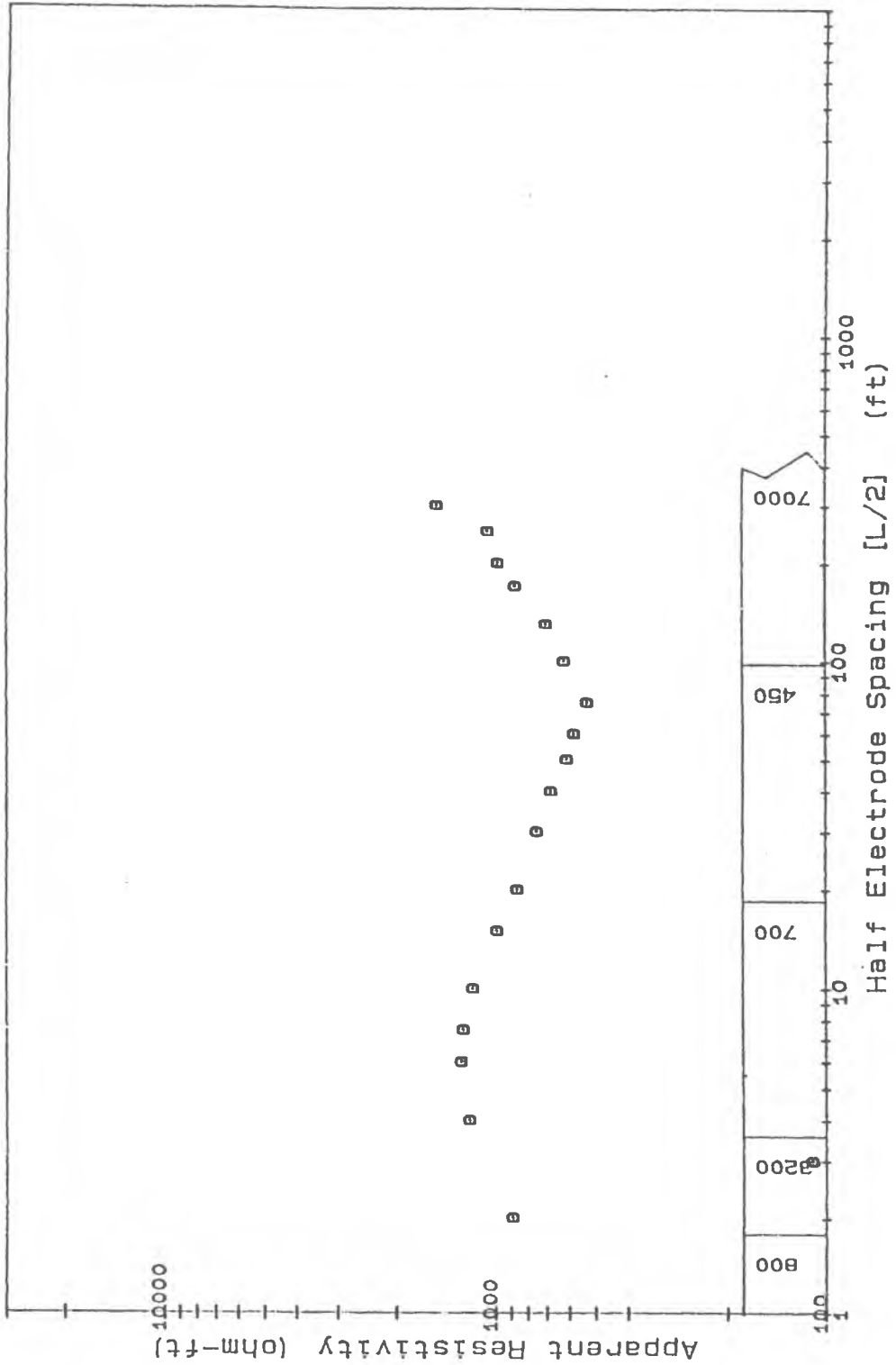


200

# GeoElectrical Depth Sounding After Schlumberger

Project : Maine Survey  
 Location :  
 Operators: Frohlich, Owen

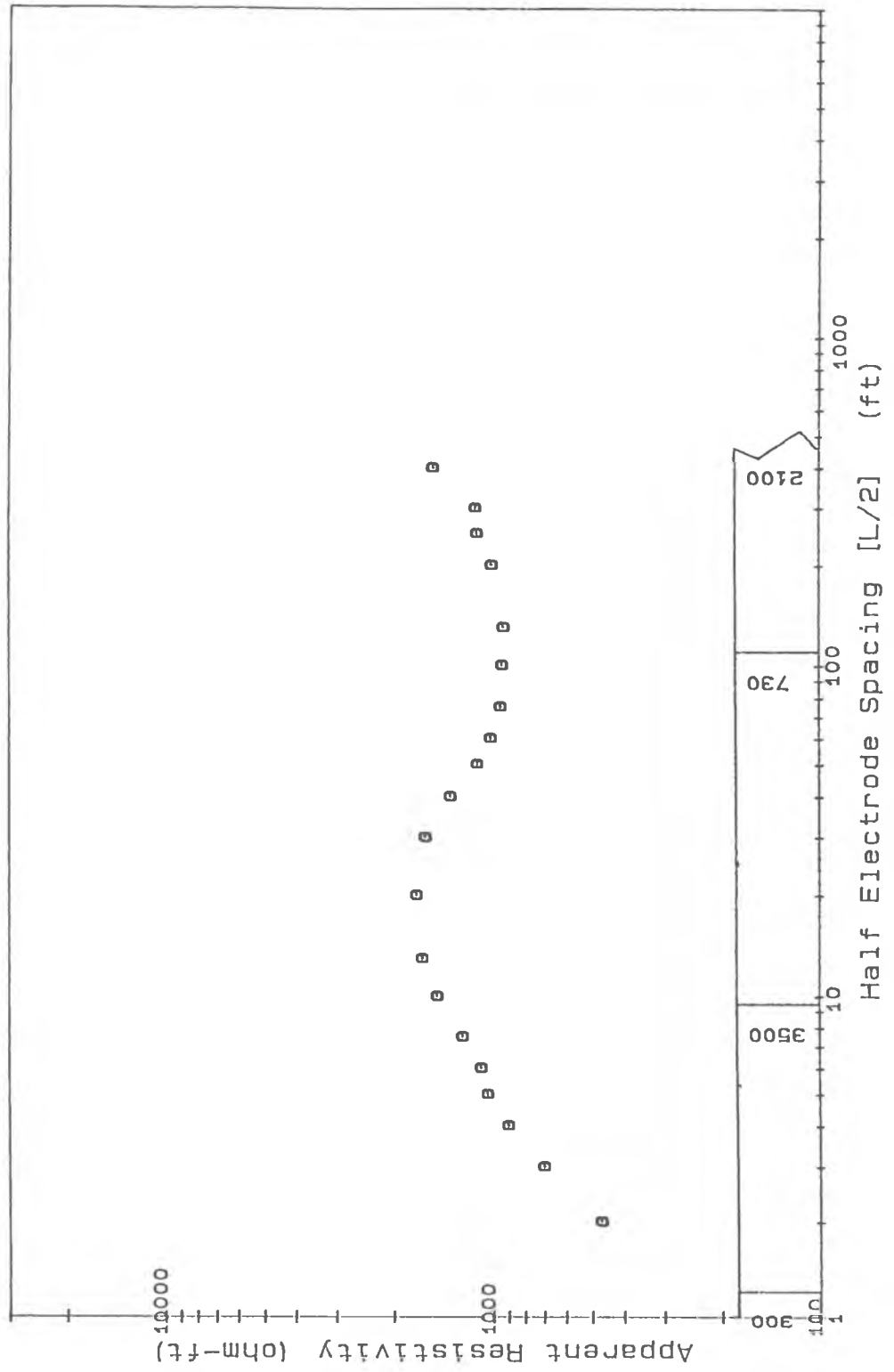
Profile : Me-3  
 Date : AUG 86



# GeoElectrical Depth Sounding After Schlumberger

Project : Maine Survey  
 Location :  
 Operators: Frohlich, Owen

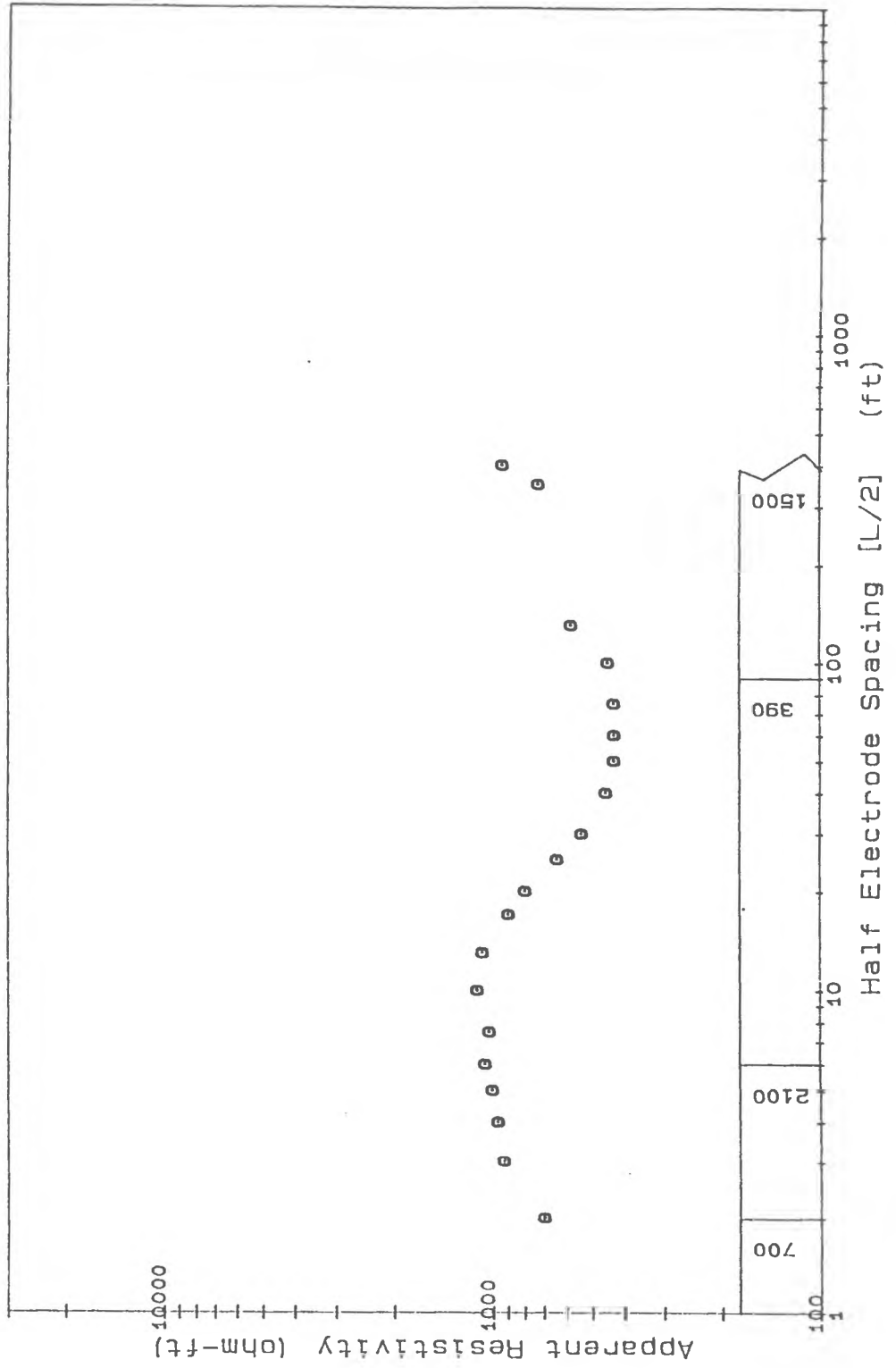
Profile : Me-4  
 Date : AUG 86



# GeoElectrical Depth Sounding After Schlumberger

Project : Maine Survey  
 Location :  
 Operators: Frohlich, Owen

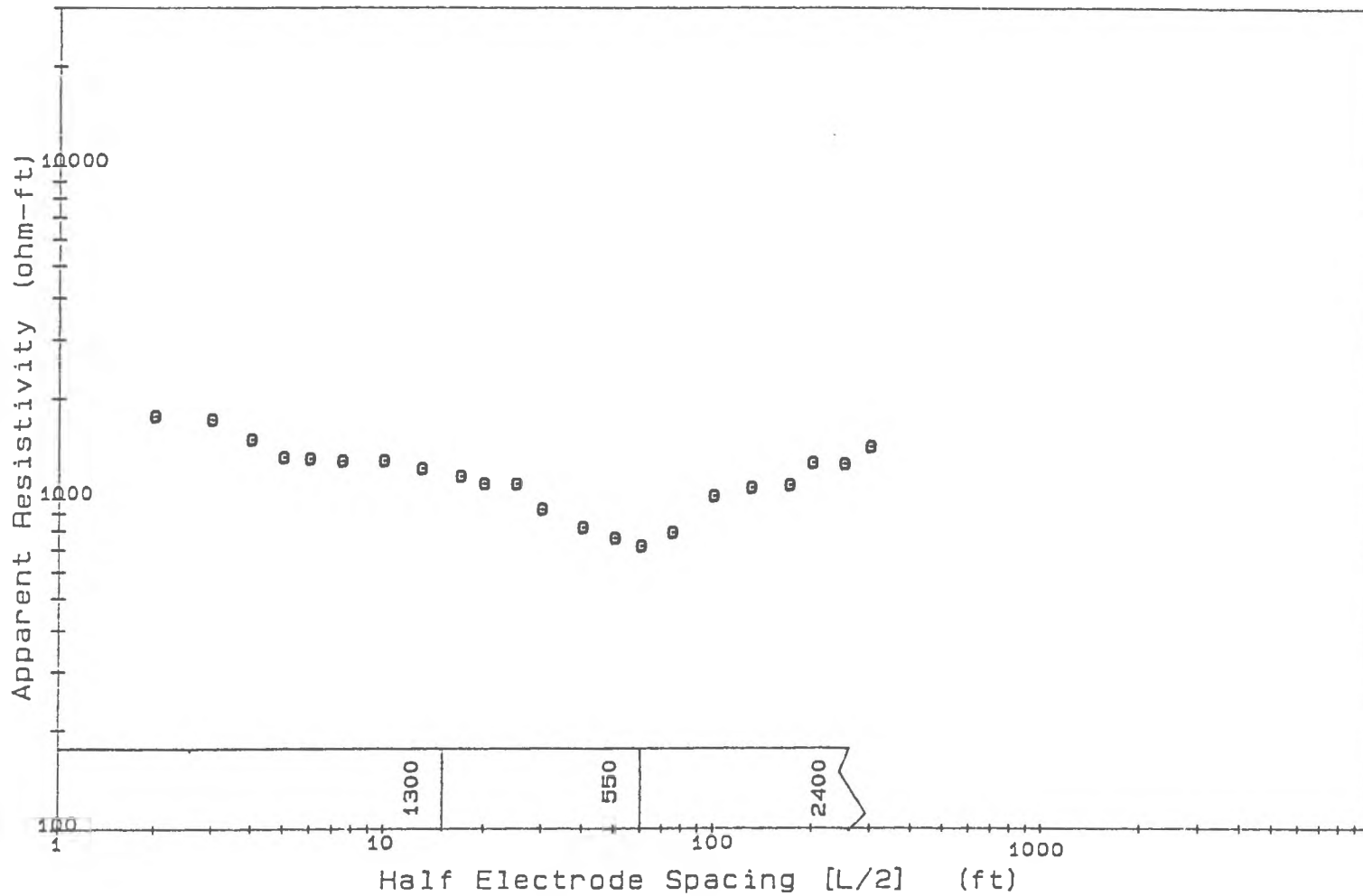
Profile : Me-5  
 Date : AUG 86



# GeoElectrical Depth Sounding After Schlumberger

Project : Maine Survey  
Location :  
Operators: Frohlich, Owen

Profile : Me-6  
Date : AUG 86

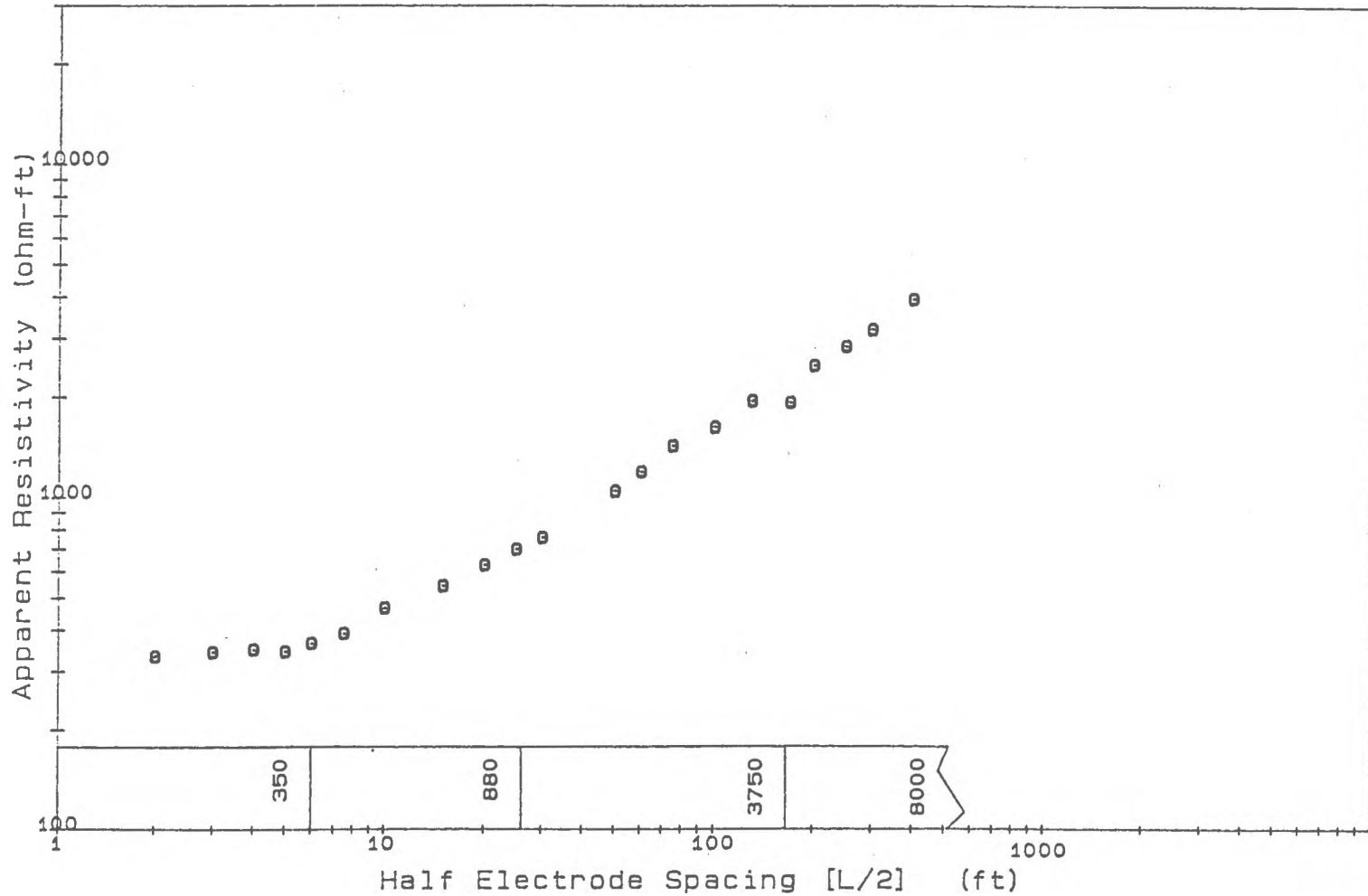


204

# GeoElectrical Depth Sounding After Schlumberger

Project : Maine Survey  
Location : Perp. to Fracture  
Operators: Frohlich, Owen

Profile : Me-7  
Date : AUG 86

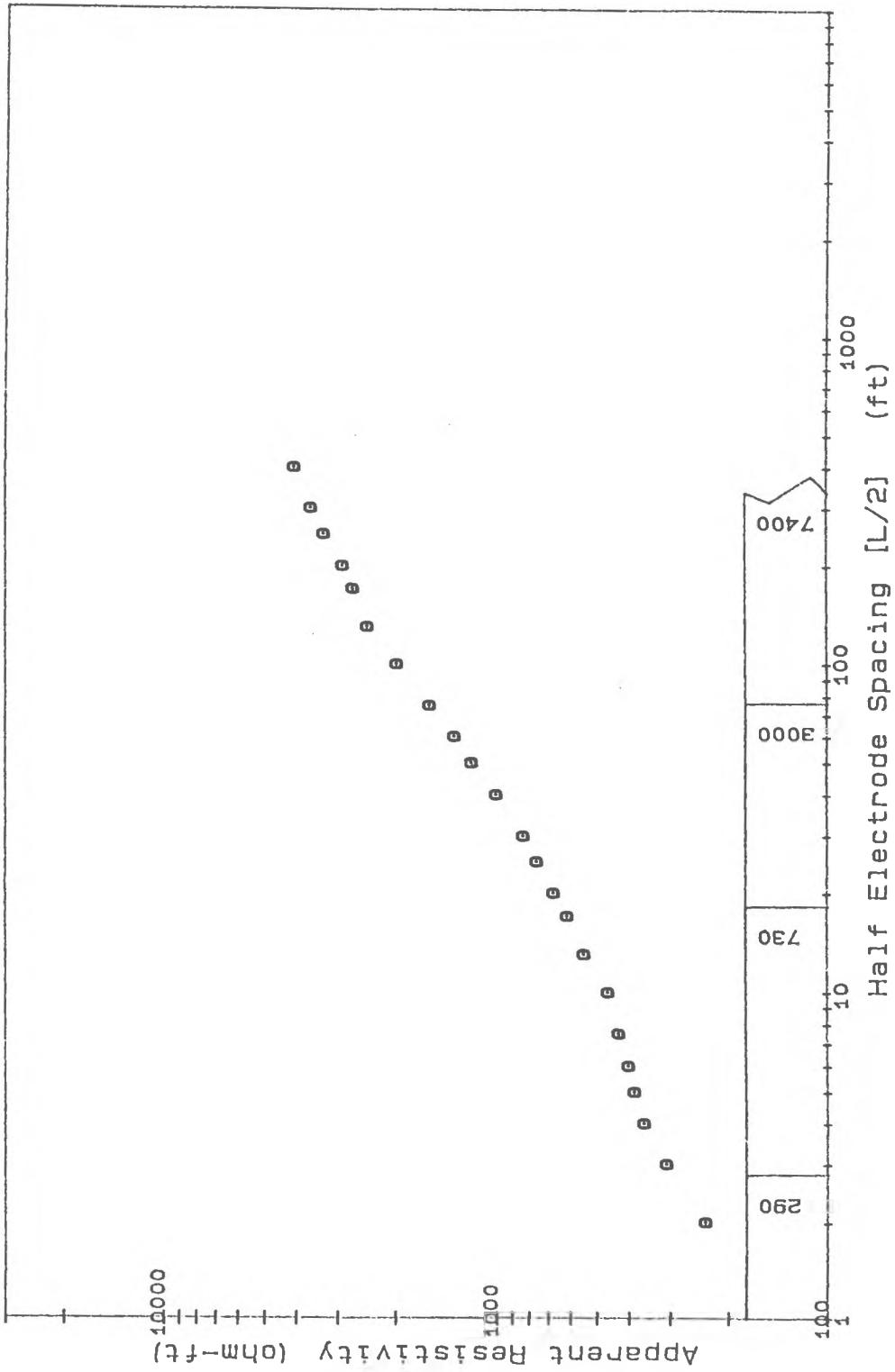




# GeoElectrical Depth Sounding After Schlumberger

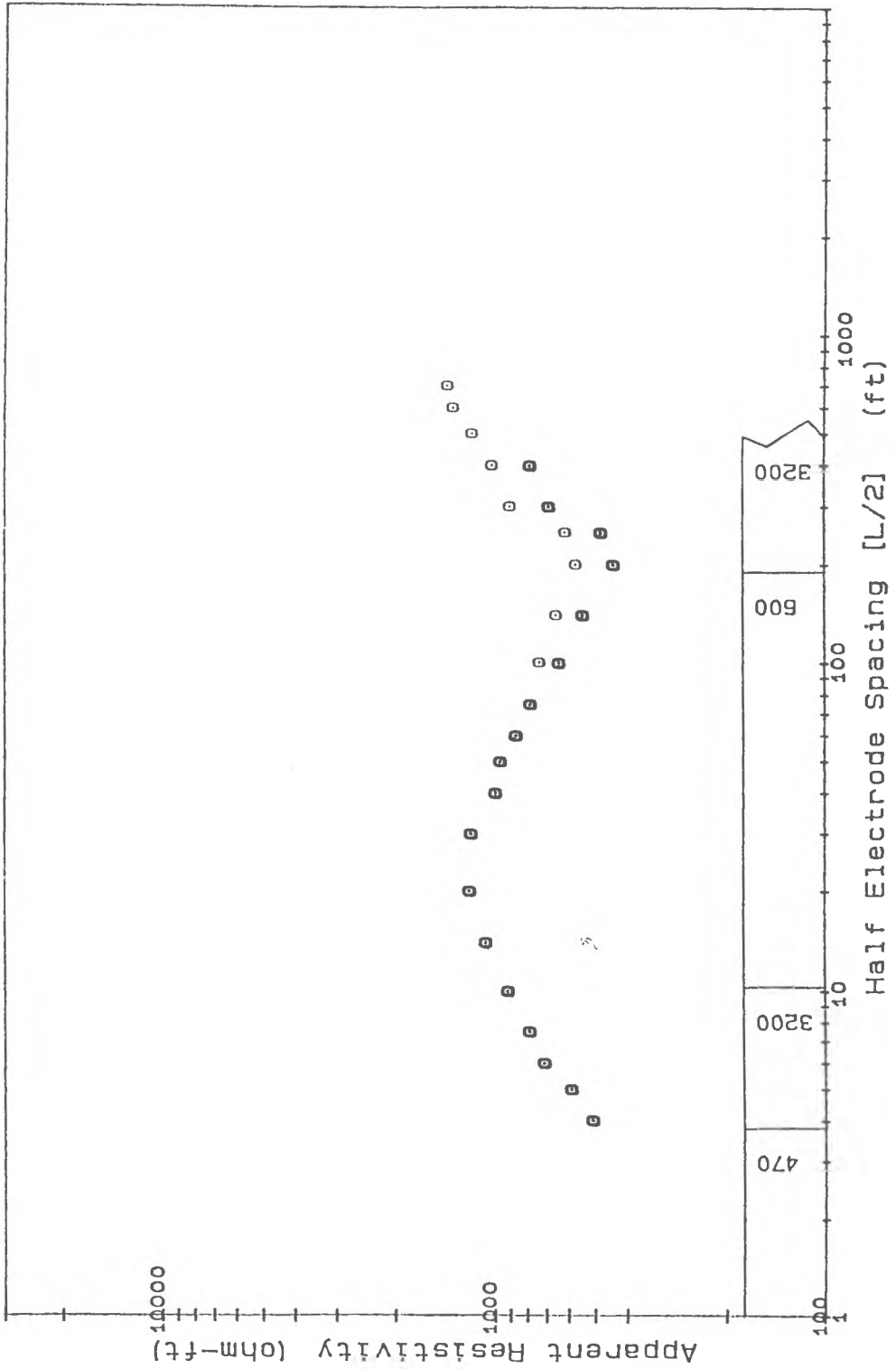
Project : Maine Survey  
 Location : Paral. to Fracture  
 Operators: Frohlich, Owen

Profile : Me-8  
 Date : AUG 86



# GeoElectrical Depth Sounding After Schlumberger

Project : Miane Survey      Profile : Me-11  
 Location : Fort Fairfield      Date : 04 AUG 87  
 Operators: Frohlich, Boland, Smith



# GeoElectrical Depth Sounding After Schlumberger

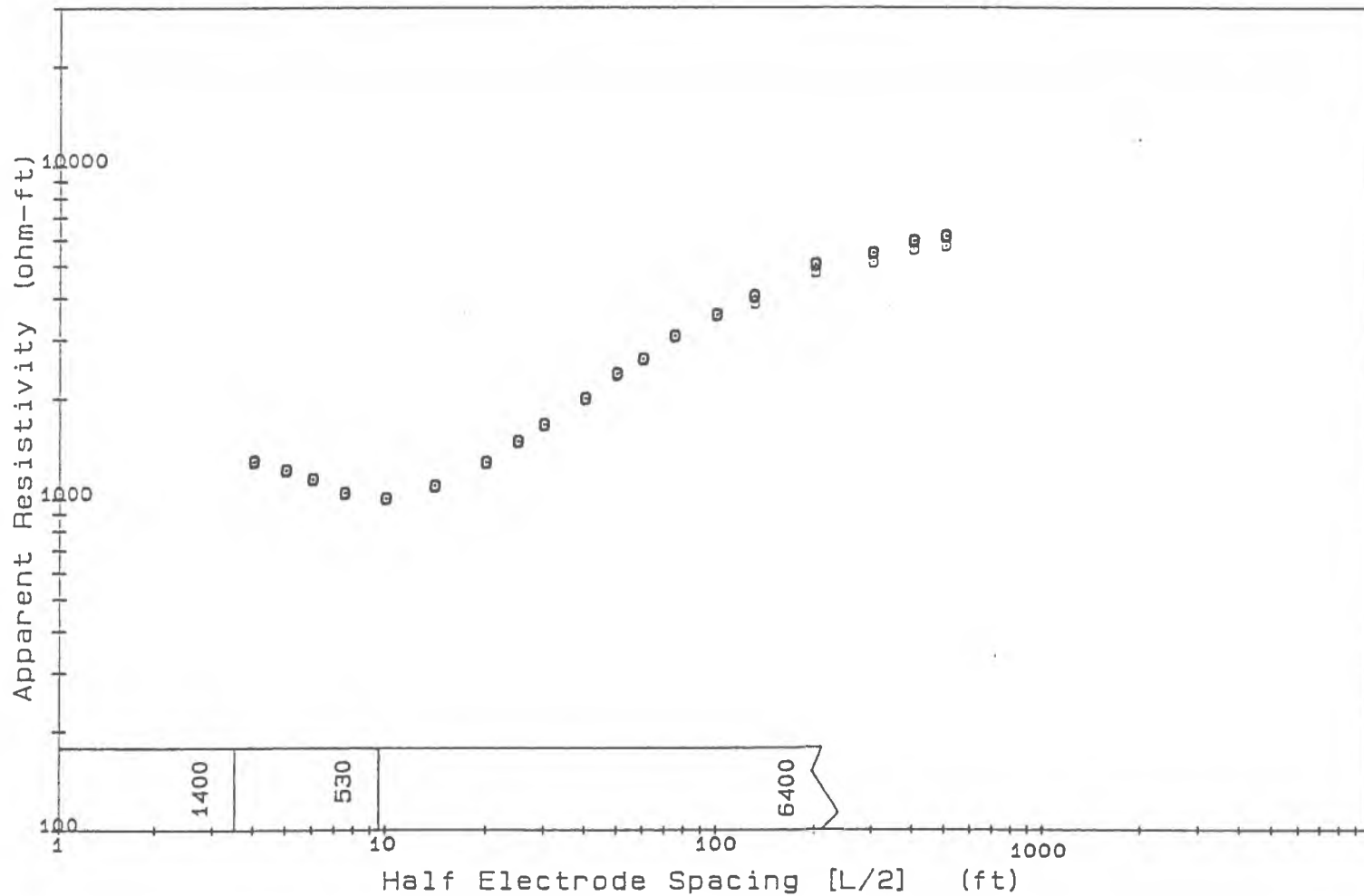
Project : Maine Survey

Location : Fort Fairfield

Operators: Frohlich, Boland, Smith

Profile : Me-12

Date : 04 AUG 87



# GeoElectrical Depth Sounding After Schlumberger

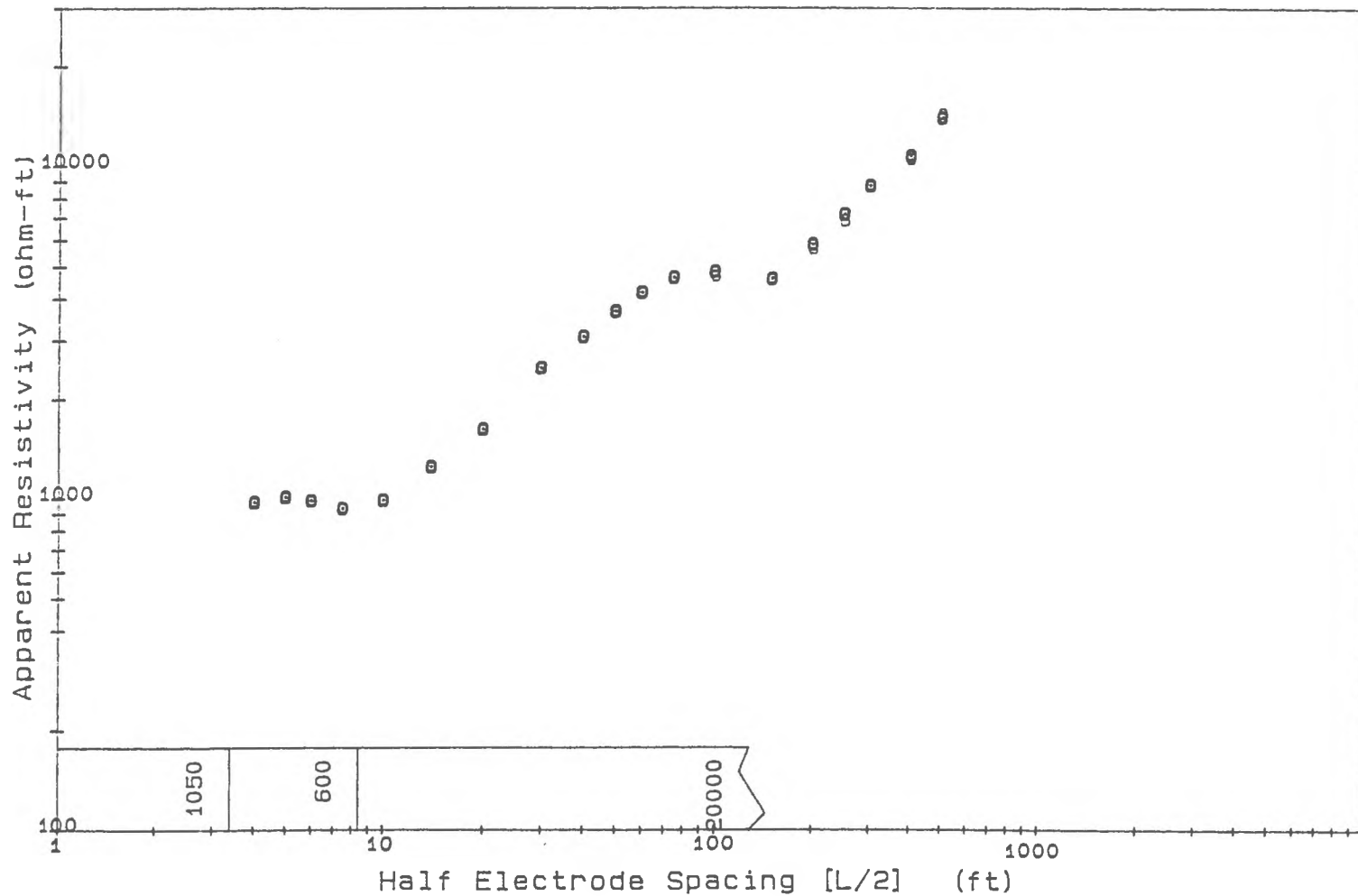
Project : Maine Survey

Location : Westfield

Operators: Frohlich, Boland, Smith

Profile : Me-13

Date : 04 AUG 87



# GeoElectrical Depth Sounding After Schlumberger

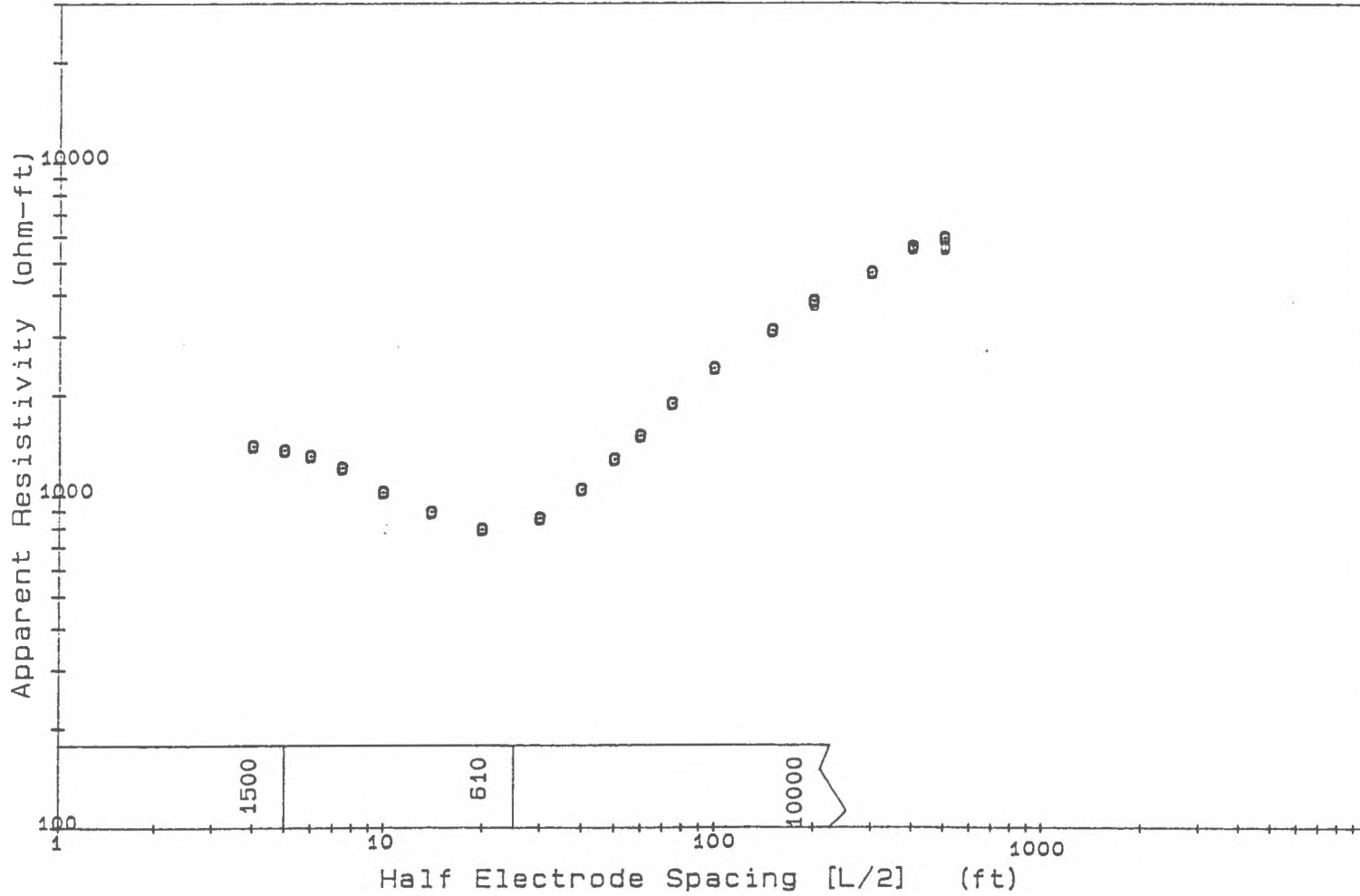
Project : Maine Survey

Location : Mars Hill

Operators: Fröhlich, Boland, Smith

Profile : Me-14

Date : 05 AUG 87



# GeoElectrical Depth Sounding After Schlumberger

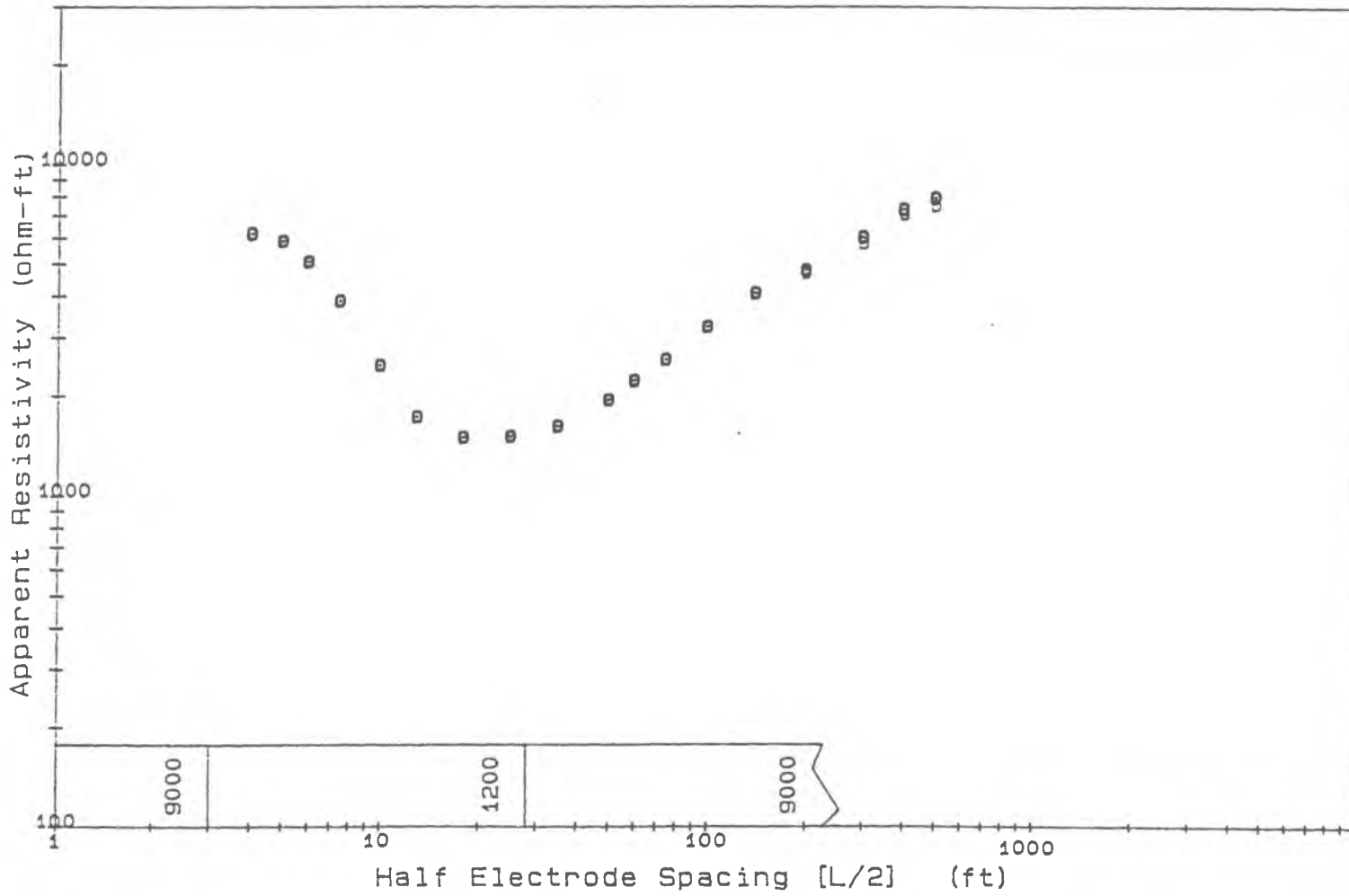
Project : Maine Survey

Location : Mars Hill

Operators: Frohlich, Boland, Smith

Profile : Me-15

Date : 05 AUG 87



# GeoElectrical Depth Sounding After Schlumberger

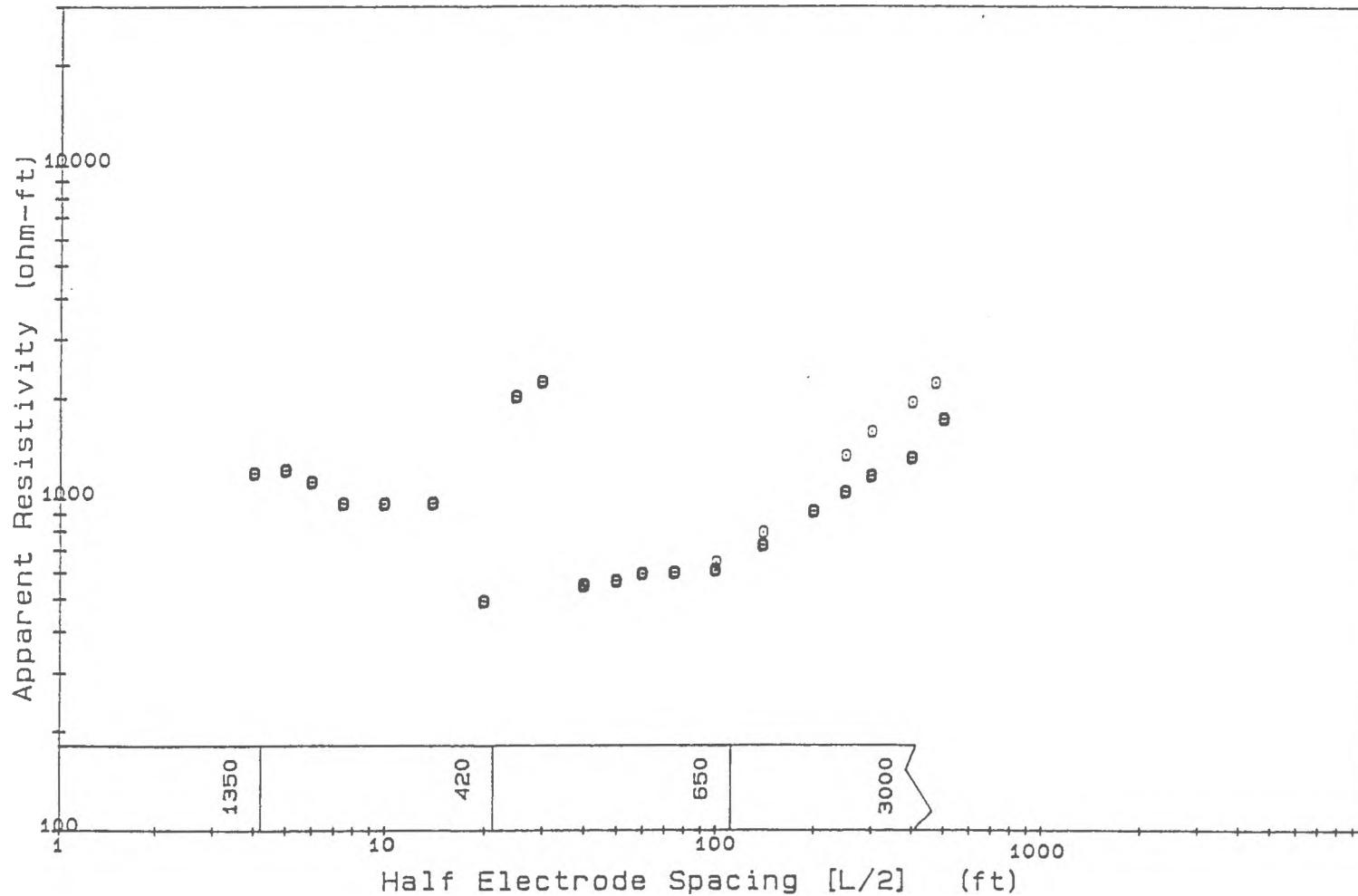
Project : Maine Survey

Location : Limestone

Operators: Frohlich, Boland, Smith

Profile : Me-16

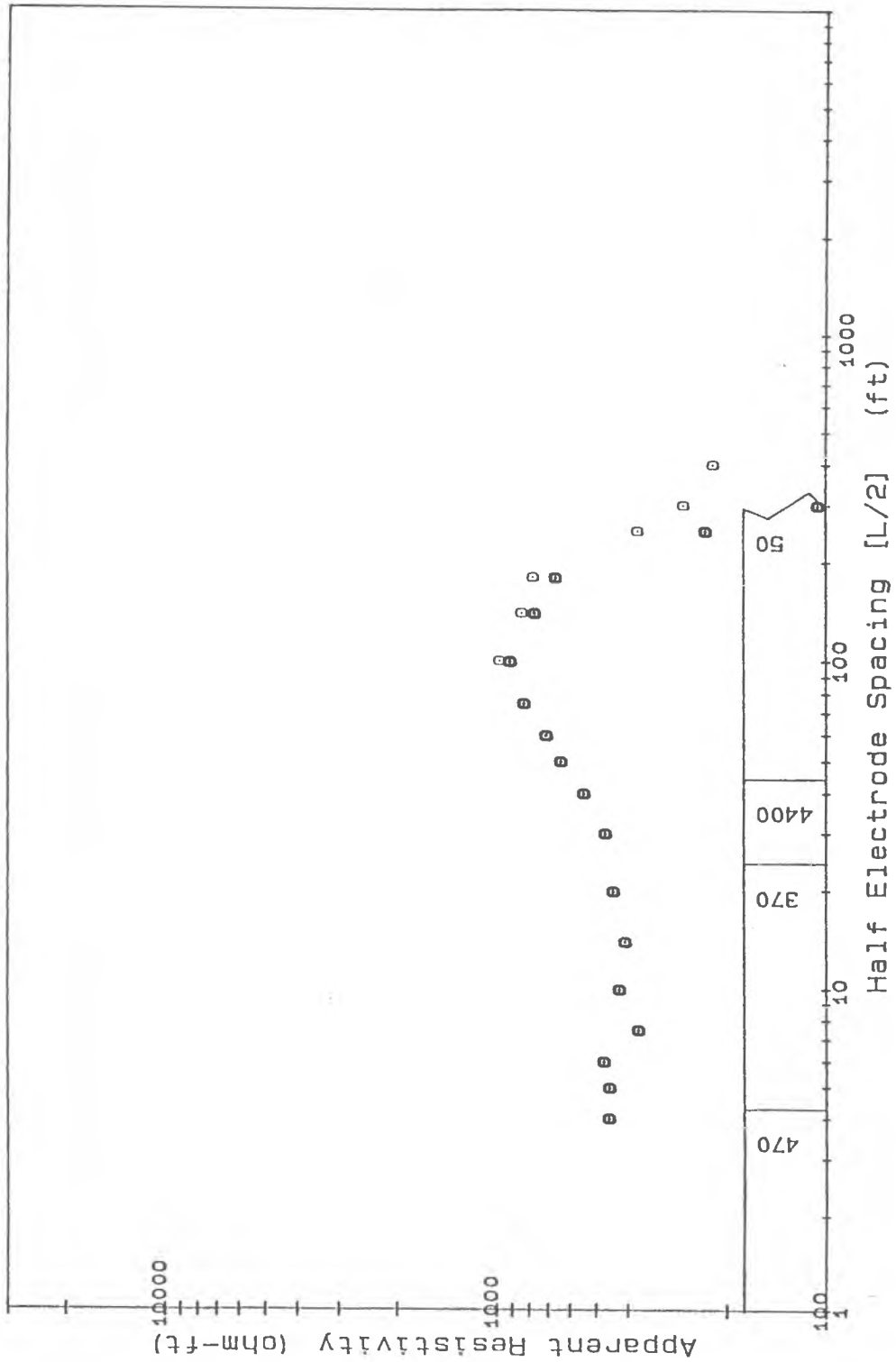
Date : 06 AUG 87



# GeoElectrical Depth Sounding After Schlumberger

Project : Maine Survey  
 Location : Fort Fairfield  
 Operators: Frohlich, Boland, Smith

Profile : Me-17  
 Date : 06 AUG 87





# GeoElectrical Depth Sounding After Schlumberger

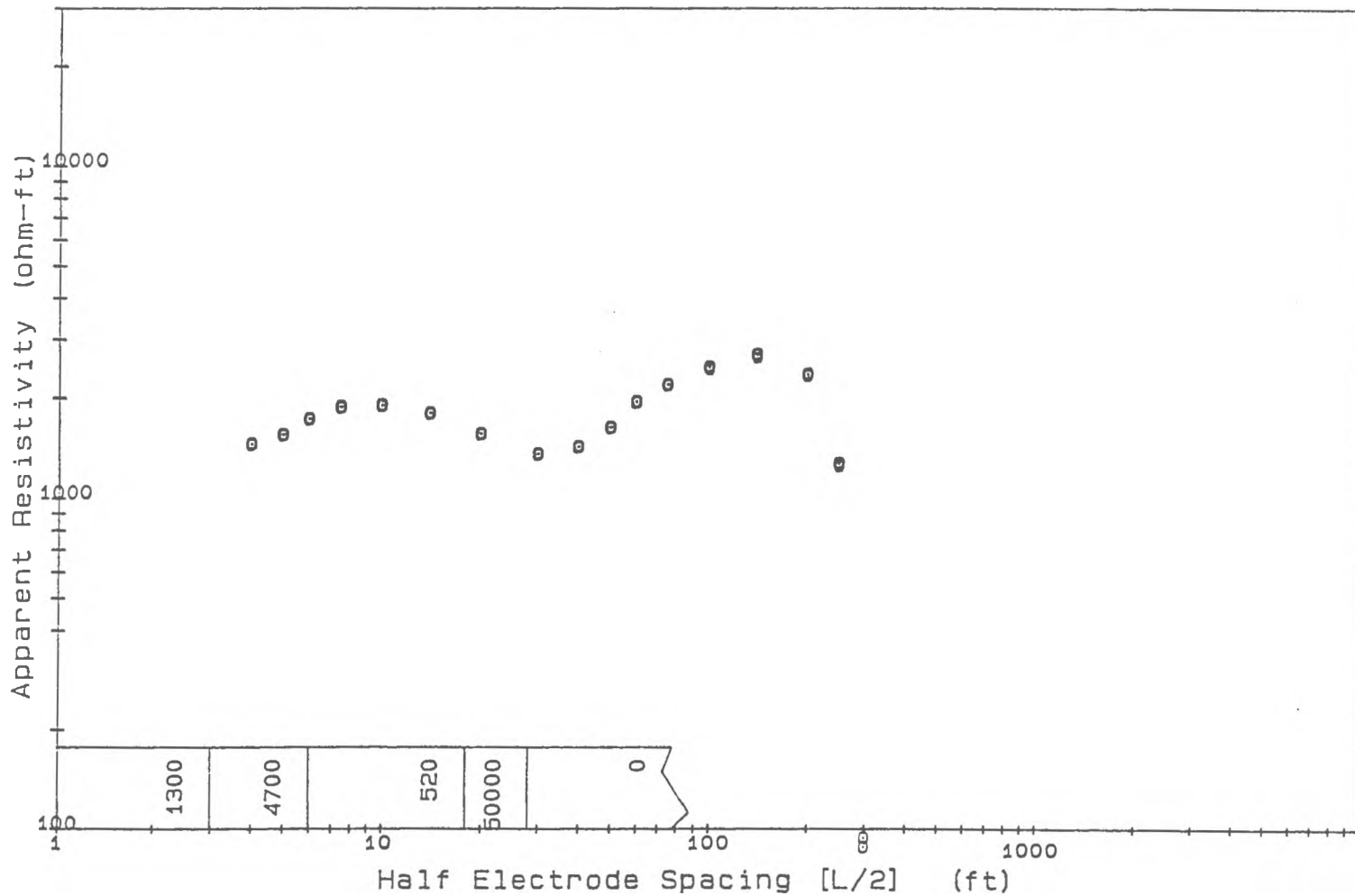
Project : Maine Survey

Location : Fort Fairfield

Operators: Frohlich, Boland, Smith

Profile : Me-18

Date : 06 AUG 87



# GeoElectrical Depth Sounding After Schlumberger

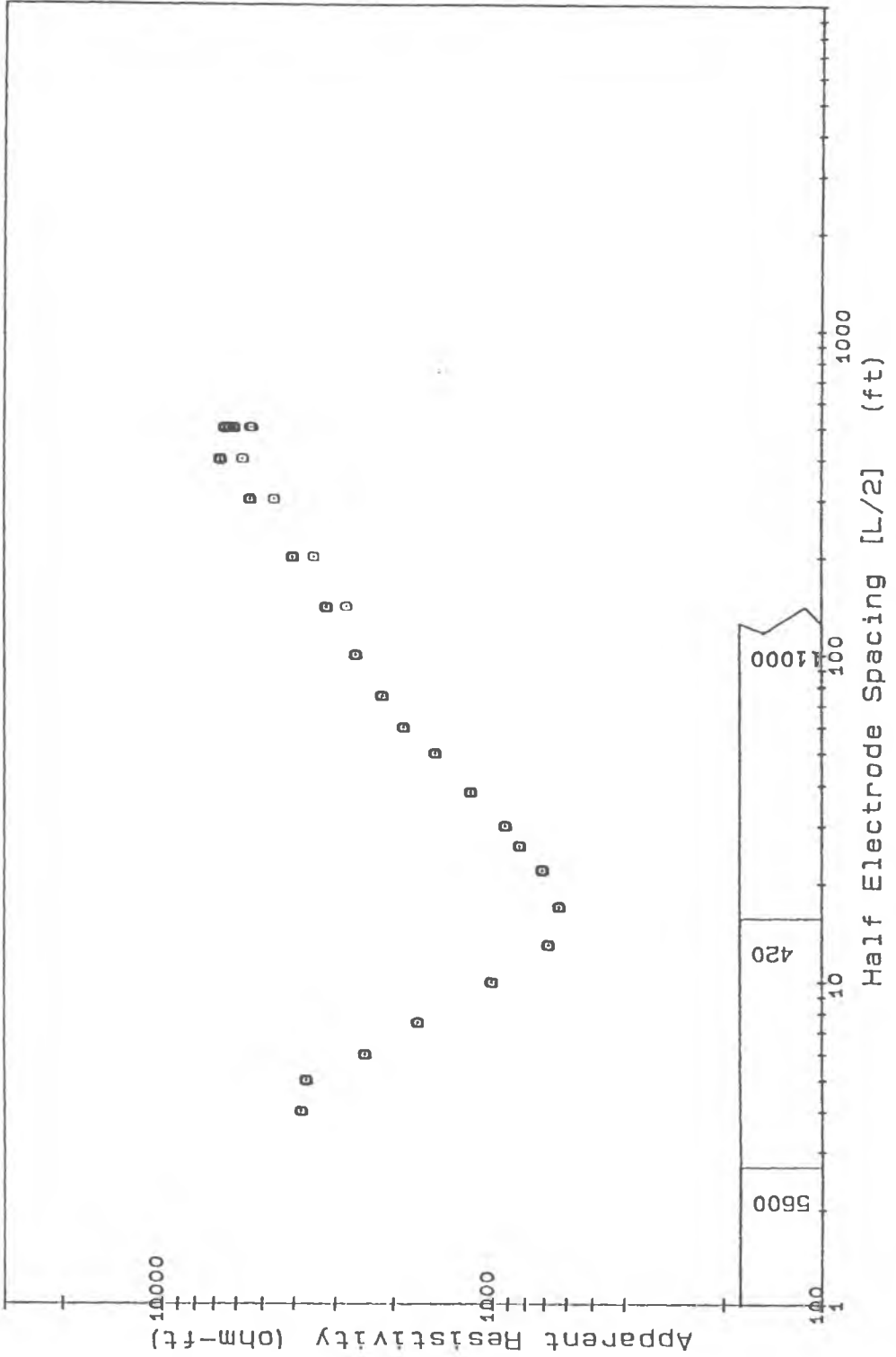
Project : Maine Survey

Location : Westfield

Operators: Frohlich, Boland, Smith

Profile : Me-19

Date : 07 AUG 87



# GeoElectrical Depth Sounding After Schlumberger

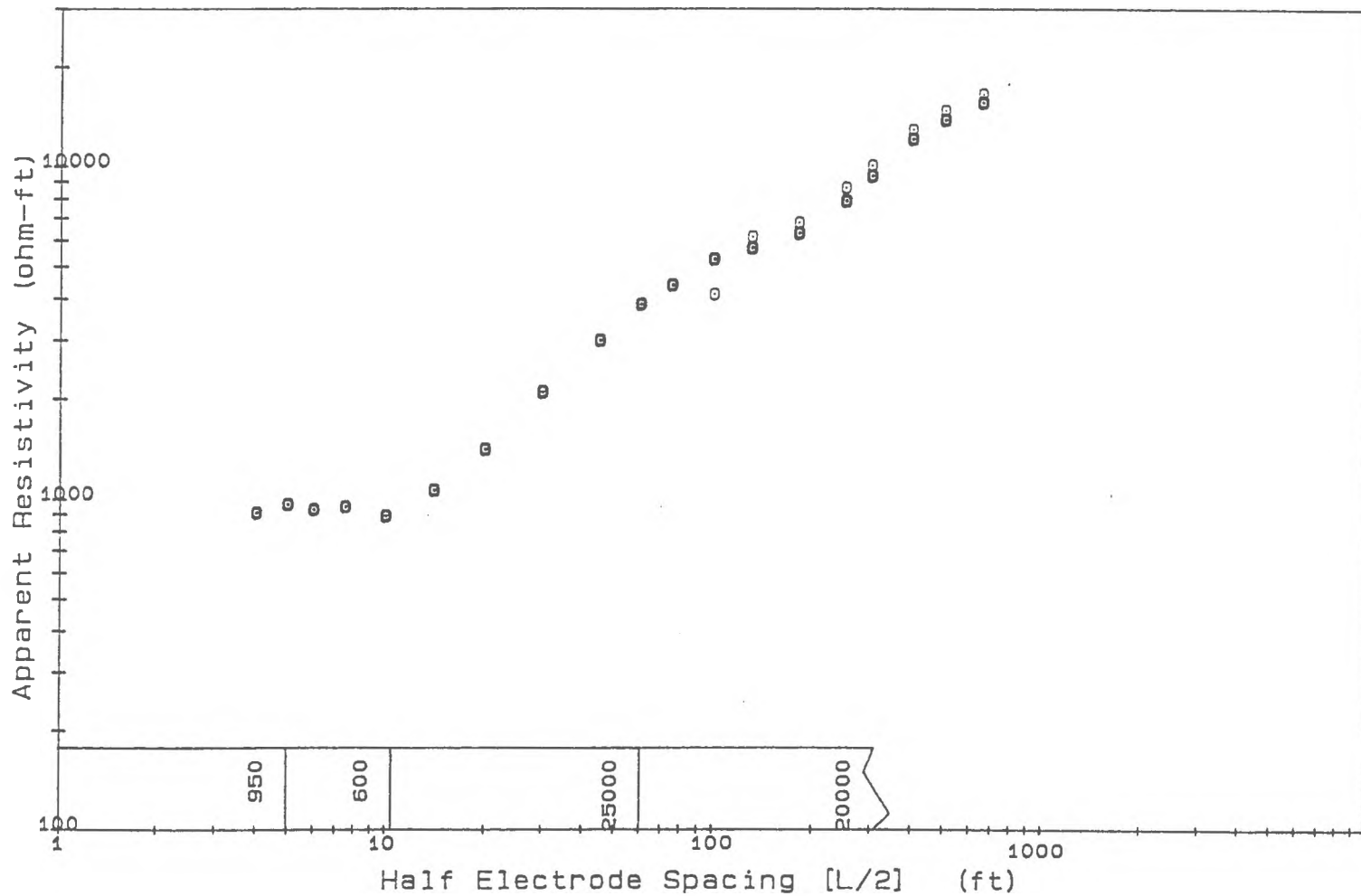
Project : Maine Survey

Location : Westfield

Operators: Frohlich, Boland, Smith

Profile : Me-20

Date : 07 AUG 87



# GeoElectrical Depth Sounding After Schlumberger

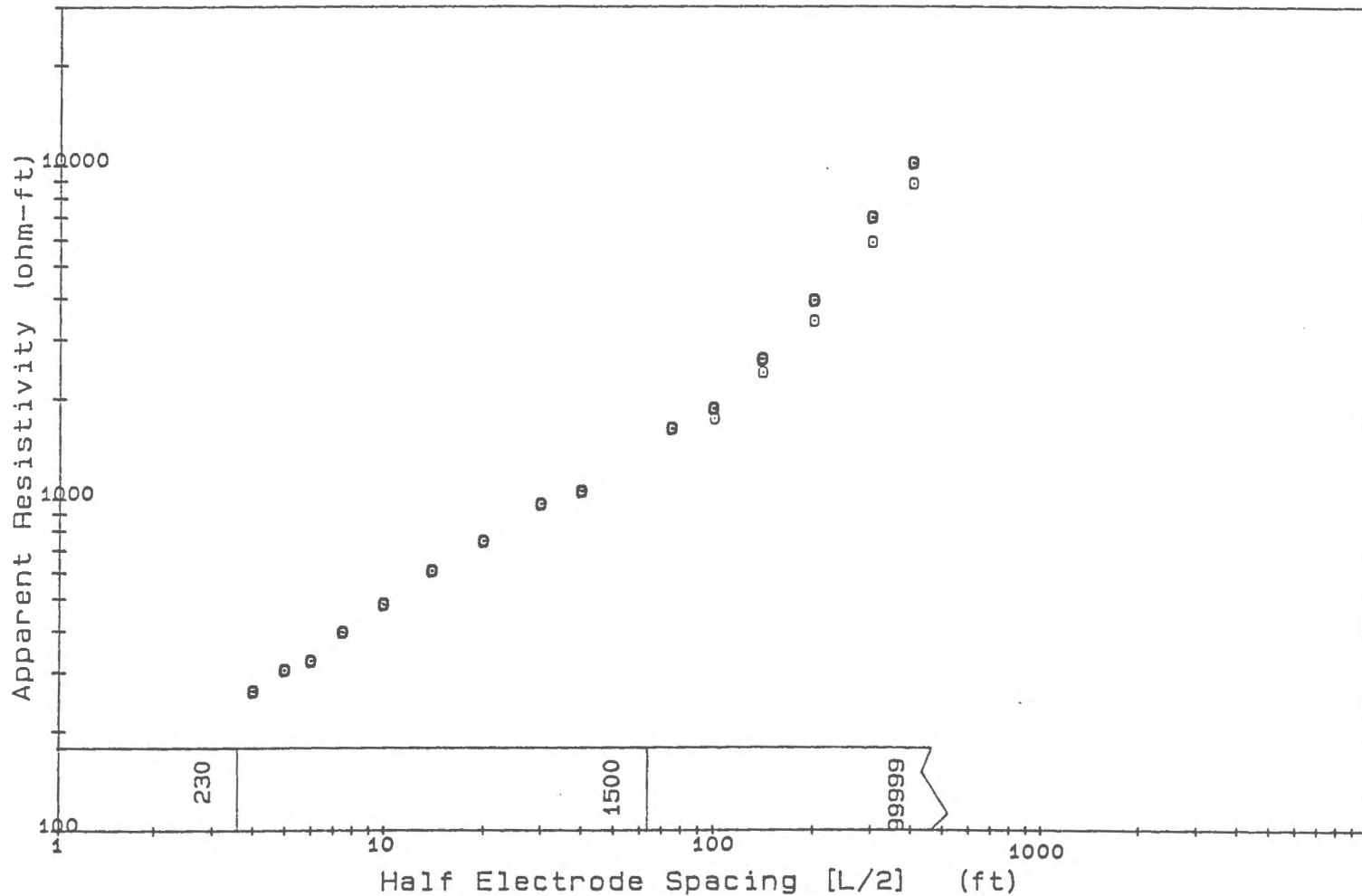
Project : Maine Survey

Location : Westfield

Operators: Frohlich, Boland, Smith

Profile : Me-21

Date : 07 AUG 87



# GeoElectrical Depth Sounding After Schlumberger

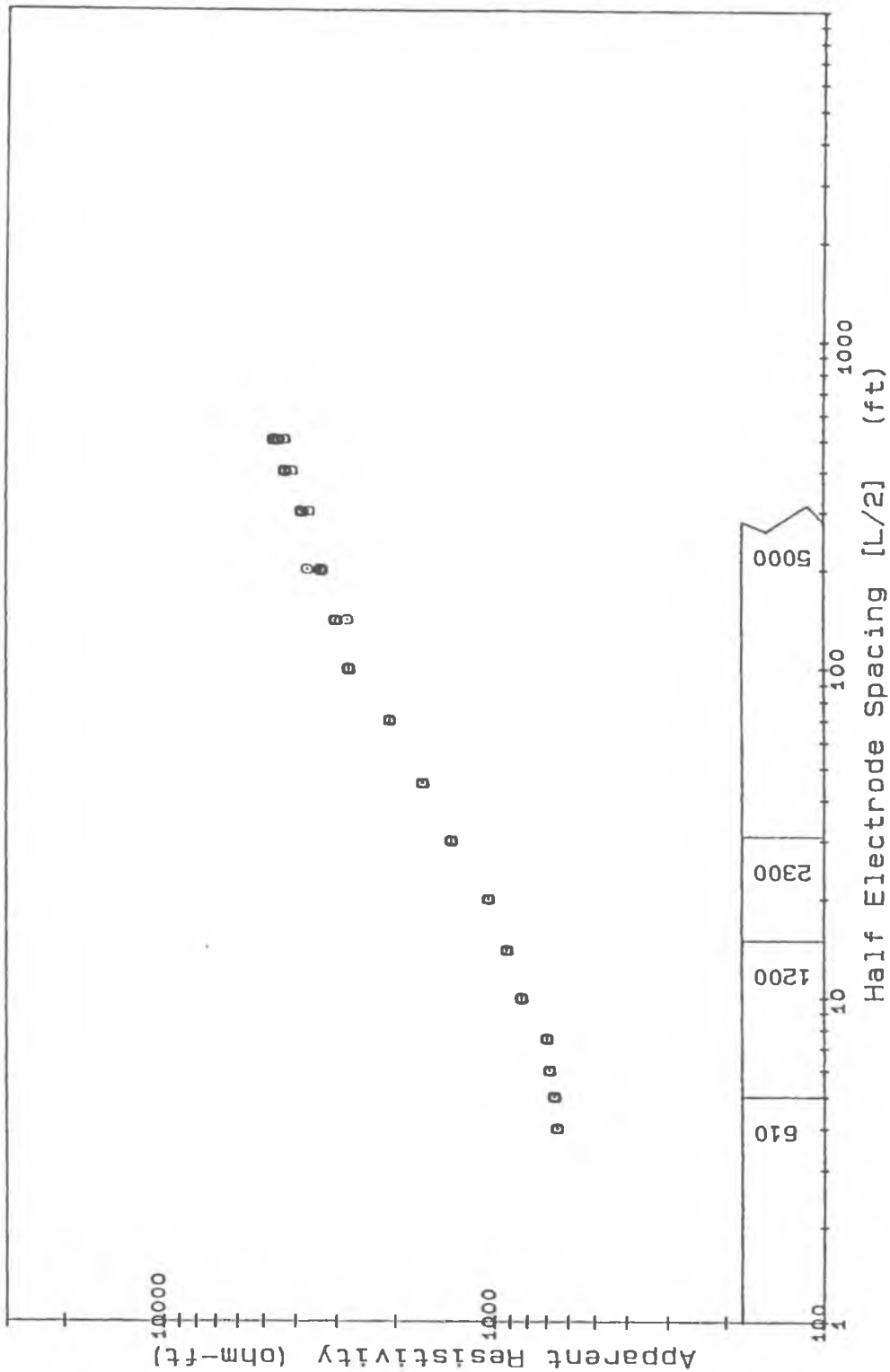
Project : Maine Survey

Location : Easton

Operators: Frohlich, Boland, Smith

Profile : Me-22

Date : 07 AUG 87



# GeoElectrical Depth Sounding After Schlumberger

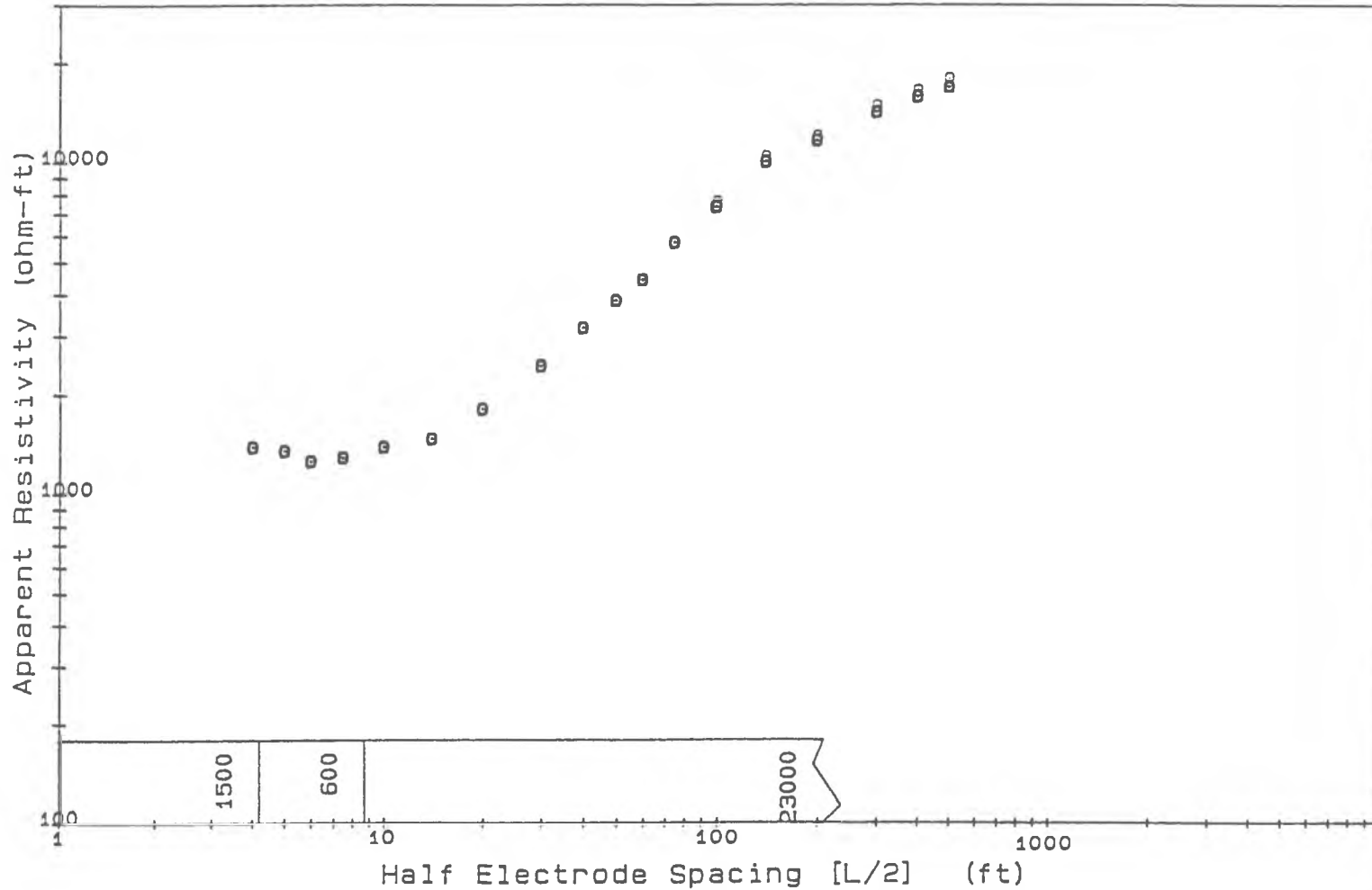
Project : Maine Survey

Location : Easton

Operators: Frohlich, Boland, Smith

Profile : Me-23

Date : 08 AUG 87



# GeoElectrical Depth Sounding After Schlumberger

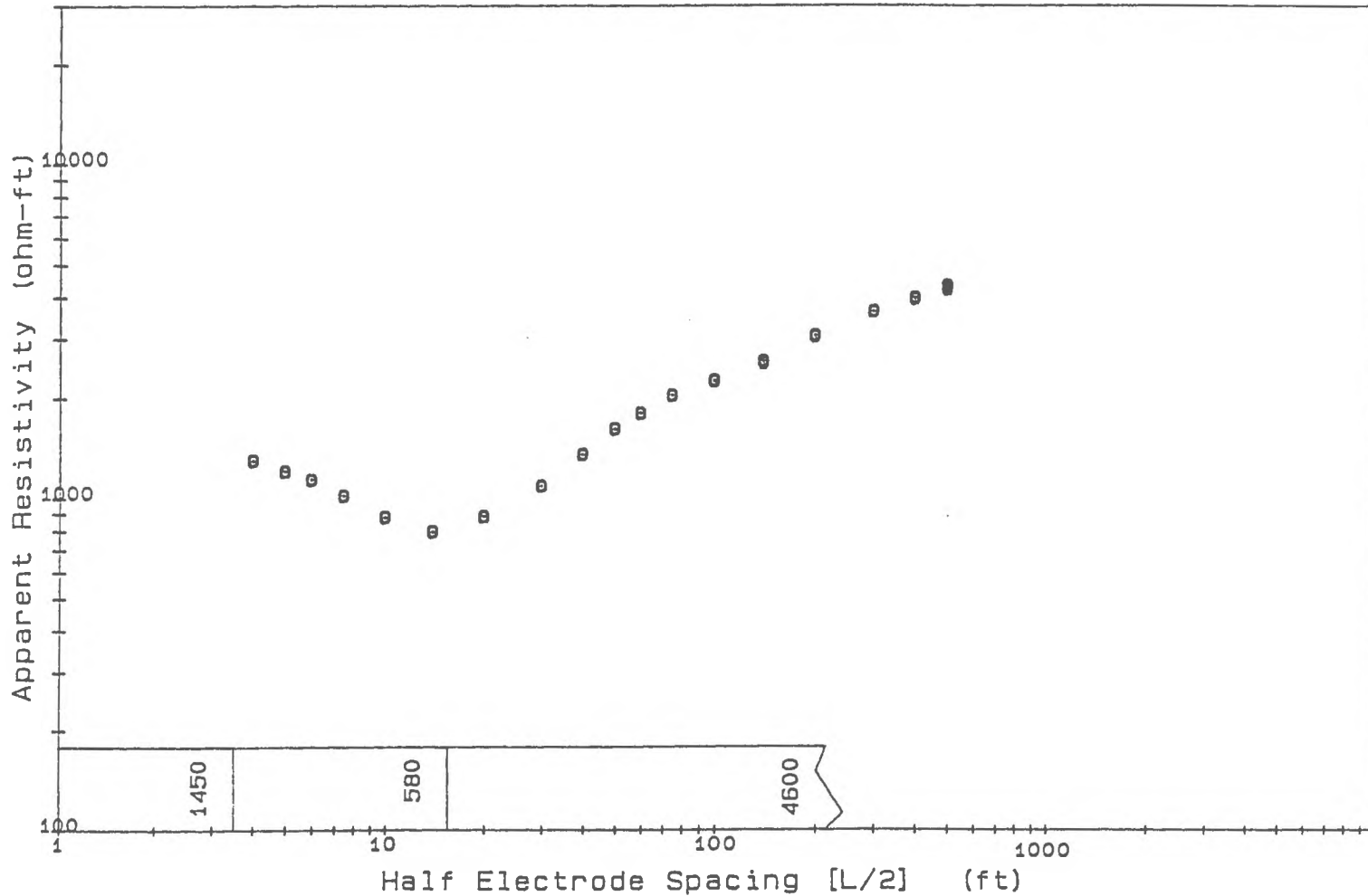
Project : Maine Survey

Location : Easton

Operators: Frohlich, Boland, Smith

Profile : Me-24

Date : 08 AUG 87



# GeoElectrical Depth Sounding After Schlumberger

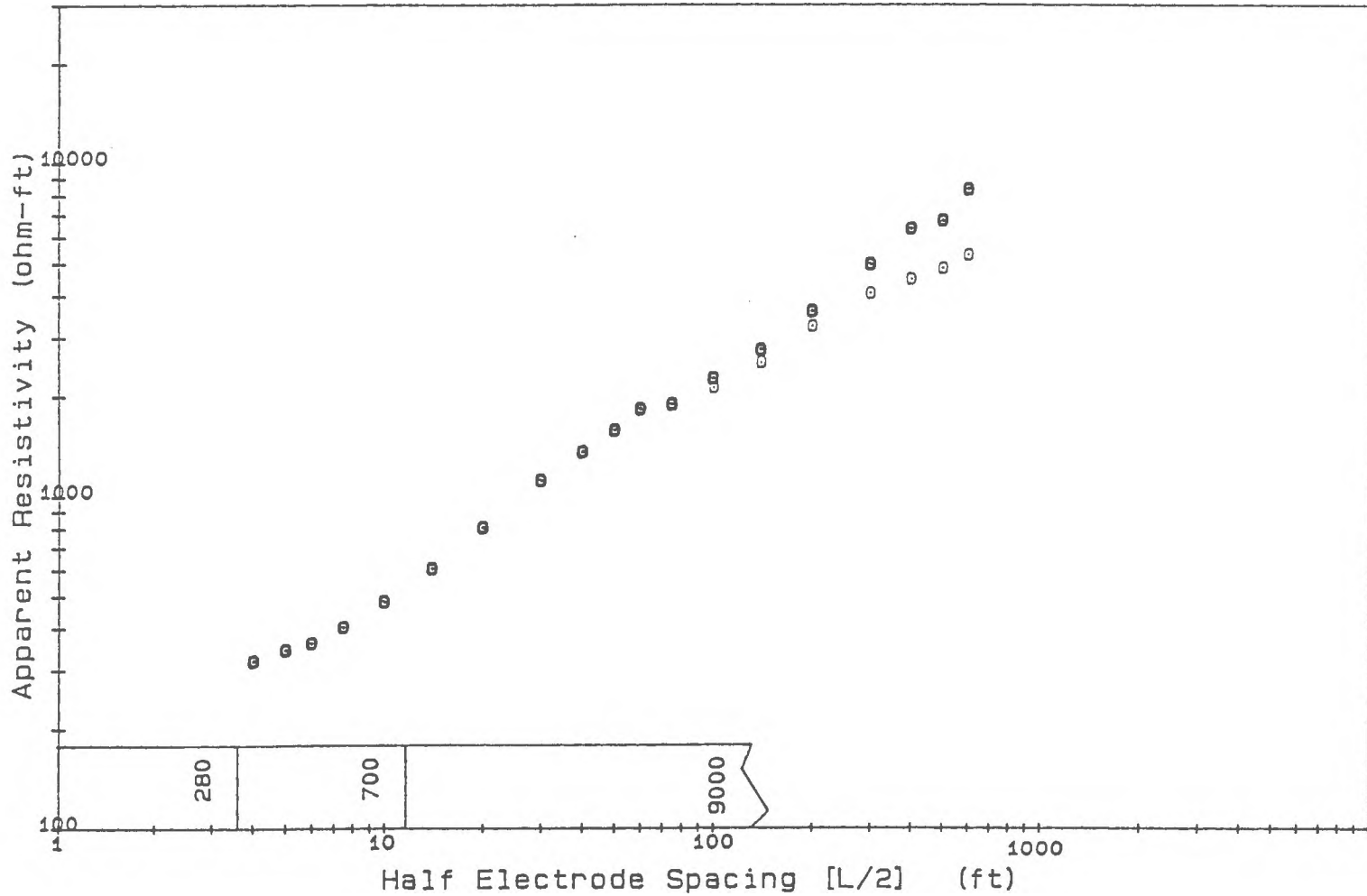
Project : Maine Survey

Location : Easton

Operators: Frohlich, Boland, Smith

Profile : Me-25

Date : 08 AUG 87

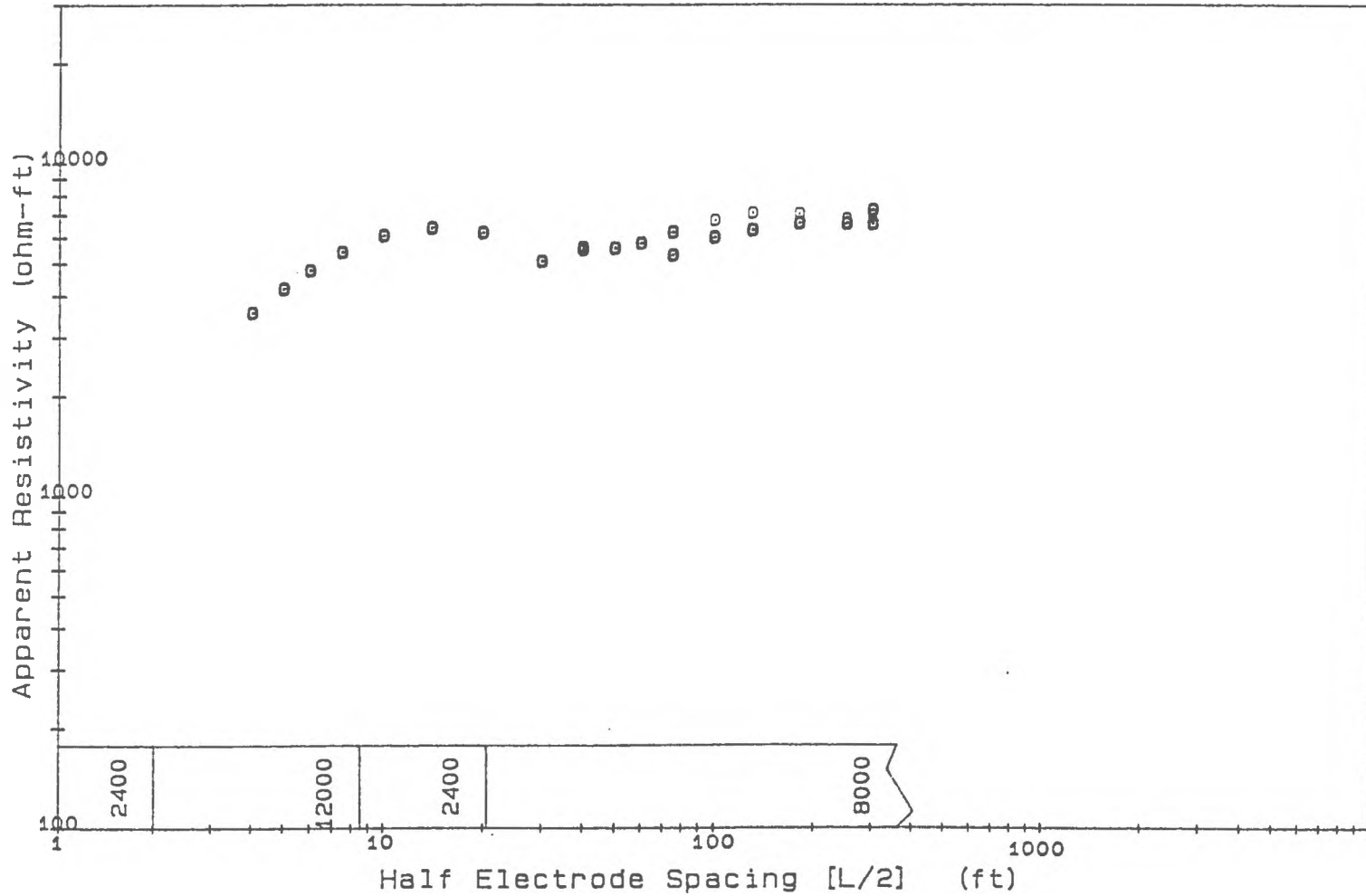




# GeoElectrical Depth Sounding After Schlumberger

Project : Maine Survey  
Location : Fort Fairfield  
Operators: Frohlich, Boland, Smith

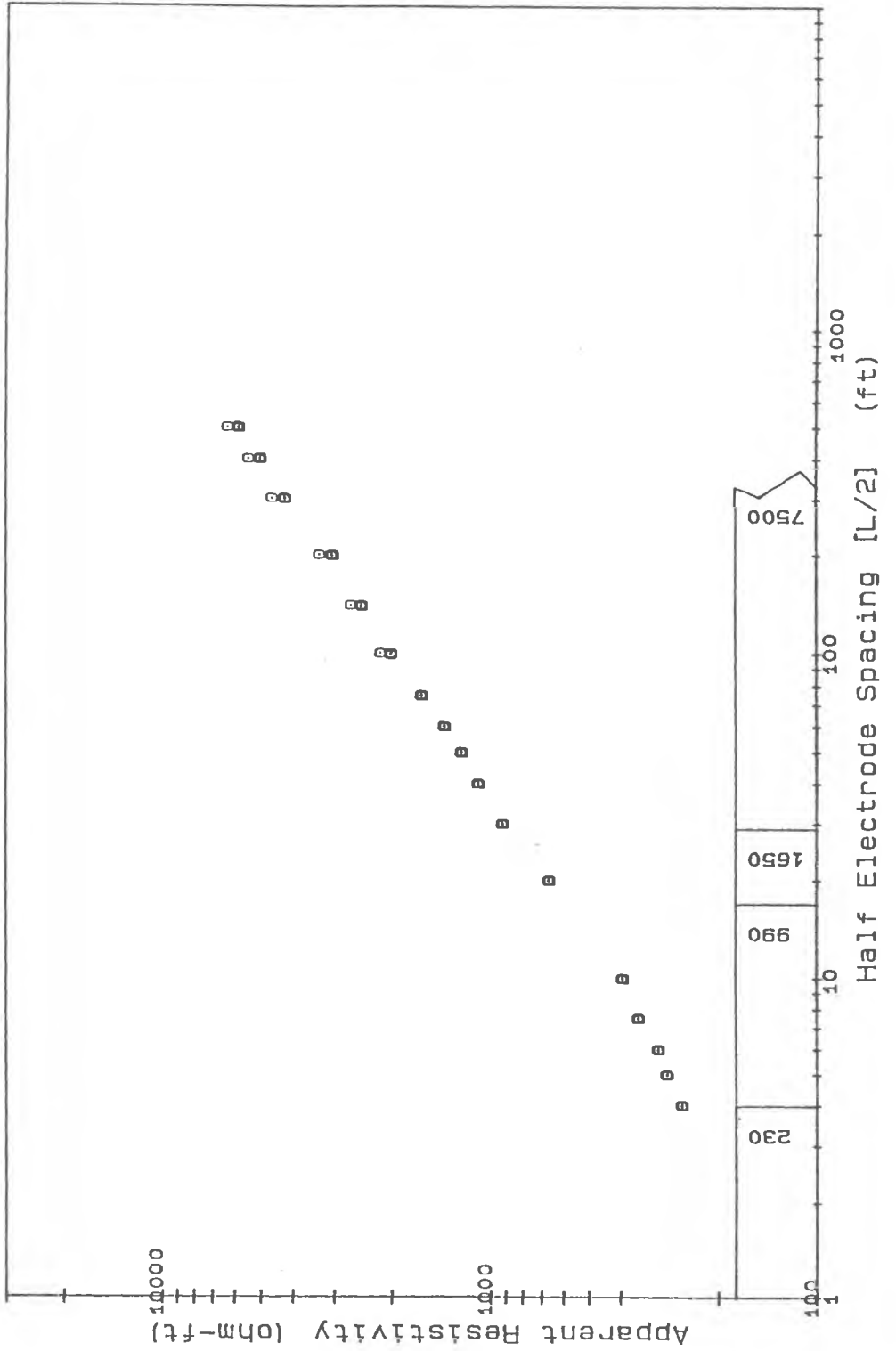
Profile : Me-26  
Date : 09 AUG 87



# GeoElectrical Depth Sounding After Schlumberger

Project : Maine Survey  
 Location : Fort fairfield  
 Operators: Frohlich, Boland, Smith

Profile : Me-27  
 Date : 10 AUG 87



# GeoElectrical Depth Sounding After Schlumberger

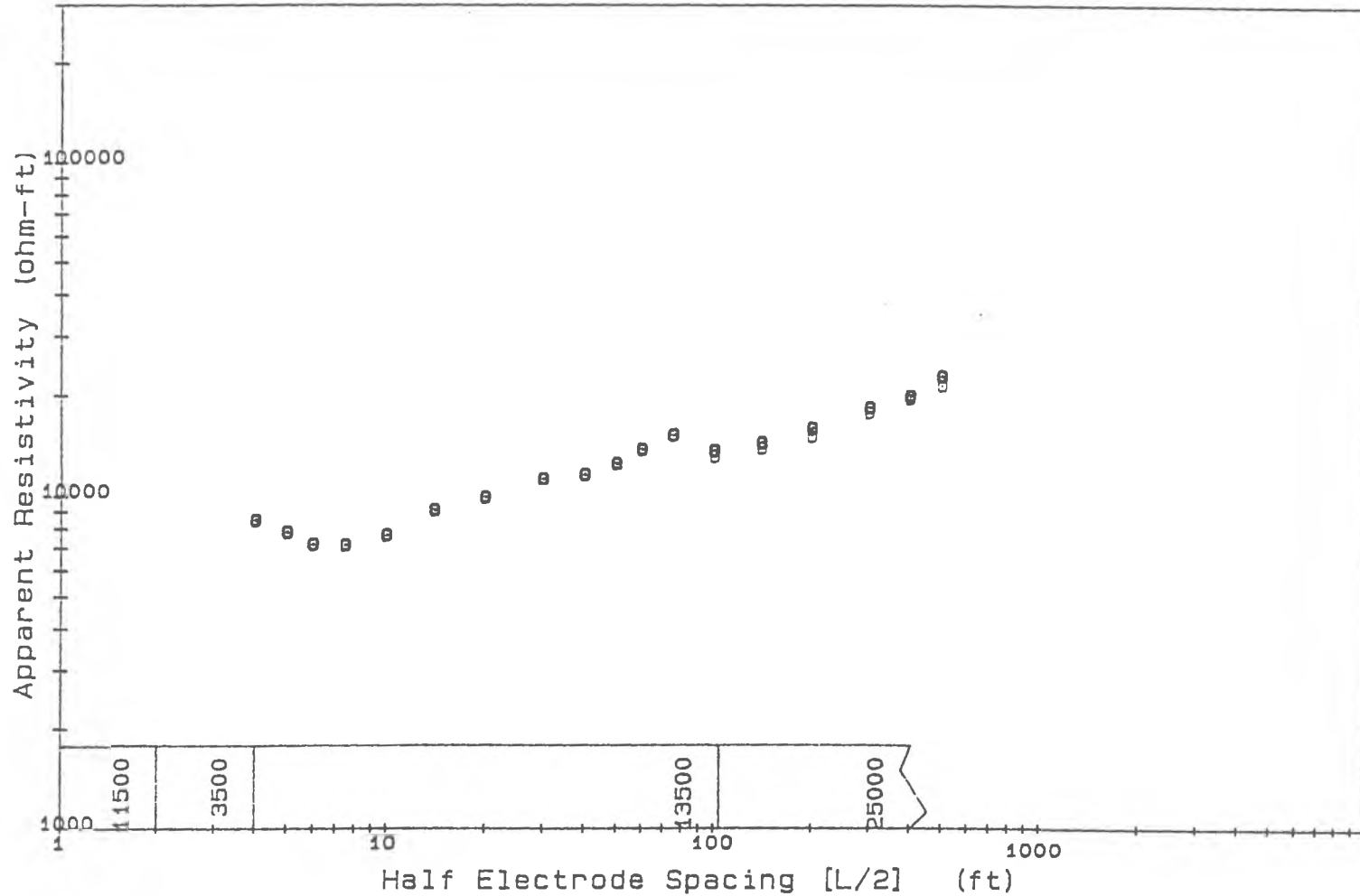
Project : Maine Survey

Location : Fort Fairfield

Operators: Frohlich, Boland, Smith

Profile : Me-27a

Date : 10 AUG 87



# GeoElectrical Depth Sounding After Schlumberger

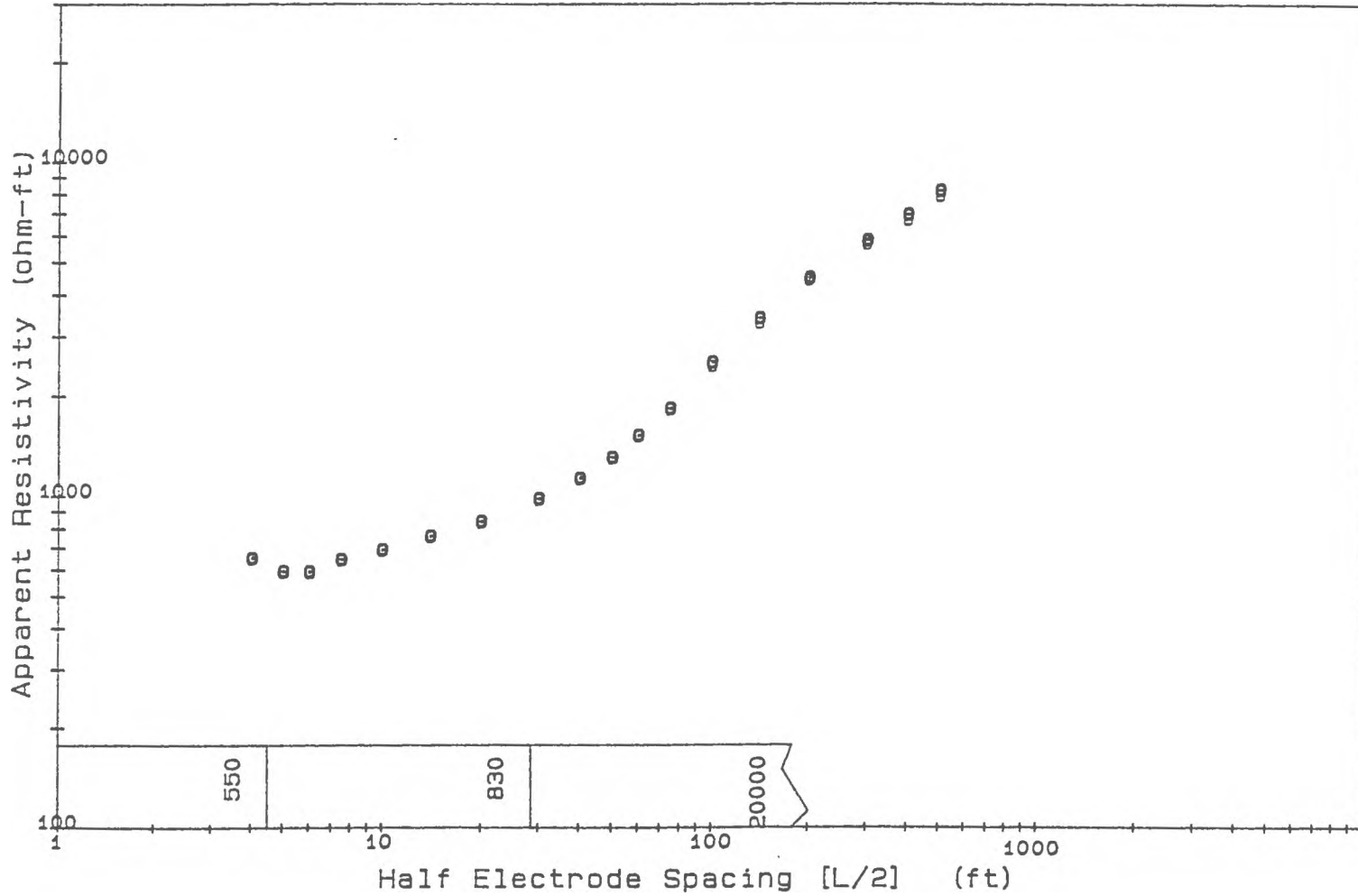
Project : Maine Survey

Location : Fort Fairfield

Operators: Frohlich, Boland, Smith

Profile : Me-28

Date : 10 AUG 87



# GeoElectrical Depth Sounding After Schlumberger

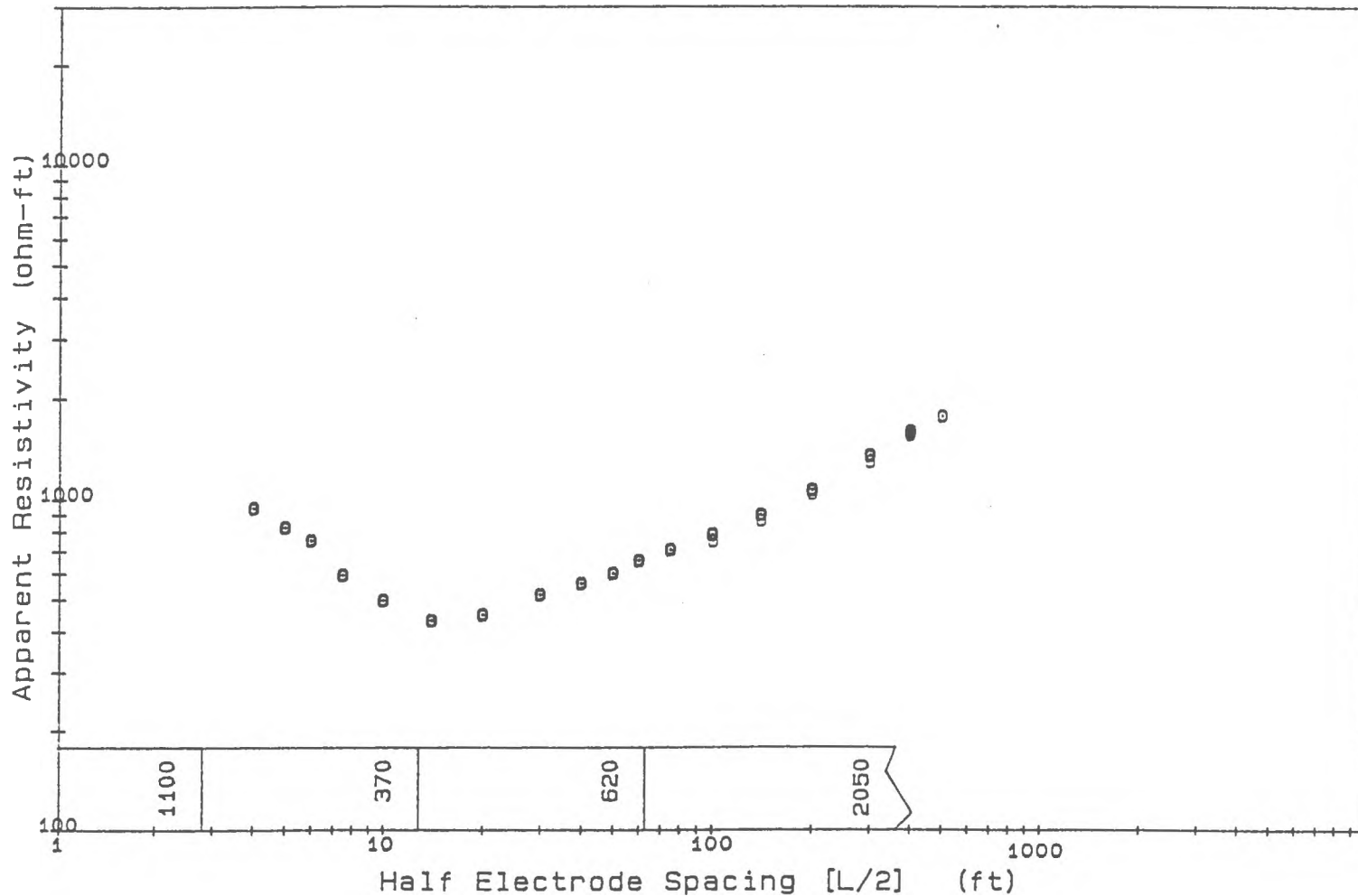
Project : Maine Survey

Location : Fort Fairfield

Operators: Frohlich, Boland, Smith

Profile : Me-29

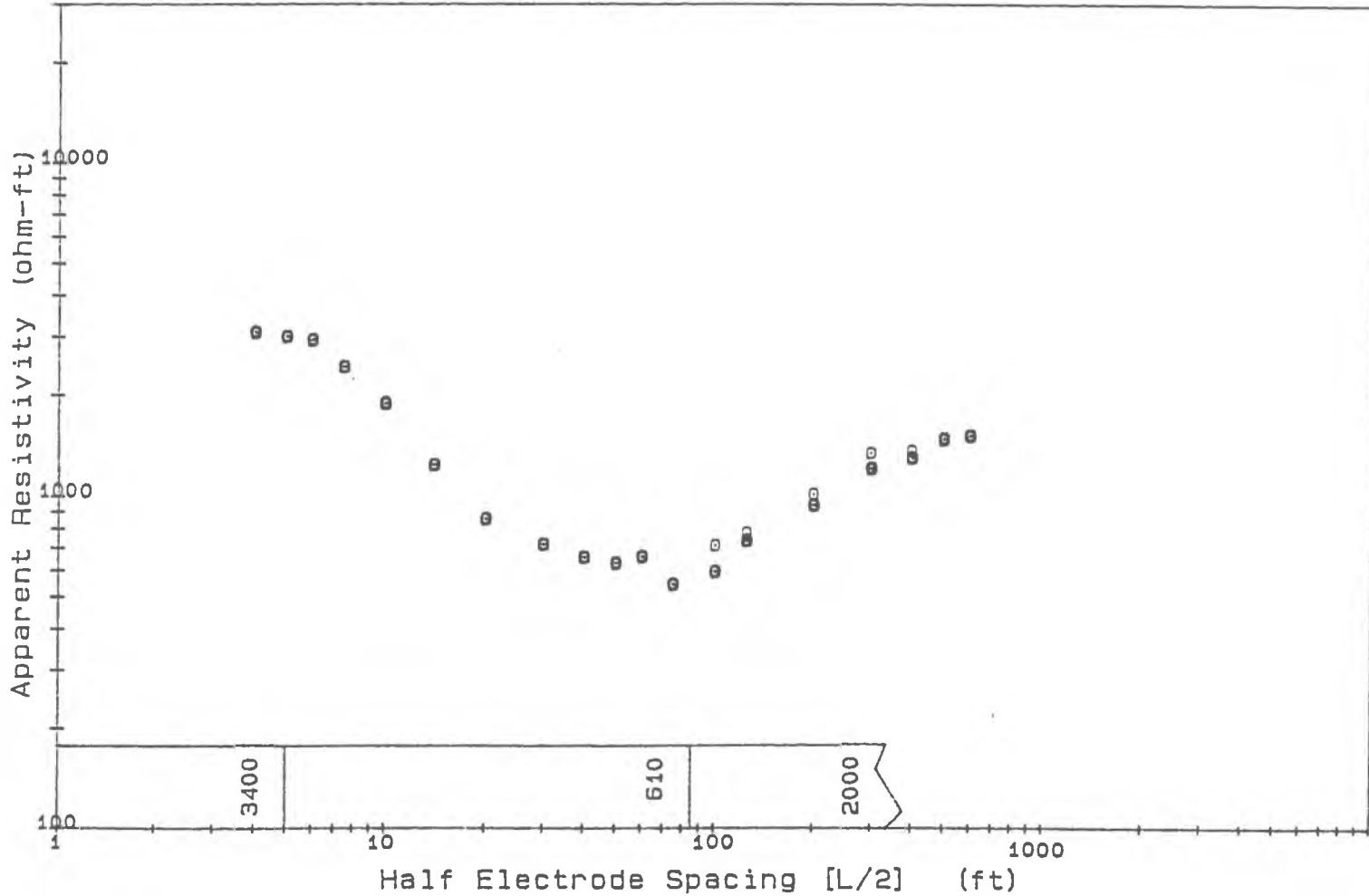
Date : 11 AUG 87



# GeoElectrical Depth Sounding After Schlumberger

Project : Maine Survey  
Location : Fort Fairfield  
Operators: Frohlich, Boland, Smith

Profile : Me-30  
Date : 11 AUG 87



# GeoElectrical Depth Sounding After Schlumberger

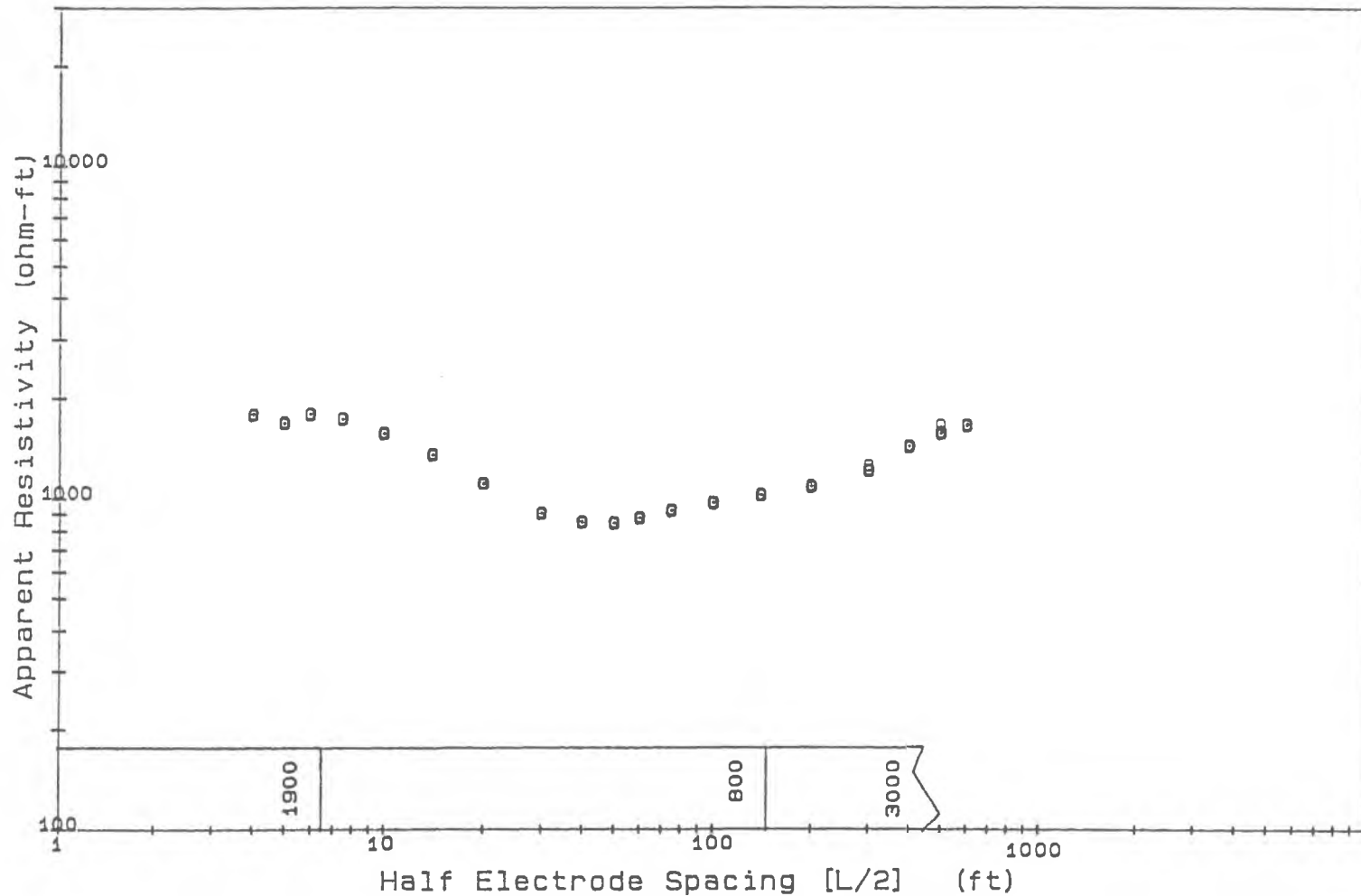
Project : Maine Survey

Location : Fort Fairfield

Operators: Frohlich, Boland, Smith

Profile : Me-31

Date : 11 AUG 87



# GeoElectrical Depth Sounding After Schlumberger

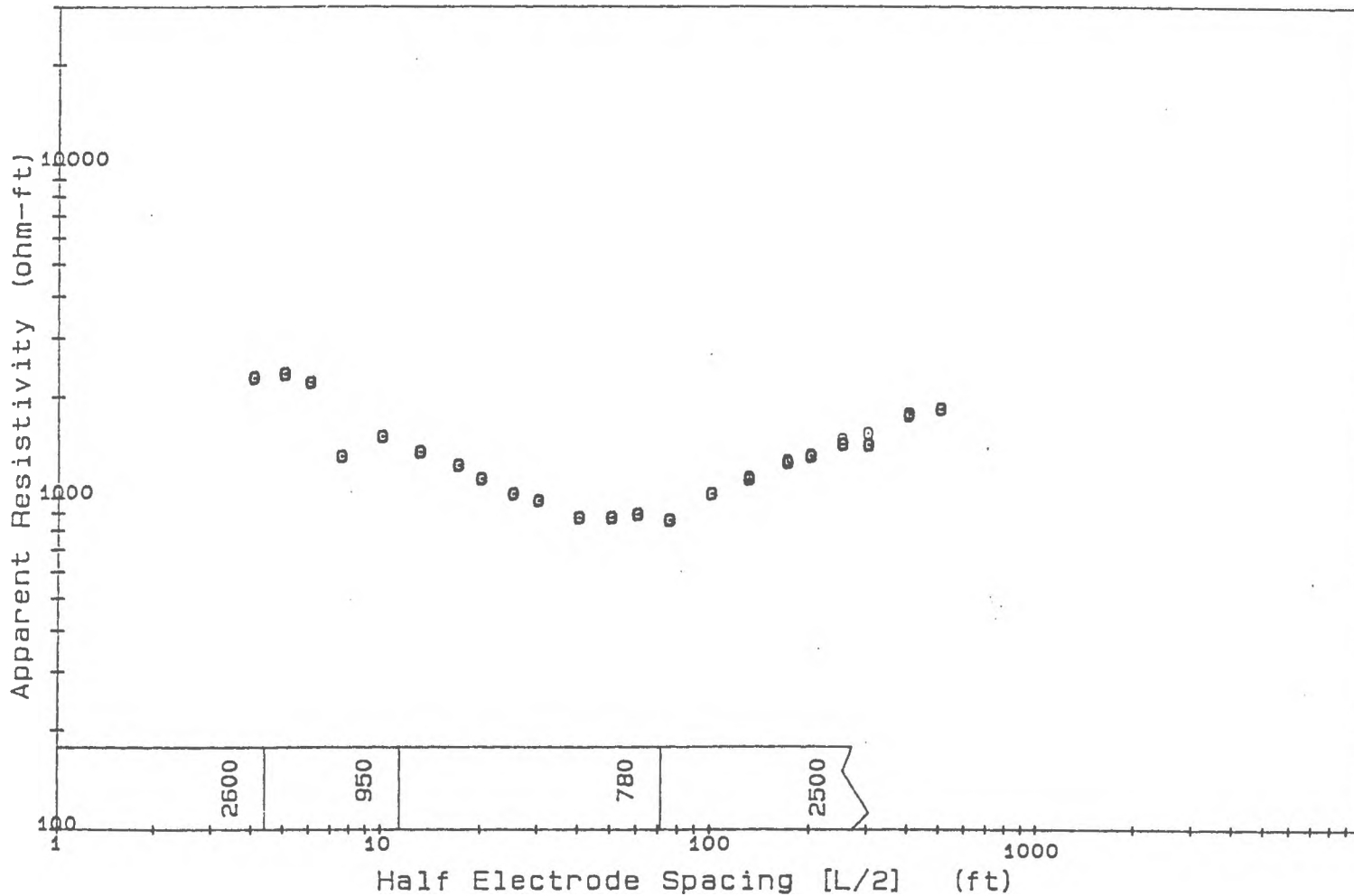
Project : Maine Survey

Location : Fort Fairfield

Operators: Frohlich, Boland, Smith

Profile : Me-32

Date : 12 AUG 87





## BIBLIOGRAPHY

- Allen, W.B. and Ryan, D.J., 1960. Ground Water Map of the Fall River Quadrangle, Massachusetts-Rhode Island. U.S. Geological Survey, GWM 7.
- Archie, G.E., 1942. Introduction to Petrophysics of Reservoir Rocks. Bull. Am. Assoc. Pet. Geol., Vol. 34, No. 5, pp. 943-961.
- Baker, R.D. and Griffiths, D.H., 1981. Surface Geophysical Methods in Hydrogeology in CASE-STUDIES IN GROUNDWATER RESOURCES EVALUATION. Ed. J.W. Lloyd, Clarendon Press, Oxford, pp. 27-43.
- Bear, J., 1972. Dynamics of Fluids in Porous Media. ed. Biswas, A.K., American Elsevier, N.Y. p. 764.
- Cartwright, K. and McComas, M.R., 1968. Geophysical Surveys in the Vicinity of Sanitary Landfills in Northern Illinois. Ground Water, vol. 6, No. 5, pp. 23-30.
- Danforth, W.W., 1986. Petrology and Structural Relations of the Western Scituate Granite (M.S. Thesis). Kingston, Rhode Island, The University of Rhode Island, 185 p.
- Fisher, J.J., Frohlich, R.K., and Urish, D., 1987. Fracture Trace/Geophysical Investigation of Central Landfill site, Johnston Rhode Island, unpublished report prepared for Goldberg, Zoino & Assoc., Inc.
- Fisher, J.J., Frohlich, R.K., Savarese, J.G., and Mulhare, M.J., 1988. Hydrocarbon Contamination Beneath Glacial Till in Bedrock Wells Detected by Hydrogeology, Remote Sensing and Geophysical Techniques: Presented at the International Conference on Fluid Flow in Fractured Rocks, Atlanta, GA, 1988 (in press).
- Freeze, R.A., and Cherry, J.A., 1979. Groundwater: Prentice-Hall. Inc., Englewood Cliffs, New Jersey, 604p.
- Frohlich, R.K., 1974. Combined Geoelectrical and Drill-Hole Investigations for Detecting Fresh-Water Aquifers in Northwestern Missouri. Geophysics, Vol. 39, No. 3, pp. 340-352.
- Frohlich, R.K. and Kelly, W.E., 1985. The Relation Between Hydraulic Transmissivity and Transverse Resistance in a Complicated Aquifer of Glacial Outwash Deposits. Journal of Hydrology, Vol. 79, pp. 215-229.
- Frohlich, R.K. and Kelly, W.E., 1988. Estimates of Specific Yield with the Geoelectric Resistivity Method in Glacial Aquifers. Journal of Hydrology, Vol. 97, pp. 33-44.
- Frohlich, R.K., Williams, J.B., and Boland, M.P., 1988. A geological Study of Hydraulic Bedrock Conditions in Aroostook County, Maine. Presented at the International Conference on Fluid Flow in Fractured Rocks, Atlanta, GA, 1988 (in press).
- Greenberg, R.J. and Brace, W.F., 1969. Archie's Law of Rocks Modeled by Simple Networks. Journal of Geophysical Research, Vol. 74, No. 8, pp. 2099-2102.

- Hanson, L.G., 1988. A Seismic Refraction Investigation of the Hydrogeology of Fractured Bedrock. (M.S. Thesis): Kingston, Rhode Island, University of Rhode Island, 198p.
- Hamidzada, N.A., and Hermes, O.D., 1984. Ductile Shear Zones in North Central Rhode Island and Their Bearing on Devonian Plutonism. Geological Society of America Abstracts with Program, p. 22.
- Hamidzada, N.A., 1988. Petrology, Geochemistry and Structure of the Northeast Part of the Scituate Pluton (M.S. Thesis): Kingston, Rhode Island, University of Rhode Island. 294p.
- Hermes, O.D., Rao, J.M., Dickenson, M.P., and Pierce, T.A., 1984. A Transitional Alkalic Dolerite Dike Suite of Mesozoic Age in Southeastern New England: Contributions to Mineralogy and Petrology, Vol. 86, p. 386-397.
- Hermes, O.D., and Zartman, R.E., 1985. Late Proterozoic and Devonian Plutonic Terrane within the Avalon Zone of Rhode Island. Geologic Society of America, Vol. 96, pp. 272-282.
- Johnson, D.L., Koplik, J., Schwartz, M., 1986. New Pore-Size Parameter Characterizing Transport in Porous Media. Physical Review Letters, Vol. 57, No. 20, pp. 2564-2567.
- Katsube, T.J., Hume, J.P., 1987. Permeability Determination in Crystalline Rocks by Standard Geophysical Logs. Geophysics, Vol. 52, No. 3, p. 342-352.
- Keller, G.V., and Frishknecht, F.C., 1966. Electrical Methods in Geophysical Prospecting: Pergamon Press. Oxford. 529 p.
- Kelly, W.E., and Reiter, P.F., 1984. Influence of Anisotropy on Relations Between Electrical and Hydraulic Properties of Aquifers. Journal of Hydrology. Vol. 74, pp. 311-321.
- Kiraly, L., 1971. Groundwater Flow in Heterogeneous, Anisotropic Fractured Media: A Simple Two-Dimensional Electric Analog. Journal of Hydrology, vol. 12, pp. 255-261.
- Klefstad, G.K., Sendlein, L.V.A., Palmquist, R.C., 1975. Limitations of the Electrical Resistivity Method in Landfill Investigations. Ground Water, Vol. 13, No. 5, pp. 418-427.
- Koefoed, O., 1979. GEOSOUNDING PRINCIPLES. 1: Resistivity Sounding Measurements: Amsterdam. Elsevier Scientific Pub. Co., 176 p.
- Kosinski, W.K., Kelly, W.E., 1981. Goelectric Soundings for Predicting Aquifer Properties. Ground Water, Vol. 19, No. 2, pp. 163-171.
- Kowalski, R.G., Sanders, D.P., 1983. Introduction to Hydrogeologic Investigations of Contamination in Fractured Rock. Rhode Island Water Resources Center. Technical Report, No. 13, 71 p.

- Merkel, R.H., 1972. The Use of Resistivity Techniques to Delineate Acid Mine Drainage in Ground Water. *Groundwater*, Vol. 10, No. 5, pp. 38-42.
- Neuzil, C.E., 1986, Groundwater Flow in Low-Permeability Environments. *Water Resources Research*, Vol. 22, No. 8, pp. 1163-1195.
- Norton, D., and Knapp, R., 1977. Transport Phenomena in Hydrothermal Systems: The Nature of Porosity. *American Journal of Science*, Vol. 277, pp. 913-936.
- O'Neil, D.J. and Merrick, N.P., 1984. A Digital Linear Filter for Resistivity Sounding with a Generalized Electrode Array. *Geophysical Prospecting*, Vo. 32, pp. 105-123.
- Osberg, P.H., Hussey, A.M., Boone, G.M., 1985. Bedrock Geologic Map of Maine. Maine Geological Survey.
- Owen, D.J., 1987. Abnormal Electrical Resistivity Effects Over Buried Bedrock Fractures: unpublished M.S. Thesis, University of Rhode Island, 114 p.
- Page, L.M., 1986, Use of the Electrical Resistivity Method for Investigating Geologic and Hydrologic Conditions in Santa Clara County, California. *Ground Water*, Vol. 6, No. 5, pp. 31-40.
- Pavrides, L., 1978. Bedrock Geologic Map of the Mars Hill Quadrangle and Vicinity, Aroostook Co., ME, U.S.G.S.G. Map, Miscellaneous investigations series, Map I - 1064.
- Quinn, A.W., 1971. Bedrock Geology of the Tiverton Quadrangle, RI-MA. U.S. Geological Survey, Bull. 1158-D, pp. D4-D5, D9-D15.
- Robinson, C.S., 1961. Surficial Geology of the North Scituate Quadrangle, Rhode Island, U.S. Geological Survey Geologic Quadrangle Map GQ143.
- Rothman, D.H., 1988. Cellular-Automation Fluids: A Model for Flow in Porous Media. *Geophysics*, Vol. 53, No. 4, pp. 509-518.
- Savarese, J.G., 1987. Hydrogeologic Evaluation of a Contaminateds Bedrock Aquifer: Tiverton, RI: unpublished M.S. Thesis, University of Rhode Island. 148p.
- Shankland. T.J., and Waff, H.S., 1974. Conductivity in Fluid-bearing Rocks. *Journal of Geophysical Research*, Vol. 79, No. 32, pp. 4863-4868.
- Sjogren, Bengt, 1984. *Shallow Refraction Seismic*, University Press, Cambridge, 268 p.
- Stollar, R.L. and Roux, P., 1975. Earth Resistivity Surveys - A Method for Defining Ground-Water Contamination. *Ground Water*, vol. 13, No. 2, pp. 145-150.
- Summers, W.K., 1972. Specific Capacities of Wells in Crystalline Rocks. *Ground Water*, Vol. 10, No. 6, pp. 37-48.
- Urish, D.W., 1981. Electrical Resistivity - Hydraulic Conductivity Relationships in Glacial Outwash Aquifers. *Water Resources Research*, Vol. 17, No. 5, pp. 1401-1408.

- Walsh, J.B., and Brace, W.F., 1984. The Effect of Pressure on Porosity and the Transport Properties of Rock. *Journal of Geophysical Research*. Vol. 89, No. B11, pp 9425-31.
- Ward, S.H., Frasher, D.C., 1967. Conduction of Electricity in Rocks. Part B of Chap. II in Mining Geophysics Vol II, ed. The SEG Mining Geophysics Volume Editorial Committee, pub. The Soc. of Exploration Geophysicists. p. 510.
- Wong, P., Koplik, J., and Tomanic, J.P., 1984. Conductivity and Permeability of Rocks. *Physical Review B*, Vol. 30, No. 11, pp. 6606-6614.
- Zen, E-an, 1983. Bedrock Geologic Map of Massachusetts. U.S. Geologic Survey: 3 map sheets.
- Zohdy, A.A.R., Eaton, G.P., Mabey, D.R., 1974. Applications of Surface Geophysics to Ground-Water Investigations. Book 2, Chap. D1. Collection of Environmental Data. Published by the U.S. Department of the Interior. Geological Survey.